4-18-2016 12:00 AM

At the interface of glycolipids and glycoproteins in the two gastro-intestinal pathogens Campylobacter jejuni and Helicobacter pylori

Najwa Zebian
The University of Western Ontario

Supervisor
Dr. Carole Creuzenet
The University of Western Ontario

Abstract

Campylobacter jejuni and *Helicobacter pylori* are phylogenetically related human gastro-intestinal pathogens. *C. jejuni* colonizes the intestine and is the leading cause of bacterial gastroenteritis worldwide. *H. pylori* colonizes the stomach of half the world's population, causing gastritis, gastric ulcers and gastric cancer. Both pathogens express glycoproteins and glycolipids (capsule, lipooligosaccharide or lipopolysaccharide (LPS)) that are important in pathogenesis. Sugar units from capsule or LPS can modify proteins in several bacteria. We reasoned that this may occur in *C. jejuni* and *H. pylori* as means to diversify their surface glycosylation and aid in colonization, immune evasion and virulence.

The putative sugar nucleotide dehydratase of *C. jejuni* NCTC 11168, Cj1319, has predicted roles in initiating the pathway for capsular heptose modification or participating in legionaminic acid synthesis for flagellin glycosylation. Alternatively, we propose that Cj1319 may use the GDP-*manno*-heptose precursor normally used for capsular heptose modification in a novel protein glycosylation pathway. We determined through enzymatic reactions with GDP-*manno*-heptose and compositional analysis of capsule from a *cj1319* knockout mutant that Cj1319 does not use GDP-*manno*-heptose and does not affect capsule. Furthermore, our comprehensive mass spectrometry (MS) analysis of flagellin glycopeptides showed that flagellin glycosylation is highly heterogeneous and includes modification by legionaminic acid. We determined that the *cj1319* mutant glycosylates flagellins with more legionaminic acid than WT, thus excluding the direct involvement of Cj1319 in legionaminic acid synthesis. This increase in legionaminic acid correlated with higher colonization of chickens but with lower virulence in *Galleria mellonella* larvae.

H. pylori NCTC 11637 expresses Lewis Y (Le^y) blood group mimics in the O-antigen of LPS which is important in immune evasion. We determined that the outer membrane protein HopE is glycosylated with Le^y through a comprehensive MS analysis of outer membrane peptides. This novel level of host mimicry is likely important for colonization and pathogenicity.

Keywords

Co-Authorship Statement

The work presented in Sections 3.3.5, 3.3.6, 3.4.4 and MS figures in Appendix B, in addition to Table 1 Table 2, have been previously published in (Zebian *et al.*, 2015). The *cj1319::CAT* mutant was created by Dr. Alexandra Merkx-Jacques and the chicken colonization experiment was performed by our collaborator Dr. Charles Dozois (INRS-Institut Armand Frappier). Ms. Paula Pittock ran samples by LC-MS and MS^2 and played a pivotal role in deconvoluting spectra where three ions co-eluted and co-isolated. I analyzed all other data including the MS data with assistance from Ms. Pittock.

The work presented in section 3.5 is currently being prepared for submission.

NHis-Cj1319 and Cj1319-CHis (with starting sequence MDGKGEKVRNIL) constructs were made by Dr. Merkx-Jacques and the NGST-Cj1319 construct was made by Ms. Melinda Demendi, MSc.

NHis-Cj1419 and NHis-Cj1426 were constructed by Ms. Anna Xie under my supervision.

Compositional analysis of the capsule and LOS was performed at the Complex Carbohydrate Research Center (Athens, GA, USA). I prepared the samples for this analysis and was in close correspondence with the technicians, providing essential information regarding the nature of our samples in order to facilitate the analysis.

Dr. Xuan Thanh Bui generated *cj1121c* and *cj1294* complement constructs and transformed them into *C. jejuni* making strains *cj1121c*comp_RSP and *cj1294*comp_RSP presented in sections 3.2-3.5.

Ms. Rachel Ford, MSc discovered the outer membrane Le^y glycoprotein candidate, Mr. Alexander Oberc extracted and purified outer membrane peptides and labelled BambL and PA-IIL with biotin, Mr. Brandon Oickle, MSc constructed the *hope::CAT* mutant and Dr. Melissa Hannauer performed the anti-Le^y Western blot of this mutant. I directed and performed the MS analysis and provided continuity to this project through guiding all members involved in this work and contributing intellectually.

Dr. C. Creuzenet modelled HopE and provided Figure 44.

Dedication

I would like to dedicate this work to my family and friends who have been there for me and supported me throughout the course of my life and work. Thank you Mom and Dad for your encouragement, patience and understanding throughout the years. I would never have reached this far without your support and love. Thank you to my brother, sisters (too many of you to call out) and sister-in-law for showing your interest and enthusiasm towards my work. Thanks to all my great friends, especially Melissa Pondexter, Marlon Badette, Lawrence Wu and Vi Nguyen. You kept me positive and encouraged me to perservere. Thank you for making my days better when I was down and for all the good times. Finally, I would like to thank everyone throughout my life who inspired my love for knowledge and education.

Acknowledgments

Table of Contents

List of Tables

List of Figures

List of Appendices

List of Abbreviations

BHI-YE	brain heart infusion yeast extract
˚C	degree Celsius
CAT	chloramphenicol resistance cassette
CE	capillary electrophoresis
cDNA	complementary DNA
CID	collision induced dissociation
CFU	colony forming units
CPS	capsular polysaccharide
CMP	cytidyl monophosphate
CTAB	cetyltrimethylammonium bromide
CV	column volume
Da	Dalton
DNA	deoxyribonucleic acid
ECD	electron capture dissociation
E. coli	*Escherichia coli*
EDTA	ethylenediaminetetraacetic acid
ESI	electrospray ionization
ETD	Electron transfer dissociation
FT	Fourier transform
FlaA	flagellin A
FlaB	flagellin B
Fuc	fucose
FucT	fucosyltransferase
g	gravitational force
Gal	galactose
GalNAc	N-acetyl-galactosamine
GDP	guanosine 5'-diphosphate
Glc	glucose
GlcNAc	N-acetyl-glucosamine
Glu	glutamic acid
h	hours
HCD	high energy collision induced dissociation
Hep	heptose
LB	Luria Bertani
LC	liquid chromatography
Leg5Ac7Ac	legionaminic acid
Leg5Am7Ac	acetamidino legionaminic acid
Leg5AmNMe7Ac	N-methylacetimidoyl derivative of legionaminic acid
Le^a	Lewis a
Le^b	Lewis b
Le^x	Lewis x
Le^y	Lewis y
LOS	lipooligosaccharide

LPS	lipopolysaccharide
MALDI	matrix assisted laser desorption ionization
Man	mannose
NANA	N-acetyl-neuraminic acid
OD	optical density
OM	outer membrane
OMP	outer membrane protein
OTase	oligosaccharyltransferase
μL	microliter
Min	minutes
Me	methyl
mL	milliliters
mRNA	messenger Ribonucleic acid
MS	mass spectrometry
MS^2	tandem mass spectrometry
MS^3	third-stage mass spectrometry
m/z	mass per charge
TSA	Trypticase Soy Agar
TSB	Trypticase Soy Broth
PBS	phosphate buffered saline
PCR	polymerase chain reaction
pgl	protein glycosylation locus
pH	potency of hydrogen
pI	isoelectric point
pse	pseudaminic acid
Pse5Ac7Ac	pseudaminic acid
Pse5Ac7Am	acetamidino pseudaminic acid
Pse5AcGriMe7Ac	dimethylglyceric derivative of pseudaminic acid
Pse5AcGriMe7Am	dimethylglyceric derivative of acetamidino pseudaminic acid
RNA	ribonucleic acid
RT	reverse transcriptase
SAM	S-adenosyl-methionine
SDS-PAGE	sodium dodecyl sulfate polyacrylamide gel electrophoresis
U	unit
Und-P	Undecaprenyl phosphate
WT	wild type

Chapter 1

1   Introduction

Campylobacter jejuni and *Helicobacter pylori* are two important phylogenetically-related gastro-intestinal human pathogens, both with major health and economic burdens (Deltenre, 2012; Kaakoush *et al*., 2015; Peleteiro *et al*., 2014; Plummer *et al*., 2015). Each of these two bacterial species possess and express glycosylation machineries for the glycosylation of both lipids and proteins (Day *et al*., 2012; Rubin and Trent, 2013). This chapter provides a detailed overview of the glycosylation machineries, the glycolipids and glycoproteins expressed by each, and their relationship to host colonization and infection. An overview of mass spectrometry analysis methods for glycoproteins is also presented as this analysis is complex but integral for the understanding of a significant amount of data presented in this dissertation.

1.1   *Campylobacter jejuni*

1.1.1   Discovery and general characteristics

Campylobacters were first reported by Escherich in 1886 who noted spirally shaped microbes in intestinal contents from 16 of 17 children who had died of diarrheal disease (Escherich, 1886). Thereafter, it was not until 1913 that these organisms were first isolated from ovine abortuses whereby the bacteria were referred to as '*Vibrio*' due to their similarity with *Vibrio cholera* (McFadyean and Stockman, 1913). However, it was shown that these microbes were genetically distinct from other vibrios due to their small genomes, non-fermentative metabolism and microaerophilic nature. In 1963, the genus *Campylobacter,* from the Greek word for curved rod, was created and used to classify these microbes to distinguish them from the *Vibrio* genus (Sebald and Veron, 1963; Veron and Chatelain, 1973). *Campylobacter* are small microaerophilic spirally shaped gram negative cells (0.2–0.8 μm × 0.5–5 μm) (On, 2001). They obtain energy from amino acids or tricarboxylic acid cycle intermediates and do not ferment or oxidize carbohydrates (Vandamme, 2000). Under unfavourable growth conditions, these bacteria form viable but

non-culturable cocci whose role is not yet understood as it is not clear if these cells can revert to a culturable form (Portner *et al*., 2007). *C. jejuni* was recognized as one of the three thermophilic species of *Campylobacter*, including *coli* and *laridis.* The interest in this strain grew exponentially as it was isolated from children with enteritis in 1973 (Butzler *et al*., 1973) and subsequently from 57 of 803 fecal samples collected from diarrheal patients in Britain over 18 months (Skirrow, 1977).

1.1.2   Clinical manifestations of *C. jejuni* and treatment

C. jejuni is the leading cause of acute bacterial enteritis in the world, contributing to an estimated 8.4% of all diarrheal disease worldwide, ranking fourth after rotavirus, typhoid fever, and cryptosporidiosis (Humphrey; Murray *et al*., 2012; Weisent, 2010). This human pathogen is a commensal in poultry, although this has been recently challenged (Humphrey *et al*., 2014), and spreads to humans usually by the consumption of contaminated poultry meat in the developed world and contaminated water in the developing world (Humphrey; Kaakoush *et al*., 2015). The economic burden of campylobacteriosis in the United States has been estimated at $1.6 billion annually (Batz *et al*., 2012). Additionally, an increase in *Campylobacter* incidence was observed from 2006 to 2008, in contrast to other gastro-intestinal pathogens, c*ryptosporidium*, *Listeria*, *Salmonella*, *Shigella*, Shiga-toxigenic *Escherichia coli* O157:H7, and *Yersinia,* whose incidence decreased over the same timeframe (Batz *et al*., 2012).

In Canada, it was found that *Campylobacter* spp*.,* mostly *C. jejuni,* had the highest frequency of occurrence among all other pathogenic bacteria in agricultural water basins across the country, with an overall prevalence of 49% (Khan *et al*., 2014). In the Waterloo region of Ontario, an average of 49.69 cases of campylobacteriosis per 100,000 people were reported from 1990 to 2004 annually (Keegan *et al*., 2009). In Quebec, 28,521 cases were reported from 1996 to 2006 (Arsenault *et al*., 2012). British Columbia was reported to have an average of 38 cases per year per 100,000 people between 2005 and 2009 (Kaakoush *et al*., 2015).

C. jejuni doses as low as a few hundred cells may lead to infection after a short incubation time of 24-48 hours (may be up to 10 days) which is followed by severe symptoms including watery or bloody diarrhoea, abdominal cramps, and fever (Hara-Kudo and

Takatori, 2011; Kaakoush *et al*., 2015; Man, 2011). Typically, the infection is self-limiting within a median of 6 days (Man, 2011). *C. jejuni* infection causes severe gastroenteritis and is a predisposing agent of inflammatory bowel disease and celiac disease (Gradel *et al*., 2009; Man, 2011; Verdu *et al*., 2007). Furthermore, there are many post-infection complications that may arise following a *C. jejuni* infection including Guillain-Barŕe syndrome (31% of cases attributed to *C. jejuni*), reactive arthritis, and Miller Fisher syndrome, and recently irritable bowel syndrome (Israeli *et al*., 2010; Nielsen, 2010; Poropatich *et al*., 2010). These clinical symptoms associated with *C. jejuni* infection are caused by several virulence factors including: adhesins and numerous toxins, *Campylobacter* invasion antigen proteins, a type 4 secretion system, capsule, lipooligosaccharide (LOS), flagella and associated motility and protein glycosylation (Dasti, 2010).

1.1.3   Genome and phase variation

 C. jejuni NCTC 11168, the first sequenced strain of *C. jejuni,* has a circular chromosome of 1,641,481 base pairs (30.6% G+C) which is predicted to encode 1,654 proteins and 54 stable RNA species (Gundogdu *et al*., 2007; Parkhill *et al*., 2000). Virtually no insertion sequences or phage-associated sequences are found and there are very few repeat sequences in its genome. Importantly, there is an abundance of hypervariable sequences determined by homopolymeric runs of nucleotides primarily found in genes encoding the biosynthesis or modification of surface structures, including capsule, LOS, and glycoproteins, or in closely linked genes (such that phase variation leads to fusion or separation of these genes) of unknown function.

Hundreds of genomes of *C. jejuni* strains have been sequenced and, as a result, it was found that there is a high degree of genetic variation among strains. This made it particularly challenging to study the pathogenesis of this organism. Much progress has been made in terms of identifying virulence factors and key interactions with host cells using *C. jejuni* strains NCTC 11168 and 81-176 as will be described below, however, to date, it remains unclear how *C. jejuni* causes illness in humans while it lives in commensalism in the gut of birds and livestock. Our laboratory has created numerous glycosylation pathway mutants

in strain NCTC 11168, a pathogenic strain in humans that was the only strain sequenced at the onset of our studies, and thus this strain was focused on for the work presented in this thesis. Importantly, as will be discussed, this strain has more genetic potential for making novel sugars for protein glycosylation.

1.1.4 Virulence factors of *C. jejuni*

1.1.4.1   Flagella and motility

Motility is an essential virulence factor of *C. jejuni* mediated by flagella and cell shape. Cells can either have a unipolar flagellum or bipolar flagella. The flagella are made of two polymerized subunits, minor subunit FlaB at the base and major subunit FlaA which makes up the majority of the flagellum. These flagellins are *O*-glycosylated as discussed in section 1.1.4.3. It has been shown that FlaA is essential for colonization as a knockout mutant of *flaA* results in a truncated flagellum with a motility defect and impaired colonization, whereas FlaB was not important for colonization and a knockout mutant of *flaB* resulted in nearly normal motility (Grant *et al*., 1993; Guerry *et al*., 1991; Nachamkin *et al*., 1993; Pavlovskis *et al*., 1991; Wassenaar *et al*., 1991, 1993).

Unlike rod-shaped bacteria, *C. jejuni* increases in motility velocity as the viscosity of the medium increases (Ferrero and Lee, 1988), which is due in part to the spiral shape of the bacterial cell that has been shown to be important for motility as this shape allows the cell to drill into the mucosal layer of the intestinal epithelium. The shape is acquired due to the activity of peptidoglycan synthesis and modifying enzymes that are still under investigation (Frirdich *et al*., 2012). Pgp1, a metal-dependent DL-carboxypeptidase cleaving monomeric disaccharide tripeptides of peptidoglycan to disaccharide dipeptides, is the first enzyme shown to be directly linked the helical morphology of *C. jejuni* 81-176 (Frirdich *et al*., 2012). Pgp1 is also conserved in other spirally shaped bacteria. A knockout mutant of *pgp1* was shown to have lost its helical shape as well as have impaired motility, decreased biofilm formation, and decreased colonization of chicken caeca. Although no defect in the ability of this mutant to invade epithelial or macrophage cell lines was detected *in vitro*

regardless of the viscosity of the mucus used to coat the eukaryotic cells, there was an increase in mNOD1 activation and IL-8 secretion.

1.1.4.2   Protein glycosylation in *C. jejuni*

Protein glycosylation was believed to be a eukaryote-exclusive post-translational modification until the S layer glycoproteins were discovered in the 1970s (Mescher and Strominger, 1976; Sleytr and Thorne, 1976). Proteins are glycosylated through the action of a glycosyltransferase (Lairson *et al*., 2008). The eukaryotic oligosaccharyltransferase (OTase) is a multimeric subunit protein, whereby a subunit termed STT3 is highly conserved among eukaryotes (Yan and Lennarz, 2002). The OTase for *N*-glycosylation PglB was discovered in *C. jejuni* which has significant homology to STT3 and is encoded in a highly conserved locus adjacent to the LOS biosynthesis cluster (Szymanski, 1999). This locus was found to encode the biosynthesis machinery for synthesis of a conserved heptasaccharide used for protein glycosylation and made of GalNAc-α1,4-GalNAc- α 1,4-[Glcβ1,3-]GalNAc-α1,4-GalNAc-α1,4-GalNAc-α 1,3-Bac-β1, where Bac is bacillosamine (2,4-diacetamido-2,4,6-trideoxyglucopyranose) (Figure 1A) (Linton *et al*., 2005; Szymanski, 1999; Wacker *et al*., 2002; Young *et al*., 2002).

N-glycosylation

 The *N*-glycosylation cluster contains *cj1120c, cj1121c,* and *cj1123c,* which encode for a dehydratase, aminotransferase, and N-acetyltransferase respectively which are responsible for Bac synthesis (Figure 1B). The *N*-glycosylation pathway involves the attachment of a Bac-containing heptasaccharide motif onto the asparagine of the consensus sequence D/E-Y-N-X-S/T (Y, X≠P) (Kowarik *et al*., 2006). This sequon was thought to be extended compared to the eukaryotic N-X-S/T (X≠P), however, new data shows that this is not the case for all bacteria (Schwarz and Aebi, 2011; Schwarz *et al*., 2011a). Over 65 proteins have been reported to be modified by the N-glycan motif (Scott *et al*., 2011). It has been reported that disruption of this protein glycosylation pathway leads to decreased adhesion and invasion of INT 407 cells by *C. jejuni* 81-176 (Szymanski *et al*., 2002), in addition to decreased invasion of Caco-2 intestinal cells *in vitro* and impaired colonization of chicken caeca by strain NCTC 11168 (Vijayakumar *et al*., 2006).

Figure 1. Schematic of the *pgl* locus and assembly of the conserved heptasaccharide for protein *N*-glycosylation.

(A) Conserved *N*-glycosylation cluster in *C. jejuni*. **(B)** Pathway for heptasaccharide synthesis. PglE, F, and G (or Cj1120c, Cj1121c, and Cj1123c respectively) function to synthesize UDP-Bac from UDP-GlcNAc. Next, Bac is transferred to undecaprenyl pyrophosphate by PglC, and additional GalNAc residues and one glucose residue are added by the glycosyltransferases PglA, J, H and I. The formed heptasaccharide is transferred from the cytoplasm to the periplasm through the action of the flippase PglK, followed by the block transfer of this glycan onto the asparagine of the *N*-glycosylation consensus sequence through the activity of the OTase PglB. Adapted from (Kelly *et al*., 2006).

A

B
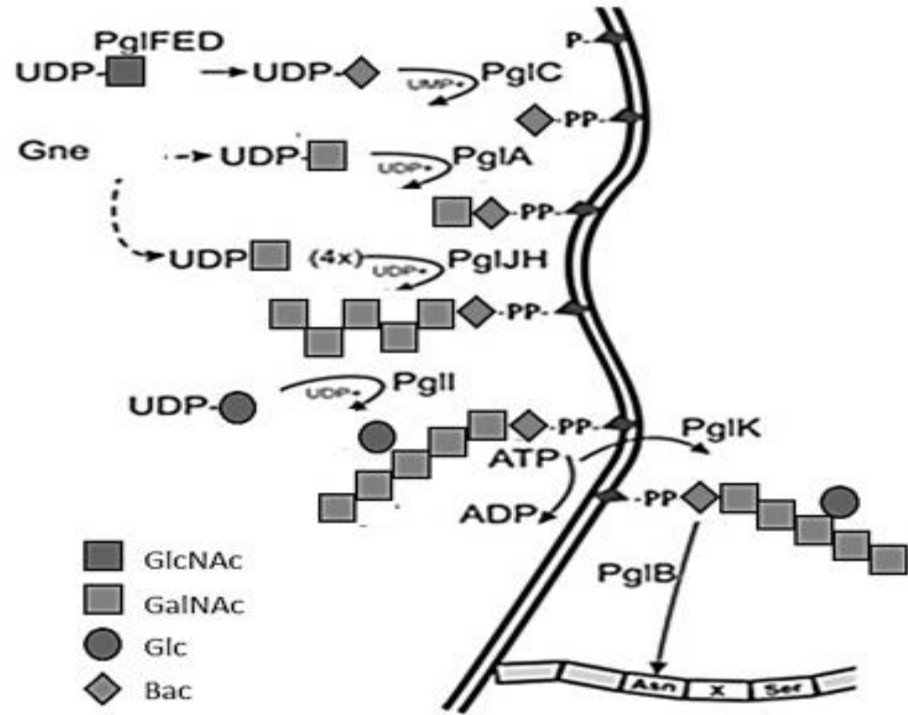
Protein *O*-glycosylation in *Campylobacter spp.*

Protein *O*-glycosylation in *C. jejuni* has been described for the flagellins of strain 81-176 (Thibault *et al*., 2001). Post-translational modification of its flagellins by pseudaminic acid (Pse5Ac7Ac) is required for assembly and function (Table 1) (Hitchen *et al*., 2010). Flagellins from *C. coli* VC167 were also shown to be glycosylated with Pse5Ac7Ac in addition to a related sugar, legionaminic acid (Logan *et al*., 2002; McNally *et al*., 2007a). *C. jejuni* NCTC 11168 was shown to produce both sugars in its metabolome (Logan *et al*., 2009), but it was not until recently that glycopeptide data were generated to show that pseudaminic and legionaminic acid and their derivatives modify flagellins in this strain (Ulasi *et al*., 2015; Zampronio *et al*., 2011; Zebian *et al*., 2015).

Recently, the major outer membrane protein (MOMP) of *C. jejuni* NCTC 11168 was identified carrying a sugar motif of Gal(β1–3)-GalNAc(β1–4)-GalNAc(β1–4)-GalNAc α1 on Thr$_{268}$. (Mahdavi *et al*., 2014). This glycosylation affects the conformation of MOMP which modulates binding to human histo-blood group antigens and promotes cell-to-cell binding, biofilm formation, adhesion to Caco-2 cells and is required for optimal colonization of chickens.

Table 1. Summary of known sugars produced in *C. jejuni* NCTC 11168 and 81-176, and in *C. coli* VC167 that have been shown on glycopeptides and/or have been identified in the metabolome.

Modification	Bacterial species and strains	References
Pseudaminic acid[a] (Pse5Ac7Ac)	*C. jejuni* 81-176	Thibault 2001[c]; McNally 2006[d]
	C. jejuni NCTC 11168	Logan 2009[d]; Ulasi 2015[e]
	C. coli VC167	Logan 2002[e] ; McNally 2007[d]
Acetamido pseudaminic acid[a] (Pse5Ac7Am)	*C. jejuni* 81-176	Thibault 2001[c]; McNally 2006[d]
	C. jejuni NCTC 11168	Logan 2009[d];
	C. coli VC167	Logan 2002[e] ; McNally 2007[d]
O-acetyl pseudaminic acid (Pse5Ac7Ac8OAc)	*C. jejuni* 81-176	Thibault 2001[c]
N-acetyl glutamic pseudaminic acid derivative (Pse5Ac7Ac8-GlnAc)	*C. jejuni* 81-176	Thibault 2001[c]
Dihydroxypropionyl pseudaminic acid derivative (PsePr)	*C. jejuni* 81-176	Thibault 2001[c]
Dimethylglyceric derivative of acetamidino pseudaminic acid (Pse5AcGriMe7Am)	*C. jejuni* NCTC 11168	Logan 2009[d]; Ulasi 2015[e]; Zampronio 2011[e]
Dimethylglyceric derivative of pseudaminic acid (Pse5AcGriMe7Ac)	*C. jejuni* NCTC 11168	Logan 2009[d]; Ulasi 2015[e]; Zampronio 2011[e]
Acetamidino pseudaminic acid-deoxypentose	*C. coli* VC167	Logan 2002[e]
O-acetyl pseudaminic acid-deoxypentose	*C. coli* VC167	Logan 2002[e]

Legionaminic acid[a] (Leg5Ac7Ac)	*C. jejuni* NCTC 11168	Logan 2009[d]; Ulasi 2015[e]; Zampronio 2011[e]
	C. coli VC167	McNally 2007[d]
Acetamidino legionaminic acid[a] (Leg5Am7Ac)	*C. jejuni* NCTC 11168	Logan 2009[d]; Ulasi 2015[e]; Zampronio 2011[e]
	C. coli VC167	McNally 2007[d]
N-methylacetimidoyl derivative of Legionaminic acid[b] (Leg5AmNme7Ac)	*C. jejuni* NCTC 11168 *C. coli* VC167	Logan 2009[d] McNally 2007[d]

[a] Pse5Ac7Ac and Leg5Ac7Ac share the same mass and could not be distinguished on peptides by MS but could be distinguished from one another by NMR. The same applies for Pse5Ac7Am and Leg5Am7Ac. To date, most NMR data were obtained via metabolomic studies (McNally *et al.,* 2007, McNally *et al.,* 2006, Logan *et al.*, 2009), the only NMR data showing pseudaminic acid on glycopeptides was obtained for *C. jejuni* 81-176 (Thibault *et al.,* 2001). No NMR analysis has been conducted on *C. jejuni* NCTC 11168 or *C. coli* VC167 flagellin glycopeptides, and thus the definitive assignment of these sugars on glycopeptides remains undetermined.

[b] The modifications present on the Leg5AmNme7Ac derivative were identified in the metabolome of *C. jejuni* NCTC 11168 (Logan *et al.,* 2009) but have never been found on pseudaminic acid. Thus the presence of its oxonium ion in MS analyses indicates specifically the presence of legionaminic acid. Its sugar oxonium ion was shown by top-down MS in *C. coli* VC167 (McNally *et al.,* 2007) but not mapped to any peptide.

[c] glycopeptide data comprising NMR evidence of sugar identity.

[d] metabolomics study comprising NMR evidence of sugar identity.

[e] MS study relying on mass of oxonium ions only.

Pseudaminic acid and legionaminic acid synthesis

The pathway for pseudaminic acid synthesis has been well characterized (Chou *et al.*, 2005; Creuzenet, 2004; Goon *et al.*, 2003; Guerry *et al.*, 2006; Obhi and Creuzenet, 2005; Schoenhofen *et al.*, 2006). In a six-step reaction, UDP-GlcNAc is converted to pseudaminic acid through the actions of PseB/Cj1293, PseC/Cj1294, PseH/Cj1313, PseG/Cj1312, PseI/Cj1317, and PseF/Cj1311 enzymes. The first three enzymes dehydrate, aminate, and acetylate UDP-GlcNAc as described for the synthesis of UDP-Bac from UDP-GlcNAc, however, the two pathways differ in their dehydratases, whereby the pseudaminic acid pathway Cj1293 enzyme also has C5 epimerase activity (Schoenhofen *et al.*, 2006).

Through analysis of the nucleotide-activated sugars in the metabolome of various knockout mutants, a putative legionaminic acid synthesis gene cluster was identified in *C. coli*, and the presence or absence of this cluster has been subsequently used to identify *Campylobacter* strains and/or species as producing legionaminic acid or not (Howard *et al.* 2009; McNally *et al.* 2007). For example, *C. jejuni* 81-176 lacks this gene cluster and consistently does not make legionaminic acid. Legionaminic acid synthesis has also been explored *in vitro* for *Legionella pneumophila* and *C. jejuni*. A pathway in each organism was proposed whereby the enzymes from both pathways are homologous and carry out similar functions, but use different substrates. The first pathway used recombinant *C. jejuni* Cj1120c, Cj1121c and Cj1123c enzymes from the general protein N-glycosylation system to perform successive dehydration, amination and acetylation of UDP-GlcNAc to make UDP-diNAcBac (Demendi and Creuzenet, 2009; Schoenhofen *et al.*, 2006; Vijayakumar *et al.*, 2006). This was followed by conversion into CMP-legionaminic acid via hydrolysis of UDP with concomitant C2 epimerisation, condensation with phosphoenolpyruvate and finally activation as a CMP derivative by homologues of sialic acid synthesis enzymes from *L. pneumophila* (Glaze *et al.*, 2008). The second pathway used recombinant *C. jejuni* Cj1319, Cj1320 and Cj1298 enzymes to produce GDP-2,4-diacetamido-2,4,6-trideoxy-α-D-glucopyranose from GDP-GlcNAc, followed by conversion into CMP-legionaminic acid using sialic acid synthesis homologues Cj1328, Cj1327 and Cj1331 (Schoenhofen *et al.*, 2009). Specifically, in the GDP-GlcNAc based pathway, Cj1319 is reported to catalyze

GDP-GlcNAc into GDP-2-acetamido-2,6-dideoxy-α-D-*xylo*-hexos-4-ulose which is further modified by Cj1320. However, homologues of these two enzymes were previously excluded from the legionaminic acid gene cluster in *C. coli* because the knockout mutant of the Cj1319 homologue produced more CMP-Leg5Ac7Ac than the wild type (WT) and the knockout mutant of the Cj1320 homologue showed no defect in CMP-Leg5Ac7Ac production (McNally *et al*., 2007a). This contradiction is intriguing and requires addressing in order to understand the complex flagellin glycosylation machinery in *C. jejuni* NCTC 11168.

1.1.4.3   Capsule

It was originally discovered during the 1990s that *Campylobacter* spp. produces surface-exposed polysaccharides that were thought to be the O-chain of lipopolysaccharide (LPS) (Aspinall *et al*., 1992, 1993, 1995a, 1995b, 1995c). However, in the early 2000s, the structures of these polysaccharides in some *Campylobacter* species were determined which indicated that these structures were not associated with LPS, but rather they resembled capsule polysaccharides (Aspinall *et al*., 1995c). It was also shown by electron microscopy and Alcian blue staining that these surface structures were indeed capsule polysaccharides (Karlyshev *et al*., 2000). There are currently eight *C. jejuni* capsule structures known, whereby they differ in the sugar content or in linkage types (Aspinall *et al*., 1992, 1995c; Chen *et al*., 2008; Hanniffy *et al*., 1999; Karlyshev *et al*., 2005a; McNally *et al*., 2005, 2007b; Michael *et al*., 2002; Muldoon *et al*., 2002). Specifically, the capsule of strain NCTC 11168 that is the focus of this study comprises β-D-Rib*p*, β-D-Gal*f*NAc, α-D-Glc*p*A6(NGro), a uronic acid amidated with 2-amino-2-deoxyglycerol at C-6, and 6-*O*-methyl-D-*glycero*-α-L-*gluco*-heptose as a sidebranch (Figure 2) (Michael *et al*., 2002). This structure is linked to a poly-(3-deoxy-D-*manno*-oct-2-ulosonic acid) (poly-Kdo) which is linked to a lipid carrier (Corcoran *et al*., 2006; Willis *et al*., 2013). *C. jejuni* strains have been classified into 47 serotypes according to a scheme called Penner or heat-stable (HS) serotyping which sorts on the basis of a combination of their capsule and LOS structures, although the capsule has a stronger influence on the serotype (Penner, 1983; Penner and Hennessy, 1980). A recent systematic review revealed that eight serotypes accounted for more than half of sporadic diarrheal diseases globally, three of which dominated inter-

regionally and globally, including HS2, the serotype of NCTC 11168 (Pike *et al*., 2013). More recently, a genotyping scheme for capsular types was developed based on the potential of a strain to express a serotype which is not sensitive to variations in capsule gene expression or affected by genes and gene products outside the capsule locus which are complications affecting the HS serotyping scheme (Poly *et al*., 2011). A number of capsule genotypes have been shown to be associated with Guillain-Barre Syndrome in combination with certain LOS structures, including HS2 (Heikema *et al*., 2015).

Figure 2. Structure of the capsule of *C. jejuni* NCTC 11168 and the organization of the capsular gene locus highlighting the three regions.

(A) Schematic of one capsule unit attached to its KDO-phospholipid anchor next to the structure of the capsule unit. **(B)** Schematic of the three genetic regions for capsule synthesis, assembly and export highlighting the heptose modification genes in region 2 and the capsule transporter gene *kpsM* in region 3. Adapted from (Wong *et al*., 2015).

A

3,6-O-Me$_2$-D-α-L-*gluco*Hep*p*-(1-3)

MeOPN-4

-2)-β-D-Rib*f*-(1-5)-β-D-Gal*f*NAc-(1-4)-α-D-Glc*p*A-(1-

MeOPN-3

GroN/EtN-6

B

Attachment   **Synthesis**   **ABC Transporter**

Region 1   Region 2   Region 3

cj1419   hddC gmhA2 hddA cj1426c wcaG mlghC cj1429c mlghB   kpsM

Precursor   **Modified heptose**
GDP-D-*glycero*-D-   GDP-3,6-OMe-L-
manno-heptose   *gluco*-heptose
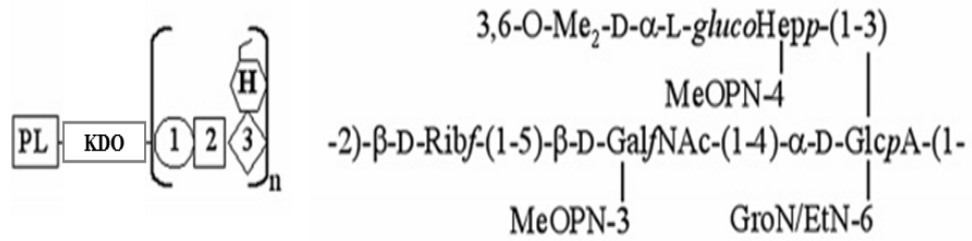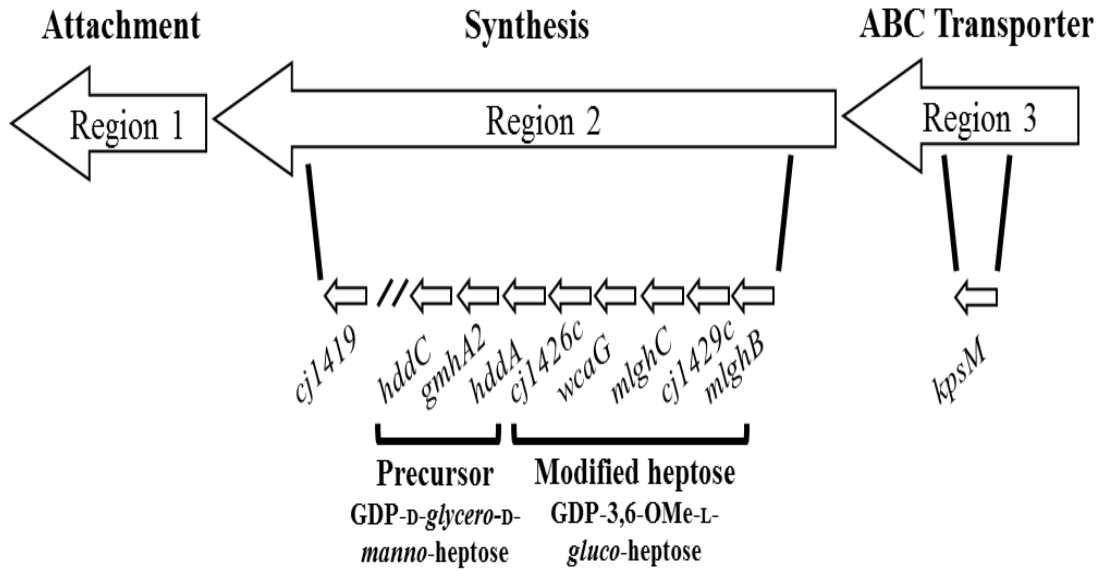
Capsule is assembled via an ABC transporter mechanism in *C. jejuni*, similar to the class 2 and 3 capsules of *E. coli* K1 and K5, *Neisseria meningitidis* and *Haemophilus influenza* (Guerry *et al*., 2012; Whitfield, 2006). The genetic organization of the capsular genes in *C. jejuni* is also similar to their organization in the said organisms, whereby there are three regions: 1 and 3 are highly conserved and involved in assembly and transport of the capsule and region 2 is a variable region involved in synthesis of the polysaccharides. Region 1 contains six genes encoding KpsF, E, D, U, C, and S. KpsE and KpsD are involved in the translocation of the polysaccharide across the periplasmic space, while KpsC and KpsS are believed to play roles in the attachment of Kdo to the phosphatidic acid, and its subsequent attachment to the reducing end of the polysaccharide. KpsF has unknown function and KpsU is a cytidine 5'-monophosphate (CMP)-Kdo synthetase enzyme, responsible for the generation of the CMP-Kdo required for the ligation step. Region 3 encodes for KpsM and KpsT, both members of the ATP-binding cassette (ABC) family of transporters, which are involved in the export of the polysaccharide from the cytoplasmic face of the inner membrane into the periplasmic space.

The phospholipid anchor of three capsule types (HS3, HS6, and HS23/36) has been determined to be dipalmitoyl-glycerophosphate with ester-linked hexadecanoic acids (Corcoran *et al*., 2006). A distinguishable feature of *Campylobacter* species capsules is the presence of a heptose found in an unusual configuration (*altro*, *ido, gulo*, *talo*) which is also sometimes found dehydrated at C6. This modified heptose may be part of the main chain or a side branch of the capsule depending on the strain (Aspinall *et al*., 1992, 1995c; Chen *et al*., 2008; Hanniffy *et al*., 1999; Karlyshev *et al*., 2005a; McNally *et al*., 2005, 2007b; Michael *et al*., 2002; Muldoon *et al*., 2002). In our strain of interest, it is a side branch (Figure 2) (Michael *et al*., 2002). In addition, an *O*-methyl phosphoramidate (MeOPN) is linked to different sugars in most *Campylobacter* strains and its presence seems to depend on that of the modified heptose in strain NCTC 11168 (Alphen *et al*., 2014; McNally *et al*., 2007b).

Modified capsular heptose

The capsule locus of *Campylobacter* species contains the highly conserved genes *gmhA2, hddA,* and *hddC* encoding enzymes responsible for the biosynthesis of GDP-ᴅ-*glycero*-ᴅ-*manno*-heptose, the precursor of the capsular modified heptose (Karlyshev *et al*., 2005a). In addition to gene product of *gmhB* (ᴅ-glycero-ᴅ-manno-heptose 1,7-bisphosphate phosphatase; shared with the LOS pathway for making heptose) encoded by the LOS cluster, the gene products of *gmhA2* (phosphoheptose isomerase), *hddA* (putative ᴅ-glycero-ᴅ-manno-heptose 7-phosphate kinase), and *hddC* (putative ᴅ-glycero-ᴅ-manno-heptose 1-phosphate guanosyltransferase) synthesize GDP-ᴅ-*glycero*-ᴅ-*manno*-heptose from ᴅ-sedoheptulose 7-phosphate (Kneidinger *et al*., 2001), a common precursor for synthesis of the heptose found in the LOS or LPS of other bacteria (Karlyshev *et al*., 2005a; Kneidinger *et al*., 2002). Noteworthy, *gmhA2* is homologous to *gmhA* which is encoded in the LOS biosynthesis gene cluster and part of the pathway for making ADP-ʟ-*glycero*- ᴅ-*manno*-heptose from ᴅ-sedoheptulose 7-phosphate. The two gene products have been shown to be redundant in function as the heptose of both capsule and LOS remained produced in either single gene knockout mutant of *gmhA* or *gmhA2*, but upon disruption of both genes, both the capsule and LOS no longer contained heptose (Karlyshev *et al*., 2005a).

The pathway for modification of GDP-ᴅ-*glycero*-ᴅ-*manno*-heptose used for capsule synthesis has been fully characterized in *C. jejuni* 81-176 (Figure 3A) (McCallum *et al*., 2012). The enzymes encoded by *cjj1426* (DdahA, C4, C6 dehydratase), *cjj1430* (DdahB, C3 epimerase) and *cjj1427* (DdahC, C4 reductase) modify this precursor to form GDP-6-deoxy-α-ᴅ-*altro*-heptose. *C. jejuni* NCTC 11168 has been shown to incorporate ᴅ-*glycero*-α-ʟ-*gluco*-heptose into its capsule (Figure 2) (Michael *et al*., 2002). The pathway for making this sugar has been partially deciphered (Figure 3, right pathway) (McCallum *et al*., 2013), whereby the enzymes encoded by *cj1430* (MlghB, C3, C5 epimerase) and *cj1428* (MlghC, C4 reductase) have been characterized. However, the proposed C4 oxidase MlghA of this pathway has yet to be found. This enzyme is expected to be homologous to the dehydratase DdahA as C4 oxidation also occurs during C4, C6 dehydration. However,

there are no proteins encoded by the NCTC 11168 capsule locus bearing similarity to DdahA aside from Cj1319, coded by a gene found in the flagellar glycosylation locus.

Figure 3. Pathways for the modification of GDP-*manno*-heptose for incorporation into capsular polysaccharide.

(A) The fully characterized pathway for capsular heptose modification in *C. jejuni* 81-176. **(B)** The partially determined equivalent pathway from strain NCTC 11168. (Adapted from McCallum *et al*., 2013).

A

Pathway established in strain 81-176

GDP-D-*glycero*-D-*manno*-heptose

DdahA | C4,C6 dehydration

GDP-6-deoxy-4-keto-
D-*lyxo*-heptose

DdahB | C3 epimerization

GDP-6-deoxy-4-keto-
D-*arabino*-heptose

DdahC | C4 reduction

GDP-6-deoxy-*altro*-heptose
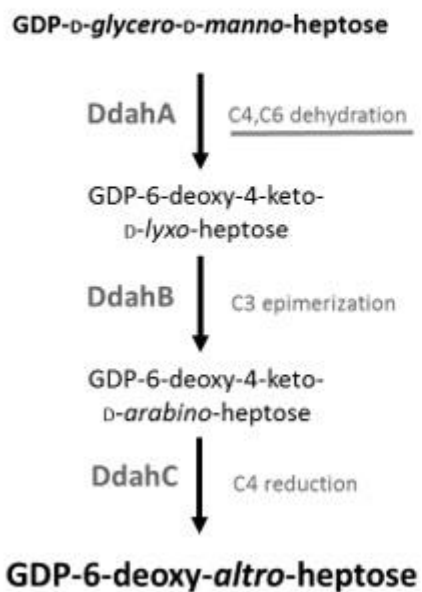
B

Partial pathway established in strain NCTC 11168

GDP-D-*glycero*-D-*manno*-heptose

C4 oxidation

GDP-3,6-R-4-keto-D-
lyxo-heptose

MlghB | C3, C5 epimerization

GDP-3,6-R-4-keto-L-
xylo-heptose

MlghC | C4 reduction

GDP-3,6-OMe-L-*gluco*-heptose
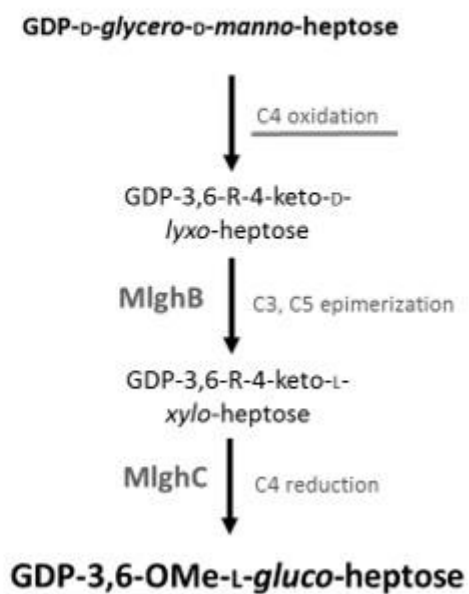
Cj1319 is predicted to be a sugar nucleotide dehydratase suggesting its involvement in a glycosylation pathway. Cj1319 is estimated to be encoded by 82% of *C. jejuni* clinical strains including NCTC 11168 (Huang et al., 2013). Although Cj1319 is homologous to GDP-*manno*-heptose dehydratases and GDP-mannose dehydratases, Cj1319 has been shown to participate in an *in vitro* pathway for legionaminic acid synthesis, a sugar that is predicted to glycosylate the flagellins of some *C. jejuni* strains, as discussed in section 1.1.4.2.

Some strains of *C. jejuni* also further methylate the capsular heptose (Karlyshev *et al*., 2005a). This modification is variable as, for example, strain NCTC 11168 produces a modified capsular heptose in a heterogeneous mixture of unmethylated, C3-*O*-methylated, C6-*O*-methylated, or C3, C6-*O*-methylated D-*glycero*-α-L-*gluco*-heptose (Michael *et al*., 2002; Wong *et al*., 2015). The expression of this modified heptose is also negatively regulated by WcaG, a C4 reductase which reduces GDP-6-deoxy-4-keto-D-*lyxo*-heptose to GDP-6-deoxy-D-*manno*-heptose (McCallum *et al*., 2011, 2013).

As *C. jejuni* NCTC 11168 expresses the modified heptose as a sidechain of the capsular polysaccharide, it was possible to study the role of this modified heptose in the virulence of *C. jejuni* specifically as the lack of the incorporation of this heptose still allows for capsular chain assembly which is in contrast with other strains that express the modified heptose within the main chain (Wong *et al*., 2015). This modified heptose was found to play a role in serum resistance and invasion of intestinal cells and that it is important for the colonization of chicken caeca. Similar findings were obtained from *Yersinia pseudotuberculosis,* which expresses a modified heptose in its LPS, which showed the lack of this heptose led to an increase in susceptibility to bile salts, polymyxin and novobiocin, as well as decreased flagellar mediated motility (Ho *et al*., 2008; Kondakova *et al*., 2008).

1.1.4.4   LOS

C. jejuni makes LOS, rather than LPS which is more commonly found in gram negatives. The LOS is composed of lipid A with a core oligosaccharide and no O-antigen repeat chain as found in LPS. The structure of the LOS core of strain NCTC 11168 has been determined

(Figure 4). The lipid A differs from that of *Escherichia coli* lipid A in that it contains the disaccharide 2,3-diamino-2,3-dideoxy-D-glucose and D-glucosamine (GlcN3N-GlcN), or variations of GlcN3N–GlcN3N and GlcN–GlcN, phosphorylated with pyrophosphorylethanolamine (*PP*Etn) and this is acylated with palmitic or lauric acid (Szymanski *et al*., 2003). These backbones further vary by having different phosphorylation patterns. WaaC is heptosyltransferase I that attaches the first heptose to Kdo and WaaF is heptosyltransferase II that attaches the second heptose to the first (Klena *et al*., 1998; Oldfield *et al*., 2002). As mentioned above in section 1.1.4.3, these heptoses are synthesized from the same precursor, D-sedoheptulose 7-phosphate, used to make GDP-*manno*-heptose for capsule synthesis, however, through the action of different enzymes. GmhA (phosphatase), GmhB (kinase), WaaE (pyrophosphorylase) and WaaD (epimerase) are responsible for the conversion of D-seduloheptulose7-phosphate into ADP-L-*glycero*-D-*manno*-heptose (Karlyshev *et al*., 2005a). *C. jejuni* also produces neuraminic acid (sialic acid) which is incorporated into some of the LOS chains. The outer core of the LOS of strain NCTC 11168, β-Gal-(1,3)-β-D-GalNAc-(1,4)-β[α-NeuAc-(2,3)]-Gal, is analogous to the human gangliosides GM1a and GM2 (Michael *et al*., 2002; Oldfield *et al*., 2002; Szymanski *et al*., 2003). These structural mimics lead to generation of cross-reacting antibodies against gangliosides which is the pathological basis for the association of preceding *C. jejuni* infection with GBS and MFS (Godschalk *et al*., 2007; Islam *et al*., 2012; Nachamkin *et al*., 1998; Yuki *et al*., 2004). Other strains have been shown to produce LOS mimics of other structures such as strain RM1221 which makes LOS mimics of P blood groups and paragloboside antigens and strain RM1503 which makes LOS mimics of lacto-*N*-biose and sialyl-Lewis c units, a pancreatic tumor-associated antigen (Houliston *et al*., 2011).

Figure 4. The biosynthesis and structure of the LOS of *C. jejuni* NCTC 11168.

The structure of the LOS from strain NCTC 11168, highlighting the transferases known or predicted to be responsible for addition of each sugar to the LOS core. (Adapted from Karlyshev *et al*., 2005b).

| Cj1139 (WlaN) | **CgtA**/NeuA1 | Cj1138? | Cj1136? | WaaF | WaaC |

P/*P*Etn
↓
6

β-Gal-(1→3)-β-D-GalNAc-(1→4)-β-Gal-(1→3)-β-Gal-(1→3)-L-α-D-Hep-(1→3)- L-α-D-Hep-(1→5)-Kdo

3
↑
2
α-Neu5Ac

2
↑
1
α-D-Gal

2
↑
1
β-D-Glc

4
↑
1
β-D-Glc

| Cst | Cj1137? | Cj1135? | Cj1135? |
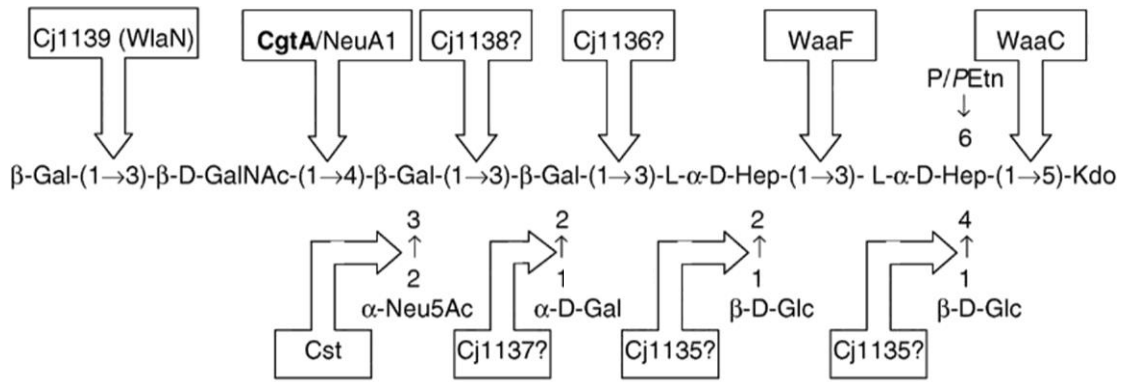
1.1.5 The role of Cj1319 in *C. jejuni*

As mentioned above, Cj1319 has predicted roles in both synthesis of a modified heptose for capsule and in legionaminic acid synthesis. The *cj1319* gene, encoding a putative sugar nucleotide dehydratase, is clustered with *cj1320* and *cj1321*, encoding a putative aminotransferase and an N-acetyl transferase respectively, which is reminiscent of the genetic arrangement of the *N-* and *O*-protein glycosylation pathways (Figure 5) (Creuzenet, 2004; Nothaft and Szymanski, 2010; Obhi and Creuzenet, 2005; Vijayakumar *et al.*, 2006). This suggests that there is a possibility that these three gene products may be part of a novel protein glycosylation pathway. Cj1319 belongs to the NDP-sugar modifying subfamily of short chain dehydrogenases/reductases which have characteristic Rossman-fold structures with helices on either side and a catalytic tetrad (N-S-Y-K) (Persson et al., 2009). Cj1319 shares similarity to the GDP-*manno*-heptose dehydratases, DmhA (45 %) and DdahA (41 %) (Ho *et al.*, 2008; McCallum *et al.*, 2011). DdahA is the first enzyme in the capsular heptose modification pathway in strain 81-176. This pathway for our strain of interest, *C. jejuni* NCTC 11168, is partially characterized, however, the enzyme initiating this pathway which is predicted to be a C4 oxidase has yet to be found (McCallum *et al.*, 2013). This oxidase role may be fulfilled by Cj1319 as C4 oxidation is also performed by C4, C6 dehydratases, whereby Cj1319 would have a central role in capsular heptose modification. Alternatively, Cj1319 may use GDP-*manno*-heptose as the precursor of a novel protein glycosylation pathway whereby its product would be further modified by Cj1320 and Cj1321. This would establish a potential link between capsule synthesis and protein glycosylation.

Cj1319 and Cj1320 have been implicated in an *in vitro* pathway for legionaminic acid synthesis for flagellar glycosylation (Schoenhofen *et al.*, 2009). In contrast, the Cj1319 and Cj1320 homologues from *C. coli* were excluded from the legionaminic acid synthesis pathway based on knockout mutagenesis and metabolic profiling (McNally *et al.*, 2007a). This contradiction remained unaddressed at onset of this work, mainly due to the lack of flagellin glycopeptide data showing that legionaminic acid is incorporated onto flagellins in *C. jejuni* and also because the effects of inactivating *cj1319* and *cj1320* have not been studied in *C. jejuni*.

Figure 5. Genetic organization of *cj1319* gene locus and the two protein glycosylation pathway genes.

N-glycosylation cluster

cj1120c   cj1121c   cj1123c

O-glycosylation cluster

cj1293   cj1294   cj1298   cj1313

cj1319 unknown cluster

cj1319   cj1320   cj1321

C4, C6 dehydratase   Aminotransferase   N-acetyltransferase
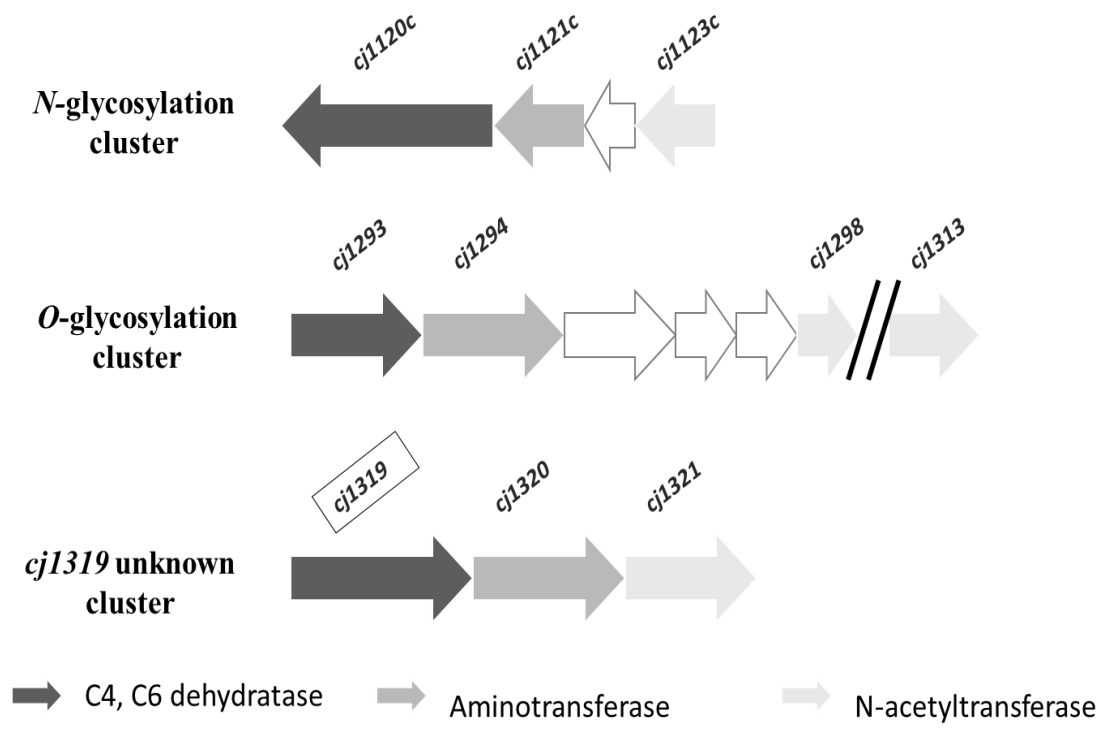
1.1.6 Host interactions

C. jejuni has long been considered a commensal colonizer of chickens, however, recently it has been demonstrated that *C. jejuni* colonization of chickens does result in inflammation and affects the well-being of the birds (Humphrey *et al*., 2014). A major difference observed between the interaction of *C. jejuni* with humans and chickens is that more bacteria invade human epithelial cells compared to those derived from chickens (Byrne *et al*., 2007; Larson *et al*., 2008; Young *et al*., 2007). The chicken intestinal mucus was shown to have an important role in inhibiting *C. jejuni* invasion of both chicken and human intestinal cells (Byrne *et al*., 2007). Thus the ability of *C. jejuni* to adhere to and invade epithelial cells is key to determine the ability of this organism to act as a pathogen or commensal. The initial interactions in the intestinal tissues are with mucins, highly sialylated and mannosylated proteins, such as MUC1 which is a decoy receptor released from the intestinal epithelium into the lumen upon binding bacteria including *C. jejuni*, and MUC2 which is significantly less sialylated compared to MUC1 and found in *C. jejuni's* favoured niche, the intestinal crypts (Linden *et al*., 2008; McAuley *et al*., 2007). *C. jejuni* was found to be able to bind to the more easily accessible fucosylated and terminal galactosylated structures found within the crypts, although no *C. jejuni* lectin has been yet identified (Day *et al*., 2009). A number of adhesins have been identified such as CadF and FlpA which have been demonstrated to bind fibronectin (Flanagan *et al*., 2009; Monteville *et al*., 2003). Whereas the importance of CadF has been demonstrated in a number of different strains and using different methods (Konkel *et al*., 1997; Scott *et al*., 2010; Ziprin *et al*., 1999), other identified adhesins, JlpA and PEB proteins have controversial roles in adherence. JlpA was described as an important adhesin (Jin *et al*., 2001), however, others were unable to show a significant defect in invasion of intestinal cells by a *jlpA* mutant (Novik *et al*., 2010). PEB proteins were also originally thought to be adhesins (Pei *et al*., 1991), however, they were found to be inner membrane proteins with transporter or chaperone roles (Del Rocio Leon-Kempis *et al*., 2006; Kale *et al*., 2011), whereby they appear to have an indirect role on cellular adherence to intestinal cells. In addition to their role in motility, the flagella have also been shown to act as a type III secretion system for

Campylobacter invasion antigens (Cia) (Konkel *et al*., 2004). However, it is not clear if the Cia proteins are secreted into intestinal cells or into the lumen. The role of the flagellar glycosylation in host cell interactions is also not clear as there still remains limited data on flagellar glycosylation in *C. jejuni* strains.

It has also been shown that *C. jejuni* pre-exposed to oxidative stress are better able to invade epithelial cells (Šikić Pogačar, 2009). However, it was recently shown that this is strain specific, as NCTC 11168 for example is unable to adhere to or invade Caco-2 intestinal cells when exposed to hydrogen peroxide (Koolman *et al*., 2016). Analysis of gene expression in 10 strains in response to hydrogen peroxide stress revealed the upregulation in *cadF* in all strains, whereas other changes in gene expression were deemed to be strain specific (Koolman *et al*., 2016). *C. jejuni* expresses a highly branched electron transport chain which allows for both aerobic and anaerobic respiration, whereby it encodes for all proteins required for a complete oxidative TCA cycle (Kelly, 2008). Aerobic respiration is preferred, however, this bacterium is also able to use alternative electron acceptors including nitrate, dimethylsulphoxide, fumarate, and tetrathionate (Liu *et al*., 2013; Pittman *et al*., 2007; Sellars *et al*., 2002). Fumarate respiration has been shown to be important for both chicken colonization and intracellular survival of *C. jejuni* (Liu *et al*., 2012b; Weingarten *et al*., 2009).

Once *C. jejuni* invades epithelial cells, it is able to avoid the lysosome and gain access to underlying tissues and reach different cellular receptors and phagocytic cells (Mihaljevic *et al*., 2007; Watson and Galán, 2008). It has been reported that *C. jejuni* can survive within macrophage for extended periods of time (6-7 days) by some (Hickey *et al*., 2005; Kiehlbauch *et al*., 1985), whereas others report this is not a common occurrence due to the finding that human derived monocytes/macrophages kill phagocytosed bacteria within 24 to 48 h, as *C. jejuni* is targeted to the lysosome in macrophages (Wassenaar *et al*., 1997; Watson and Galán, 2008). The internal survival of *C. jejuni* within phagocytes is largely believed to be strain-dependent. Within macrophages, *C. jejuni* needs to survive the reactive oxygen and nitrogen species produced by the host cell and may overcome them at least in part by the expression of catalase and nitric oxide response regulator (Day *et al*., 2000; Gundogdu *et al*., 2011; Iovine *et al*., 2008).

1.1.7 Role of biofilm formation and interaction with amoeba in survival during transmission in the environment

Unlike other foodborne pathogens, *Campylobacters* have fastidious growth requirements and lack many of the adaptive responses correlated to the resistance of different stress conditions (Park, 2002). They are highly sensitive to oxygen levels, have a limited pH and temperature range for growth, and very sensitive to osmotic stress and dryness. Conversely, these organisms are still able to survive in the environment, allowing for their transmission among different hosts which leads to the infection of humans. The mechanisms by which *C. jejuni* are able to survive outside of their hosts are still under investigation.

Under unfavourable growth conditions, *Campylobacter* spp. have been shown to enter a viable but nonculturable (VBNC) form whereby the cells maintain limited metabolic activity while retaining their spiral shape or degenerating into a coccoid form, but do not replicate and cannot be cultured (Bronowski *et al*., 2014; Murphy *et al*., 2006; Oliver, 2005; Park, 2002). There remains controversy regarding the role of this cell form, but it has been suggested that cells may maintain this form to survive unfavourable environmental conditions, and they may revert back into a replicating viable and culturable form once they enter a host.

The formation of biofilms by *C. jejuni* is an important survival mechanism still undergoing extensive study. These bacteria have been shown to be able to form biofilms in water systems, on abiotic surfaces, and in natural aquatic environments (Lehtola *et al*., 2006; Maal-Bared *et al*., 2012). *C. jejuni* has been shown to form three types of biofilm forms, including a pellicle at the liquid air interface, surface attachment, and free unattached aggregates termed 'flocs' (Joshua *et al*., 2006). Multiple studies have shown that stressful conditions, such as exposure to oxygen, detergents and bile, induce and enhance biofilm formation of *C. jejuni* (Allen and Griffiths, 2001; Reuter *et al*., 2010; Svensson *et al*., 2009, 2014). The extracellular matrix of the biofilm has yet to be fully characterized, as there have only been a few recent studies aimed at determining its composition. Some studies have demonstrated that it is composed of extracellular DNA by demonstrating its sensitivity to Dnase treatment and through the induction of the release of DNA in response

to bile which in turn induced biofilm formation (Brown *et al*., 2015; Svensson *et al*., 2014). In contrast, another study demonstrated that the *C. jejuni* can produce an α-dextran in response to pancreatic amylase and this dextran represents the exopolysaccharide (Jowiya *et al*., 2015). It is possible that both components are required to form the extracellular matrix.

Whereas *C. jejuni* encodes very limited metabolic pathways (Kelly, 2001), it has many transport systems which suggests that the potential this organism may exploit the resources produced by other organisms (Dorrell and Wren, 2007). As such, although *C. jejuni* is able to form biofilms on its own (Joshua *et al*., 2006), it has been shown that it has enhanced attachment and survival when co-cultured with *Pseudomonas aeruginosa* and has been suggested that *C. jejuni* are secondary colonizers of pre-existing biofilms sampled from poultry farm environments (Hanning *et al*., 2008; Ica *et al*., 2012; Trachoo *et al*., 2002).

The interaction of *C. jejuni* with protozoa in water has also been suggested as a mechanism for bacterial survival. It has recently been shown that amoeba deprive their local environment of oxygen, thus creating favourable respiratory conditions for surrounding *C. jejuni* (Bui *et al*., 2012a). It has also been shown that environmental stress factors promote *C. jejuni* internalization in amoeba, although the internal survival was reported to be short-lived and limited to several hours (Bui *et al*., 2012b). Other studies have shown that *C. jejuni* can survive within amoeba for several days, whereby live non-replicating *C. jejuni* were maintained in non-digestive vacuoles and heat-killed bacteria were found in one large digestive vacuole (Olofsson *et al*., 2013). To address the discrepancy found between the described studies, a modified gentamycin protection assay was performed to remove as much variability among assays as possible. The results of this study were in support of the prior studies, suggesting internalization of *C. jejuni* occurs at a very low negligible rate (Dirks and Quinlan, 2014). Furthermore, cocultures of *C. jejuni* and amoeba in unpasteurized milk and juice prolonged the survival of extracellular *C. jejuni* (Olofsson *et al*., 2015).

1.2   *Helicobacter pylori*

1.2.1 Discovery and clinical manifestion

Helicobacter pylori, originally called *Campylobacter pylori*, was regularly observed in stomach biopsies and assumed to be related to inflammation nearly 35 years ago (Marshall and Warren, 1984). Despite this, it was not accepted by the scientific community that a bacterium would be able to survive the harsh conditions of the stomach and cause disease. *H. pylori* was first isolated in 1982 and, through drinking *H. pylori* cultures which lead to the development of symptoms of gastritis that could be relieved by antibiotic treatment, Dr. Marshall was able to prove that this organism is able to cause gastritis (Marshall *et al*., 1985). This significant finding later led to Dr. Marshall and Dr. Warren, whom he worked with, being awarded the Nobel Prize in Physiology or Medicine in 2005. This pathogen is now considered the leading cause of gastric cancer and gastric ulcers and has been determined to be a class I carcinogen by the World Health Organization (Malfertheiner *et al*.,1994). It is estimated that gastric cancers caused by *H. pylori* account for ~6% of all cancers worldwide (Plummer *et al*., 2015). The prevalence of colonization is currently estimated to be 70-90% in developing countries and 25-50% in developed countries (Malfertheiner *et al*., 2014; Papamichael and Mantzaris, 2012). Colonization rates can vary drastically within countries, as observed in Canada where prevalence can range from 23% to 95% across different ethnic groups (Naja *et al*., 2007).

In order to prevent these *H. pylori* caused-illnesses, early eradication of this bacterium is the most effective method and can also reduce the risk of gastric cancer (Ford *et al*., 2014). Triple therapy was the popular method of treatment which includes two antibiotics combined with a proton pump inhibitor, however this strategy has been losing efficacy due to the increase in antibiotic resistance and thus to overcome this, quadruple therapies are being used which include an additional antibiotic (Delchier *et al*., 2014; Gatta *et al*., 2013; Ierardi *et al*., 2013; Jheng *et al*., 2015; Malfertheiner *et al*., 2012; Yang *et al*., 2014). However, both triple and quadruple therapies result in harsh side effects in a significant portion of patients (23% for sequential therapies and 46% for concomitant therapies) (Delchier *et al*., 2014; Gisbert *et al*., 2015; Jheng *et al*., 2015). A number of studies also

suggest there is a high rate of ineffective treatment (up to 67%) (Masoodi *et al*., 2015). Other efforts have been put into combining probiotics with the above treatments in which some probiotics have been deemed to possibly improve the efficacy of treatment and reduce some of the negative side effects associated with treatments (McFarland *et al*., 2015). Efforts are being put into finding novel treatments other than antibiotic therapy that would specifically target *H. pylori* and eradicate it with minimal side effects.

1.2.2 Flagella and other protein glycosylation

As in *C. jejuni,* the *H. pylori* flagella are made of the two subunits FlaA and FlaB at a ratio of 10 to 1 respectively (Josenhans *et al*., 1995). FlaA is required for motility whereas FlaB only enhances motility since a *flab* knockout mutant was found to have impaired motility (30-40% reduction compared to WT). The flagella of a number of *H. pylori* strains have been shown to be *O*-glycosylated with pseudaminic acid (Josenhans *et al*., 2002; Merkx-Jacques *et al*., 2004; Schirm *et al*., 2003, 2005). The glycosylation has been shown to be required for motility, however, since the flagella are sheathed, the sugars are not exposed to the host and thus it is not apparent that they play a role in host interaction (Geis *et al*., 1993; Merkx-Jacques *et al*., 2004). The sheath is composed of outer membrane (Geis *et al*., 1993), thus contains both outer membrane proteins and LPS. The role of this sheath is not yet well understood, however, it is believed that it may provide a protective barrier for the flagella, shielding them from the acidic pH of the stomach and preventing depolymerization of the FlaA and B subunits, shield the antigenic properties of the flagella, as well as aid in adhesion as some outer membrane protein adhesins are found in the sheath.

Our group identified other glycoprotein candidates through selective biotin-hydrazide labelling of sugars and detection with fluorescently-labelled streptavidin via Western blot, in addition to extracting the sugars from glycoproteins and analyzing them by MS (Hopf *et al*., 2011). These findings were confirmed by another group who used selective azide-labelling of glycoproteins (by supplementing *H. pylori* growth media with azide-labelled free sugars) in conjunction with Staudinger ligation of a FLAG-His-tag to azide-labelled sugars to purify glycoproteins. β-elimination was used to release *O*-linked sugars and these proteins were analyzed by mass spectrometry (Champasa *et al*., 2013). By doing so, 125

O-linked glycoproteins were identified through the detection of Staudinger-glycan ligation adducts which were released only after β-elimination. These proteins localized to different parts of the cell and are of diverse biological function, some with roles in pathogenesis. Of these glycoproteins, only the urease proteins UreA and UreB were validated biochemically. Urease is an important virulence and colonization factor which is secreted by *H. pylori* to cleave urea and neutralize the local environment in the stomach to provide a favourable niche for *H. pylori* to persist within (Eaton *et al*., 1991; Scott *et al*., 1998). Urease also functions to raise the pH of the periplasm, increase the membrane potential, and induce protein synthesis at acidic pH (Scott *et al*., 1998).

1.2.3   Lewis mediated host mimicry of LPS as a virulence factor

1.2.3.1   Lewis-containing O-antigen and host mimicry

Gram-negative bacteria are unique in that they express LPS which cover ~75% of their cell wall (Lerouge and Vanderleyden, 2002). These negatively charged structures, composed of lipid A, a core oligosaccharide and a variable O-antigen repeat chain, provide a permeability barrier to large negatively charged and/or hydrophobic molecules and contribute to the structural properties of the cell envelope. The *H. pylori* LPS is unique in that its O-antigen is composed of host-related Lewis blood group antigens, carbohydrates that are also expressed by the gastric epithelium in humans (Figure 6). Lewis y (Le^y) and Lewis x (Le^x) are the predominant Lewis antigens expressed in *H. pylori* clinical isolates (80-90%) (Heneghan *et al*., 2000; Marshall *et al*., 1999; Simoons-Smit *et al*., 1996; Wirth *et al*., 1996). In humans, Le^y and Le^x are tumour-associated markers and these antigens and their derivatives can interact with selectins, mediating cell-to-cell adhesion (Hakomori, 1992). This pathogen also expresses other related antigens at a lower frequency including Lewis a, Lewis b, Lewis c, sialyl-Le^x and H-antigens (Monteiro *et al*., 1998, 2000, 2000). Lewis b, found on gastric epithelial cell surfaces, is an acceptor for the attachment of *H. pylori* (Borén *et al*., 1993)*.* The expression of these Lewis O-antigens by *H. pylori* is a mechanism of molecular mimicry, which has two function in pathogenesis. *H. pylori* can protect itself from recognition by the host immune system and thus aid in its prolonged persistence in the host, however, upon recognition by the immune system over time, the

formation of antibodies towards these antigens results in auto-antibodies towards the Lewis expressing gastric epithelium and thus resulting in inflammation (Appelmelk *et al.*, 1996, 1997; Moran *et al.*, 1996; Negrini *et al.*, 1996).

Figure 6. Diagramatic representation of the Lewis antigens *O*-glycosylating gastric mucins.

Lewis antigen structures highlighting the different compositions and linkages of the glycans. Le^x, Le^y and H-type antigens are also expressed by *H. pylori* (Adapted from Juge, 2012).
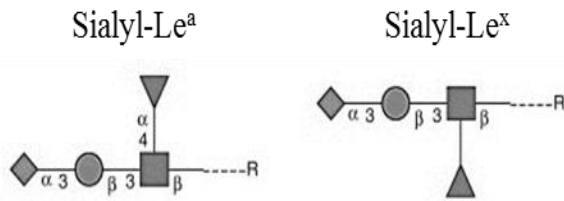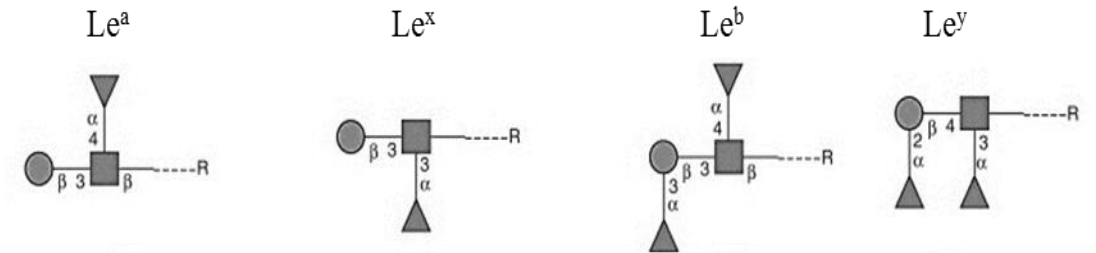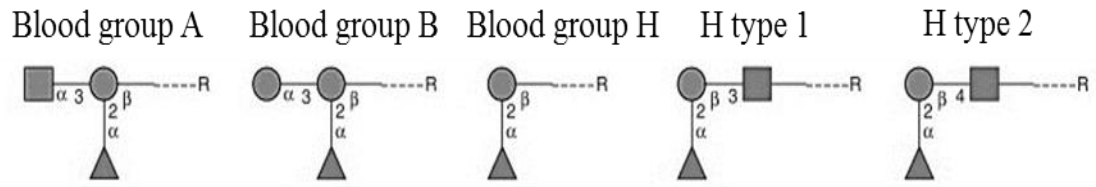
Blood group A   Blood group B   Blood group H   H type 1   H type 2

Le^a   Le^x   Le^b   Le^y

Sialyl-Le^a   Sialyl-Le^x

Key:

▲ Fuc   ● Gal   ▢ GalNAc   ▪ GlcNAc   ◆ Neu5Ac

Le^y and Le^x are made by the addition of fucose onto Galβ1-4GlcNAc repeat units of the O-antigen chain (Wang *et al*., 2000). Three fucosyltransferases, FutA, B and C, are responsible for O-antigen biosynthesis. FutA and B have α 1,3 and α 1,4 fucosyltransferase activity for the synthesis of Le^x and Le^a antigens respectively. FutC is a α 1,2 fucosyltransferase that adds an additional fucose to form Le^y and Le^b antigens respectively (Ma *et al*., 2006; Moran, 2008). *H. pylori* uses the mechanism of slipped-strand mispairing to yield the different LPS variants due to the presence of long stretches of C-residues at the ends of the three genes encoding each of the three fucosyltransferases described (Appelmelk *et al*., 1999; Wang *et al*., 1999). In addition, both FutA and B contain molecular rulers depicted as heptad repeats of DD/NLRV/INY, whereby the number of these repeats reflects the number of Galβ1-4GlcNAc repeat units that become fucosylated (Nilsson *et al*., 2006). The length of the chains has also been shown to be affected by the environment and different cells within the same bacterial population can have varying O-antigen chain length as well as different O-antigen types (Appelmelk *et al*., 1999; Nilsson *et al*., 2006, 2008). The expression of Le^y and Le^x is influenced by both pH and iron concentrations as well as location in the gastric tissue (Keenan *et al*., 2008; Moran *et al*., 2002; Nilsson *et al*., 2006; Skoglund *et al*., 2009). *H. pylori* is able persist in colonization by expressing different LPS variants that bind to DC-SIGN of dendritic cells which leads to modulation of the host T-helper cell immune response (Bergman *et al*., 2004; Skoglund *et al*., 2009).

1.2.3.2 General assembly of LPS

LPS biosynthesis in *H. pylori* follows a novel mechanism compared to that of other gram negatives (Hug *et al*., 2010). The pathway involves glycosyltransferases, a flippase, and an O-antigen ligase (Figure 7). WecA is responsible for initiating the pathway by transferring a GlcNAc-phosphate from UDP-GlcNAc to UndP. Next a number of glycosyltransferases, GalT, GlcNAcT and FucTs, assemble the O-chain by addition of galatose, GlcNAc and fucose respectively to UndPP-GlcNAc. As described above, the fucosyltransferases expressed govern the degree of fucosylation which leads to the determination of the O-antigen Lewis type. The flippase Wzk, which is homologous to protein *N*-glycosylation

flippases, translocates the UndPP-O-antigen chain to the periplasm. This chain is then ligated to the lipid A-core oligosaccharide through the O-antigen ligase WaaL.

Figure 7. LPS biosynthesis pathway in *H. pylori*

The *H. pylori* O-antigen chains are assembled in the cytoplasm onto a polyisoprenoid membrane anchor. O-antigen synthesis is initiated by the UDP-GlcNAc transferase WecA. Glycosyltransferases (GalT and GlcNAcT) alternately add Gal and GlcNAc residues, producing the linear O chain backbone. Fucosyltransferases (FucTs) attach fucose residues on selected locations of the O-antigen backbone, generating Lewis antigens. The flippase, Wzk, transfers the O-polysaccharide to the periplasm, where it is attached onto the lipid A-core via the O-antigen ligase WaaL. The LPS molecule can then be transported to the outer leaflet of the *H. pylori* outer membrane by Lpt proteins. (Adapted from (Hug *et al.*, 2010)).
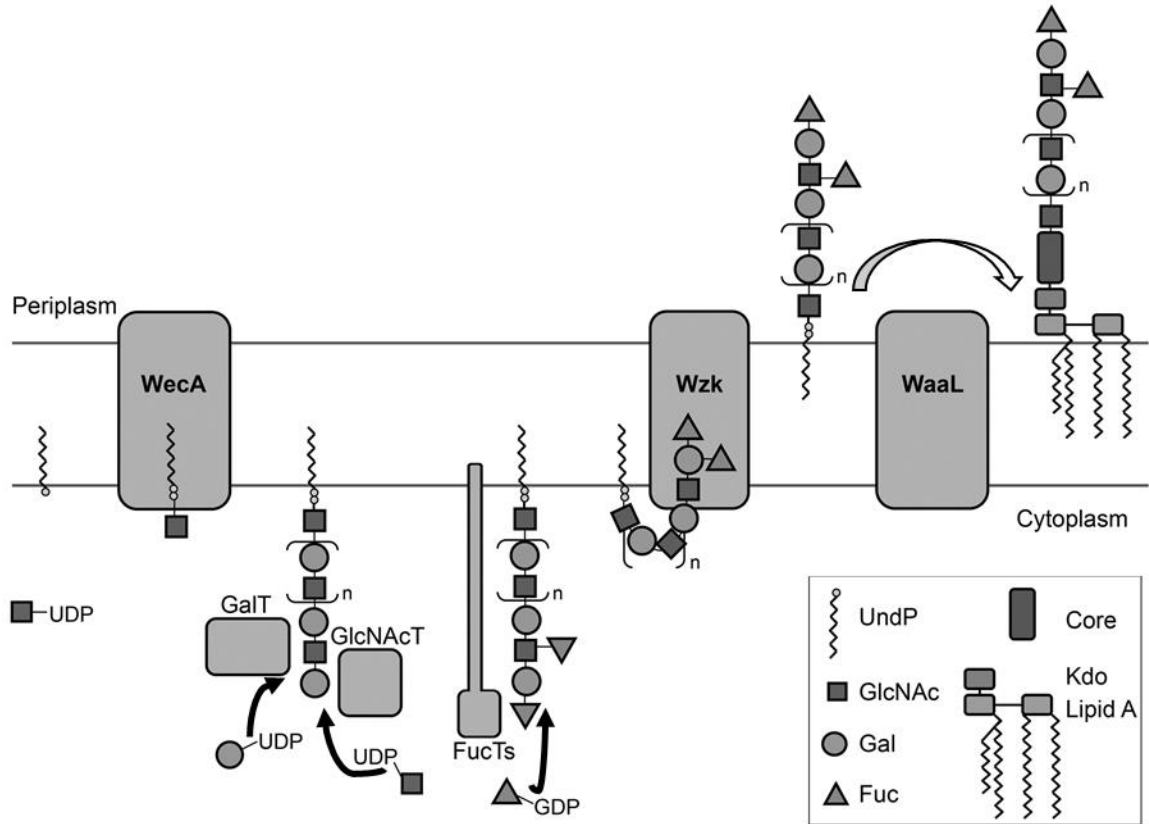
1.2.4 Adhesins

Three major outer membrane adhesins expressed by *H. pylori* bind to glycoconjugates of the gastric mucus layer and epithelial cells (Magalhães *et al*., 2010; Rossez *et al*., 2014). BabA is a blood group binding adhesin which recognizes Lewis b blood group antigens expressed in glycoproteins from the gastro-intestinal tract (Ilver *et al*., 1998; Magalhães *et al*., 2009). SabA is a sialic acid binding adhesin which recognizes α 2,3-sialylated structures including sialyl-Lewis a and sialyl-Le^x found on glycosphingolipids and glycoproteins (Mahdavi *et al*., 2002). Most recently, the adhesin LabA has been discovered which adheres to di-*N*-acetyllactosamine motifs found on the MUC5AC gastric mucin (Rossez *et al*., 2014). All three adhesins function through recognition of sugar motifs and this glycan-mediated adhesion has been shown to act as an important trigger for translocation of several virulence factors into host cells as specifically found in the case of BabA (Ishijima *et al*., 2011). These factors include CagA and peptidoglycan which modulate the host signaling NF-κB and NOD1 pathways respectively (Brandt *et al*., 2005; Viala *et al*., 2004).

1.3   Relationship between protein glycosylation and LPS synthesis

Bacterial protein *O*-glycosylation and LPS biosynthesis are evolutionarily related. This stems from the conserved Wzy_C domain for substrate recognition that is found in both OTases and *O*-antigen ligases (Power *et al*., 2006; Qutyan *et al*., 2007). The link between the two glycosylation processes was first shown in *Pseudomonas aeroginosa* 1244 whereby pili were demonstrated to be glycosylated with a single O-antigen unit from the LPS through the action of PilO, an OTase distinct from the O-antigen ligase WaaL which is also present in this bacterium (Castric *et al*., 2001; DiGiandomenico *et al*., 2002). The OTase of *C. jejuni,* PglB, is used for the transfer of the heptasaccharide for protein *N*-glycosylation but has relaxed substrate specificity such that it can transfer O-antigen of LPS from *E. coli* and *P. aeruginosa* to proteins (Feldman *et al*., 2005). The capsule units of *Acinetobacter baumaunnii* have been shown to glycosylate some proteins (Lees-Miller *et al*., 2013). It is possible that the link between protein glycosylation and capsule or LPS

synthesis is a more common phenomenon and occurs in other bacteria including *C. jejuni* and *H. pylori*.

1.4 Protein glycosylation analysis

Protein glycosylation is the most common and complex post-translational modification as the process of glycosylation is a non-template driven process that relies on the action of many enzymes without any proofreading machinery (Lisowska and Jaskiewicz, 2001). The synthesis of the final glycosylation products relies on several factors including the availability of the sugar substrates and the production of the enzymes required for biosynthesis and transfer of the glycan onto a protein which may be expressed at different growth stages (Raman *et al*., 2005). These factors allow for several magnitudes of structural heterogeneity of the glycan and the glycosylation of the recipient protein. The selectivity of certain proteins for certain glycans relies majorly on the sugar substrate specificity of the glycosyltransferase and whether this enzyme attaches sugars to serine/threonine or asparagine residues (Ielmini, 2011; Lundborg, 2010). Furthermore, asparagine residues need to be within a minimum consensus sequence of N(X)S/T (X≠P) for *N*-glycosylation in eukaryotes (Bause, 1983). This sequence was thought to be extended to D/E-Y-N-X-S/T (Y, X≠P) in bacteria, however, this is not true in most cases (Kowarik *et al*., 2006; Nita-Lazar *et al*., 2005; Schwarz *et al*., 2011b). Glycosylation sites are restricted even more based on their accessibility to the glycosyltransferase which is governed by the glycoprotein's structure (Slynko *et al*., 2009; Zielinska *et al*., 2010). These factors aid in analysis of glycoproteins and predicting sites of glycosylation.

1.4.1 Challenges of glycoprotein analysis

There are several challenges for glycoprotein analysis which have largely lead to the slow progression of the glycoproteomics field. Bacteria produce unconventional sugars synthesized through complex sugar pathways. This heterogeneity likely contributes to immune evasion due to the structural diversity provided by the glycosylation. Bacteria produce more simple glycan structures compared to eukaryotes which use limited types of

well-known conventional sugars (including mannose, fucose, galactose, N-acetylglucosamine and N-acetylgalactosamine) to form large complex glycan chains (Stanley *et al*., 2009). More than 70% of eukaryotic proteins are estimated to be glycosylated, whereas in bacteria, it is not currently known what the extent of protein glycosylation is, though it is now thought to be a normal occurence rather than a rare event (Dell *et al*., 2011). The large size of the glycan, low abundance of many glycoproteins, the poor ionization of glycoproteins and glycopeptides in mass spectrometers, the size of some glycans (particularly eukaryotic glycans), the branched nature of glycan chains and the heterogeneous nature of glycosylation all contribute to the difficulty in glycoprotein analysis (Liu *et al*., 2014). These factors lead to poor detection of glycoproteins by mass spectrometry, the gold standard for glycopeptide characterization, and thus a number of strategies have been employed to overcome this problem.

1.4.2 Strategies to simplify and improve the analysis of glycoproteins

In order to simplify glycoprotein analysis, many studies have used the strategy of deglycosylation of glycoproteins either chemically or enzymatically (Edge, 2003; Wilson *et al*., 2002). Upon deglycosylation, the deglycosylated peptides and released sugars/glycans are analyzed separately by mass spectrometry. To facilitate the sugar analysis, the sugars are typically derivatized by permethylation or other stabilizing signature tags (Morelle and Michalski, 2007). The information from the peptide and sugars are combined to infer the glycosylation of the protein from which these glycopeptides were released. This approach is lacking in its ability to demonstrate unarguably that the sugars detected were indeed linked to the peptide identified as no linkage information is produced. Other approaches focus on methods for glycoprotein/glycopeptide enrichment to increase their detection by mass spectrometry. Enrichment methods may be targeted toward certain glycoproteins, whereby lectins with specific sugar binding preferences may be used (Ongay *et al*., 2012). Other untargeted methods make use of the hydrophilic nature of the sugars on proteins which allows their enrichment through reverse phase chromatography (Calvano *et al*., 2008; Scott *et al*., 2011; Yu *et al*., 2009). It is also possible to label sugars with a number of tags, for example with biotin hydrazide based on a Schiff-base reaction

after oxidation that specifically labels sugars (Ruhaak *et al*., 2010). Affinity chromatography targeting the incorporated tags can then be used to purify the glycoproteins/glycopeptides.

1.4.3 Mass spectrometry analysis of glycoproteins and glycopeptides

Mass spectrometry is considered the gold standard for glycoprotein analysis, whereby this technique allows for the determination of the identities of the protein and sugar(s) in addition to being able to map the site(s) of glycosylation. There are two methods of MS analysis for proteins including glycoproteins: 'top-down' and 'bottom-up' (Chait, 2006). Top-down MS describes the fragmentation of intact glycoproteins by MS and tandem MS (MS^2), providing protein sequencing ladders and *in situ* localization of the glycosylation without prior extensive separation or proteolytic digestion (Hanisch, 2011; Schirm *et al*., 2005). This method has been applied to studying the glycosylation of flagellins of some bacterial pathogens (Schirm *et al*., 2005). The bottom-up MS approach is the most widely used strategy for glycoprotein analysis which differs from the top-down approach in that it requires extensive preprocessing of samples prior to MS analysis, including proteolytic digestion and chromatography techniques (Zhang *et al*., 2013). The glycoproteins may be chemically or enzymatically deglycosylated and the resulting peptides and sugars can be analyzed as described above. Alternatively, and more popular with recent MS advances, the glycoproteins can be treated with a protease and the resulting glycopeptides may be enriched if needed and analyzed by MS directly in order to simultaneously obtain peptide, sugar, and glycosylation site information.

Two major ionization technologies are employed for glycoprotein and glycan analysis: electrospray (ESI) and matrix-assisted laser desorption ionization (MALDI) (Han and Costello, 2013). ESI is able to generate multiply charged ions of glycopeptides, which is advantageous when studying intact glycoproteins although increasing the complexity of the data generated. Furthermore, ESI can be coupled with liquid chromatography (LC) which allows for online LC-MS analysis. The advantage in MALDI is that it generates singly charged species when analyzing glycoproteins which simplifies the analysis.

Derivatization of the glycan by permethylation, for example, can help stabilize the labile glycosidic bonds and aid their detection when using either ionization type.

Different mass analyzers are used for the analysis of glycoproteins, including the orbitrap and Fourier transform ion cyclotron resonance (FT-ICR) mass spectrometers which are now commonly used for glycoprotein analysis (Han and Costello, 2013; Patrie *et al*., 2013; Zhou and Håkansson, 2011). The FT-ICR-MS has the highest mass accuracy and ultrahigh resolution, but comes at a high monetary cost. The orbitrap also has ultrahigh resolution and is compatible with LC and can be used for three different fragmentation modes including collision-induced dissociation (CID), higher collision-induced dissociation (HCD), and electron transfer dissociation (ETD). Orbitraps have been combined with linear ion traps for the analysis of glycoproteins, whereby the MS occurs in the linear ion trap and MS^2 is set up to take place in the orbitrap, thus leading to rapid and accurate mass detection of peptide and sugar fragments (Ye *et al*., 2013).

1.4.3.1 Fragmentation methods

In CID, the peptide ions are accelerated by an electrical potential to high kinetic energy and then collided with neutral molecules (helium, nitrogen or argon) (Mitchell Wells and McLuckey, 2005). Some of the kinetic energy is converted into internal energy which results in bond breakage and ions are detected in the linear ion trap. In HCD, peptide ions are injected into a collision cell and fragment ions are then analyzed by an orbitrap analyzer where more accurate mass/charge (m/z) for the fragment ions can be measured (Olsen *et al*., 2007). Peptide fragmentation patterns and nomenclature of fragment ions are represented in Figure 8. Two types of fragment ions, b- and y-ions (peptide fragments originating from sequential losses of amino acids from the C- and N-terminus respectively), are frequently observed in MS^2 spectra obtained by CID and HCD fragmentation. Glycosylation typically decreases the fragmentation efficiency of peptide backbones when these fragmentation methods are used. As the collision energy is mostly absorbed by the glycan, glycosidic bonds usually break first, leading to inefficient peptide bond breakage if any. This results in different fragmentation patterns of glycopeptides compared to their non-glycosylated counterparts. This issue has been resolved through the use of HCD, which supplies sufficient energy for peptide bond breakage even in the presence of a glycan

and also results in the release and detection of sugar oxonium ions which are signatures of sugar release (Olsen *et al*., 2007). HCD can be used to map glycosylation sites as has been demonstrated in the case of peptides modified by GlcNAc (Segu and Mechref, 2010).

On the other hand, ETD produces fragment ions dominantly by breaking peptide bonds while the glycan/sugar or other post-translational modification remains attached (Kim and Pandey, 2012; Mikesh *et al*., 2006). Electrons are transferred to a multiply protonated peptide or protein, or radical cations are generated in the case of a multiply protonated peptide or protein, which leads to the cleavage of the N–Cα backbone bonds to generate c- and z-ions (Figure 8) (Syka *et al*., 2004).

Figure 8. Peptide fragmentation pattern and nomenclature of major ions formed by mass spectrometry.

Nomenclature is based on the Roepstorff Nomenclature Scheme (Roepstorff and Fohlman, 1984). Fragment ions arising from the charge being retained on the N-terminus are denoted as a, b, and c. Fragments arising from the charge being retained on the C-terminus are denoted as x, y, and z. (Adapted from Maleknia and Johnson, 2011).

A

x_3 y_3 z_3 x_2 y_2 z_2 x_1 y_1 z_1

H^+

R1 O   R2 O   R3 O   R4

$H_2N-C-C-N-C-C-N-C-C-N-C-COOH$

H   H H   H H   H H   H

a_1 b_1 c_1 a_2 b_2 c_2 a_3 b_3 c_3

B

R1 O   R2

$H_2N-C-C-N^+-C-$

H   H H

a_2

R3 O   R4

$O{\equiv}C-N-C-C-N-C-COOH$

H H   H H

x_2

R1 O   R2

$H_2N-C-C-N-C-C{\equiv}O^+$

H   H H

b_2

R3 O   R4

$H_2N^+-C-C-N-C-COOH$

H   H H

y_2

R1 O   R2 O

$H_2N-C-C-N-C-C-NH_3^+$

H   H H

c_2

R3 O   R4 H^+

$-C-C-N-C-COOH$

H   H H

z_2
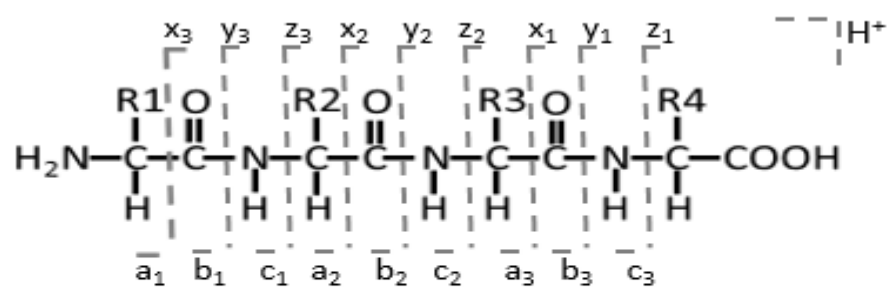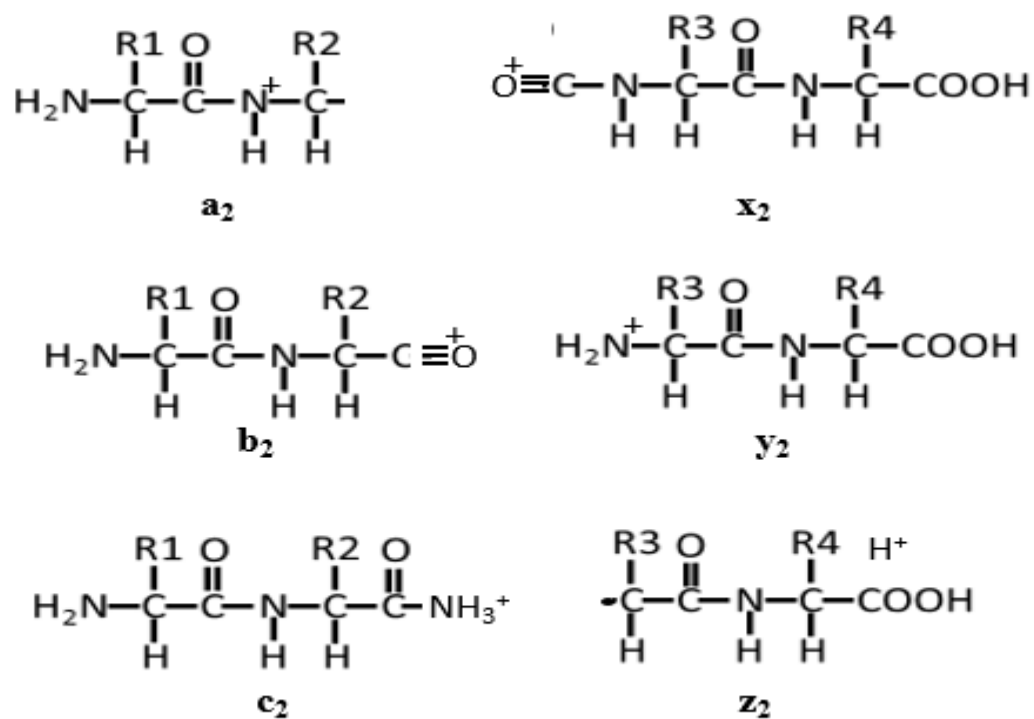
1.4.3.2   Data analysis

Once the raw spectral data is generated by the mass spectrometer, the data can be analyzed using specialized software in order to determine peptide sequences and their protein origin. Database search and *de novo* sequencing are the two mainly used computational approaches for spectral data interpretation, whereby the major difference between the two approaches is the requirement of protein databases. In the first approach, the protein sequences in a protein database are digested *in silico* to generate peptides, then an MS^2 spectrum is compared with each possible peptide to calculate a peptide-spectrum match (PSM) score, a calculated measurement of the similarity between a peptide and a spectrum. The peptide from the database with the top PSM score is determined to match the MS^2 spectrum. As protein databases do not incorporate post-translational modification (PTM) data, database searching misses the identification of modified peptides. *De novo* sequencing is a recent advance in spectral analysis which constructs the peptide sequence directly from an MS^2 spectrum, thus it is often used for novel protein identification. *De novo* searches all amino acid combinations to find the optimal peptide sequence. PEAKS and PepNovo are two state-of-the-art de novo software tools (Frank and Pevzner, 2005; Ma, 2003). Accurate *de novo* sequencing, accompanied by different enzymatic digestions, has been proven to be able to calculate the whole sequence for a purified protein sample (Liu *et al.*, 2009). However, the accuracy of the peptide sequence obtained from *de novo* sequencing approaches is often lower than the one obtained from database search approaches, although the two combined approaches have resulted in superior results than either alone (Zhang *et al.*, 2012). PEAKS software also allows to search for fixed or variable PTM modifications whose corresponding mass can be manually inputted by the user to facilitate analysis of modified peptides.

1.4.4   Mass spectrometry analysis of *C. jejuni* flagellins

A detailed description of *Campylobacter* flagellin glycosylation is presented here as an example of bacterial glycoprotein analysis where a combination of the various MS methods described above needed to be implemented to overcome the challenges presented by the complex and highly heterogeneous flagellin glycosylation. This information is imperative to the understanding of the work presented in sections 3.3.5 and 3.3.6.

The glycopeptides of *C. jejuni* 81-176 flagellins have been mapped (Thibault *et al.* 2001), whereby 19 of the 107 Ser/Thr residues were shown to be O-glycosylated with Pse5Ac7Ac, Pse5Ac7Am, Pse5Ac7Ac8OAc, and Pse5Pr7Pr (Table 1). The glycopeptides of *C. coli* VC167 flagellins have been mapped by MS and contain both Pse5Ac7Ac (316.127 Da) and its acetamidino derivative, Pse5Ac7Am (315.143 Da), and two unknown sugars with masses 431 Da and 432 Da (Table 1) (Logan *et al.*, 2002). Additionally, it was shown by metabolome analysis that this bacterium makes CMP-legionaminic acid (CMP-Leg5Ac7Ac), its acetamidino derivative (CMP-Leg5Am7Ac), and a N-methylacetimidoyl derivative (CMP-Leg5AmNMe7Ac). This was the first report of legionaminic acid being produced in *Campylobacter* (McNally *et al.*, 2007a), but it was not known whether these legionaminic acid derivatives contributed to flagellin glycosylation in *C. jejuni*. Interestingly, many chicken, bovine, and ovine livestock isolates of *C. jejuni* encode the putative legionaminic acid synthesis cluster derived from *C. coli* analyses, including strain NCTC 11168 (Champion *et al.* 2005).

Early attempts at characterizing the flagellin glycopeptides of *C. jejuni* NCTC 11168 were unsuccessful (Thibault *et al.* 2001), but metabolomics data indicate that this strain makes CMP-linked Pse5Ac7Ac, Pse5Ac7Am, two dimethylglyceric derivatives of pseudaminic acid (Pse5AcGriMe7Ac, 390.164 Da and Pse5AcGriMe7Am, 389.180 Da), and, consistent with the presence of the putative legionaminic acid synthesis gene cluster, it also makes CMP-linked Leg5Ac7Ac (316.127 Da), Leg5Am7Ac (315.143 Da) and Leg5AmNMe7Ac (329.159 Da) (Table 1) (Logan *et al.* 2009). Pse5AcGriMe7Ac and Pse5AcGriMe7Am were further shown to glycosylate flagellins in two independent studies, one identifying two peptides (residues 203-222 and 463-479), although the precise glycosylation sites were undetermined (Logan *et al.*, 2009), and the other showing that S_{181} and S_{207} were each modified by Pse5AcGriMe7Ac or Pse5AcGriMe7Am and that T_{465} or T_{464} was modified by Pse5AcGriMe7Am (Zampronio *et al.* 2011). It is also important to note that the 5AcGriMe7Ac and 5AcGriMe7Am modifications are unique to pseudaminic acid and have not been found associated with legionaminic acid to date, and thus can be used to unambiguously show that pseudaminic acid is glycosylating the flagellins. No glycopeptide evidence of flagellin modification by legionaminic acid was demonstrated in these studies. This is because pseudaminic acid and legionaminic acid are both structurally

related to sialic acid and have the same mass (Table 2) and cannot be distinguished by mass spectrometry, preventing assignment of either legionaminic acid or pseudaminic acid to flagellin glycopeptides based on detection of their oxonium ions. The same problem applies to their acetamidino derivatives. In contrast, the 5AmNMe7Ac modification has only been found associated with legionaminic acid and not with pseudaminic acid to date, which allows assignment of legionaminic acid to the flagellins upon detection of the unique oxonium ion of Leg5AmNMe7Ac at m/z 330.167 during glycopeptide analysis. This principle was used to demonstrate by top-down MS that the *C. coli* flagellins are indeed modified by legionaminic acid (McNally *et al.* 2007).

Very recently, improved methodology allowed a more thorough characterization of the flagellin glycopeptides (Ulasi *et al*., 2015). The use of collision induced dissociation (CID) and electron capture dissociation (ETD) with high field asymmetric waveform ion mobility spectrometry (FAIMS), combined with either trypsin or proteinase K treatment, resulted in detection of multiple glycopeptides within the amino acid region 387 to 463 of flagellin A. This highly glycosylated region had been missed in previous work. Overall 16 glycosylation sites were identified in addition to those found in the previous studies, several of them presenting a high level of heterogeneity in glycosylation. However, even in this study, no glycopeptide evidence showing specifically the presence of legionaminic acid via the unique 329.159 Da Leg5AmNMe7Ac modification was obtained. The reported presence of legionaminic acid was only based on detection of ions that are common to pseudaminic and legionaminic acids. Thus the presence of legionaminic acid on flagellins of *C. jejuni* NCTC 11168 remained hypothetical. Recently, as a result of the work presented in this dissertation (Section 3.3.5), legionaminic acid was conclusively found to glycosylate the flagellins of this strain (Zebian *et al*., 2015).

Table 2. Monoisotopic and oxonium ion masses of sugars produced by *C. jejuni* NCTC 11168 based on metabolome analysis (Logan *et al*., 2009).

Sugars	Monoisotopic Mass (Da)	Oxonium Ion Mass (Da)
Pseudaminic acid OR Legionaminic acid (Pse5Ac7Ac OR Leg5Ac7Ac)	316.127 ▲	317.136 ▲
Acetamidino pseudaminic acid OR Acetamidino legionaminic acid (Pse5Ac7Am OR Leg5Am7Ac)	315.143 ⬡	316.151 ⬡
Dimethylglyceric derivative of pseudaminic acid (Pse5AcGriMe7Ac)	390.164 ⬠	391.172 ⬠
Dimethylglyceric derivative of acetamidino pseudaminic acid (Pse5AcGriMe7Am)	389.180 ◆	390.188 ◆
N-methylacetimidoyl derivative of Legionaminic acid (Leg5AmNme7Ac)	329.159 ✦	330.167 ✦

1.5   Rationale and hypothesis

As discussed, *C. jejuni* NCTC 11168 has several glycosylation pathways that have been extensively studied. However, there are still missing links in these pathways, including the OTases for flagellin glycosylation, and many genes within the annotated glycosylation islands are of yet unknown functions. Cj1319 is a putative sugar nucleotide dehydratase which has potential roles in both protein glycosylation and capsule synthesis.

In *H. pylori*, we and others have shown that novel glycoproteins other than the well characterized flagellin glycoproteins exist (Champasa *et al*., 2013; Hopf *et al*., 2011). Additionally, the pathway for LPS synthesis has been recently deciphered and signifies an evolutionary connection between *N*-protein glycosylation and LPS biosynthesis (Hug *et al*., 2010). Combined with the fact that the *H. pylori* LPS O-antigen represents human Lewis blood group mimics and this O-antigen has an important role in both host evasion and immune modulation through molecular mimicry, it would not be surprising if *H. pylori* used these host mimicking structures for protein glycosylation as well.

Based on the above, we **hypothesize** that there are links between the machineries used for glycosylation of lipids and proteins in *C. jejuni* and *H. pylori,* whereby the sugar precursors of glycolipids or O-units can serve for protein glycosylation to generate glycoproteins that have not been identified to date. These novel glycoproteins may have important roles in virulence and would also contribute to the heterogeneity of glycosylated structures found on the cell surface.

To address this **main hypothesis**, we have **two major objectives**. Our first goal is to investigate a relationship between capsule synthesis and protein glycosylation in *C. jejuni* through the study of the enzyme Cj1319, a sugar nucleotide dehydratase, which has predicted roles in both protein glycosylation and capsule synthesis. We also aim to determine the contribution of this enzyme and its predicted glycosylation pathway in colonization and virulence. Secondly, our purpose is to show that *H. pylori* can glycosylate proteins with the O-antigen of its LPS by MS analysis of glycoprotein candidates to show that their glycopeptides contain O-antigen in addition to identifying the glycosylation site(s).

In **chapter 3** of this thesis, **sections 3.1-3.4** aim to examine the role of Cj1319 in *C. jejuni* and its contribution to colonization and virulence. Our **hypothesis** is Cj1319 is sugar nucleotide dehydratase participating in a novel protein glycosylation pathway with a link to capsule modified heptose synthesis through the use of a common precursor and contributes to the virulence of *C. jejuni* NCTC 11168. To address this specific hypothesis, we have three main objectives:

1) **To determine the enzymatic function of Cj1319 by determining its substrate and product.**

   Determining the enzymatic function of Cj1319 is a key piece of information that will aid greatly in determining which glycosylation pathway(s) this enzyme functions within. We assessed its activity on GDP-*manno*-heptose to determine if it has a role in capsular heptose modification or if it shares the said precursor of this pathway. Additionally, we tested its activity on GDP-mannose, as there is functional similarity between heptose and hexose modifying enzymes. We controlled positively for its activity using GDP-GlcNAc which was described as the substrate of Cj1319 within the *in vitro* legionaminic acid synthesis pathway (Schoenhofen *et al*., 2009).

2) **To show legionaminic acid decorates WT flagellins and investigate its presence in the *cj1319::CAT* mutant to determine if Cj1319 is involved in legionaminic acid synthesis.**

   Here we address the controversial role of Cj1319 in legionaminic acid synthesis through mass spectrometry analysis of flagellin glycopeptides from the WT, a *cj1319::CAT* mutant, and its complemented strain. Since limited flagellin glycopeptide data was available for our strain of interest at the onset of our work and legionaminic acid was only implied but not demonstrated to glycosylate the flagellins of *C. jejuni*, we performed a comprehensive flagellin glycopeptide analysis using LC-HCD-MS[2] with an emphasis on determining the presence of legionaminic acid on the flagellins of our strains.

3) **To determine phenotypes associated with the *cj1319::CAT* mutant to shed light on its biological activity.**

In order to understand the importance of Cj1319 and the role of the glycosylation pathway this enzyme may participate in on *C. jejuni* and on its interactions with host cells, we examined the composition of the capsule and LOS of *cj1319::CAT* mutant, in addition to this mutant's glycoprotein profile compared to WT. We further investigated functions of *C. jejuni* that are affected by glycosylated structures including motility. In addition, we studied the interaction of the WT and our mutant strain with several eukaryotic cells. Lastly, we examined the role of Cj1319 *in vivo,* specifically in chicken colonization and infection in an insect model.

Chapter 3, section 3.5 aims to identify a novel glycoprotein from *H. pylori* NCTC 11637 that is modified by a Lewis O-antigen. **We hypothesize** that *H. pylori* synthesizes the O-antigen Le^y for protein glycosylation, specifically for outer membrane proteins which can interact with the host, in addition to incorporation into its LPS. For this we have **three specific objectives:**

1) **To isolate Le^y-modified peptide candidates from outer membranes.**

Previous preliminary data from our laboratory indicates that at least one Le^y-modified protein is found in the outer membrane. Since the outer membrane proteins copurify with LPS by ultracentrifugation during cell fractionation, we trypsinolyzed the outer membranes to release soluble peptides and glycopeptides into the supernatant. These peptides were passaged through a fucose binding lectin column to enrich for Le^y containing peptides.

2) **To analyze glycopeptides by mass spectrometry for the Le^y modification.**

In order to identify the Le^y-modified protein, we analyzed the peptide samples with LC-HCD-MS^2. Upon identification of the glycopeptide, we continued to analyze the sample with LC-CID/ETD-MS^2 in order to map the glycosylation site(s).

3) **To verify Le^y-modified glycoproteins identified by mass spectrometry through knockout mutagenesis and Western blot analysis using anti-Le^y.**

To verify that the glycoprotein identified in objective 2 is the Le^y-modified protein candidate observed in our preliminary data, we constructed a knockout mutant of the gene encoding the glycoprotein identified. Anti-Le^y Western blot was used to verify that the Le^y glycoprotein candidate originally found in the WT is not present in the mutant.

Chapter 2

2 Methods

2.1 Bacterial strains and culture conditions

C. jejuni NCTC 11168 was grown in a microaerobic atmosphere (85% N_2, 10% CO_2 and 5% O_2) at 37°C on trypticase soy agar (TSA) supplemented with 5% sheep blood (Cedarlane) and $10\,\mu g\,mL^{-1}$ vancomycin and $5\,\mu g\,mL^{-1}$ trimethoprim as background antibiotics. Where appropriate, the medium was supplemented with $15\,\mu g\,mL^{-1}$ chloramphenicol and/or $30\,\mu g\,mL^{-1}$ kanamycin. The cells were grown overnight from freezer stocks on TSA containing appropriate antibiotics. Cells were harvested and normalized to an OD_{600nm}=0.1 and 100 µL were spread onto TSA blood plates containing only the background antibiotics using glass beads and strains were allowed to grow for 20–24 h. The cells were harvested and normalized to the same OD_{600nm} before use for phenotypic analyses unless otherwise specified. The viability of the bacterial suspensions that were used as the inoculum for phenotypic assays was assessed by colony forming unit (CFU) measurements.

H. pylori NCTC 11637 cells were grown under microaerobic conditions, as indicated above, for approximately 48 h on agar plates containing 37 g L^{-1} Brain Heart Infusion (BHI) media (EMD), 2.5 g L^{-1} yeast extract (Bioshop), and 0.05% sodium pyruvate, supplemented with 7.5 % horse serum (Gibco), 4 µg mL^{-1} amphotericin B (Calbiochem), 5 µg mL^{-1} trimethoprim (Sigma) and 10 µg mL^{-1} vancomycin (EMD Biosciences). Cells were revived from freezer stocks on standard BHI plates in the case of the wild type strain and BHI supplemented with 15 µg mL^{-1} chloramphenicol in the case of the *hopE::CAT* mutant strain. After 48 h of growth, the bacteria were spread to a new plate using a sterile cotton swab soaked in BHI and grown for another 48 h. The full plates were each expanded to 8 plates and grown for 48 h. Standard BHI plates (without chloramphenicol) were used in the final expansion of both wild type and mutant strains whereby each plate was further expanded to another 8 plates. The bacteria were harvested in 1 mL of sterile 0.85 % saline solution per plate of confluent growth. The harvested bacteria were centrifuged at 4,000 *g*

for 30 min at 4˚C in a 5810 R centrifuge (Eppendorf). The supernatant was discarded and the pellet was frozen at -20˚C until further use.

E. coli was routinely grown on Luria Bertani (LB) agar (Fisher Scientific) in a 37˚C incubator. Alternatively, *E. coli* was grown in LB broth in a shaking incubator (200 rpm) at 37˚C. Antibiotics were supplemented where appropriate at the following concentrations: 100 µg mL^{-1} ampicillin, 30 µg mL^{-1} kanamycin, 34 µg mL^{-1} chloramphenicol and 4 µg mL^{-1}.

2.2 Preparation of chemically competent *E. coli* and transformation of these cells

A 3 mL overnight culture of *E. coli* grown in LB broth was used to inoculate 100 mL LB. The bacteria were incubated until an OD$_{600}$ of 0.6 was reached. The bacteria were pelleted at 5,000 *g* (Eppendorf 5415D, Eppendorf) for 10 min at 4˚C, resuspended in 20 mL of cold 50 mM calcium chloride solution and incubated on ice for 30 min. The cells were then pelleted as described above and resuspended in 5 mL of 50 mM calcium chloride solution and incubated on ice for 5 h. The cells were resuspended in 5 mL of 50 % cold glycerol in 50 mM calcium chloride and aliquoted for storage at -80˚C.

The competent *E. coli* cells were thawed on ice and 100 µL were added to 10 µL of plasmid DNA (~25 ng µL^{-1}) or a ligation mixture was added and mixed gently into the competent cells and incubated on ice for 30 min. The cells were heat shocked for 90 s at 42˚C and then placed on ice for 1 min. Then 600 µL of LB broth was added to the cells prior to incubation for 1.5 h at 37˚C in a shaking incubator. The cultures were then plated on LB agar plates supplemented with the appropriate antibiotics for selection. The plates were incubated at 37˚C for up to 16 h and colonies were patched onto LB plates and screened by colony PCR. Positive clones were grown in 3 mL of LB overnight and freezer stocks were prepared in 25% glycerol for storage at -80˚C. Plasmids were extracted with a plasmid extraction kit (Froggabio) as per manufacturer's instructions for sequencing.

2.3 Construction of His-tagged and GST-tagged recombinant enzymes

NHis-Cj1319 was made by cloning *cj1319* into a pET23 derivative vector using CJ1319P1 and CJ1319P2 (Appendix B, Table 9). Cj1319-CHis was made by cloning *cj1319* into a pET30a vector using CJ1319P9 and CJ1319P10 (protein start sequence MDGKGEKVRNIL) or using CJ1319P23 and CJ1319P24 (protein start sequence MVRNIL). NGST-Cj1319 was created by cloning *cj1319* into a pGEX-2T vector using CJ1319P13 and CJ1319P14. NHis-Cj1320 was made by cloning *cj1320* into a pET23 derivative vector using CJ1320P1 and CJ1320P2. NHis-Cj1419 and NHis-Cj1426 were created by cloning *cj1419c* and *cj1426c* into a pET23 derivative vector using primer pairs CJ1419P1 and CJ1419P2 or CJ1426P1 and CJ1426P2 respectively. The primers used for making all constructs contained sequences cleavable by restriction enzymes, such that the PCR products and the plasmids were digested accordingly and ligated with T4 DNA ligase (NEB Biolabs). The constructs were transformed into *E. coli* DH5α and clones were selected by growth on LB agar supplemented with the appropriate antibiotics and screened by colony PCR and verified by DNA sequencing (Robarts Sequencing).

pNRC173.1, pNRC136.1, and pNRC175.1 were generously provided by Ian Schoenhofen (National Research Council, Canada) for the expression of PgmL, PtmE and GlmU respectively. These plasmids were constructed as detailed in (Schoenhofen *et al.*, 2009).

NGST-HP0044 and DdahA-CHis were constructed as detailed previously (Butty *et al.*, 2009; McCallum *et al.*, 2011).

2.4 Protein expression and purification

Protein expression was performed in *E. coli* BL21(DE3) for His-tagged clones and *E. coli* DH5α for GST-tagged clones. Unless specified otherwise, cells were grown in LB broth shaking at 200 rpm at 37°C until an $OD_{600nm}=0.6$ was reached and then recombinant protein expression was induced for 3 h at 37°C (or overnight at room temperature for GST-tagged clones) by the addition of 0.15 mM isopropyl β-D-1-thiogalactopyranoside. The cells were pelleted at 14,000 *g* for 15 min and stored at -20°C until needed.

For purification of over-expressed His-tagged proteins, cell pellets were re-suspended in 30 mL cold binding buffer (5mM imidazole, 0.1 M NaCl, 50 mM sodium phosphate pH 7.5). The cells were lysed by passaging through a cell disruptor (Constant Systems LTD IS6/40/BA/AA model) at 25,000 psi. The cellular debris and insoluble proteins were removed by centrifugation at 14,000 g for 30 min at 4°C, followed by the removal of membranes by ultracentrifugation (Beckman) at 100,000 g for 1 h at 4°C. The His-tagged proteins were purified by nickel chelation chromatography using Fast Protein Liquid Chromatography (FPLC) system with a POROS 1.6 mL column (Applied Biosciences). The column was washed initially with 5 column volumes (CV) of water before being charged with 30 CV of 0.1 M nickel sulphate. After the column was charged, the column was washed with 7.5 CV of 0.1 M NaCl and 5 CV of water. The column was equilibrated with 10 CV binding buffer that was adjusted to pH 7.5 for Cj1319 purifications and pH 8 for Cj1419 and Cj1426 purifications. After loading the sample, the column was washed with 10 CV of 1X binding buffer to remove proteins that were non-specifically bound to the column. Bound proteins were eluted with an imidazole gradient from 50 mM to 1.0 M in 0.1M NaCl and 50 mM sodium phosphate that was adjusted to the same pH as the 1X binding buffer. Elution fractions were collected and separated by SDS-PAGE to determine which fraction contained the protein of interest. Purified proteins were stored in 50 % glycerol at -20°C.

The GST-tagged proteins were purified by affinity chromatography using a 1 mL GSTrap FF column (GE Healthcare) that had been equilibrated in PBS binding buffer. The cell pellets obtained after overexpression of the GST-tagged proteins were resuspended in 30 mL of PBS binding buffer, pH 8 (140 mM NaCl, 2.7 mM KCl, 10 mM Na2HPO4, 1.8 mM KH2PO4). The cells were disrupted using a cell disruptor (Constant Systems LTD IS6/40/BA/AA model) at 25,000 psi. Cellular debris and insoluble proteins were removed by centrifugation for 30 min at 14,000 g and by filtration through a 0.2 μm filter. GST affinity purification was completed on an FPLC system using a 1 mL GSTrap FF column (GE Healthcare) that had been equilibrated in PBS binding buffer. The column was washed with 10 CV of binding buffer. The GST-tagged proteins were eluted with 3 CV of 0.01 M reduced glutathione. The glutathione was removed from the sample by overnight dialysis (cutoff of 3500 Da) in 50 mM Tris-HCl, pH 8, at 4°C. For HP0044, the GST tag was

removed by on-column incubation with thrombin for 2 h at 37°C, and the protein was eluted in 5 CV of 50 mM Tris-HCl buffer, pH 8. The purified proteins were analyzed by SDS-PAGE and Coomassie staining and were stored in 50% glycerol at -20°C.

2.5   Enzymatic reactions and analysis

Enzymatic reactions for making GDP-GlcNAc from D-glucosamine-6-phosphate were performed as described previously (Schoenhofen *et al*., 2009).

GDP-*manno*-heptose substrate was prepared enzymatically from sedoheptulose 7-phosphate (GlycOTeam) using overexpressed and purified GmhA/B/C and D enzymes from *Aneurinibacillus thermoaerophilus* as described previously (Butty *et al*., 2009). GDP-*manno*-heptose was purified by anion-exchange chromatography using a 5 ml High Q Econopac column (Bio-Rad Laboratories) and a linear gradient of 20 CV of TEAB (triethylammonium bicarbonate), pH 8.5, (50 mM–1 M) at 1 ml min^{-1} as described previously (Obhi and Creuzenet, 2005). After freeze-drying, substrate quantification was performed using a NanoDrop spectrophotometer and using ϵ_{GTP}=12000 mol^{-1}·l·cm^{-1}.

Reactions were typically performed by incubating 50 ng–2 μg of enzyme with 0.1 mM substrate (GDP-*manno*-heptose or GDP-GlcNAc prepared as described above or commercial GDP-mannose (Sigma)) in a final volume of 10 μl of 200 mM Tris/HCl pH 8.5 for DdahA and HP0044 or 25 mM sodium phosphate, pH 7.3, 25 mM NaCl for Cj1319 and other enzymes. Coenzymes were added at a concentration of 0.1 mM each. For reactions with Cj1320, 0.8 mM PLP, 8 mM L-Glu, and 1.2 mM acetyl-CoA were added. Reactions with Cj1419 and Cj1426 additionally contained 1 mM S-adenosylmethionine (SAM). Reactions were normally incubated for 3 h at 37°C. The reaction products were analysed by capillary electrophoresis.

2.6   Capillary electrophoresis (CE) of sugar nucleotides

CE was performed on a Beckman Gold instrument using the 32 Karat software and a 75 cm inner diameter bare silica capillary. The initial conditioning of the capillary was performed by washing the capillary with 0.1 N HCl for 30 min at 20 psi, followed by 10

min of water. For sample analyses, the capillary was washed for 2 min with 200 mM borax, pH 9, buffer. The sample was injected by pressure for 4 s and separation was performed by applying 26 kV to both ends of the capillary that were maintained in the borax buffer. Migrating compounds were monitored at 254 nm in a window placed at 50 cm from the beginning of the capillary. The capillary was washed 2 min with water, 2 min with 0.1 M NaOH, and 2 min again with water between each run. Substrate conversion was estimated by integration of the areas under the substrate and product peaks using the 32 Karat software.

2.7   Extraction of chromosomal DNA from *C. jejuni* and *H. pylori*

For chromosomal DNA extraction from total cells, half a plate of confluently grown bacteria were harvested into 1 mL of 0.85 % saline solution and pelleted at 14,000 g for 1 min and washed once prior to resuspension in 500 µL of cetyltrimethylammonium bromide (CTAB) buffer (100 mM Tris-HCL pH 8.8, 1.4 M NaCl, 0.02 M EDTA, 1% (w/v) CTAB). A solution of phenol:chloroform:isoamyl alcohol (25:24:1) was added to the cell suspension (1:1) and the mixture was vortexed until an emulsion formed following by centrifugation at 14,000 g for 5 min. The aqueous phase was collected and added to 500 µL of chloroform-isoamyl alcohol (24:1) and centrifuged at 14,000 g for 5 min to remove residual phenol. The aqueous phase was recovered and 0.08 volumes of cold 7.5 M ammonium acetate and 0.54 volumes of chilled isopropanol were added to precipitate the DNA. The contents were mixed by inversion 30 times and incubated at room temperature for 10 minutes. The precipitated DNA was collected by centrifugation at 14,000 g for 10 min at 4°C. The DNA pellet was washed once with cold 70 % ethanol and air dried. The final DNA pellet was resuspended in 50 µL of autoclaved distilled water and stored at 4°C.

2.8 Construction of knockout mutant and complement strains

2.8.1 Construction of *cj1319*::*CAT* knockout mutant

Construction of the *cj1319::CAT* knockout mutant was performed as previously described for the *cj1294::CAT* mutant using a CAT cassette for selection and natural transformation (Vijayakumar *et al*., 2006). Primers CJ1319P1 and CJ1319P2 were used to clone *cj1319* into the pET23 vector derivative (Newton and Mangroo, 1999) and primers CJ1319P3 and CJ1319P4 were used for inverse PCR (Appendix B, Table 9). The CAT cassette was amplified from pRYIII vector using primers CATCOLIP3 and CATCOLIP2 (Vijayakumar *et al*., 2006; Yao *et al*., 1993). The knockout mutant was checked by PCR with primers flanking outside the gene.

2.8.2 Construction of *cj1319* complement strains

Complementation was performed by chromosomal integration in the 16S–23S rRNA region as reported previously (Karlyshev and Wren, 2005) and detailed by (Wong *et al*., 2015). Briefly, *cj1319* was fused together with the promoter of *ompE* and a downstream *kan* resistance cassette using primers CJ1319P16, CJ1317, CJ1319P18, and CJ1319P19 by the primer overlap extension method (Heckman and Pease, 2007) (Appendix B, Table 9). The final construct was cleaved with *Nhe*I and inserted into the XbaI site of the pBluescript plasmid, generating pBSK-*cj1319*comp_RSP. This was sequenced (Robarts Sequencing Facility, London, Ontario) and transformed into the *cj1319::CAT* mutant by natural transformation.

Alternatively, primers 1318Pr-Bglll and Cj1319p25-NdeI were used to amplify *cj1319* with two upstream predicted promoter sequences based on RNA-seq data (Dugar *et al*., 2013). The *kan* resistance cassette was amplified with primers Aph3-For-His-NdeI and Aph3-p3. The two PCR products were digested with NdeI and ligated together. The blunt ended product was ligated into blunt ended pBSK-16S-23S cut with *Sma*I to generate pBSK-*cj1319*comp_RSP. To generate pBSK-*cj1319*comp_ONP, the blunt ended product

and pET23-*cj1320* were digested with BglII and NcoI and the two digested products were ligated together.

2.8.3 Construction of *hopE::CAT* mutant

The 500 bp upstream of the hp0706 gene was PCR-amplified from chromosomal DNA from *H. pylori* strain NCTC 11637 and the CAT cassette and 500 bp downstream of hopE were amplified by PCR from the hopEHisCat PCR SOEing product. The upstream and CAT downstream products were blunt-end ligated using T4 ligase (New England Biolabs). The ligated product was finally inserted into pUC18 digested with PstI and EcoRI forming phopE::CAT. Proper integration of the CAT cassette is verified by PCR. The knockout hopE mutant of strain NCTC 11637 was generated using this construct by electroporation-mediated allelic exchange, with selection on 12 µg mL^{-1} chloramphenicol. Potential transformants were analyzed for gene integration by PCR amplification of the gene knockout using primers that hybridize to DNA that was outside of the fragment used for recombination. Finally, correct insertion was confirmed by sequencing of the amplicons generated from the chromosomal DNA of selected mutants.

2.9   Purification of BambL, PAII-L and BC2L-A

pET25-BambL, pET25pa2l, and pRSETbcla were generously obtained from Dr. A. Imberty (CERMAV-CNRS, Grenoble, France) and constructed as described previously (Audfray *et al*., 2012; Lameignere *et al*., 2008; Mitchell *et al*., 2005). The plasmids were transformed into *E. coli* BL21(DE3) cells. The transformed cells were grown in LB broth containing 100 µg ml^{-1} ampicillin to an OD_{600nm}=0.6 and induced with 0.5 mM IPTG for 5 h at 30°C. The cells were centrifuged at 7,000 *g* for 15 min and resuspended in equilibration buffer (20 mM Tris pH 7.5, 100 µM $CaCl_2$, 0.15 M NaCl) followed by passaging through a cell disruptor (Constant Systems LTD IS6/40/BA/AA model) at 25,000 psi. The lysate was centrifuged at 14,000 *g* for 30 min to pellet cellular debris and insoluble proteins. The supernatant was further centrifuged at 50,000 *g* for 30 min, and the resulting supernatant was filtered through a 0.45 µm filter. Affinity chromatography on a mannose-agarose column (Sigma-Aldrich) was performed on the supernatant, whereby 1 mL of resin was loaded into a column and the beads were washed with 10 CV milliQ water

and 10 CV equilibration buffer. The purified lectins were allowed to bind to immobilized mannose in equilibration buffer and after washing with (20 mM Tris-HCl pH 7.5, 1 M NaCl), they were eluted with 2 CV of 100 mM mannose in equilibration buffer. Purified protein was dialyzed extensively using a 3.5 kDa MW cutoff against ultrapure water overnight, lyophlized and stored at 4 °C.

2.10   Labelling lectins with biotin

Pure BambL, PA-IIL, and BC2L-A was resuspended in 0.1 M sodium carbonate, pH 9.5, 0.1 % NaN_3 at a concentration of 20 mg mL^{-1}. Biotin-hydroxysuccinimide ester in DMSO was added to each lectin at a ratio of 10 mol biotin/mol of lectin and the mixture was allowed to incubate for 4 h at room temperature. To quench the reaction, 20x phosphate buffer (10 mM sodium phosphate, 150 mM NaCl pH 7.4, 0.1 % NaN_3) was added to the mixture and the sample was dialyzed extensively against phosphate buffer using a 3.5 MW cutoff.

2.11   Coupling BambL to sepharose for purification of glycopeptides

Lyophilized BambL (3 mg) was resuspended in 1 mL of coupling buffer (0.1 M $NaHCO_3$ pH 8.3, 0.5 M NaCl) and added to sepharose (1 mL/0.2g dried sepharose). The column was washed with 4 CV of coupling buffer and the sepharose was blocked by adding 5 CV of 0.1 M Tris-HCl pH 8.0. The column was equilibrated in 10 CV of equilibration buffer (20 mM Tris pH 7.5, 0.15 M NaCl, 100 uM $CaCl_2$). The soluble outer membrane tryptic peptides were allowed to bind to immobilized BambL in equilibration buffer and after washing with (20 mM Tris-HCl pH 7.5, 1 M NaCl), glycopeptides were eluted with 2 CV of each of 100 mM and 200 mM mannose in equilibration buffer.

2.12   Agarose gel electrophoresis

Agarose gel electrophoresis was used to separate DNA fragments. For most DNA fragments, a 0.7 % agarose gel was prepared in TAE buffer (40 mM Tris-acetate pH 8.0, 1 mM EDTA), and ethidium bromide was added to a final concentration of 0.01 %. For smaller fragments (~200 bp), a 1.4 % agarose gel was prepared in a similar manner as

above. Samples were mixed with DNA loading buffer (4x TAE buffer, 50 % glycerol, 0.01 % bromophenol blue) before loading and sizes were compared to a 1 kilobase pair DNA ladder standard (Invitrogen, Frogga). Electrophoresis was carried out at 80 volts until proper separation was achieved. DNA bands were visualized using UV light (254 nm).

2.13   Natural transformation of *C. jejuni* and *H. pylori*

C. jejuni were grown under microaerobic conditions as described above and the cells were harvested into TSB and adjusted to an $OD_{600}=0.2$. A total of 2 µg of plasmid DNA was added to the cells to a final volume of 80 µL. A negative transformation control consisted of 70 µL of cells and 10 µL of water. The transformation mixtures were diluted by the addition of 300 µL of TSB. Four spots of 75 µL each were placed onto TSA plates supplemented with 5% sheep blood and cells were allowed to recover for 8 hours under microaerobic conditions at 37°C. The spots were resuspended in 300 µL of TSA broth and 75 µL plated onto TSA agar plates containing the appropriate antibiotics for selection using glass beads. Plating onto TSA plates, with no antibiotics, to ensure viability after transformation, was also done in parallel. These plates were grown for 2-3 days under microaerobic conditions at 37°C until colonies were observed.

Similarly, *H. pylori* were transformed according to the above protocol with the following modifications: Transformation mixtures were done in BHI and cells were grown on BHI agar supplemented with 7.5% horse serum. Plates were allowed to incubate for 5-7 days until colonies were observed.

2.14   Growth curves of *C. jejuni* strains

C. jejuni was grown as described above and re-suspended in MH broth to an OD_{600} of 1.0. A sidearm flask containing 20 mL MH broth and background antibiotics was first equilibrated under microaerobic conditions overnight. The MH broth was then inoculated with 1.5 mL of the bacterial suspension to achieve a starting OD_{600} of 0.075. Nitrogen gas was injected into the flask for approximately 1 min through a sterile Pasteur pipette which

was inserted into the flask, and partially sealed with a rubber stopper, to allow gas to fill the remaining volume of the flask, creating a microaerobic environment. The flasks were then sealed and incubated under agitation (120 rpm) at 37˚C for up to 24 h. Growth was monitored using a Klett colony meter (600 nm filter) over 24 h.

2.15   SDS-PAGE and Western blotting

Bacterial proteins were denatured in SDS loading buffer (0.625 M Tris pH 6.8, 2% SDS, 2 % β-mercaptoethanol, 10 % glycerol, and 0.002 % bromophenol blue) and incubated for 5 min at 100^0C, unless otherwise indicated. Proteins were separated on 12% SDS polyacrylamide gels by the Laemmli system (Bio-Rad, mini-gel system). Electrophoresis was performed at 12 mA. Proteins were visualized by Coomassie blue staining (10% acetic acid, 25% ethanol, 0.001% (w/v) Brilliant Blue R-250), silver nitrate staining or Western blotting.

LPS preparations were separated by 12 % SDS-polyacrylamide gels. Carbohydrates were visualized by silver nitrate staining or Western blotting.

The antibodies and Western blot conditions used in this study are summarized in Table 3. Western blotting was performed after electrophoretic transfer of proteins or LPS to nitrocellulose (Bio-Rad). Wet transfer was performed for 90 min for membrane protein samples and 60 min for all other protein and LPS samples in Tris-Glycine Transfer buffer (192 mM glycine, 25 mM Tris, 20 % methanol, 0.01 % SDS) with a constant current of 180 mA (Bio-Rad transblot system). After transfer, the membrane was rinsed in distilled water and stained with Ponceau S (0.1% (w/v) Ponceau S (Sigma-Aldrich) in 1 % (v/v) acetic acid) to visualize the transfer of proteins to the membrane. The Ponceau S stain was removed from the membrane by two 20 mL washes with phosphate buffered saline (PBS) buffer (137 mM NaCl, 2.7 mM KC1, 8 mM Na2HPO4, 1.46 mM KH2PO4, pH 7.2). The membrane was blocked overnight at 4^0C followed by an hour at room temperature with gentle shaking on a gel surfer (Dia-med) in 2.5 % skim milk, Odyssey Blocking Buffer (Licor), or 10 % Horse Serum (Gibco), as appropriate for the antibodies to be used (Table

3). After blocking, all steps were performed at room temperature and with gentle shaking on the gel surfer. The membrane was washed twice in 20 mL PBS-Tween-20 (PBS with 0.1 % Tween-20) and once in PBS buffer for 5 min each and then incubated with primary antibody for 1 h at room temperature. After incubation, the membrane was washed four times in PBS-Tween-20 and once in PBS for 5 min each and then incubated with secondary antibody for 30 min in the dark. The membrane was washed in the dark with PBS-Tween-20 and PBS as above. All antibodies were centrifuged at 6,300 g for 10 min prior to use. Proteins or LPS were detected by the Licor Infrared Imaging system at wavelengths of 700 nm or 800 nm.

Table 3. Antibodies and Western blotting conditions used in this thesis

Epitope detected	Blocking buffer	Primary antibody /label and dilution	Secondary antibody and dilution used	Wavelength detected (nm)
Biotin	10% horse serum	Glycoprotiens labelled with biotin-hydrazide	Streptavidin conjugated to AlexaFluor 680 (Invitrogen), 1μg/mL	700
6xHistag	2.5% skim milk	Anti-polyHistidine (mouse) (Sigma), 1/3000	Anti-mouse (goat) conjugated to IRDye 680 (Licor), 1/10000	700
Fucose	10% horse serum	Biotin-conjugated PAII-L or BambL lectins	Streptavidin conjugated to AlexaFluor 680 (Invitrogen), 1μg/mL	700
Heptose	10% horse serum	Biotin-conjugated BC2L-A lectin	Streptavidin conjugated to AlexaFluor 680 (Invitrogen), 1μg/mL	700
FlaA and FlaB	2.5% skim milk	Anti-FlaA/B (rabbit), 1/2500	Anti-rabbit (goat) conjugated to IRDye 800 (Rockland Immunochemicals), 1/5000	800
Lewis Y	2.5% skim milk	Anti-Lewis y, clone F3 (mouse) (Calbiochem), 1/100	Anti-mouse (goat) conjugated to IRDye 680 (Licor), 1/10000	700

2.16   RNA extraction and cDNA synthesis

C. jejuni was grown for 20-24 h under microaerobic conditions at 37˚C on one TSA plate. For RNA isolation, approximately 5.0×10^9 cells were resuspended in 200 µL TE buffer, as recommended by the manufacturer, prior to lysis. RNA was isolated using the RNA midi spin kit (GE Health Sciences) as per the manufacturer's instructions. The final elution step was done in 500 µL of RNAse free water, following the manufacturer's instructions. In addition to the on column DNAse I treatment as suggested by the manufacturer, the samples were treated using 60 units of DNAse I (Roche, Canada) for 40 minutes at 37°C. Following the reaction, the DNAse was inactivated via the addition of 8.4 µL 100 mM ethylenediaminetetraacetic acid (EDTA) and heating at 70˚C for 10 minutes. The amount of RNA was quantified using a ND-1000 Nanodrop spectrophotometer (Nanodrop, USA). RNA samples were diluted in RNAse free water to a final concentration of 10.5 ng/µL. cDNA was generated using iScript reverse transcriptase (BioRad, Canada). Each reaction contained 30 µL of DNAse-treated RNA, 8 µL 5x iScript reaction mix, and 2 µL of iScript reverse transcriptase. Negative control samples contained 10 µL of the iScript reaction mix and 30 µL of RNA. The reverse transcription reaction was carried out using a BioRad thermocycler (BioRad, Canada) and the program used was as follows: 5 minutes at 25˚C for annealing of the random primers, 30 minutes at 42˚C for extension, 5 minutes at 85˚C for inactivation of reverse transcriptase, and a final 4˚C hold. Following the generation of cDNA, the samples were stored at -20˚C until use.

2.17   qPCR analysis

Real-time PCR analysis was carried out using the Rotor-Gene 6000 (Corbett Life Science, Canada) to measure the transcription levels of the *cj1141*, *cj1142, cj1143, cj1426c*, *cj1427c*, *cj1428c*, *cj1429c, cj1430c*, *cj1120c*, *cj1121c*, *cj1293, cj1294, cj1318, cj1319, cj1320,* and *cj1321* genes in the wild type and mutant strains. The gene *cj1537c* encoding an acetyl CoA synthetase (a housekeeping gene) was used as a reference for normalization within each strain (intrastrain). *C. jejuni* chromosomal DNA was used as a positive control for the amplification of each fragment. When determining the expression level of each gene of interest, samples were set up in triplicate. For determination of gene expression, 2 µL of

cDNA were added to 2 μL of the appropriate primer mix (1 μL of each primer, at 7 pmol/μL (see Appendix B Table 9 for primer sequences)), 10 μL SYBR green mix, containing all necessary components for qPCR, (BioRad, Canada), and 6 μL of water. Negative controls for the qPCR contained cDNA but did not contain the SYBR Green mix. An additional negative control consisted of the SYBR Green mix and RNA which did not undergo reverse transcription. This control was used to ensure there was no chromosomal DNA contamination.

Reactions were carried out as follows: 95˚C (initial denaturation) for 5 minutes, 95˚C (denaturation) for 45 seconds, 59.5˚C (annealing) for 30 seconds, and 72˚C (elongation) for 20 seconds. Steps 2-4 were repeated for 40 cycles.

For each primer pair, efficiencies were determined using the dynamic range of chromosomal DNA and amplifying the desired fragments. Following amplification, the data were plotted and a standard curve was generated based on the C_T (the cycle number at which enough amplified product accumulates to yield a detectable fluorescence signal above a set threshold) values for the amplification from the different chromosomal DNA concentrations covering the dynamic range. The primer amplification efficiency was determined from the slope of the standard curve by performing the following calculation: E (efficiency) = $10^{-1/slope}$, which was converted into a percentage using the following: %Efficiency = (E-1) x 100.

The dynamic range of cDNA for downstream qPCR analysis was determined using varying concentrations of cDNA. For this, DNA fragments were amplified from serial dilutions of cDNA. The C_T value for each reaction was determined and a standard curve was generated by plotting C_T against the cDNA concentration. The cDNA concentrations yielding the best standard curve (i.e. the C_T values were evenly spaced and a linear standard curve results in a slope indicative of the maximum amplification efficiency (i.e. a doubling of DNA per cycle)) were used in each experiment to determine gene expression.

Two methods of comparison were used to determine differences in gene expression: intrastrain and interstrain comparisons. In intrastrain comparisons, the fold difference of expression of each gene was normalized to an internal housekeeping gene, *cj1537c* (a gene

which encodes acetyl CoA synthetase). For interstrain comparisons, the ΔCT of each gene compared to the housekeeping gene was calculated. The $\Delta\Delta$CT between the WT and mutant genes was calculated and the fold change compared to WT was calculated as such: fold $= 2^{\Delta\Delta CT}$. The standard deviation (SD) of the CT values of biological replica was determined for each gene and the propagated error incorporated into the fold change calculation was determined using the following equation $E = \sqrt{(S1^2 + S2^2)}$, where S1 is the SD of the gene of interest and S2 is the SD of the housekeeping gene. This error is calculated within the WT to give E1 and in the mutant strain to give E2. The final propagated SD is calculated by $SD = \sqrt{(E1^2 + E2^2)}$.

2.18   Motility assay

Campylobacter jejuni strains were adjusted to OD$_{600nm}$ of 1.0. Motility plates (0.3 % agar in TSA) were stabbed in triplicate with the wild type or mutants and incubated under microaerobic conditions at 37°C. The diameter of the motility halo was recorded after 48 h.

2.19   Electron microscopy

Electron microscopy was performed at the Biotron at Western University led by Dr. R. Gardiner with uranyl acetate staining as previously described (Merkx-Jacques *et al.*, 2004).

2.20   Flagellin purification

C. jejuni strains were grown as described above and cells were harvested from four petri dishes and washed in 0.85 % saline. The cells were resuspended in 10 ml of 0.85 % saline and surface appendages were sheared off using a tissue homogenizer for 4 x 30 s with cooling on ice in between shearing. The cells were pelleted twice at 4,000 *g* for 20 min at 4°C. The supernatant containing the extracted flagella was centrifuged at 100,000 *g* for 1 h at 4°C. The pelleted flagella were resuspended in water for further analyses.

2.21   Capsule, LOS, and LPS extraction and purification

2.21.1 Crude extraction

Crude CPS, LOS and LPS samples were prepared by SDS-solubilization as previously described by Hitchcock and Brown (Hitchcock and Brown, 1983). Briefly, *C. jejuni* from one TSA plate (or *H. pylori* from one BHI plate) was resuspended into 1 mL of PBS and pelleted at 14,000 *g* (Eppendorf 5415D, Eppendorf). The resuspended bacteria were diluted to an OD_{600} of 0.375 and 1 mL aliquoted. This aliquot was respun at 14,000 *g* to pellet the bacteria. The bacterial pellet was resuspended in 200 µL of SDS solubilization buffer (2 % SDS, 4 % 2-mercaptoethanol, 10 % glycerol, 1 M Tris pH 6.8, pinch of bromophenol blue) and boiled for 10 min. To each sample, 5 µL of 20 mg mL^{-1} Proteinase K was added and incubated for one hour at 60 °C. Samples were run on a SDS-PAGE gel as described above.

2.21.2 Ultra-pure extraction and separation of *C. jejuni* capsule and LOS

For the purification of capsule from *C. jejuni* NCTC 11168 wild type, *cj1319::CAT, cj1427*::CAT, *cj1428*::CAT, *cj1430*::CAT, and *KpsM* mutants, and *cj1319* complement strains, cells were grown on TSA plates as aforementioned and approximately 4 TSA plates were used to inoculate 600 mL of Brucella broth (BBL Sciences, Canada), containing 7.5% horse serum and 25 mM sodium pyruvate to an OD_{600} of approximately 0.05. After 24 h of growth (OD_{600} approximately 0.3), the bacteria were spun down at 4,200 *g* (Avanti J-25I, Beckman-Coulter) for 30 min. Purification of capsule was performed using the hot water/phenol extraction method (O. Westphal, 1964). Briefly, wet cell pellets of approximately 1 g were re-suspended in 20 mL of MilliQ water pre-heated to 68°C. An equal amount of liquified phenol (Fisher) preheated to 68°C was added to the pellet and sealed in a 50 mL phenol resistant centrifuge tube. The samples were incubated in a 68°C water bath for 10 minutes with intermittent rigorous vortexing. The sample was allowed to cool to 10°C on ice and centrifuged for 30 min at 6,300 *g* (Eppendorf 5810R, Eppendorf), and 10°C. The aqueous (top) phase was collected, and an equal amount of water was added to the remaining organic phase. The procedure was repeated and the aqueous phases were

pooled. The aqueous phases were dialyzed (molecular weight cut off 12-14000 Da, Spectra/Por, Spectrum Labs) against running water for 2-3 days until no phenol remained. The sample was lyophilized and re-suspended in double distilled water. Ultracentrifugation of the sample for 30 h at 4°C and 100,000 *g* (Optima Max-XP Ultracentrifuge, Beckman-Coulter) pelleted most of the LOS, while CPS remained in the supernatant. The sample was lyophilized and resuspended in 500 μL double distilled water. Treatment with 200 mg of Proteinase K (Biobasic, Markham, Canada) was carried out for 2 h at 60°C to degrade any remaining proteins that may not have been removed during the hot water/phenol procedure. Capsule samples were stored at -20°C until further required.

For compositional analysis of the capsule and LOS, the procedure was performed on 6 L of cell cultures, whereby all volumes were adjested accordingly. In addition to the above, the samples were further treated twice with both DNase I and RNase and twice more with Proteinase K to ensure the removal of peptides and nucleic acids. In between treatments, the samples were centrifuged at 100,000 *g* for 10 h and the pellet was recovered. To separate the LOS from capsule, isopropanol was added to a final concentration of 50 % (v/v) and the samples were spun at 14,000 *g* for 10 min. The supernatant containing the capsule was removed and speedvaccuumed to drynesss and resuspended in water. The pellet containing the LOS was resuspended in the same volume of water as the capsule. Samples were frozen at -20°C until further use.

2.22   Silver staining of carbohydrates

The silver staining protocol of Fomsgaard *et al* was followed (Fomsgaard *et al*., 1990). Briefly, carbohydrates were first separated on a 10% SDS-PAGE and then oxidized in a solution of 0.7% periodic acid, 40% ethanol and 5% acetic acid in milliQ water with shaking for 20 min. The oxidation was followed by five washes over 15 min in milliQ water. The gel was then stained with silver nitrate in a staining solution with the following final concentrations: 0.19% (v/v) 10 N NaOH, 1.3% (v/v) ammonium hydroxide, 0.7% (w/v) silver nitrate. Gels were stained for 10 min, followed by five washes over 15 min in

milliQ water. Following the wash, the gels were developed using 0.005% (w/v) citric acid and 0.05% (v/v) formaldehyde (37%) in milliQ water until bands became visible. The gels were then washed several times with milliQ water and scanned.

2.23   Compositional analysis of capsule and LOS

Glycosyl composition analysis was performed by combined gas chromatography/mass spectrometry (GC/MS) of the per-*O*-trimethylsilyl (TMS) derivatives of the monosaccharide methyl glycosides produced from the sample by acidic methanolysis.

Between 300 µg and 400 µg was used for the analysis. The samples were placed into test tubes and 20 µg of inositol was added. Methyl glycosides were then prepared from the dry samples by methanolysis in 1 M HCl in methanol at 80°C (16 h), followed by re-N-acetylation with pyridine and acetic anhydride in methanol (for detection of amino sugars). The samples were then per-*O*-trimethylsilylated by treatment with Tri-Sil (Pierce) at 80°C (0.5 hours). These procedures were carried out as previously described in (Merkle and Poppe, 1994; York *et al*., 1986). GC/MS analysis of the TMS methyl glycosides was performed on an Agilent 7890A GC interfaced to a 5975C MSD, using an Supelco Equity-1 fused silica capillary column (30m ´ 0.25 mm ID).

2.24   Cell fractionation by differential centrifugation

The cell pellet was resuspended in 30-40 mL of 50 mM sodium phosphate pH 7.2, 0.3 M NaCl to a final OD_{600} of 6-10. The cells were subsequently lysed by passage through a cell disrupter (Constant Systems LTD IS6/40/BA/AA model) at 25,000 psi. All centrifugation steps were performed at $4\,^0$C. Cellular debris and unlysed cells were pelleted by centrifugation at 5,000 *g* for 30 min. Insoluble proteins were removed from the supernatant by centrifugation at 13,000 *g* for 1 h. Membrane proteins were pelleted by ultracentrifugation (Optima-XL 100K ultracentrifuge, Beckman Coulter, 70-Ti rotor) at 100,000 *g* for 1 h at $4\,^0$C. The supernatant recovered containing soluble proteins underwent a second ultracentrifugation spin at 100,000 *g* for 1 h. The initial membrane pellet was washed in 500 μL 50 mM sodium phosphate pH 7.2, 0.3 M NaCl, and pelleted by

ultracentrifugation in a micro-ultracentrifuge (Optimax ultracentrifuge, Beckman Coulter, TLA-110 rotor at 100,000 g). The supernatant was discarded and the total membrane pellet was used for separation of inner and outer membrane proteins.

2.25 Separation of inner and outer membrane proteins by differential solubilization in N-laurylsarcosine

Differential solubilization of inner and outer membrane by lauryl sarcosine has been documented as an efficient method to separate both types of membranes in various bacteria (Creuzenet and Lam, 2001; Filip *et al*., 1973). To solubilize inner membrane proteins, the washed total membrane pellet was resuspended in 500 μL of solubilization buffer (50 mM sodium phosphate pH 7.2, 0.3 M NaCl, with 1% N-lauryl sarcosine (w/v) (Sigma-Aldrich)) and mixed on nutator for 1 h at room temperature and overnight at 4 ^{0}C. Outer membrane proteins were pelleted by ultracentrifugation at 100,000 g (Optimax ultracentrifuge, Beckman Coulter, TLA-110 rotor) for 1 h at 4 ^{0}C. To further enhance the separation, the supernatant containing inner membrane proteins was ultracentrifuged at 100,000 g for 1 h at 4 ^{0}C three more times until no pellet was visible. Similarly, the original outer membrane pellet was resuspended and washed in solubilization buffer, mixed for 1 h at room temperature, and pelleted again by ultracentrifugation at 100,000 g for 1 h at 4 ^{0}C. The final outer membrane pellet was resuspended in 50 mM sodium phosphate pH 7.2, 0.3 M NaCl for protein analysis by SDS-PAGE.

The membrane fractions were analyzed by SDS-PAGE (12% polyacrylamide) (Laemmli, 1970). Proteins were visualized directly by Coomassie blue staining or silver nitrate staining, or after transfer onto nitrocellulose membrane by Ponceau S Red staining, biotin-hydrazide labelling or Western blotting. To ascertain proper separation of inner and outer membranes, the samples were tested for lactate dehydrogenase activity (inner membrane marker) according to published procedures (Osborn *et al*., 1972).

2.26 Digestion of outer membrane proteins

Outer membranes were resuspended the in equilibration buffer (20 mM Tris pH 7.5, 0.15 M NaCl, 100 μM CaCl2) and trypsin was added at a ratio of 1:100 to the weight of the

outer membranes and the sample was incubated at 37°C overnight. Ultracentrifugation at 100, 000 g was performed for 1 h in order to separate the soluble released peptides from the membranes. Further digestion was performed in the presence of 1 % Tween-20 for 18 h at 37°C.

2.27   Chemical labelling of glycoproteins

The protein content of sample fractions was assessed by Bradford assay and normalized to 1 µg µL^{-1}. From each fraction, 20 µL was used for the labelling reaction. To oxidize the carbohydrates of the glycoproteins, 2 µL of 100 mM sodium periodate were added to the sample and allowed to incubate in the dark for 20 min at room temperature. To quench the oxidizing reaction, 2 µL of 200 mM of sodium bisulphite in 200 mM sodium acetate pH 5.5 was added to the reaction and allowed to incubate for 5 min at room temperature. The samples were split into two tubes each of equal volume, where one received an addition of 2.5 µL of 5 mM biotin-hydrazide (Sigma) in dimethylformamide (DMF) and the other was mock labelled with 2.5 µL of DMF. The samples were incubated for 1 h at room temperature. The reaction was stopped by adding SDS-PAGE loading buffer to final concentration of 1X.

The biotin hydrazide-labelled and mock labelled samples were boiled for 2 min at 100°C and loaded onto a 15-well 12 % 1D SDS-PAGE gel and run at 12 mA. The gel was blotted onto a nitrocellulose membrane (BioRad) and protein transfer occurred at 180 mA for 45 min. Total proteins were stained by PonceauS Red on the membrane and then scanned. The membrane was de-stained in Tris-buffered saline (TBS) (10 mM Tris-HCl pH 7.5, and 150 mM NaCl) for 10 min and was blocked overnight in 10 % horse serum in water at 4°C. The membrane was then washed in TBS-Tween-Triton (50 mM Tris, 140 mM NaCl, 2 % Triton X-100, 0.5 % Tween-20, pH 7.5) for 10 min twice and once in TBS for 10 min. The membrane was probed with 15 ml of 1 µg ml^{-1} streptavidin-AlexaFluor-680 conjugate (Molecular Probes) in 0.01 M Potassium Phosphate pH 7.5, 0.8% NaCl for 30 min in the dark. It was then washed in TBS-Tween-Triton for 10 min three times and once in TBS for

10 min. The membrane was scanned at 700 nm on a Licor (Odyssey) infra-red scanner to detect the fluorescent streptavidin conjugate.

2.28   Adhesion and Invasion assay of *C. jejuni* to Caco-2 cells

Caco-2 cells (kindly given by D. McKay, University of Calgary) were routinely grown on 75 cm^2 tissue culture flasks in DMEM medium containing high glucose (25 mM) and supplemented with 10% fetal bovine serum (FBS, Gibco), 1.5 g L^{-1} sodium bicarbonate, 0.1 mM non-essential amino acids, 1 mM sodium pyruvate, 100 U ml^{-1} penicillin, and 100 µg/ml streptomycin. Caco-2 cells were grown in a CO_2 incubator containing 5% CO_2 and 37˚C until confluent, and passaged every 4-5 days. Passage of Caco-2 cells was carried out by releasing the cells from the flask surface via the addition of 0.25% Trypsin-EDTA (Gibco), followed by incubation in the CO_2 incubator at 37˚C for 2-3 min. Once released, the trypsin-EDTA was neutralized via the addition of fresh DMEM. Cells were then centrifuged at 200 *g* (Eppendorf 5702, Eppendorf) for 5 minutes to remove any excess trypsin.

Caco-2 cells were grown for three days until they formed a confluent monolayer (approximately 6.5 x 10^5 cells per well in 24-well plates). Approximately 6.5 x 10^7 CFU of *C. jejuni* were added to the Caco-2 cells for a multiplicity of infection (MOI) of 100:1 and the cells were allowed to incubate for 5 h. The plates were spun briefly (300 *g* (Eppendorf 5870R, Eppendorf) for 5 min at room temperature) to maximize contact between the bacteria and the cell monolayer. To determine total bacterial cell association (adherent and internalized bacteria), Caco-2 cell monolayers were washed three times, lysed with 0.1 % Triton X-100 for 10 min and viable bacterial counts were determined by plating the serial dilutions. To determine the number of internalized bacteria, the Caco-2 cell monolayers were treated with 200 µg mL^{-1} gentamicin for two hours to kill extracellular bacteria. The cells were then washed and treated as above to determine bacterial viable counts.

2.29   Internal survival of *C. jejuni* in *A. castellanii*

A. castellanii ATCC 30234 was obtained from the American Type Culture Collection. The protozoa were maintained in PYG medium in 75 cm^2 tissue culture flasks (BD, Mississauga, ON, Canada) at 25°C without aeration and routinely subcultured every 5 days. Amoeba cells were seeded at a density of ~2.5 x 10^5 cells mL^{-1} in a 24-well plate in a media free of nutrients and that does not support the replication of the amoeba cells and allowed to attach for 2 h. The *C. jejuni* strains are added to the wells at an MOI of 100:1 and allowed to incubate for 2 h, followed by 1 h of incubation with 300 µg/mL gentamycin at 25°C under aerobic conditions. For 0 h post infection, amoeba were lysed in Triton-X solution and a sample was taken and serially diluted for enumerating intracellular surviving bacteria. For 2.5 h and 5 h post infection, ameoba were fed heat inactivated *E. coli* to prevent them from starving during the time of incubation following the gentamycin treatment, and then similarly the amoeba were lysed and a sample was taken to enumerate surviving bacteria. Serial dilutions for each experiment were done in duplicate per well and 3 spots of 10 µl per dilution were plated for CFU mL^{-1} enumeration. Controls included amoeba only to ensure no contaminating bacteria were present, amoeba only for enumerating amoeba cells post infection time, bacteria only to determine the number of viable bacteria, bacteria only with gentamycin, and bacteria of the viability control treated with Triton-X to determine the effect of Triton-X on the bacteria.

2.30   Adhesion, invasion and internal survival of *C. jejuni* in Raw macrophages

RAW 264.7 macrophages (ATCC) were grown in 75 cm^2 tissue culture flasks (BD Falcon) in DMEM (Invitrogen) containing high glucose (25 mM), 10% FBS, 0.1 mM non-essential amino acids, 100 U/ml penicillin, and 100 µg/ml streptomycin in a CO_2 incubator containing 5% CO_2 and at 37°C. They were grown from freezer stocks until 80% confluent and then passaged every 3-4 days to a maximum of 5 passages. Passaging involves washing the macrophages in 1x PBS (Wisent) and detaching them by the addition of 5 mL 0.25% Trypsin/EDTA (Gibco) and incubation in a CO_2 incubator for 2-3 min. The cells were detached by allowing 15 mL of fresh DMEM to run over them. Cells were then

centrifuged at 200 g (Eppendorf 5702, Eppendorf) for 5 minutes to remove any excess trypsin. To seed new cells, 1 mL of cells was taken and added to 19 mL of fresh DMEM medium in a 75 cm^2 flask and incubated in a CO$_2$ incubator until needed.

Freezer stocks of RAW 264.7 macrophages were made with 45% cells, 45% FBS and 10% dimethyl sulfoxide (DMSO, Sigma-Aldrich). Cells were aliquoted into 2 mL cryotubes and stored at -80˚C until required.

Cells were seeded at approximately 2.1×10^5 cells per well of a 24 well plate and incubated overnight in DMEM without antibiotics. *C. jejuni* wild type or mutants were added at a MOI of 100. The plates were centrifuged for two minutes at 300 g (Eppendorf 5870R, Eppendorf) to synchronize bacteria-macrophage interaction.

For adhesion experiments, the plates were incubated with bacteria at 4°C for 30 min, washed with cold PBS five times and the cells were lysed in sterile double distilled water. The bacteria were then serially diluted and plated for CFU counts.

For intracellular survival experiments, cells were seeded as above and infected with bacteria at an MOI of 100 for two hours in a CO$_2$ incubator. The cells were washed three times using PBS and incubated with fresh DMEM containing 225 μg/mL gentamicin for one hour to kill extracellular bacteria. Macrophages were then washed and incubated in fresh DMEM for the times indicated. At each time point, the macrophages were washed three times with PBS and lysed using sterile double distilled water. Samples were serially diluted and plated for CFU counts.

For infection time course experiments, macrophages were seeded as above and infected with bacteria at an MOI of 100 for the times indicated. The macrophages were washed three times in PBS and incubated in fresh DMEM containing 225 μg/ml gentamicin for one hour, followed by lysis as described above and surviving bacteria were enumerated by CFU counts.

2.31   Biofilm assay

C. jejuni was grown as usual and cells were resuspended in TSB at an $OD_{600nm}=1$ and incubated for 24 h at 37°C. The strains were normalized to an $OD_{600nm}=1$ (~10^9 cell/mL) in TSB and 1 mL was added to borosilicate glass tubes. The tubes were allowed to incubate at 37°C over 6 days. At days 3, 4, 5 and 6, three tubes per strain were washed extensively in water and dried. Attached biofilms were stained with 1 % (w/v) crystal violet in water for 30 min and then washed extensively and dried and then treated with 1 mL 30% (v/v) acetic acid to dissolve the stain. The biofilms were quantified through transfer of 200 µL of the solution to 96-well microtest plate and absorbance was measured at 590 nm.

2.32   Nitrosative and oxidative stress assays

For nitrosative stress assays, *C. jejuni* were grown as described and harvested in BHI and normalized to an $OD_{600nm}=0.1$. To promote the production of reactive nitrogen species, sodium nitrite was dissolved in BHI pH-adjusted to 5.0 at different concentrations (Gundogdu *et al*., 2011; Iovine *et al*., 2008). The acidified media was added to the cells in 96-well plates (Sarstedt) and they were allowed to incubate for 30 min under static microaerobic conditions at 37°C. Each strain was treated in duplicate with each concentration of sodium nitrite and cells serially diluted after incubation. The serial dilutions were plated in triplicate for CFU enumeration.

In order to compare the susceptibility of strains to oxidative stress in the short term, 100 µL of bacteria at an $OD_{600}=0.1$ were incubated with different concentrations of H_2O_2 (15, 1.5, 0.15, or 0 mM) in a 96-well plate for 30 min at 37°C under microaerobic conditions and then serially diluted and plated on TSA blood plates. CFUs were counted after 2 days.

In order to compare the sensitivity of our strains to oxidative stress in the long term, 100 µL of bacteria at an $OD_{600}=2$ were spread onto TSA blood plates and allowed to dry. Sterile filter discs treated with 10 µl of 3%, 10%, or 30% H_2O_2 and dried were aseptically placed onto the agar. The plates were incubated under microaerobic conditions for 24 h at 37°C and the zone of inhibition was measured.

To determine the sensitivity of strains to serum, 10 μL of bacteria at an OD_{600nm}=0.1 was added to wells of a 96-well plate dish and 90 μL of serum diluted in BHI broth to a final concentration of 25 % (v/v). The plates were then incubated for 1.5 h in microaerobic conditions at 37°C. Following incubation, samples were serially diluted and plated for CFU counts.

2.33   SDS and polymyxin B minimum inhibitory concentration (MIC) determination

To determine the MIC SDS and polymyxin B on our strains, 10 μL of bacteria at an OD_{600nm}=0.1 was added to wells of a 96-well plate dish containing SDS or polymyxin B serially diluted from 0.02 to 0 % (w/v) SDS or 100 to 0 μg/mL polymyxin B. The plates were incubated for 48 h at 37°C and a spectrophotomer was used to measure the OD_{600nm}.

2.34   Infection of *Galleria mellonella*

Final instar *G. mellonella* larvae (Recorp Inc.) were maintained on wood chips at 15°C. *C. jejuni* strains were grown as usual followed by resuspension in 1.5 mL of Brucella broth supplemented with 0.25 mM sodium pyruvate and incubation at 37°C for 4 h with shaking at 120 rpm. The cells were spun down gently and resuspended in 0.85% saline at an OD_{600nm}=3. Larvae were infected with *C. jejuni* strains in 10 μL inocula by microinjection (Hamilton) in the right foreleg. The larvae were incubated at 37°C and survival was recorded after 24 h of infection. Saline-injected and uninjected controls were used. The bacterial input was measured by serially dilutions and CFU enumeration 2 days later.

2.35   Structural modeling

Homology modeling approach was used to model the structure of HopE. SWISS-MODEL workspace (http://swissmodel.expasy.org/) was used to build the structure model (Arnold *et al*., 2006). The model was exported from SWISS-MODEL as a protein data bank file (PDB). The 3D structure was then visualized and analyzed using PyMol software (https://www.pymol.org/).

2.36 Statistical analysis

Raw data was input into Graphpad Prism 6 software following templates provided for each statistical test. All calculations including means and standard errors and statistical analyses were performed using this software.

2.37 Mass spectrometry analysis of glycoproteins

2.37.1 In-gel trypsin digest

Samples for mass spectrometry were prepared according to the procedure outlined by the University of Western Ontario Biological Mass Spectrometry Laboratory (BMSL). Briefly, after separation of proteins by SDS-PAGE and protein staining with Coomassie Blue stain, the protein band of interest was excised from the polyacrylamide gel and cut into $1mm^3$ pieces and combined in a 1.5 mL eppendorf tube. The gel pieces were washed with 1 volume of autoclaved and filtered distilled water with occasional vortexing throughout. The distilled water was removed and the gel pieces were treated three times with 1 volume of 1:1 distilled water and acetonitrile for 15 min. The liquid was removed and the gel pieces were incubated with enough acetonitrile to just cover the gel pieces until the gel pieces visibly shrunk in size, appeared white in colour, and stuck together (approximately 5-10 minutes). The gel pieces were subsequently spun down in a microcentrifuge and the acetonitrile was removed. The gel pieces were rehydrated in 1 volume of 0.1 M ammonium bicarbonate for 5 min. One volume of acetonitrile was added, resulting in a 1:1 mixture of acetonitrile and 0.1 M ammonium bicarbonate, and the gel pieces were incubated for an additional 15 min. The liquid was removed and the gel pieces were dried in a vacuum centrifuge (Eppendorf) on the organic phase setting. Once completely dry, the gel pieces were rehydrated in 1 volume of 10 mM DTT, 0.1 M ammonium bicarbonate, and incubated for 45 min at $56^{o}C$ to reduce the protein. The remaining liquid was removed and 1 volume of 55 mM iodoacetamide, 0.1 M ammonium bicarbonate was added. The gel pieces were incubated in the dark for 30 min and then washed with 1 volume of 0.1 M ammonium bicarbonate for 5 minutes and 1 volume of 50 % acetonitrile in distilled water for 15 min. The wash solution was removed and 1 volume of acetonitrile was added and incubated

until the gel pieces became white and sticky (approximately 5-10 min). The liquid was removed and an additional 0.1M ammonium bicarbonate and acetonitrile washing cycle was performed to remove residual Coomassie stain. The samples were completely dried in a vacuum centrifuge. The gel pieces were rehydrated in 1 volume of trypsin digestion buffer (50 mM ammonium bicarbonate, 5 mM CaCl2, 10 ng/μL trypsin) and incubated for 45 min on ice. The gel pieces were spun down in a microcentrifuge and the supernatant removed. The gel pieces were covered with digestion buffer minus trypsin (50 mM ammonium bicarbonate, 5 mM CaCl2) and incubated overnight at 37^0C. To extract peptides, the gel pieces were spun down in a microcentrifuge and the supernatant removed to a clean 1.5 mL eppendorf tube. One volume of 25 mM ammonium bicarbonate was added to the gel pieces until they were completely covered. The gel pieces were incubated for 15 min with vortexing every 2-3 min. One volume of acetonitrile was added to make a 1:1 solution of 0.1 M ammonium bicarbonate and acetonitrile and the gel pieces were incubated for an additional 15 min. The supernatant was removed and combined with the initial supernatant following overnight digestion. To the gel pieces, 1 volume of 5% formic acid was added and incubated for 15 min. The same volume of acteonitrile was added and incubated for an additional 15 min. The gel pieces were spun down and the supernatant was combined with the earlier steps. An additional extraction cycle with 5% formic acid and acetonitrile was performed and the supernatant combined. To the pooled supernatant, DTT was added to a final concentration of 1 mM. Lastly, the combined supernatant was completely dried in a vacuum centrifuge and submitted to the BMSL facility for mass spectrometry analysis. All steps were performed at room temperature unless otherwise stated.

2.37.2 Analysis of *C. jejuni* flagellins

Two rounds of proteolytic digestion were performed, the first with trypsin, the second with trypsin and chymotrypsin, and peptides were collected and processed separately for each round. The first set of peptides (trypsin digest) was subjected to reversed phase ultra pressure liquid chromatography (LC) using a Waters nanoAcquity system coupled to a fourier transform (FT) Thermo Scientific Orbitrap Elite mass spectrometer using a Nanoflex source. The samples were trapped and then eluted onto a Waters BEH C18 75

um x 25 cm column using a gradient of 5% to 40% buffer B (Acetonitrile + 0.1% formic acid) over 90 minutes. The MS mass range was set at 400 to 1800 m/z with a high resolution set at 120,000 and the MS^2 scans were set using a fixed first mass of 100 Da using a FT/FT/HCD data dependant acquisition scheme. HCD scans were detected in the Orbitrap with a three step collision energy of 38 +/- 20% to optimize fragmentation data generated from glycopeptides. The second set of peptides (trypsin/chymotrypsin digest) were treated similarly using the same column but using a gradient of 5% to 37.5% buffer B over 80 minutes and using the Thermo Scientific QExactive mass spectrometer with the MS mass range set at 400 to 1500 m/z. The MS^2 scans were set using a fixed first mass of 100 Da using a FT/FT/HCD data dependant acquisition scheme. HCD scans were detected in the orbitrap with a normalized collision energy of 23%. For targeted MS^3 experiments, data were acquired using FT/IT(CID)/FT(HCD) ($MS/MS^2/MS^3$) with an FT Orbitrap Elite mass spectrometer with a resolution set at 60,000 using a normalized collision energy of 50%. MS^3 was set to trigger from MS^2 scans generating the 373.160 m/z ion, with a preferential MS^2 fragmentation of ions 704.3585 m/z and 772.7425 m/z (+3 charge ions previously found carrying the 372.145 modification). Raw data were visualized with the Qual Browser feature of the Thermo Scientific XCalibur software, and data analysis was performed using PEAKS 7.0 (Bioinformatic Solutions Inc.) software and peptide sequences were generated by *de novo* sequencing. The data were also searched against the NCBI database to match unmodified peptides. Unmatched peptides were further analyzed by manual addition of the mass of each sugar found in the metabolome of *C. jejuni* NCTC 11168, summarized in Table 2, and those found to be modifying flagellins of *C. jejuni* 81-176 into the variable modification list of the PEAKS software. Matches and partial matches were manually inspected to validate glycopeptides and to remove false hits.

2.37.3 Analysis of *H. pylori* outer membrane tryptic peptides

The tryptic peptides released from the outer membranes of *H. pylori* NCTC 11637 were separated on a Tris-glycine based gel (4%-16%-20%) in a Tris-Tricine system (run at 80 V till sample gets into separating, and 200 V till the end. The sample is run 30 min after the dye has run off the gel for best resolution of lower masses) and then the gel is stained with Coomassie Brilliant Blue. The area of 9-12 kDa containing anti-Le^y reactive bands

was carefully excised from the gel and the peptides were digested further with trypsin and extracted from the gel as described above for MS analysis. The peptides were separated by reversed phase ultra high pressure liquid chromatography (UPLC) using a Waters nanoAcquity system coupled to a Thermo Scientific Orbitrap Elite™ Hybrid Ion Trap-Orbitrap Mass Spectrometer, using a Nanoflex source. The peptides were trapped and then eluted onto a Waters BEH, 1.7 um, C18, 75 um x 25 cm column using a gradient of 5% to 40% buffer B (Acetonitrile + 0.1% formic acid) over 90 min. The MS mass range was set at 400 to 1800 m/z with resolution set at 120,000 and the top five most abundant precursor ions were selected for MS^2 by HCD fragmentation using a FT/FT/HCD data dependent acquisition scheme. HCD scans were detected in the orbitrap with a stepped collision energy of $38 \pm 20\%$.

Peptides were also analyzed using alternating CID/ETD fragmentation. The MS mass range was set at 400 to 2000 m/z with a high resolution set at 120,000 and the top two most abundant precursor ions were selected for MS^2 using a FT/FT/ETD/CID data dependant acquisition scheme. ETD and CID scans were detected in the orbitrap with a normalized collision energy (NCE) of 40% and 35% respectively. Raw data were visualized with the Qual Browser feature of Thermo Scientific XCalibur software, and data analysis was performed using PEAKS 7.5 (Bioinformatic Solutions Inc.) software and peptide sequences were generated by *de Novo* sequencing then searched against the NCBI database to match unmodified peptides. Unmatched or DeNovo only peptides were further analyzed by manual addition of the mass of Le^y and related sugars presented in Table 4, into the variable modification list of the PEAKS software. Matches and partial matches were manually inspected to validate glycopeptides and to remove false hits.

Table 4. Masses of Le^Y and its fragments ions arising from glycosidic bond breakage.

Sugar/glycan	Monoisotopic mass (Da) of sugar/glycan residues released from peptide	Oxonium ion (m/z)
Fucose	146.0579	147.0658
Gal	162.0528	163.0607
GlcNAc	203.0794	204.0873
GlcNAc + Fucose	349.1373	350.1452
Gal + GlcNAc + Fuc	511.1901	512.1980
Gal + Fucose	308.1107	309.1186
Full Le^y	657.2480	658.2515
Gal + GlcNAc	365.1322	366.1401

Chapter 3

3   Results

In this chapter, we investigated links between protein glycosylation and different glycolipids. We first examined the role of Cj1319 in the modification of GDP-*manno*-heptose to determine if this enzyme participates in heptose modification for capsule and/or protein glycosylation. We show through enzymology studies and a compositional analysis of the capsule from a *cj1319::CAT* knockout mutant that this enzyme is not involved in heptose modification. We further addressed the controversial role of Cj1319 in legionaminic acid synthesis, whereby we show it is not required for making this sugar. To determine an alternative role for this enzyme in non-heptose related protein glycosylation, we compared the *cj1319::CAT* mutant to mutants of each of the two known protein glycosylation pathways in phenotypes related to survival in the environment, host colonization and virulence. Through this, we determined Cj1319 has an important role in serum resistance, biofilm formation and infection of *Galleria mellonella.* Although we did not find a link between glycoproteins and glycolipids in *C. jejuni*, we expanded our study to its close relative *H. pylori.* We present data showing that an outer membrane porin is glycosylated with the Le^y O-antigen of the LPS, thus providing direct evidence that protein glycosylation is related to LPS synthesis in *H. pylori.*

3.1   Investigating the function of Cj1319 via an enzymology approach

Rationale**:** Cj1319 is a putative sugar biosynthetic enzyme which we **hypothesize** has a role in protein glycosylation in *Campylobacter jejuni* via a GDP-*manno*-heptose dehydratase activity. This is based on the homology of the enzyme to other GDP-*manno*-heptose dehydratases, DmhA and DdahA (Ho *et al*., 2008; McCallum *et al*., 2011), and on the fact that *cj1319* is clustered with a putative aminotransferase and an N-acetyl transferase, Cj1320 and Cj1321, which is reminiscent of the genetic arrangement found in

the two known protein glycosylation pathways (Nothaft and Szymanski, 2010; Vijayakumar *et al*., 2006). GDP-*manno*-heptose is the precursor of a dedicated pathway for the creation of a modified heptose that is incorporated into the capsule of *C. jejuni* strains and this heptose is important in virulence and chicken colonization (Karlyshev *et al*., 2005a; Wong *et al*., 2015). This pathway for our strain of interest, *C. jejuni* NCTC 11168, is partially characterized, however, the C4 oxidase needed to initiate this pathway has yet to be found (Figure 3) (McCallum *et al*., 2013). The oxidase role may be fulfilled by Cj1319 as C4 oxidation is also performed by C4, C6 dehydratases, whereby Cj1319 would have a central role in this pathway, or Cj1319 may use GDP-*manno*-heptose as the precursor of a novel protein glycosylation pathway which would be a potential link between capsule synthesis and protein glycosylation. It has been shown in other bacteria that O-antigen from the LPS or capsule units can serve as the glycosylation motif for protein glycosylation (Castric *et al*., 2001; DiGiandomenico *et al*., 2002; Lees-Miller *et al*., 2013).

Expression of various tagged forms of Cj1319

Previous laboratory members have attempted to express and purify Cj1319 to study its function enzymatically. Both C- and N-terminal His-tagged Cj1319 (Cj1319-CHis and NHis-Cj1319) were cloned and transformed into *E. coli* BL21(DE3)pLysS, however, little to no soluble expression of either recombinant protein was reported. As such, N-terminal GST-tagged Cj1319 (NGST-Cj1319) was cloned and transformed into *E. coli* DH5α in order to increase the solubility of Cj1319. Although induction of soluble NGST-Cj1319 was successful, the fusion protein was not found to be active on either GDP-*manno*-heptose or GDP-mannose. As the lack of activity could be explained by the presence of the GST tag which could interfere with the binding of Cj1319 to its substrate, the GST tag was removed through digestion by thrombin. However, thrombin digestion was largely inefficient and still no activity was found on either substrate. It is possible that the enzyme may be unstable and lost activity during thrombin digestion. Therefore, we expressed and purified NGST-Cj1319 to produce untagged Cj1319 following thrombin digestion under modified digestion conditions to resassess the activity of this enzyme (Appendix B, Figure 46D).

In addition, we sought to determine conditions for expression of soluble His-tagged Cj1319 in order to avoid GST tag cleavage. We transformed both NHis-Cj1319 and Cj1319-CHis constructs into BL21 (DE3) without pLysS, and analyzed them for inducible expression of Cj1319. The Cj1319-CHis clone showed the most inducible expression and thus was chosen for purification by nickel affinity chromatography (Appendix B, Figure 46A, B and C).

Since the Cj1319-CHis construct was made with a slightly longer starting sequence (MDGKGEKVRNIL) due to the ambiguity of the start codon at the time of its design (gtg, coding for valine, rather than atg), the full enzyme was recloned with a shorter starting sequence (MRNIL), as the additional starting amino acids may have caused a change in Cj1319's structure, rendering it inactive. This new clone matched exactly what was used by Schoenhofen *et al.* 2009, who showed that Cj1319 is active on GDP-GlcNAc, although activity was limited.

Testing Cj1319 on GDP-GlcNAc

It has been shown that Cj1319 is active on GDP-GlcNAc and Cj1320 is active on GDP-2-acetamido-2, 6-dideoxy-α-D-*xylo*-hexos-4-ulose generated by Cj1319 (Schoenhofen *et al.*, 2009). Thus, in order to show that Cj1319 and Cj1320 were active prior to testing on our two predicted substrates, we tested both enzymes on GDP-GlcNAc. As this sugar nucleotide is not available commercially, we needed to synthesize GDP-GlcNAc. We accomplished this using commercial 6-glucosamine-1-phosphate and enzymes PgmL, PtmE, and GlmU according to Figure 9. Constructs for expression of these enzymes were obtained from (Schoenhofen *et al.*, 2009). We expressed and purified these three enzymes and followed the reaction conditions described in (Schoenhofen *et al.*, 2009). PgmL and PtmE were used to make GDP-GlcN from 6-glucosamine-1-phosphate. This sugar nucleotide was then purified by anion exchange chromatography and the pure sugar nucleotide is shown in Figure 10, trace A. GlmU was then reacted with GDP-GlcN to make GDP-GlcNAc shown is trace B. Once GDP-GlcNAc was obtained, reactions with Cj1319-CHis and NHis-Cj1320 were performed. After 4.5h incubation with Cj1319-CHis, no evidence of product formation was detected in trace C. We additionally monitored the

reaction at 8 h, and still no product had formed. However, after extending the reaction overnight (~20 hours), almost 100% of GDP-GlcNAc is converted to GDP-2-acetamido-2, 6-dideoxy-α-D-xylo-hexos-4-ulose in trace D. This extended incubation time was also reported by (Schoenhofen *et al*., 2009). To confirm that the new peak that emerged was GDP-2-acetamido-2, 6-dideoxy-α-D-xylo-hexos-4-ulose, Cj1320 was added to the reaction and the emergence of GDP-4-amino-4, 6-dideoxy-α-D-GlcNAc is observed in trace D, although the yield is very limited, and concomitant decrease in the Cj1319 product was observed. The peak identification is based on direct comparison to the peaks reported by (Schoenhofen *et al*., 2009). The slow reaction kinetics of Cj1319 and Cj1320 on these intermediates of this pathway suggest that these substrates are unlikely to be the native substrates of these enzymes. Thus we continued to pursue the potential of Cj1319 to act on GDP-mannose and GDP-*manno*-heptose. The activity on GDP-GlcNAc was used to positively control for enzyme activity.

Figure 9. *In vitro* **pathway for the synthesis of legionaminic acid adapted from (Schoenhofen *et al*., 2009) showing only the first few steps of GDP-GlcNAc synthesis and subsequent enzymatic steps carried out by Cj1319 and Cj1320.**

6-glucosamine-1-phosphate

PgmL

GlcN-1-P

PtmE

GDP-GlcN

GlmU

GDP-GlcNAc

Cj1319

GDP-2-acetamido-2, 6-dideoxy-α-D-xylo-hexos-4-ulose

Cj1320

GDP-4-amino-4, 6-dideoxy-α-D-GlcNAc
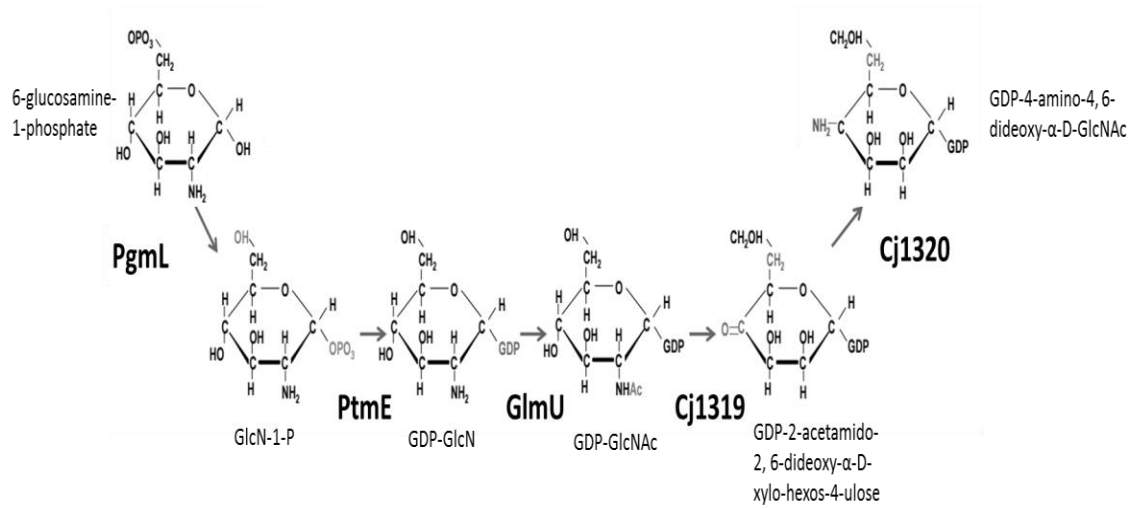
Figure 10. Analysis of the synthesis of GDP-GlcNAc by CE and the limited activity of Cj1319-CHis on this substrate.

Trace A shows GDP-GlcN made using PgmL and PtmE from 6-glucosamine-1-phosphate. Trace B shows the formation of GDP-GlcNAc from GDP-GlcN by the activity of GlmU. Trace C represents 4.5 h after addition of Cj1319-CHis to B. Trace D represents C incubated for 20 h. Trace E represents NHis-Cj1320 added to D for 20 h.

Testing activity of Cj1319 on GDP-*manno*-heptose and GDP-mannose

The purified enzymes were incubated with GDP-*manno*-heptose or GDP-mannose and coenzymes (NAD$^+$ and NADP$^+$) under different buffering conditions (pH 6-11 in 0.5 unit increments). Control reactions with equivalent amounts of either DdahA (GDP-*manno*-heptose dehydratase) and HP0044 (GDP-mannose dehydratase) were performed in parallel. All reactions were analyzed by capillary electrophoresis (CE) using UV detection. Representative traces of reaction results are shown in Figure 11. No activity on either GDP-*manno*-heptose was observed regardless of the buffer, pH or coenzyme used. Neither dialysis following purification to remove excess NaCl and imidazole nor the use of β-mercaptoethanol (Schoenhofen *et al*., 2009) had an affect on the activity of Cj1319. Different growth conditions for protein expression were tested (temperature and media) in addition to testing the supplementation of the cell lysate with the required coenzyme NAD$^+$. No condition had any apparent advantage over the other as no activity from Cj1319 was detected in any case. To address if there was an inhibitory artifact within the reactions containing Cj1319, we added either DdahA or HP0044 dehydratases to Cj1319 reaction cocktails which had been analyzed by CE and reincubated them. These two enzymes performed their activities as usual, thus demonstrating the reaction conditions were appropriate for these dehydratases.

Reactions were also performed on Cj1319-CHis prior to Ni^{2+} affinity purification to determine if the enzyme was active before purification. This was done by adding cell free extract containing overexpressed Cj1319-CHis to the reaction mixture containing both NAD$^+$ and NADP$^+$ and either of GDP-mannose or GDP-*manno*-heptose. As a control, cell free extract from *E. coli* Bl21(DE3) containing no plasmid was added to the same combinations of reaction mixes. No product was observed in this case compared to the control.

Testing Cj1319 in the presence of downstream reductase and aminotransferase to stabilize its product

Enzymatic reactions with Cj1319 were also tested with WcaG, a GDP-4-keto-6-deoxy-*manno*-heptose reductase that we hypothesized could stabilize the Cj1319 4-keto

intermediate product (McCallum *et al.*, 2011). This also did not lead to detectable activity from Cj1319. In case Cj1319 is an unstable enzyme that loses activity rapidly and cannot withstand freeze thaw cycles, the NGST-Cj1319 expressing strain was grown and the enzyme was purified in a single day without any freezing steps, and enzymatic reactions were performed immediately following purification. This included reactions performed on the GST-trap column during thrombin digestion. Despite this, the enzyme displayed no activity on either substrate.

Furthermore, we cloned, expressed and purified NHis-Cj1320, the next proposed enzyme of the Cj1319-initiated pathway, in order to determine if Cj1319 requires an interaction with Cj1320 in order to complete its function. In this pathway, Cj1320 is anticipated to aminate the 4-keto product of Cj1319. No activity was observed when both enzymes were present in the reaction mixture. In case no activity from Cj1320 was detected because Cj1319 was not active, control reactions with DdahA and HP0044, together with Cj1320 were performed. The dehydrated intermediates are proposed substrates of Cj1320 following the hypothesis that Cj1319 is C4, C6 dehydratase working upstream of Cj1320, however, Cj1320 was not active on the dehydrated intermediates. However, if Cj1319 only utilizes its potential as a C4 oxidase, then the products of DdahA and HP0044 would be surrogate substrates of the pathway and thus Cj1320 may not be active on these intermediate sugar nucleotides.

Figure 11. Cj1319 has no activity on GDP-*manno*-heptose or GDP-mannose.

(A) Trace A is a negative control reaction where no enzyme was added, showing GDP-*manno*-heptose and the two coenzymes, NAD^+ and $NADP^+$. Trace B is a representative trace of reactions with Cj1319 alone (NGST-Cj1319 cleaved or Cj1319-CHis) or both of Cj1319-CHis and NHis-Cj1320. Trace C is a representative trace of reactions with DdahA alone, a known GDP-*manno*-heptose dehydratase, or both of DdahA and NHis-Cj1320, showing the formation of the DdahA product which was not used by Cj1320. **(B)** Trace A is a negative control reaction where no enzyme was added, showing GDP-mannose and the two coenzymes, NAD^+ and $NADP^+$. Trace B is a representative trace of reactions with Cj1319 alone (NGST-Cj1319 cleaved or Cj1319-CHis) or both of Cj1319-CHis and NHis-Cj1320. Trace C is a representative trace of reactions with HP0044 alone, a known GDP-mannose dehydratase, or both of HP0044 and NHis-Cj1320, showing the formation of the HP0044 product which was not used by Cj1320.

A

NAD+

Expected GDP-4-keto-
6-deoxy-*lyxo*-heptose

NADP+

C. A + DdahA (GDP-*manno*-heptose dehydratase)
or DdahA + NHis-Cj1320
(Representative trace)

B. A + Cj1319 or Cj1319-CHis + NHis-Cj1320
(Representative trace)

GDP-*manno*-
heptose

A. No enzyme control

A_{254} nm

7   Time (min)   10

B

NAD+   NADP+

Expected GDP-4-
keto-6-deoxy-
mannose

C. A + HP0044 (GDP-mannose dehydratase)
or HP0044 + NHis-Cj1320
(Representative trace)

B. A + Cj1319 or Cj1319-CHis + NHis-Cj1320
(Representative trace)

GDP-mannose

A. No enzyme control

A_{254} nm

7   Time (min)   10

Testing if Cj1319 uses methylated substrates of the capsular heptose modification pathway

As the heptose found in the capsule of our strain of interest can be O-methylated at C3 and/or C6 (Michael *et al*., 2002; Wong *et al*., 2015), we investigated the possibility that Cj1319 may use a methylated heptose intermediate, namely GDP-3(and/or 6)-*O*-Me-*manno*-heptose, as a substrate. However, at the onset of the study, the identity of the 3- and 6-*O*-methyltransferases were unknown. Knockout mutagenesis of *cj1426c* later revealed that Cj1426 is responsible for 6-*O*-methylation, although it was never confirmed enzymatically (Sternberg *et al*., 2013). By examining the capsule cluster for putative methyltransferases that have not been studied, we identified *cj1419* as a tentative 3-*O*-methyltransferase. Both *cj1419c* and *cj1426c* were cloned with an N-terminal His-tag and expressed and purified from *E. coli* and enzymatic reactions were carried out on GDP-*manno*-heptose and intermediates of the heptose modification pathway. Neither enzyme showed activity on GDP-*manno*-heptose, while Cj1419 was found active on GDP-4-keto-6-deoxy-*lyxo*-heptose, the C4-oxidized surrogate intermediate generated by DdahA (Figure 12). Since the product of Cj1419 elutes in the same time range as does GDP-*manno*-heptose, we coinjected GDP-*manno*-heptose with the product of Cj1419 and ascertained that this was a new product. Although it was not confirmed by MS or NMR, since the surrogate intermediate is dehydrated at C6, we presume that Cj1419 methylated at C3 and thus the product formed is GDP-3-*O*-Me-4-keto-6-deoxy-*lyxo*-heptose which would follow the logic of the pathway for making the modified heptose expressed by our strain and determined by NMR (McCallum *et al*., 2013; Wong *et al*., 2015). Therefore, we could conclude that Cj1319 is not active on GDP-3-*O*-Me-*manno*-heptose since this product is not made *in vivo*. Since the surrogate intermediates of this pathway are dehydrated at C6, we did not expect to find activity from Cj1426 on these sugar nucleotides, and thus we could not conclude whether or not Cj1319 can use GDP-6-*O*-Me-*manno*-heptose.

Attempt to identify the Cj1319 substrate using a *cj1319* knockout mutant

In the absence of Cj1319 in a *cj1319* knockout mutant, we presume that there could be an accumulation of the substrate of this enzyme assuming that there is no negative feedback regulatory mechanism at play that would prevent its buildup. Therefore, in an attempt to find the substrate of Cj1319, we extracted the metabolites of the WT and *cj1319::CAT* (see section 3.2 for details) using perchloric acid (PCA), methanol or acetone extraction and analyzed the metabolites by CE. We did not find any difference in the traces (data not shown) that would allude to an accumulation of an intermediate. However, we also compared this to a PCA extract of the *cj1430::CAT* mutant, whereby Cj1430 is the MlghB epimerase acting after the oxidase in the heptose modification pathway in our strain of interest (Figure 3B). The PCA extract of this mutant also showed no difference compared to that of the WT. Thus we concluded that either not all the metabolites were extracted with PCA or no accumulation of the metabolites occurred due to feedback regulation on the glycosylation pathways. In conclusion, we were unable to identify any other potential substrate of Cj1319.

Figure 12. Cj1419 methylates an intermediate of the capsular modification pathway.

A schematic of the reaction is shown to facilitate understanding of the traces. Trace A is a negative control with GDP-*manno*-heptose with no enzymes added. Trace B shows the formation of P1 after the addition of DdahA. Trace C shows the formation of P7 after the addition of Cj1419 to P1, although complete conversion was not achieved. Trace D shows coinjection of trace C with GDP-*manno*-heptose.

H: GDP-*manno*-heptose

DdahA

P1: GDP-6-deoxy-4-keto-D-*lyxo*-heptose

Cj1419

P7: GDP-3-*O*-Me-6-deoxy-4-keto-D-*lyxo*-heptose
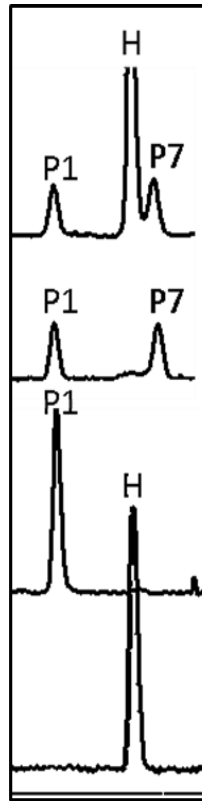
D. C+ GDP-*manno*-heptose

C. A + DdahA + Cj1419

B. A + DdahA

A. No enzymes

3.2 Generation and characterization of mutant and complements to explore the function of Cj1319

Rationale: This section introduces all the knockout and complement mutant strains used in this study in order to facilitate the readability of the thesis. Schematic representations of these strains are summarized in Figure 13. All constructs for strain generation were analyzed by PCR and confirmed by sequencing prior to transformation of *C. jejuni*. Strains were also verified by PCR analysis and sequencing.

Mutants used in this study

C. jejuni NCTC 11168 was chosen for this study since it was the first sequenced strain and our laboratory has already constructed protein glycosylation and capsular heptose mutants in this strain (Wong *et al*., 2015). It also encodes for Cj1319 which we had surmised could initiate the capsular heptose synthesis pathway. Cj1319 is not found in all strains of *C. jejuni,* but has been found in 82% of isolates (of 151 strains tested, 3 from chickens and the rest from patients) (Huang *et al*., 2013). In addition, this strain has one of the most complex protein glycosylation islands compared to other *C. jejuni* strains (Gundogdu *et al*., 2007; Parkhill *et al*., 2000). The *cj1319* knockout mutant, *cj1319::CAT,* was constructed by disruption of the gene with a chloramphenicol resistance cassette (Zebian *et al*., 2015).

For analysis of capsule related phenotypes, we compared the *cj1319::CAT* mutant to mutants of the capsule heptose modification pathway, *cj1427::CAT, cj1428::CAT, cj1429::CAT* and *cj1430::CAT,* as well as the capsuless mutant *KpsM* (Wong *et al*., 2015). Cj1427 or WcaG, is a negative regulator of the pathway (McCallum *et al*., 2011). Cj1430 and Cj1428 are the MlghB epimerase and MlghC reductase of this pathway respectively (Figure 3B) (McCallum *et al*., 2013). Cj1429 is thought to be a regulator of capsule synthesis, but its function is unknown (Wong *et al*., 2015). We also compared the *cj1319::CAT* mutant to a protein *N*-glycosylation pathway mutant, *cj1121c::CAT,* whereby Cj1121c is the aminotransferase of this pathway (Vijayakumar *et al*., 2006), and a mutant of the protein *O*-glycosylation pathway, *cj1294::CAT,* whereby Cj1294 is the

aminotransferase of this pathway (Obhi and Creuzenet, 2005; Vijayakumar *et al*., 2006) in order to investigate if Cj1319 is related to either of these two pathways or if it could be part of an independent protein glycosylation pathway. These studies also complemented our laboratory's previous studies on the role of protein glycosylation in virulence.

Figure 13. Schematic summary of strains used and created for this study.

For each strain, *cj1319* and its flanking genes are shown as well as the three copies of 16S and 23S rRNA genomic regions used for complementation as the site for chromosomal integration. Drawing not to scale. 'R' indicates that the complementation construct integrated into a copy of 16S 23S r̲RNA genomic region. 'O' indicates the complementation construct replaced the genes in the o̲riginal *cj1319* locus. 'SP' denotes 's̲trong p̲romoter' and corresponds to the use of the constitutive strong promoter of OmpE to drive expression of the genes in the complementation construct. 'NP' denotes 'n̲ative p̲romoter' whereby the native promoter of *cj1319* was cloned into the complementation construct. The *CAT* and *KAN* antibiotic resistance cassettes are in the same orientation as *cj1319.*

WT
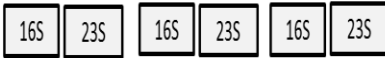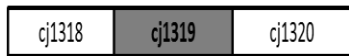
| cj1318 | **cj1319** | cj1320 |

| 16S | 23S | 16S | 23S | 16S | 23S |

cj1319KO

| cj1318 | CAT | cj1320 |

| 16S | 23S | 16S | 23S | 16S | 23S |

WT*cj1319*comp_RSP

| cj1318 | **cj1319** | cj1320 |

| 16S | OmpE | **cj1319** | KAN | 23S |

| 16S | 23S | 16S | 23S |

***Cj1319*comp_RSP**

| cj1318 | CAT | cj1320 |

| 16S | OmpE | **cj1319** | KAN | 23S |

| 16S | 23S | 16S | 23S |

WT*cj1319*comp_RNP

| cj1318 | **cj1319** | cj1320 |

| 16S | cj1318 | **cj1319** | KAN | 23S |

| 16S | 23S | 16S | 23S |

***Cj1319*comp_RNP**

| cj1318 | CAT | cj1320 |

| 16S | cj1318 | **cj1319** | KAN | 23S |

| 16S | 23S | 16S | 23S |

WT*cj1319*comp_ONP

| cj1318 | **cj1319** | KAN | cj1320 |

| 16S | 23S | 16S | 23S | 16S | 23S |

***Cj1319*comp_ONP**

| cj1318 | **cj1319** | KAN | cj1320 |

| 16S | 23S | 16S | 23S | 16S | 23S |
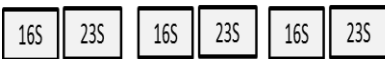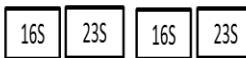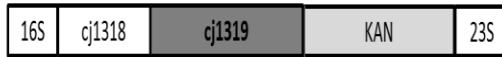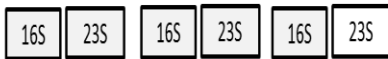
Generation and qRT-PCR characterization of complements

In this study, we originally complemented the *cj1319* knockout mutant according to a published method for *C. jejuni* chromosomal integration-based complementation (Karlyshev and Wren, 2005). Due to the instability of shuttle vectors in *C. jejuni,* this method of chromosomal integration of the complement construct into one of the three copies of 16S-23S rRNA genomic regions was chosen. Briefly. we cloned the strong constitutive promoter of the outer membrane protein, OmpE, as described by (Karlyshev and Wren, 2005) upstream of *cj1319* and inserted a kanamycin resistance cassette downstream of *cj1319.* This was done using gene splicing by overlap extension (SOEing). This construct was flanked by a region of 16S rRNA upstream and 23S rRNA downstream. This construct was transformed into both the *cj1319* knockout mutant and the WT by natural transformation and homologous recombination into a 16S-23S rRNA genomic region, generated *cj1319*comp_RSP and WT*cj1319*comp_RSP respectively where 'RSP' indicates that the complement construct integrated into a redundant 16S 23S region and that *cj1319* at this site is under the control of the strong constitutive promoter of OmpE. This complement was used in the majority of the work in this thesis. Similarly, complement constructs using *cj1121c* and *cj1294* instead of *cj1319* were made and transformed into either *cj1121c::CAT* or *cj1294::CAT* and WT, yielding *cj1121c*comp_RSP and WT*cj1121c*comp_RSP as well as *cj1294*comp_RSP and WT*cj1294*comp_RSP respectively.

As *cj1319*comp_RSP was able to complement some phenotypes, but not others, we hypothesized that this complement may be overexpressing Cj1319, and thus not restoring the phenotype to that of WT. We determined by qRT-PCR that the level of *cj1319* gene expression in *cj1319*comp_RSP was ~7 fold higher compared to that of the WT (Figure 14). Therefore, at the latest stages of this work, we altered the complement construct to encode the native promoter of *cj1319* rather than that of *ompE.* This construct was transformed into the *cj1319* knockout mutant and WT as described above, yielding *cj1319*comp_RNP and WT*cj1319*comp_RNP respectively, where 'RNP' indicates that the complement construct integrated into a redundant 16S 23S rRNA region and that *cj1319*

at this site is under the control of its nature promoter (Figure 13). The *cj1319*comp_RNP expressed WT levels of Cj1319 (Figure 14).

To determine if secondary mutations occurred in the *cj1319::CAT* mutant that contribute to the phenotypes that we tested, we constructed a third complement, whereby we replaced the *cj1319* gene disrupted with CAT in the knockout mutant with a complete *cj1319* gene under its native promotor. We inserted a KAN cassette downstream of *cj1319* in order to select for the new complement. This construct was introduced into the *cj1319*::*CAT* mutant and WT as described above resulting in strains *cj1319*comp_ONP and WT*cj1319*comp_ONP respectively, where 'ONP' indicates the complement construct replaced the knockout construct and *cj1319* is under the control of its native promoter. As these two new strains are theoretically genetically identical, they should not differ in phenotypes.

Figure 14. Fold change of *cj1319* locus in *cj1319*comp_RSP and *cj1319*comp_RNP compared to WT as determined through qRT-PCR.

Genetic organization of the genes targeted for the qRT-PCR analysis is depicted (not drawn to scale). The interstrain change in gene expression is reported in the table shown as a heat map of low to high gene expression compared to the WT. The fold change in expression was determined from two biological replicates, each tested in duplicate. The brackets indicate $2^{(\Delta\Delta CT-SD)}$ and $2^{(\Delta\Delta CT+SD)}$, where SD represents the standard error propagated through the fold calculations. No significant difference was determined by Student's t test.
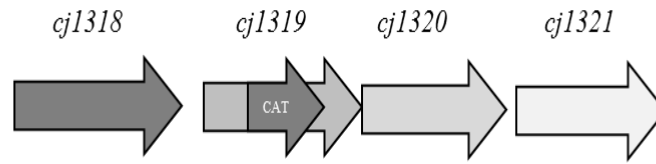
	cj1319::CAT	*cj1319*comp_RSP	*cj1319*comp_RNP
cj1318	1.26 (0.42-3.82)	12.21 (4.07-36.59)	3.57 (0.95-13.46)
cj1319	-	6.75 (3.27-13.94)	0.96 (0.14-6.45)
cj1320	2.13 (0.73-6.18)	20.36 (18.24-22.71)	6.67 (4.47-9.94)
cj1321	1.24 (0.41-3.72)	20.71 (17.94-23.91)	5.67 (2.66-12.10)

Heat map of gene fold expression compared to WT

Low | 0.01 | 0.1 0.5 | **no change** | 2 10 | >10 | High
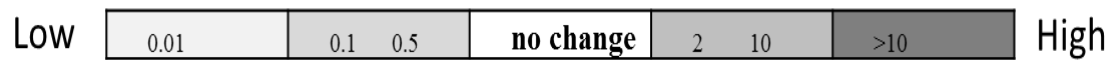
3.3   Effect of inactivation of *cj1319* on *C. jejuni* and comparison to other glycosylation knockout mutants

Rationale: In section 3.1, we determined that Cj1319 was not part of the pathway for making a modified heptose for capsule and likely not able to use a methylated intermediate of this pathway. Thus, we hypothesis that Cj1319 is initiating a protein glycosylation pathway independent of GDP-*manno*-heptose. Therefore, in order to explore alternative functions for Cj1319, we examined phenotypes of a *cj1319* knockout mutant compared to WT. For a more comprehensive analysis, we also compared this mutant to mutants of the protein glycosylation pathways or capsular heptose modification pathway as described in the previous section (3.2).

3.3.1 Effect of *cj1319* on growth rate

To determine if any of the mutations introduced for the creation of our strains affected the fitness of the cells under normal laboratory growth conditions, we assessed the growth rates of all strains. Cells were grown in MH broth preconditioned in microaerobic conditions in a closed system and growth was monitored using a Klett spectrophotomer until cells reached stationary phase. We determined that all the knockout mutants and their respective complement strains grow at approximately double the rate of the WT (Table 5). The complement constructs did not affect the growth rate of the WT with the exception of WTcomp_ONP which also grew at double the rate of the WT. Thus we concluded that none of our strains suffered from detrimental growth defects as a result of the engineered mutations. However, we noted the increased growth rate of the mutants and complement strains.

Table 5. Growth rates of *C. jejuni* strains used in this study.

Strain	Growth rate constant (g/h)[a]	Significantly different from WT?[b]
WT	0.37 ± 0.04	na.
cj1319::CAT	0.75 ± 0.04	Yes (***)
cj1319comp_RSP	0.84 ± 0.05	Yes (****)
WTcj1319comp_RSP	0.53 ± 0.01	No
cj1319comp_RNP	0.88 ± 0.04	Yes (****)
WTcj1319comp_RNP	0.56 ± 0.06	No
cj1319comp_ONP	0.83 ± 0.11	Yes (****)
WTcj1319comp_ONP	0.83 ± 0.03	Yes (****)
cj1121c::CAT	0.71 ± 0.02	Yes (**)
cj1121ccomp_RSP	0.72 ± 0.05	Yes (**)
WTcj1121ccomp_RSP	0.43 ± 0.07	No
cj1294::CAT	0.76 ± 0.05	Yes (***)
cj1294comp_RSP	0.82 ± 0.08	Yes (***)
WTcj1294comp_RSP	0.46 ± 0.09	No

[a] g represents the number of generations.

[b] na. for not applicable. (**) indicates $P<0.01$, (***) indicates $P<0.001$, (***) indicates $P<0.0001$.

3.3.2 Effect of *cj1319* inactivation on capsule and LOS

We did not find a role for Cj1319 in the capsular heptose modification pathway as per enzymatic assays. To further investigate this in our *cj1319* knockout mutant, we analyzed the gene expression of the capsular heptose modification genes, including *cj1419c* (which we showed codes for the 3-*O*-methyltransferase in this pathway) and *cj1426c* (which codes for the predicted 6-*O*-methyltransferase of this pathway (Sternberg *et al*., 2013)) in the WT and *cj1319::CAT* (Figure 15). We did not find any change in the expression of these genes, signifying that they are not affected by the absence of Cj1319. This further supports that Cj1319 does not play a role in heptose modification for capsule synthesis.

To ascertain that Cj1319 does not play a role in heptose modification for capsule synthesis, we extracted and analyzed the capsules of *cj1319::CAT, cj1319*comp_RSP, and WT*cj1319*comp_RSP and compared them to those of the WT, acapsular mutant, *KpsM,* and three mutants lacking modified heptose as determined by NMR, *cj1427::CAT, cj1428::CAT* and *cj1430::CAT* (Wong *et al*., 2015)*.* We used a hot water and phenol extraction method for capsule purification that is compatible with downstream mass spectrometry and NMR analysis (Westphal, 1964). Since the LOS copurifies with capsule, we used ultracentrifugation to separate capsule from the LOS, as the latter was reported to pellet and the former was reported to remain soluble (Michael *et al*., 2002). In order to maximize resolution of the capsule/LOS species by SDS-PAGE, gel compositions developed for resolving peptide and small proteins using a tris-tricine buffering system were exploited (Schägger, 2006). We found that using these gel compositions (now on refered to as 'peptide gels') in a tris-glycine buffering system increased the resolution of the capsule.

Figure 15. Fold change in capsular heptose modification genes in the *cj1319::CAT* mutant compared to WT as determined by qRT-PCR.

Genetic organization of the genes targeted for the qRT-PCR analysis is depicted (not drawn to scale). The interstrain change in gene expression compared to the WT is reported in the table shown. The fold change in expression was determined from two biological replicates, each tested in duplicate. The brackets indicate $2^{(\Delta\Delta CT-SD)}$ and $2^{(\Delta\Delta CT+SD)}$, where SD represents the standard error propagated through the fold calculations. No significant difference was determined by Student's t test.

cj1419c *cj1426c* *cj1427c* *cj1428c* *cj1429c* *cj1430c*

← ← ← ← ← ←
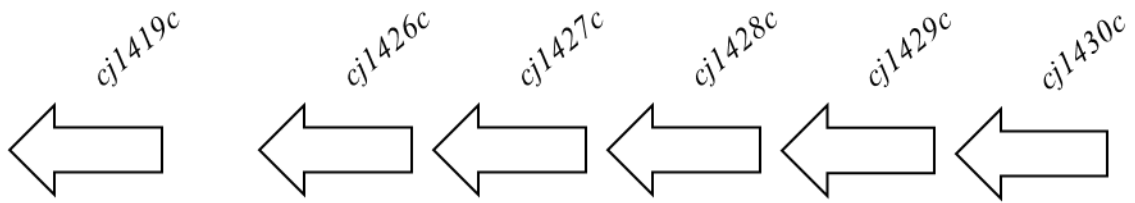
	cj1319::CAT
cj1419c	1.30 (0.44-3.90)
cj1426c	0.82 (0.36-1.89)
cj1427c	0.81 (0.36-1.85)
cj1428c	0.76 (0.20-2.84)
cj1429c	0.76 (0.33-1.74)
cj1430c	1.08 (0.26-4.53)

Separation and identification of capsule and LOS by ultracentrifugation and SDS-PAGE

We analyzed both the pellet and supernatant following ultracentrifugation by SDS-PAGE and silver staining (Figure 16). The smallest species is the LOS, mostly found in the pellet as expected, but is also found in small amounts in the supernatant. The intermediate molecular weight species is capsule based on its absense in the *KpsM* mutant. Against expectation a significant amount of capsule was recovered in the pellet. High molecular weight species with a ladder-like appeareance very reminiscent of LPS were recovered mostly in the pellet along with the LOS.

As *C. jejuni* strains generally do not produce LPS, it was initially intriguing that we observed this regularly spaced high molecular weight species that no one has described previously in our strain. However, it has been published that the LOS of other strains of *C. jejuni* form aggregates above a certain concentration which gives rise to the visualization of regular ladder repeating units by SDS-PAGE and silver staining (Logan and Trust, 1984). Therefore, to test if this was the case for our strain, we separated the pelleted capsule/LOS sample on a 12.5% peptide gel. Part of the gel was silver stained and used as a ruler to accurately excise specific bands from the unstained gel. These gel slices were then inserted into the wells of a second 12.5% peptide gel and re-separated by SDS-PAGE and silver stained. The resulting gel (Figure 17A) shows that these higher molecular weight bands are indeed LOS aggregates, as they give rise to low molecular weight LOS.

Effect of *cj1319* inactivation on LOS as assessed by SDS-PAGE

Importantly, *cj1319::CAT* and *cj1319*comp_RSP showed downshifted bands indicative of truncated repeat units of this high-molecular weight species compared to the WT and the other strains. As our results indicate that the high molecular weight species is LOS, this infers that *cj1319* affects the LOS. To show this, we performed serial dilutions of the WT and *cj1319* mutant pellet capsule/LOS samples and resolved them on a 16% peptide gel (Figure 17B). The diluted sample allowed the visualization of two LOS bands distinctly, corresponding to the full LOS structure (top band) and LOS lacking the branched sialic acid residue (bottom band) (Linton *et al*., 2000), showing the truncation occurs at the level

of the LOS core of the *cj1319* mutant. Thus this truncation of the core LOS would consistently give rise to LOS aggregates of smaller size compared to those of WT.

<u>The effect of *cj1319* inactivation on capsule as assessed by SDS-PAGE</u>

The *cj1319::CAT* mutant also showed a higher abundance of the high molecular weight capsule bands compared to WT. This phenotype was not reversed back to WT levels in *cj1319*comp_RSP, signifying this phenotype is likely due to a secondary mutation or due to the high expresion of *cj1319* by the strong promoter. Interestingly, WT*cj1319*comp_RSP showed reduced capsule production compared to WT. Trace amounts were detected if any. The spacing between the repeat units does not appear altered compared to WT, however, the heptose modification mutants also do not appear different compared to WT even though we have shown they lack the modified heptose by NMR (Wong *et al.*, 2015). So it is possible that the capsule composition in the *cj1319* mutant differs from that of WT.

Figure 16. Analysis of the supernatant and pellet by SDS-PAGE of a 16% peptide gel stained with silver following ultracentrifugation of the total capsule/LOS extracted samples.

(A) Supernatant showing semi-pure capsule. **(B)** Pellet showing LOS, second capsule species not previously reported, and high molecular weight species.

A   **B**

WT*cj1319comp_RSP*
cj1319comp_RSP
cj1319::CAT
WT
KpsM::KAN
cj1427::CAT
cj1428::CAT
cj1430::CAT

High MW species

Capsule

LOS

Supernatant   **Pellet**
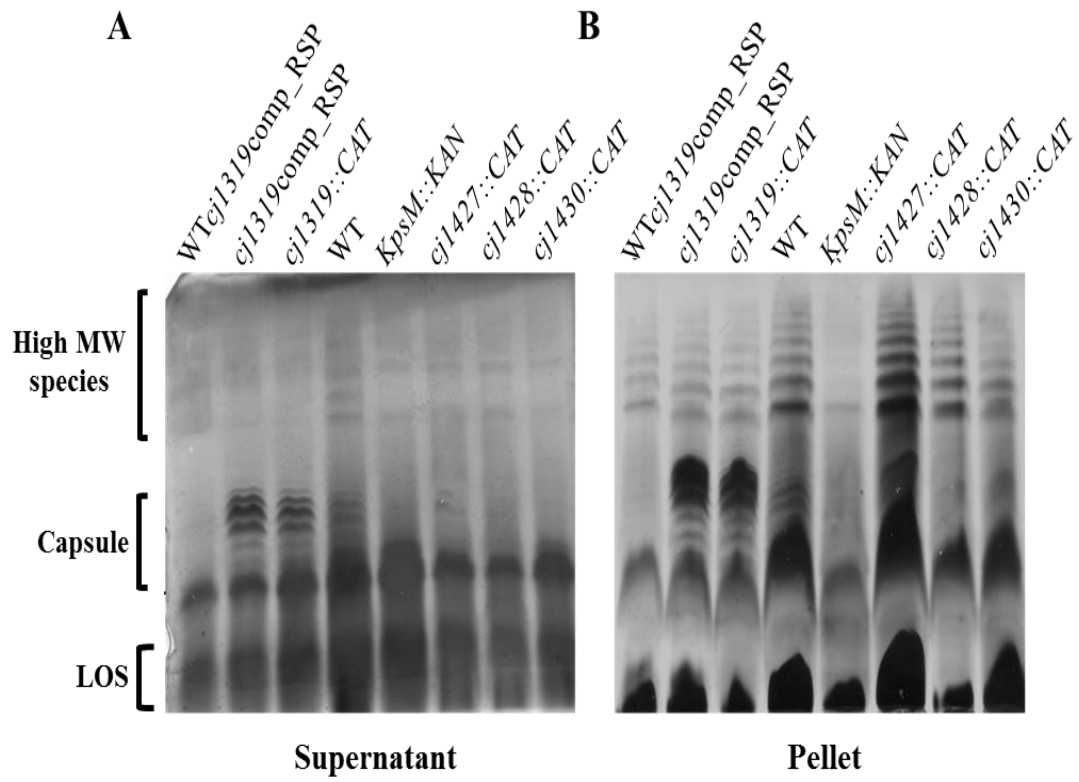
Figure 17. Analysis of high molecular weight species reveals it is LOS and highlights the truncation of the LOS core.

(A) SDS-PAGE of bands excised from a 12% peptide gel showing the high molecular weight species are LOS aggregates. **(B)** Serial dilutions of WT and *cj1319* knockout mutant pellet capsule/LOS samples on a 16% peptide gel stained with silver highlighting the truncation of the inner core of the LOS in the mutant.

A
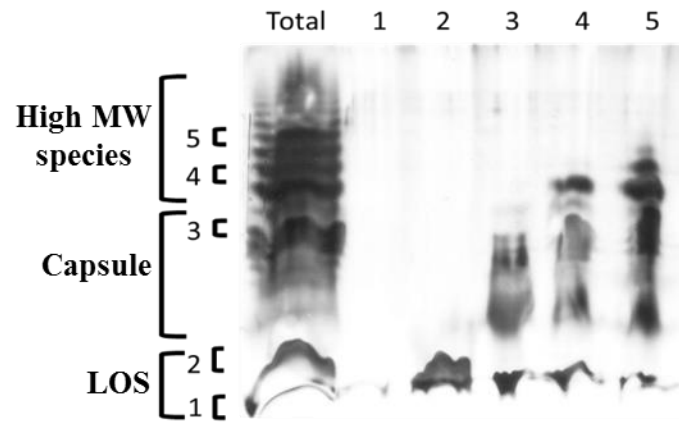
B
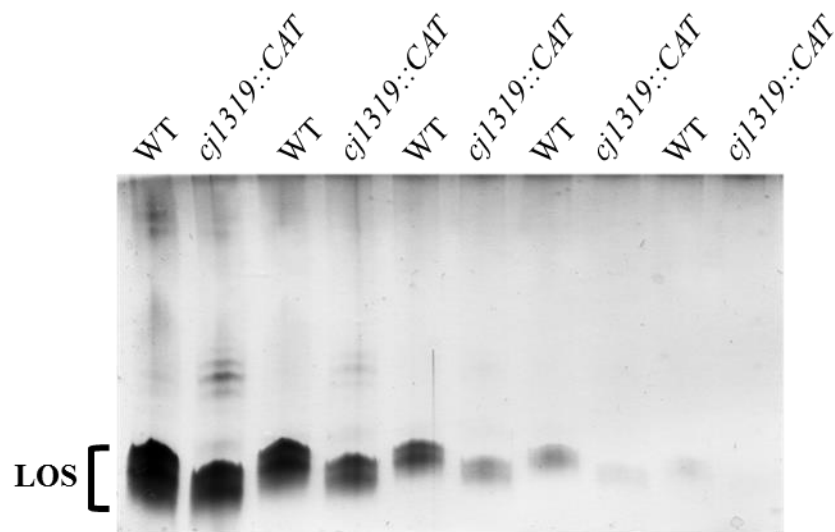
Effect of *cj1319* inactivation on capsule and LOS as assessed by compositional analysis

To aid the interpretation of the band shifts observed by SDS-PAGE, a compositional analysis of the samples was performed at the Complex Carbohydrate Research Center (CCRC), Athens, GA. The bulk of the capsule and LOS pelleted following ultracentrifugation, thus this sample was used for the compositional analysis (Figure 16). To simplify the analysis, we separated the capsule from the LOS by taking advantage of the different solubility tendencies of the two species in alcohol. Isopropanol and ethanol were tested at different concentrations, and it was determined that isopropanol was the best solvent in separating the LOS from capsule at an optimal concentration of 50%, whereby the LOS pellets at a low speed spin and the capsule remains soluble (Figure 18). Both the corresponding CPS and LOS samples of the WT and *cj1319* knockout mutant were processed by per-O-trimethylsilylation and GC-MS for compositional analysis at the CCRC and the results are summarized in (Appendix B, Table 10). The structures of the LOS and capsule which have been published for our strain are presented in (Figure 2A and Figure 4B).

Figure 18. Separation of capsule from LOS by differential solubility in 50% isopropanol.

Pellet samples shown in Figure 16B separated into insoluble LOS and soluble CPS following addition of isopropanol to a final concentration of 50% (v/v).
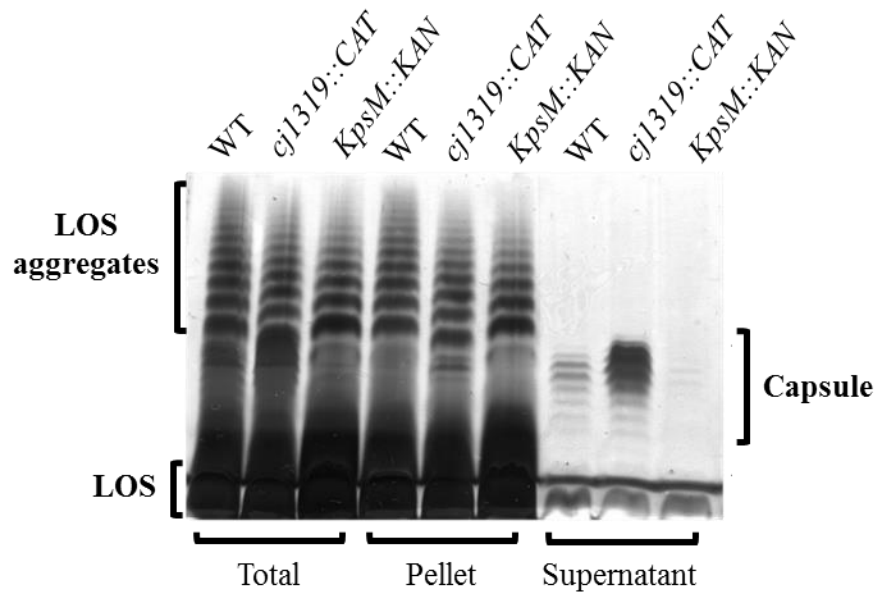
No change in the capsule composition of the *cj1319::CAT* mutant

As shown in Table 10 (Appendix B), there was no difference in the capsule composition between the WT and mutant. Since *cj1319::CAT* still makes the modified heptose, this is in line with our enzymology work, where we excluded Cj1319 from this heptose modification pathway.

Furthermore, the enhanced capsule phenotype observed in the *cj1319::CAT* mutant could not be complemented (data not shown). In light of this, we concluded that the enhanced expression of higher molecular weight capsule chains is likely due to a secondary mutation rather than due to the disruption of *cj1319*. Five genes in the capsule locus of our strain contain hypervariable sequences, four of which code for methyltransferases, including *cj1426c* which encodes the probable C6-*O*-methyltransferase for heptose modification (Sternberg *et al*., 2013)*,* and one of unknown function, *cj1429c* (Parkhill *et al*., 2000). We did not expect that methylation would affect the amount of capsule produced because previous studies of capsule methylation phase variants did not show that there were differences in capsule abundance among variants (Szymanski *et al*., 2003). However, since *cj1426c* is of interest in our study, we examined this gene for phase variation. We determined through sequencing that *cj1426c* did not phase vary from WT by slipped-strand mutagenesis in its phase variable poly-G tract, however, we did find two point mutations which lead to a change of C111 to W. The impact of this mutation is not known. We also examined *cj1429c* since its function is unknown and we found it was expressed in both the WT and the *cj1319::CAT* mutant.

Change in LOS composition leads to the identification of secondary mutations in *cj1319::CAT*

We found that the mutant had a reduced amount of galactose in the LOS, consistent with the truncation we observed by SDS-PAGE and silver staining. Through sequencing phase variable genes in the LOS cluster (Table 6), we found that the truncation was due to a point mutation in a β-1,3-galactose transferase gene*, cj1139*, which leads to an immature stop in translation and thus no functional transferase is made (Linton *et al*., 2000). Thus the truncation of the LOS is not caused by the *cj1319* mutation, which is further supported by

finding the same mutation in the *cj1319*comp_RSP which also produces truncated LOS. Interestingly, we found another point mutation in *cj1144/45*, encoding a putative α1,4 galactosyltransferase whose precise function is unknown, however, it has been found associated with alterations in the LOS composition (Semchenko *et al*., 2012). This gene was found in the 'OFF' state in WT, but in the 'ON' state in the mutant, suggesting that the *cj1319* mutant expresses a galactosyltransferase not expressed in the WT. However, it does not appear to be compensating for the loss of Cj1139 based on the composition analysis of the LOS. Therefore, it is not clear what phenotypic change this mutation created in the *cj1319* mutant. We found the same truncated phenotype in the *cj1319*comp_RNP and *cj1319*comp_ONP, further emphasizing that this truncation is due to phase variation that occurred while the *cj1319::CAT* mutant was generated and is unrelated to *cj1319*. In light of this discovered phase variation, a new *cj1319::CAT* mutant was generated and the above phase variable genes were sequenced and verified to match that of the WT. However, as these variations were detected at the latest stages of this work, the *cj1319::CAT* mutant with these variations was used in all the phenotypic analyses presented in this work. With the three complement strains, we were able to conclude whether or not each phenotype studied was related specifically to Cj1319 or not.

Table 6. Phase variation of LOS and CPS genes.

gene	WT	*cj1319::CAT*	*cj1319*comp_RSP
cj1139	Poly-8G = ON	Poly-9G = OFF	Poly-9G = OFF
cj1144/45	Poly-9G = OFF	Poly-10G = ON	Poly-10G = ON
cj1426c	Poly-10G= ON	Poly-10G= ON	Poly-10G= ON
		*C111W	*C111W
cj1429c	Poly-10G= ON	Poly-10G= ON	Poly-10G= ON

3.3.3 Effect of *cj1319* inactivation on SDS, polymyxin B and serum resistance

Truncations of the LOS usually affects SDS and polymyxin B sensitivity (Naito *et al*., 2010), thus we sought to determine if the loss of the terminal galactose residue resulted in increased susceptibility of the c*j1319::CAT* mutant to these compounds. We did not find any significant difference in the sensitivity of the mutant to SDS or polymyxin B (MIC of 0.01% and 25 µg/mL respectively).

Capsule has been shown to play an important role in serum resistance (Keo *et al*., 2011), and recently the modified heptose of the capsule was shown to play an important role in this function (Wong *et al*., 2015). We determined that the *cj1319::CAT* mutant produced more high molecular capsule weight chains compared to the WT. Although we later determined that this phenotype was not related to *cj1319*, but rather to a secondary mutation, we investigated the effect of active serum on the *cj1319::CAT* mutant.

Interestingly, despite the abundance of capsule, we found that our mutant was significantly more sensitive to killing by the serum compared to WT ($P<0.05$). We could restore this phenotype to WT in the *cj1319*comp_RNP strain, signifying that this phenotype was specific to *cj1319*.

Figure 19. The *cj1319* knockout mutant is significantly more sensitive to active serum compared to WT.

Bacteria were incubated with or without the addition of active horse serum for 2.5 hours at 37°C and then serially diluted and plated for CFU enumeration. The graph displays the mean of three independent experiments performed in duplicate wells and spot plated in triplicate. * $P<0.05$, ** $P<0.01$, and ***$P<0.001$ by two-way ANOVA. ns. Not significant.
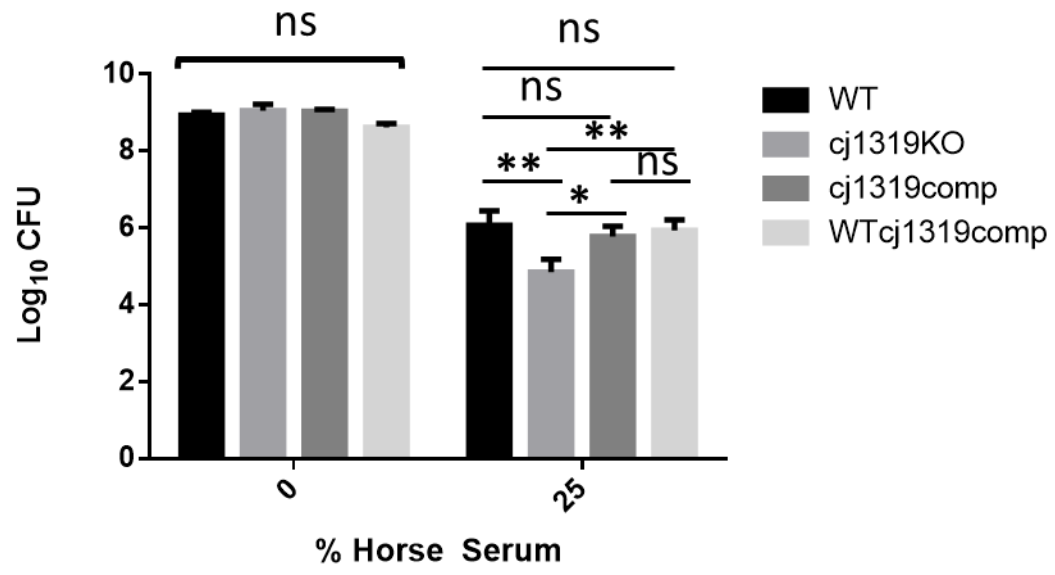
3.3.4 Effect of *cj1319* on motility

An important feature and virulence factor of *C. jejuni* is motility which is affected by general *N*-protein glycosylation (Vijayakumar *et al*., 2006). In addition, mutants of enzymes playing a role in flagellin *O*-glycosylation often have defects in flagellin production, export, and/or flagella formation (Ewing *et al.* 2009; Goon *et al.* 2003). We verified this through testing *cj1121c::CAT* and *cj1294::CAT* and their complemented strains respectively in a soft agar stabbing assay. We found the mutants were not motile and the complement strains partially restored motility (Figure 20A). Since Cj1319 could have a role in protein glycosylation, we examined also examined motility in the *cj1319* mutant. We found no defect in flagellin production as per anti-flagellin Western blot (Figure 20B), no defect in flagella assembly as per electron microscopy (Figure 20C), and no defect in motility compared to WT as per stabbing in semi-solid agar (Figure 20A). The *cj1319*comp_RSP was oddly nonmotile when *cj1319::CAT* had no motility defect. This complement still made full length flagella as determined by EM (Figure 20C). It was apparent that complement constructs with the strong promoter were not optimal due to only partial restoration of motility in *cj1121c*comp_RSP and *cj1294*comp_RSP and abolishment of motility in *cj1319*comp_RSP. Thus we constructed *cj1319*comp_RNP and *cj1319comp_*ONP as detailed in section 3.2, which both express *cj1319* under the regulation of its native promoter. Interestingly, both these complements showed motility defects, although not as drastic as cj1319comp_RSP, whereas WT*cj1319*comp_RNP and WT*cj1319*comp_ONP had no defects in motility. This highlights the importance of the stoichiometry of Cj1319. Furthermore, we did not find any difference in the ability of the *cj1319::CAT* mutant or any of its complement strains to autoagglutinate (data not shown), a feature of *C. jejuni* that has been shown to be correlated with flagellar expression (Misawa and Blaser, 2000).

Figure 20. Cj1319 does not play an integral role in motility or flagellum production.

 (A) Motility halo measurements on 0.3% agar plates (n=6 for all strains except *cj1319*comp_RNP, *cj1319*comp_ONP and their respective WT controls where n=2). Statistical analysis was done by one-way ANOVA. Same letters indicate no significant difference with *P*>0.05. Different letters indicate significant difference with *P*<0.05. **(B)** Western blot analysis of flagellins purified by mechanical shearing. PonceauS Red stain of total proteins (top panel) and anti-flagellin Western blot (bottom panel). MW, molecular weight. **(C)** Electron micrographs of WT (19,000x magnification), *cj1319* knockout mutant (10,500x magnification) and *cj1319*comp_RSP (49,200x magnification). Black arrows point to flagella.

A

B

PonceauS Red

kDa

Anti-flagellin

C
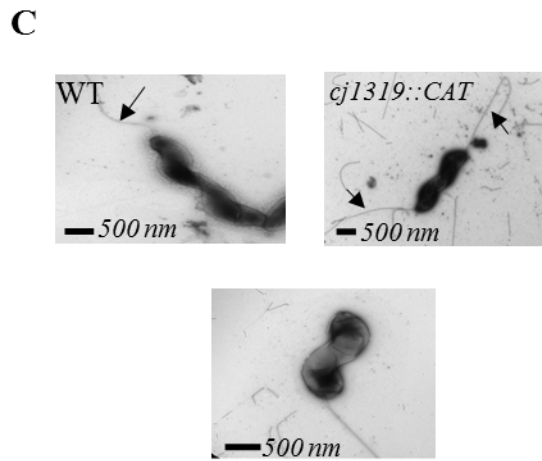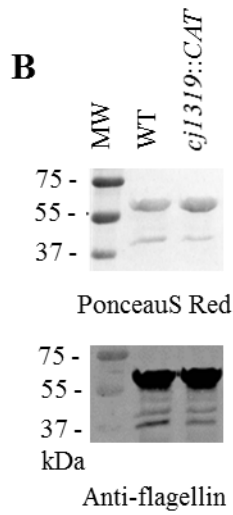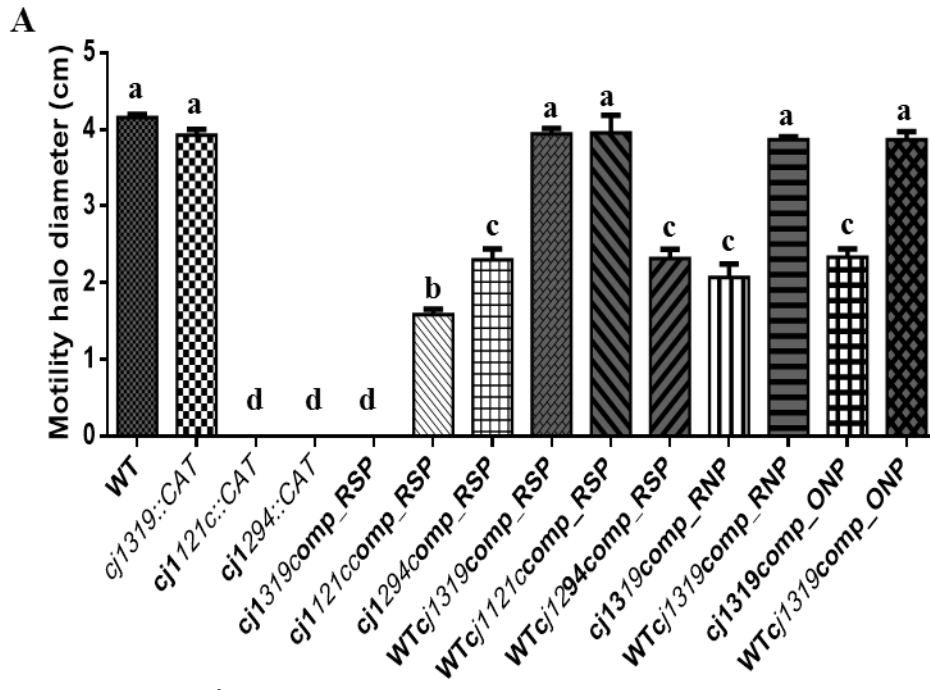
3.3.5 Mass spectrometry analysis of WT *C. jejuni* NCTC 11168 flagellins by HCD-MS[2]

As we observed that the *cj1319* complement strains have motility defects despite assembling normal flagella, we reasoned this may be due to aberrant flagellar glycosylation. Since Cj1319 has been implicated in an *in vitro* pathway for making legionaminic acid for flagellar glycosylation (Schoenhofen *et al*., 2009), dysregulation of *cj1319* expression could lead to altered glycosylation profiles. However, as mentioned previously, there is no *in vivo* data supporting a role for Cj1319 in legionaminic acid synthesis, nor had legionaminic acid been shown to decorate *C. jejuni* flagellins at the onset of this study. Furthermore, flagellin glycopeptide data for *C. jejuni* NCTC 11168 was very limited until the latest stages of our study (Ulasi *et al*., 2015). Therefore, we performed an extensive MS analysis of the WT flagellins of this strain in parallel with *cj1319::CAT* and *cj1319*comp_RSP.

To analyze the flagellin glycopeptides of *C. jejuni* NCTC 11168, the flagella were sheared off the bacterial surface mechanically and concentrated by ultracentrifugation. Bands corresponding to flagellins were excised from SDS-PAGE gels and subjected to in-gel trypsinolysis for MS analysis. The portion of the flagellins that is proposed to be heavily glycosylated, based on sequence alignments with *C. jejuni* 81-176 and *C. coli* VC167, comprises three large tryptic peptides of 2826, 3036 and 4294 Da in flagellin A, corresponding to residues 339-336, 388-420, and 421-463 respectively (Figure 21). The recovery of such large peptides and of their even larger glycosylated forms after in-gel trypsinolysis was anticipated to be low. Thus, after extraction of the tryptic peptides, the gel pieces were further treated with chymotrypsin to reduce the sizes of remaining peptides and maximize extraction. Both sets of peptides were analyzed separately by LC-MS and HCD-MS[2]. This method, not previously used for flagellins, allows to concomitantly detect oxonium ions derived from sugars, acquire peptide sequence, and map glycosylation sites (Segu and Mechref, 2010). Glycopeptides were identified by manual addition of the mass of each sugar found in the metabolome of *C. jejuni* NCTC 11168 (Table 2) into PEAKS software as variable modifications and by manual search for characteristic oxonium ions.

Figure 21. Amino acid sequence of flagellin A from *C. jejuni* NCTC 11168 summarizing glycopeptide and protein coverage data determined by this study and available at onset of this study.

Blue font: peptides covered in nonglycosylated form (this study). Red font: glycopeptides covered (this study). Black font: peptides not detected (this study). Yellow highlight: glycosylation sites previously determined in *C. jejuni* NCTC 11168 (Zampronio *et al*., 2011). Underline: conserved amino acid found glycosylated in *C. jejuni* 81-176 (Thibault *et al*., 2001). Bold: conserved amino acid found glycosylated in *C. coli* VC167 (Logan *et al*., 2002). Black box: Large tryptic peptides predicted to be heavily glycosylated.

```
1    MGFRINTNVA ALNAKANADL NSKSLDASLS RLSSGLRINS AADDASGMAI ADSLRSQANT
61   LGQAISNGND ALGILQTADK AMDEQLKILD TIKTKATQAA QDGQSLKTRT MLQADINRLM
121  EELDNIANTT SFNGKQLLSG NFINQEFQIG ASSNQTVKAT IGATQSSKIG LTRFETGGRI
181  STSGEVQFTL KNYNGIDDFQ FQKVVISTSV GTGLGALADE INKNADKTGV RATFTVETRG
241  IAAVRAGATS DTFAINGVKI GKVDYKDGDA NGALVAAINS VKDTTGVEAS IDANGQLLLT
301  SREGRGIKID GNIGGGAFIN ADMKENYGRL SLVKNDGKDI LISGSNLSSA GFGATQFISQ
361  ASVSLRESKG QIDANIADAM GFGSANKGVV LGGYSSVSAY MSSAGSGFSS GSGYSVGSGK
421  NYSTGFANAI AISAASQLST VYNVSAGSGF SSGSTLSQFA TMKTTAFGVK DETAGVTTLK
481  GAMAVMDIAE TAITNLDQIR ADIGSVQNQV TSTINNITVT QVNVKAAESQ IRDVDFAAES
541  ANYSKANILA QSGSYAMAQA NSVQQNVLRL LQ
```

Using this approach, we were able to detect 7 different glycopeptides from the WT, five of which were in multiple glycoforms (Table 7). The peptide $T_{464}T_{465}$AFGVKDETAGVTTLK for example, was found unmodified (Figure 22A) and modified by sugar masses consistent with Pse5Ac7Am/Leg5Am7Ac, or Pse5Ac7Ac/Leg5Ac7Ac (Figure 22B and C). It was also found modified by either one of Pse5AcGriMe7Ac or Pse5AcGriMe7Am (Figure 22D and E) as previously reported (Zampronio *et al.* 2011). This peptide was additionally found carrying an unknown sugar of 372.145 Da (Figure 23A), as a peak at 373.160 m/z signifying a potential sugar oxonium ion was observed for this glycopeptide. We were able to identify the glycosylation site through the presence of b-ions (peptide fragments originating from sequential losses of amino acids from the C- terminus) which, compared with b-ions of the unmodified peptide, comprise the additional mass of a sugar. For example, two ions at 518.243 m/z (b_2 + 315.143 Da) and 589.281 m/z (b_3 + 315.143 Da) are consistent with TT and TTA each carrying Pse5Ac7Am/Leg5Am7Ac, respectively (Figure 22B). This indicates that glycosylation occurs on T464 or T465. Glycosylation was also mapped at the same two positions for all other glycoforms of this peptide (Figure 22C, D, E and Figure 23A). As the glycosylation occurred at the N-terminus, no y-ions (originating from sequential losses of amino acids from the N- terminus) were observed carrying a sugar.

Similarly, the peptide IS_{181}TSGEVQF was also found in four different glycoforms (Appendix B, Figure 47 and Figure 23B) and we mapped the glycosylation to residue S181 as determined by the ion of 516.265 m/z (b_2 + 315.143 Da) for modification by Pse5Ac7Am/Leg5Am7Ac (Appendix B, Figure 47A), 590.307 m/z (b_2 + 389.180 Da) for modification by Pse5AcGriMe7Am (Appendix B, Figure 47B), and 591.283 m/z (b_2 + 390.164 Da) for modification by Pse5AcGriMe7Ac (Appendix B, Figure 47C). A longer peptide, encompassing IS_{181}TSGEVQF, was found modified by an unknown sugar of 372.145 Da, but found consistently modified at S181 by detection of the fragment ion 1321.640 m/z (b_9 + 372.145 Da), although modification on T182 could not be excluded for this glycoform (Figure 23B).

Table 7. Summary of glycopeptide data collected in *C. jejuni* NCTC 11168 from this study showing the extensive microheterogeneity of flagellin glycosylation.

Peptide sequence[a]	WT	*cj1319::CAT*	*cj1319*comp_RSP
I**S**TSGEVQF[b]	⬢◆⬠▲	⬢◆⬠▲✶	⬢◆⬠▲
VVI**ST**SVGTGL[c]	⬢◆⬠▲▲	⬢◆⬠▲▲✶	⬢◆⬠▲▲
NDGKDILI**S**G**S**NL**SS**AGF[d]	⬢▲, ⬢⬢ ◆◆, ◆⬠	⬢▲, ⬢⬢ ◆◆, ▲▲ ▲▲✶	⬢▲, ⬢⬢ ◆◆
GVVLGGYSSVSAYMSSAGSG FSSGSGYSVGSGK	⬢▲✶▲	Peptide not detected	Peptide not detected
NY**S**TGF	⬢	⬢	Peptide not detected
SQFATMK	◆	Peptide not detected	Peptide not detected
TTAFGVKDETAGVTTLK[e]	⬢◆⬠▲▲	⬢◆⬠▲▲✶	⬢◆⬠▲▲✶

[a] Glycosylation sites were determined as, or narrowed down to, the bold underlined residues.

[b] Additionally detected as FETGGRISTSGEVQFTLK

[c] Additionally detected as VVISTSVGTGLGALADEINKNADK and VVISTSVGTGLGALADEINK

[d] Additionally detected as DILISGSNLSSAGFGATQFI SQASVSLR, NDGKDILISGSNLSSAGFGATQFISQASVSLR, and DILISGSNLSSAGF

⎣⎯⎦ indicates two glycans detected on this peptide – one at S5 or S7 and one at S10 or S11

[e] Also found unmodified in all strains

Sugars are simplified in symbol form as described in table 2 in addition to: unknown putative sugar 372.154 m/z (▲).

Figure 22. HCD-MS^2 analysis of a WT flagellin peptide showing multiple glycoforms and nonglycosylated form.

(A) Unmodified peptide. The same peptide glycosylated with **(B)** Pse5Ac7Am or Leg5Am7Ac (⬤ 315.143 Da), **(C)** Pse5Ac7Ac or Leg5Ac7Ac (▲ 316.127 Da), **(D)** Pse5AcGriMe7Am (◆ 389.180 Da), and **(E)** Pse5AcGriMe7Ac (⬟ 390.164 Da). For all figures, the respective oxonium ion for each sugar is represented on the spectra using the same symbol with a (+) sign and important ions representing peptide + sugar masses are highlighted on spectra.

A TTAFGVKDETAGVTTLK

PEPTIDE[1+]
1738.9130

TT
b₂ 203.103

TTA
b₃ 274.140

AFGVKDETAGVTTLK
y₁₅ 1536.842

B TTAFGVKDETAGVTTLK

b₂ + 315.143
518.243

TT

b₃ + 315.143
589.281

TTA

b₆ + 315.143
892.438

b₁₀ + 315.143
1365.650

AFGVKDETAGVTTLK
y₁₅ 1536.842

b₉ + 315.143
1264.602

316.149

C TTAFGVKDETAGVTTLK (▲ partially mapped)

AFGVKDETAGVTTLK
y₁₅ 1536.842

317.134

b₁₀ + 316.127
1366.640

D TTAFGVKDETAGVTTLK

390.187

TTA

b₃ + 389.180
663.319

b₁₀ + 389.180
1439.687

AFGVKDETAGVTTLK
y₁₅ 1536.842

E TTAFGVKDETAGVTTLK (⬠ partially mapped)

391.170

b₁₀ + 390.164
1440.677

AFGVKDETAGVTTLK
y₁₅ 1536.842

Figure 23. HCD-MS^2 analysis showing three peptides carrying an additional mass of 372.145 Da ( ), indicative of a possible novel glycan in NCTC 11168.

(A) TTAFGVKDETAGVTTLK, **(B)** FETGGR<u>ISTSGEVQF</u>TLK, and **(C)** VVISTSVGTGLGALADEINK with the oxonium ion (373.16 m/z).

A

TTAFGVKDETAGVTTLK

Intensity (%)

50

25

+ 373.160

y$_6$

y$_{10}$

y$_{11}$

y$_{13}$

y$_{15}$

TTAFGVKD

b$_8$ + 372.145
1192.565

PEPTIDE[1+]
1738.916

PEPTIDE[1+]
2111.056

-372.145 Da

500   1000   1500   m/z

B

FETGGR<u>IST</u>SGEVQFTLK (partially mapped)

Intensity (%)

50

25

b$_2$

+ 373.160

b$_{12}$

FETGGRIST

b$_{13}$ /
b$_9$ + 372.145
b$_{14}$ 1321.640

500   1000   1500   2000   m/z

C

<u>VVIST</u>SVGTGLGALADEINK

Intensity (%)

100

50

b$_2$

+ 373.160

y$_6$

VVIS

b$_4$ + 372.145
771.382

VVISTS

b$_6$ + 372.145
959.508

y$_9$

VVISTSVGTG

b$_{10}$ + 372.145
1273.669

y$_{13}$

500   1000   1500   m/z

The peptide $VVIS_{207}T_{208}SVGTGL$ was also found carrying five different sugars individually, including the unknown 372.145 Da sugar (Appendix B, Figure 48 and Figure 23C) and out of its four potential O-glycosylation sites, we narrowed the glycosylation site down to S207 or T208 for two of its glycoforms based on its b_5 ion (Appendix B, Figure 48B and C) and to S207 based on the b_4 ion for another glycoform (Figure 23C).

Overall, a total of three different peptides were found carrying the unknown sugar of 372.145 Da (Figure 23), each showing the same oxonium ion peak at m/z 373.160, showing several ions arising from the combined mass of a b ion and this unknown sugar mass, and in one example also showing a 372.145 Da mass difference between the modified and unmodified full peptides (Figure 23A). We pursued the identification of this sugar by targeted third-stage MS (MS^3) of the 373.160 m/z ion (Appendix B, Figure 49). A number of diagnostic ions were observed, namely an ion at 89.002 m/z that is typical of a singly positively charged sugar backbone (C_6O_1 of mass 87.995 Da), an ion at 74.060 m/z that potentially corresponds to the CH_3-CHOH-CH-NH portion of a CH_3-CHOH-CH-NH-CO-CH_3 side chain, mass 73.053 Da, carrying a single positive charge as previously reported (Logan *et al*., 2009), an ion at 59.050 m/z that potentially stems from a singly positively charged N-acetyl side chain (CH_3-CO-NH, mass 58.029 Da), and two ions at 134.060 m/z and 180.066 m/z which were reported as C_1-C_9 sugar backbone ions found in Pse5Ac7Ac and Pse5Am7Ac (Thibault *et al.,* 2001). Of note, in our MS^2 spectra, this 372.145 Da sugar candidate was often found associated with a 391.172 m/z ion (Pse5AcGriMe7Ac), whose break down also releases a 373.160 m/z ion, which prevented us from making a definitive assignment of its identity. Notwithstanding its precise identity, this sugar modification confers further heterogeneity to the flagellins and its biological relevance will be worth investigating.

Moreover, we found the peptide $NDGKDILIS_{343}GS_{345}NLS_{348}S_{349}AGF$ carrying four different combinations of two sugars at once (Appendix B, Figure 50). The 1529.749 m/z (b_{12} + 315.143 Da) ion representing $NDGKDILIS_{343}GS_{345}$ carrying Pse5Ac7Am/Leg5Am7Ac and the 783.355 m/z (y_5 + 315.143 Da) ion representing $S_{348}S_{349}AGF$ carrying Pse5Ac7Am/Leg5Am7Ac in one of the glycoforms (Appendix B, Figure 50A) show that glycosylation occurs at one site comprised of S343 or S345 and at

a second site comprised of S348 or S349. This was consistently shown to be the case with another glycoform (Appendix B, Figure 50C) and two partially mapped glycoforms (Appendix B, Figure 50B and D).

Compared to the tryptic digest alone, the addition of chymotrypsin allowed the detection of two additional glycosylated peptides, NYSTGF and SQFATMK (Appendix B, Figure 51). Their glycosylation was mapped to the serine residue based on the 680.294 m/z (b_3 + 315.143 Da) ion, consistent with NYS carrying Pse5Ac7Am/Leg5Am7Ac, and the 605.278 m/z (b_2 + 389.180 Da) ion, consistent with SQ carrying Pse5AcGriMe7Am. The sequential digest also improved the quality of the data by providing shorter glycopeptide fragments which aided the interpretation of many of the spectra.

We detected a large mass of 5193.280 Da, resulting from the tryptic digest alone, whose HCD-MS^2 spectrum shows oxonium ions 316.150, 317.130 and 330.166 m/z indicative of Pse5Ac7Am/Leg5Am7Ac, Pse5Ac7Ac/Leg5Ac7Ac and Leg5AmNMe7Ac, respectively, as well as ion 373.159 m/z corresponding to the unknown sugar (Figure 24A). Large ions showing sequential losses of 315.143 Da and 316.127 Da were determined by manual analysis to correspond to residues G388 to K420 (3036.3891 Da), which form one of the predicted highly glycosylated peptides indicated in Figure 21. Our manual analysis allowed us to assign the mass of 3982.777 Da to this peptide carrying a total of two Pse5Ac7Am/Leg5Am7Ac (315.143 Da) and one Pse5Ac7Ac/Leg5Ac7Ac (316.127 Da). The additional sugar oxonium ions and extra unassigned mass of the 5193.280 Da glycopeptide that those fragments originated from suggest more extensive glycosylation, however we did not detect fragment ions above 3982.777 Da to further characterize this peptide.

Similarly, we found the same peptide (based on unmodified b and y ions) present as a different glycoform (5231.382 Da), with the strong oxonium ion of 330.166 m/z in addition to large ions showing a loss of 329.159 Da indicative of Leg5AmNMe7Ac (Figure 24B). This shows that the peptide fragment is modified by at least one Leg5AmNMe7Ac residue. We could not fully characterize this fragment which is thus annotated as "partial peptide". This spectrum also shows oxonium ions of 316.150, 317.130 and 373.160 m/z indicative

of Pse5Ac7Am/Leg5Am7Ac, Pse5Ac7Ac/Leg5Ac7Ac and the unknown 372.145 Da species respectively. Overall, the large mass and sugar oxonium ions further highlight the highly glycosylated nature of this peptide. Importantly, these results show for the first time glycopeptide evidence that WT *C. jejuni* NCTC 11168 flagellins carry the Leg5AmNMe7Ac modification, thus directly demonstrating that legionaminic acid is used for flagellin glycosylation in this strain. As mentioned previously, this is based on the fact that the 5AmNMe7Ac modification is unique to legionaminic acid.

Noteworthy, we did not find any peptide modified with O-acetyl pseudaminic acid, N-acetyl glutamic pseudaminic acid derivative or dihydroxypropionyl pseudaminic acid derivative, three sugars shown to modify the flagellins of *C. jejuni* 81-176. Additionally, every glycopeptide found was not detected in an unglycosylated form except for one (Figure 22A).

Figure 24. A highly glycosylated peptide shown carrying Leg5AmNMe7Ac (✿ 329.159 Da).

(**A**) Manual analysis of a HCD-MS^2 spectrum identifying the peptide carrying Pse5Ac7Ac/Leg5Ac7Ac (▲ 316.127 Da), Pse5Ac7Am/Leg5Am7Ac (● 315.143 Da), Leg5AmNMe7Ac, and the unknown putative sugar (▲ 372.145 Da). (**B**) Manual analysis of the HCD-MS^2 spectrum of a second glycoform of this peptide, highlighting the modification by Leg5AmNMe7Ac.

A GVVLGGYSSVSAYMSSAGSGFSSGSGYSVGSGK

B GVVLGGYSSVSAYMSSAGSGFSSGSGYSVGSGK
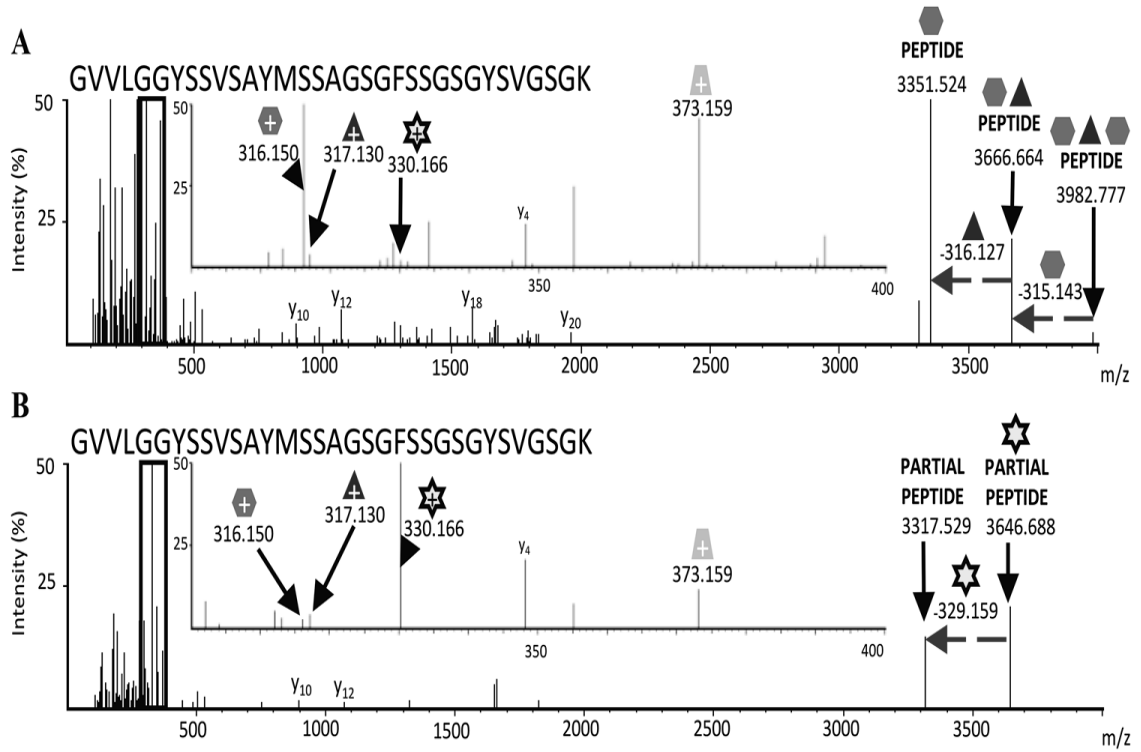
3.3.6 The cj1319 knockout mutant glycosylates its flagellins with Leg5AmNMe7Ac

In *C. coli* VC167, a knockout mutant of a *cj1319* homologue was found to produce significantly more CMP-Leg5Ac7Ac compared to WT (McNally *et al.* 2007). If a *cj1319* mutant of *C. jejuni* also exhibited the same phenotype, this would further demonstrate flagellin glycosylation by legionaminic acid in *C. jejuni* and would exclude Cj1319 from the legionaminic acid synthesis pathway. Thus we investigated the presence of legionaminic acid on the flagellins of our *cj1319* mutant. We showed that this mutant had no defects in flagellin production, export, and assembly nor in motility (Figure 20), and thus the flagellins purified from the mutant were processed and analyzed by MS as described for WT. We found that the *cj1319* mutant still glycosylates its flagellins with all the same modifications as determined in the WT (Table 7). Importantly, we also detected Leg5AcNMe7Ac (329.159 Da) on four different peptide sequences, contributing to four of the total 23 glycoforms detected in this mutant (Figure 25, Table 7). The addition of Leg5AcNMe7Ac to these peptides did not otherwise change the glycosylation sites as highlighted by ions representing peptide fragments with the bound sugar (Figure 25A, B and D). These results show that legionaminic acid can be used for flagellin glycosylation without drastically altering the global flagellin glycosylation pattern and that Cj1319 is not required for legionaminic acid synthesis, although it does affect its incorporation onto flagellins.

To assess if this phenotype was specific to *cj1319,* we complemented *cj1319* in *cis* using a strong constitutive promoter to ensure the expression of Cj1319. The flagellins of this complemented strain were analyzed using the same method and the glycopeptide data are summarized in Table 7. We only detected Leg5AmNMe7Ac on one peptide in this strain, compared to four peptides in the *cj1319* knockout mutant but readily detected peptides glycosylated by pseudaminic acid and its derivatives, suggesting successful (although partial) complementation. This shows that the enhanced incorporation of legionaminic acid on the flagellins of the *cj1319* knockout mutant is indeed due to Cj1319 specifically.

Figure 25. HCD-MS^2 analysis of the *cj1319* knockout mutant reveals four different peptide sequences glycosylated with Leg5AmNMe7Ac (✡ 329.159 Da).

(A) ISTSGEVQF, **(B)** VVISTSVGTGLGALADEINK, **(C)** NDGKDILISGSNLSSAGFGATQFISQASVSLR (additionally modified with Pse5Ac7Ac/Leg5Ac7Ac (▲ 316.127 Da)), and **(D)** TTAFGVKDETAGVTTLK.
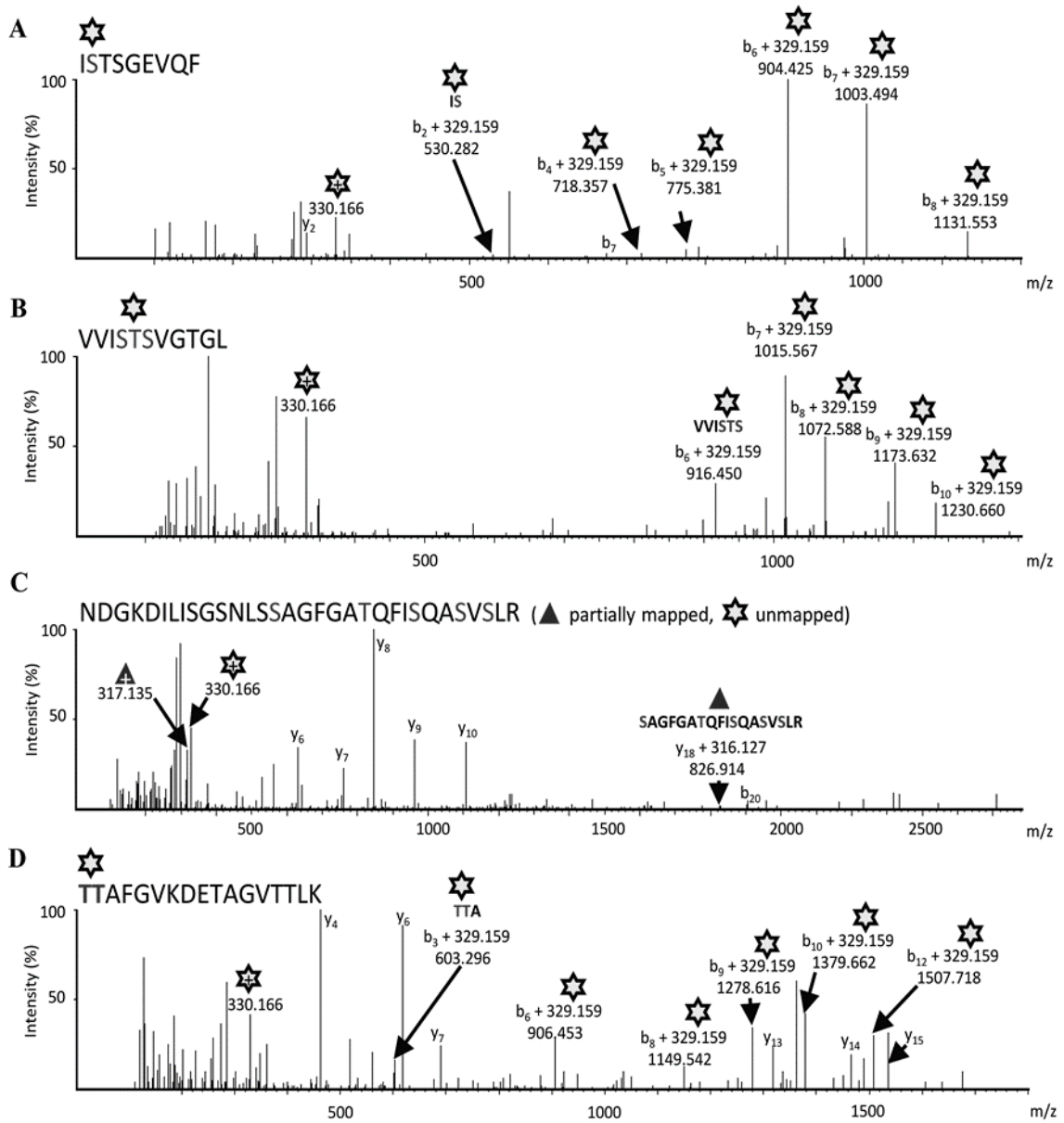
Legionaminic acid synthesis in *L. pneumophila* has been demonstrated *in vitro* using the neuraminic acid synthesis enzymes on UDP-bacillosamine, which is produced by the *N*-glycosylation pathway in *C. jejuni* (Glaze *et al*., 2008). These enzymes are homologous to the *C. jejuni* enzymes used for making the sialic acid of LOS. Although deemed highly unlikely, we acknowledged that these enzymes may compensate for the lack of Cj1319, if Cj1319 normally is involved in making legionaminic acid, by using UDP-bacillosamine produced by the *N*-glycosylation pathway. If so, we expect there would be an increase in the expression of these enzymes that would allow them to compete for UDP-bacillosamine and result in making legionaminic acid. Therefore, we used qRT-PCR to measure the level of expression of these sialic acid synthesis genes in the WT and *cj1319::CAT* strains. No significant difference was determined in the level of expression of these genes between the two strains (Figure 26). Thus there was no apparent compensatory mechanism occurring.

Figure 26. Fold change in sialic acid synthesis genes in the *cj1319::CAT* mutant compared to WT as determined by qRT-PCR.

Genetic organization of the genes targeted for the qRT-PCR analysis is depicted (not drawn to scale). The interstrain change in gene expression compared to the WT is reported in the table shown. The fold change in expression was determined from two biological replicates, each tested in duplicate. The brackets indicate $2^{(\Delta\Delta CT-SD)}$ and $2^{(\Delta\Delta CT+SD)}$, where SD represents the standard error propagated through the fold calculations. No significant difference was determined by Student's t test.

UDP-GlcNAc

↓ Cj1142

↓ Cj1141

↓ Cj1143

CMP-NANA

	cj1319::CAT
cj1142	0.72 (0.27-1.90)
cj1141	0.91 (0.35-2.36)
cj1143	1.50 (0.28-8.18)
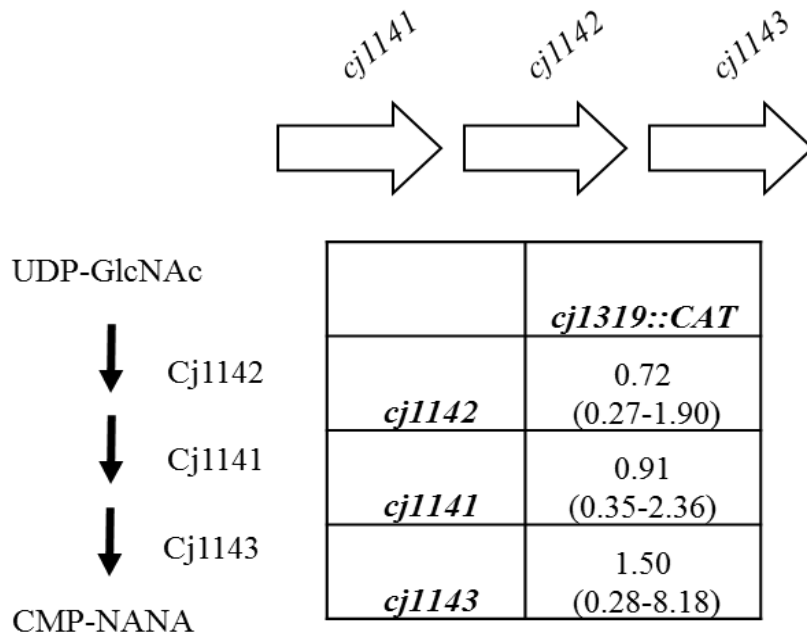
3.3.7 Investigation of the role of Cj1319 in non-flagellar protein glycosylation

We determined that Cj1319 does not have a role in capsular heptose modification based on enzymology studies and that it is not required for legionaminic acid synthesis. Therefore, we hypothesized that Cj1319 likely plays a role in non-flagellar protein glycosylation. To address this, we screened cell free extracts of the *cj1319::CAT* mutant compared to those of the WT and the *cj1121c::CAT* and *cj1294::CAT* protein glycosylation pathway mutants. To increase the resolution of the screening, cell free extracts were fractionated into soluble and membrane proteins. The membranes were further divided into inner membrane and outer membrane fractions based on the differential solubility of the inner membrane in the detergent N-laurylsarcosine. We labelled glycoproteins with biotin hydrazide post mild periodate-based oxidation and the proteins were separated by SDS-PAGE and analyzed by Western blot using fluorescently labelled streptavidin (Figure 27). We did not observe any striking difference in the glycoprotein profiles of *cj1319::CAT* compared to WT in any of the protein fractions using this method. However, an important observation to note is that the *cj1121c::CAT* mutant's glycoprotein profile only differed to the WT in the outer membrane proteins, where glycoproteins at ~50-52 kDa are missing in this mutant, but are restored upon complementation (Figure 27D). It is also interesting to note that *cj1294::CAT* is missing a major outer membrane protein of ~60-62 kDa which is consistent with the flagellins, however, this protein is not restored to the outer membrane upon complementation. The same protein in the *cj1319::CAT* mutant is more abundant and reactive with biotin hydrazide compared to the WT and its complement.

Figure 27. Western blot analysis of the glycoprotein profiles of *C. jejuni* **strains using biotin hydrazide labelling.**

Representative blots of glycoprotein profiles of **(A)** soluble proteins, **(B)** total membrane proteins, **(C)** inner membrane proteins, and **(D)** outer membrane proteins pre-labelled with biotin hydrazide. The bracket indicates area where differences were perceived in the outer membrane samples. Detection was accomplished using fluorescently labelled streptavidin.

A

MW WT *cj1319::CAT* *cj1121c::CAT* *cj1294::CAT* *cj1319comp_RSP* *cj1121ccomp_RSP* *cj1294comp_RSP*

WT *cj1319::CAT* *cj1121c::CAT* *cj1294::CAT* *cj1319comp_RSP* *cj1121ccomp_RSP* *cj1294comp_RSP*

97
66
45
31
21
kDa

Soluble

B

66
45
31
21
14
kDa

Total membrane

C

66
45
31
21
14
kDa

Inner membrane

D

92
52
29
21.5
kDa

Outer membrane

PonceauS Red

Biotin hydrazide/streptavidin
(Chemical)
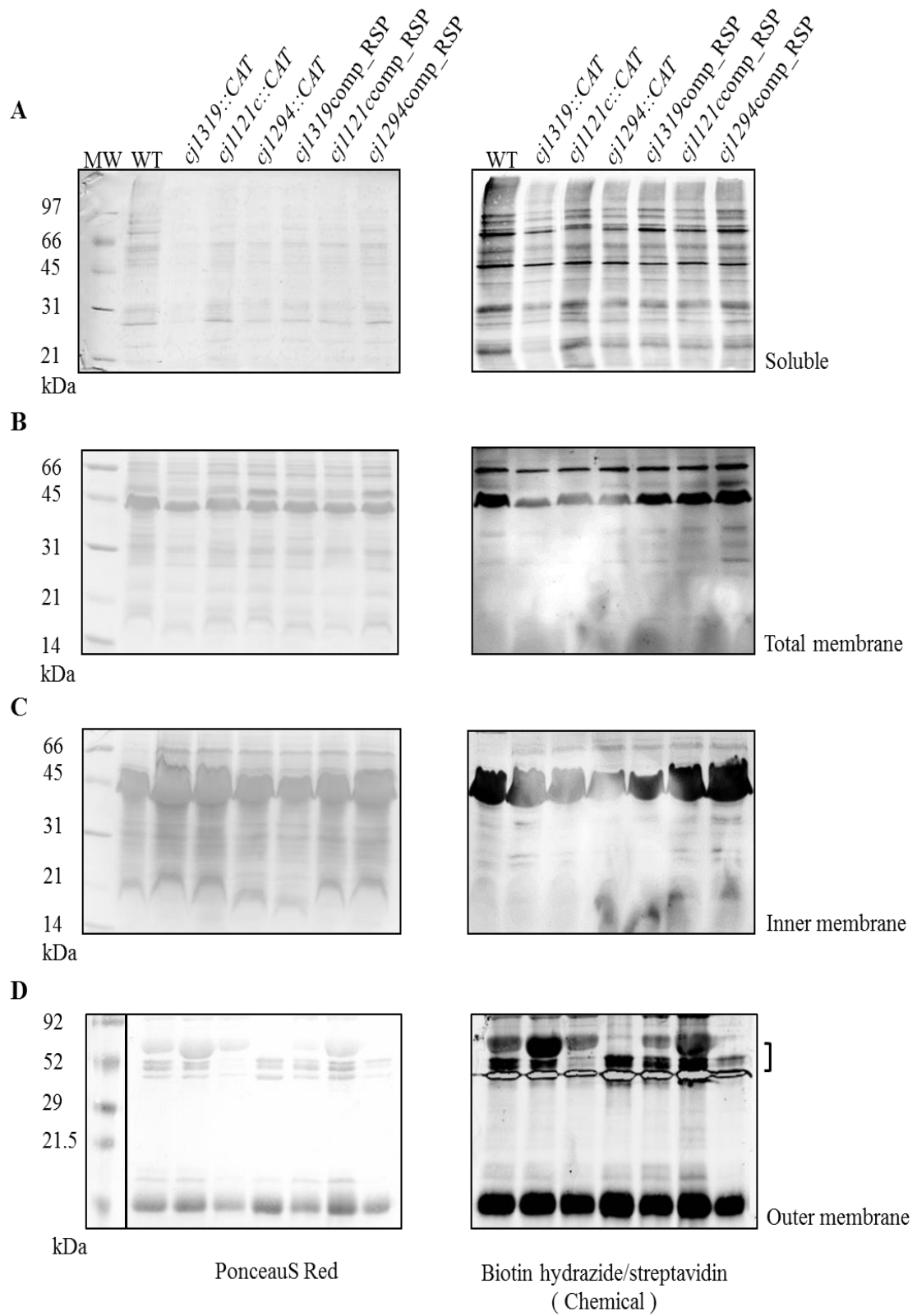
The prior glycoprotein detection method did not perceive differences between the *cj1121* mutant and the WT although we know Cj1121c is part of the *N*-glycosylation pathway which glycosylates over 60 proteins, both soluble and membrane proteins (Scott *et al.*, 2011). Thus we could conclude that the biotin hydrazide labelling method was either labelling more than just glycoproteins or that there were glycoproteins beyond those modified by the general *N*-glycosyltaion pathway that were masking the signals disappearing in the *cj1121c* mutant. Therefore, we used the soybean-agglutinin (SBA) lectin which was originally used to detect the *N*-glycosylated proteins in *C. jejuni* by Western blot (Young *et al.*, 2002). This lectin binds terminal α- and β-GalNAc residues which are found in the *N*-linked heptasaccharide. Similar to the biotin hydrazide labelling method, we did not perceive any obvious difference between the *cj1319* mutant and the WT (Figure 28). In *cj1121c::CAT*, we still observed many glycoprotein bands and only glycoproteins at ~50-52 kDa are missing in the membrane fraction, but restored upon complementation (Figure 28B).

Figure 28. Western blot analysis of glycoprotein profiles of *C. jejuni* strains using anti-SBA.

Representative blots of glycoprotein profiles of **(A)** soluble proteins and **(B)** total membrane proteins using anti-SBA for the detection of glycoproteins containing terminal GalNAc. The bracket indicates area where differences were perceived in the membrane samples.

A

MW WT *cj1319::CAT* *cj1121c::CAT* *cj1294::CAT* *cj1319comp_RSP* *cj1121ccomp_RSP* *cj1294comp_RSP*

97
66
45

31

21

14

kDa

WT *cj1319::CAT* *cj1121c::CAT* *cj1294::CAT* *cj1319comp_RSP* *cj1121ccomp_RSP* *cj1294comp_RSP*

Soluble

B

97
66

45

31

21

kDa

PonceauS Red

Anti-SBA

Total membrane
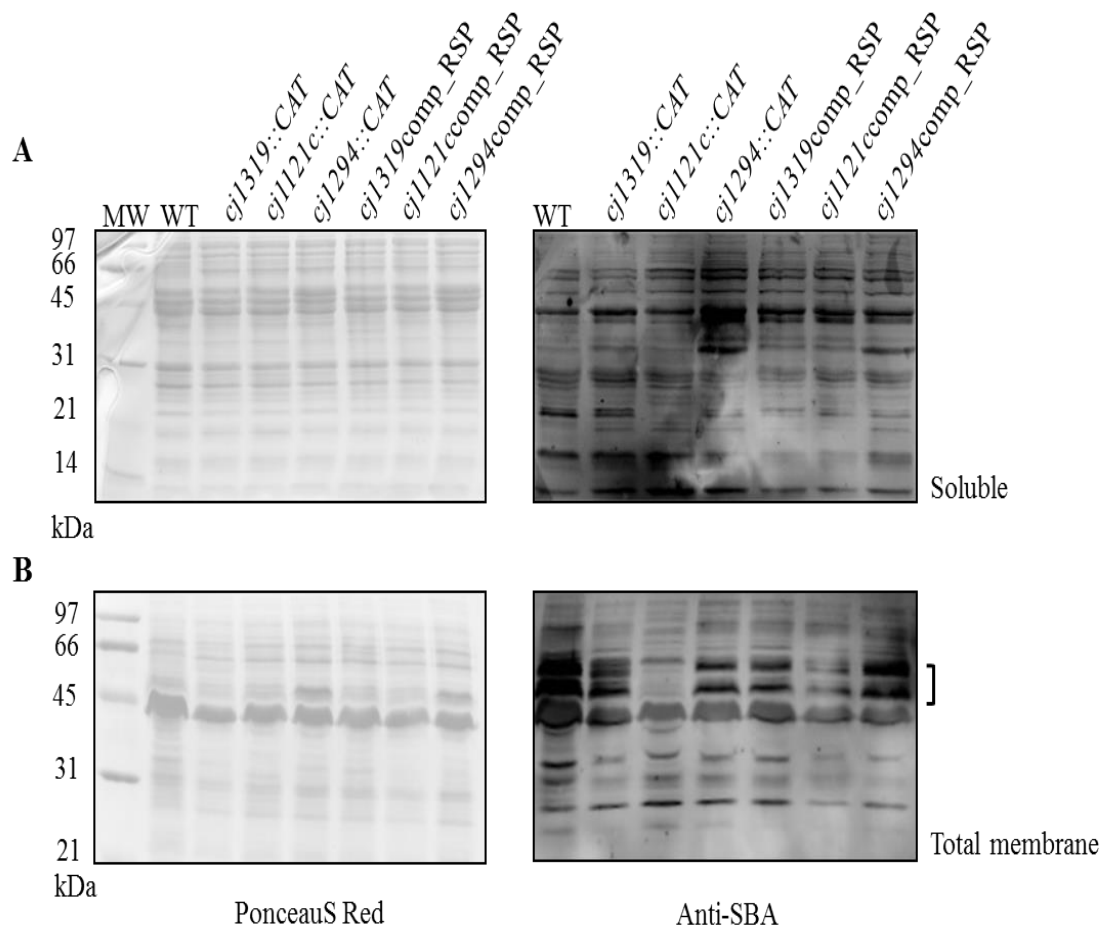
GDP-mannose can be used to make GDP-fucose through the action of a dehydratase and a 3,5-epimerase/4-reductase. If Cj1319 can dehydrate GDP-mannose, it is possible that fucose would be the end product on the Cj1319 pathway and serve for protein glycosylation. Although we had determined enzymatically that Cj1319 could not use GDP-mannose as a substrate, we had concurrently tested for the presense of fucosylated proteins in *C. jejuni* using two fucose binding lectins, BambL (Audfray *et al*., 2012) and PAII-L (Mitchell *et al*., 2005), in Western blot analysis of protein fractions. Interestingly, both lectins were able to bind some soluble proteins, but no membrane proteins (Appendix B, Figure 52). However, in agreement with our enzymatic assays, we found no differences between the fucosylated glycoprotein profiles of the WT and *cj1319* mutant. Similarly, we screened for heptose modified proteins using a heptose binding lectin, BC2L-A (Marchetti *et al*., 2012), by Western blot. However, this lectin did not bind to any proteins (data not shown). This lectin could also not bind the modified heptose of the capsule as per Western blot (data not shown) and thus we concluded that this lectin is specific to unmodified heptose and was not suitable for detection of modified heptoses that could be produced by the Cj1319 pathway. However, to our knowledge, such a lectin does not exist and since we did not find a role for Cj1319 in heptose modification enzymatically, we did not pursue this analysis further.

Although we were limited by the resolution of the 1D Western blot analysis of glycoprotein profiles, we were able to conclude that there were glycoproteins modified by a pathway other than the general *N*-protein glycosylation pathway as marked by the analysis of the *cj1121c* mutant. In addition, although we did not perceive any differences in glycoprotein profiles of the *cj1319* mutant compared to WT, we could not exclude the possibility that enzymes of the other two protein glycosylation pathways may act to compensate for the loss of Cj1319 or vice versa. To determine if this could occur, we used qRT-PCR to measure the level of gene expression of protein glycosylation genes and *cj1319* in the *cj1319* mutant compared to WT and the two protein glycosylation pathway mutants, including their respective complemented strains. There were no notable changes in gene expression in any of the genes tested among the strains, and thus no compensatory mechanism could be inferred (Figure 29). Importantly, these results show that in the

complementation was successful at the level of gene expression, as all three complement strains show high levels of gene expression, owing to the promoter of OmpE.

Figure 29. Fold changes of protein glycosylation pathway genes in our strains of interest compared to WT as determined via qRT-PCR.

Genetic organization of the genes targeted for the qRT-PCR analysis is depicted (not drawn to scale). The interstrain change in gene expression is reported in the table shown as a heat map of low to high gene expression compared to the WT. The fold change in expression was determined from three biological replicates, each tested in duplicate in the case of *cj1319::CAT* and *cj1319*comp_RSP or one biological replicate tested in duplicate for the other strains. The brackets indicate $2^{(\Delta\Delta CT-SD)}$ and $2^{(\Delta\Delta CT+SD)}$, where SD represents the standard error propagated through the fold calculations. No significant difference was determined by Student's t test.

cj1120c cj1121c cj1122c cj1123c

pgl cluster
(*N*-glycosylation)

cj1293 cj1294 cj1298 cj1313

pse cluster
(*O*-glycosylation)

cj1318 cj1319 cj1320 cj1321

Unknown cluster
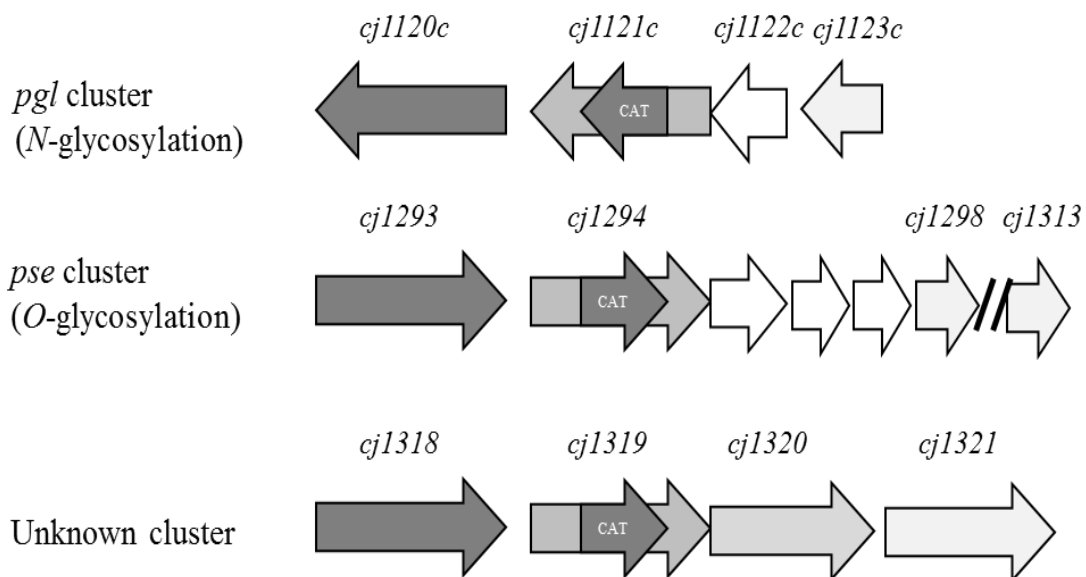
	cj1319::CAT	*cj1121c::CAT*	*cj1294::CAT*	*cj1319comp_RSP*	*cj1121ccomp_RSP*	*cj1294comp_RSP*
cj1319	-	1.52 (1.11-2.07)	1.19 (0.96-1.47)	6.75 (3.27-13.94)	5.77 (4.65-7.15)	1.83 (1.39-2.41)
cj1120c	1.06 (0.63-3.66)	-	-	0.95 (0.84-1.07)	-	-
cj1121c	0.26 (0.22-1.85)	-	0.71 (0.59-0.86)	0.70 (0.62-0.80)	83.94 (68.59-102.54)	1.27 (1.07-1.49)
cj1293	0.85 (0.48-2.85)	-	-	1.88 (1.82-1.93)	-	-
cj1294	0.78 (0.60-4.14)	0.80 (0.68-0.94)	-	0.94 (0.80-1.10)	0.55 (0.40-0.76)	72.10 (46.85-110.66)

Heat map of gene fold expression compared to WT

Low | 0.01 | 0.1 | 0.5 | no change | 2 | 10 | >10 | High
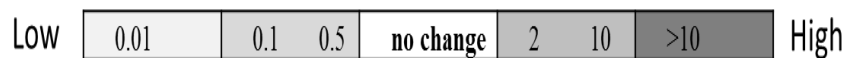
3.3.8 Effect of *cj1319* inactivation on sensitivity to nitrosative and oxidative stress

Despite not finding the biochemical role of Cj1319 in *C. jejuni*, we sought to determine the role of this protein in the interaction of *C. jejuni* with environmental or host stressors. A PhD thesis by Blackwell, 2010 (Dr. Charles Penn, University of Birmingham) suggests that *cj1319* and surrounding genes are regulated by *Nssr*, which regulates the response to nitric oxide. Although the work remains unpublished, it is interesting that genes involved in synthesizing sugars may be regulated in reponse to nitric oxide. Therefore, we sought to determine the effect of nitrosative stress in our strains of interest. Nitric oxide radicals were produced from sodium nitrite at different concentrations in media pH-adjusted to 5.0. The bacteria were allowed to incubate in this media for 30 min and then serially diluted and spot-plated for CFU counts. As a negative control, cells were incubated in the same media without any sodium nitrite. We did not find any significant difference among strains in their sensitivity to nitrosative stress (Figure 30).

Figure 30. *cj1319::CAT* and protein glycosylation mutants do not differ in their sensitivity to nitrosative stress compared to WT.

Data represent the means of six independent experiments for the WT and knockout mutants and two independent experiments for the complement strains, all performed in duplicate wells and spot plated in triplicate. Two-way ANOVA showed no significant difference among strains.

Legend:
- WT
- *cj1319::CAT*
- *cj1121c::CAT*
- *cj1294::CAT*
- *cj1319*comp_RSP
- *cj1121c*comp_RSP
- *cj1294*comp_RSP

Y-axis: CFU/mL

X-axis: Concentration of Nitric oxide — 0 mM, 10 mM, 50 mM, 100 mM
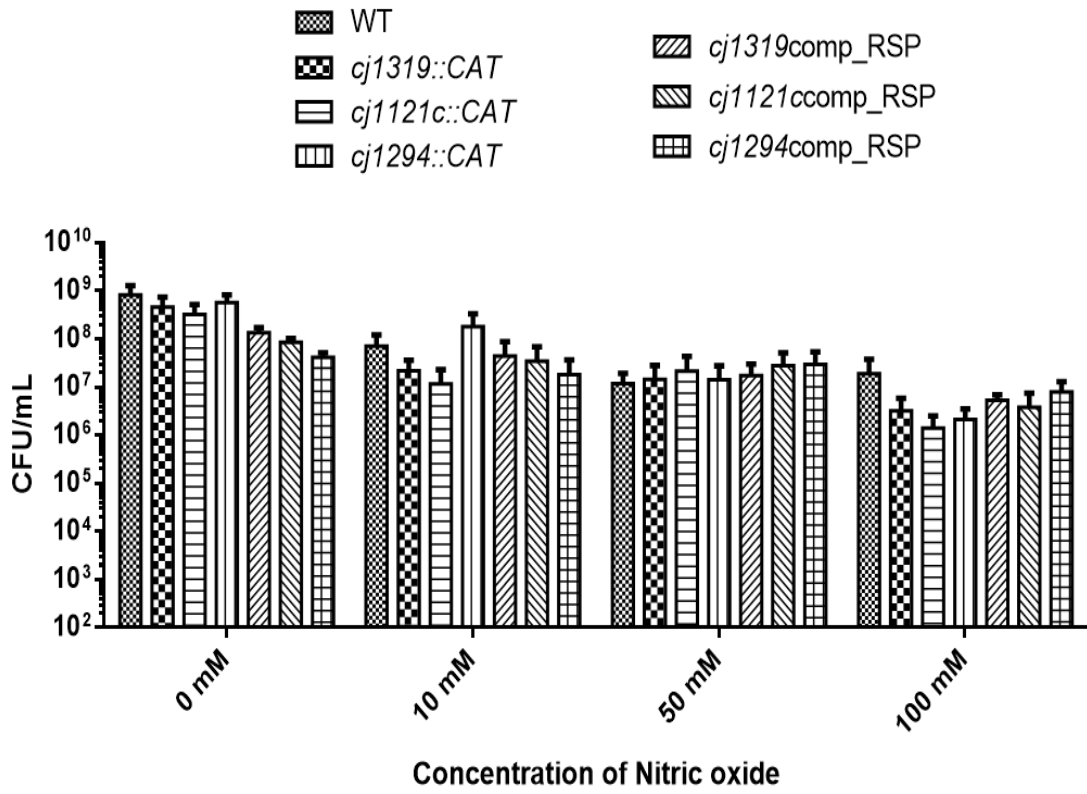
Since *C. jejuni* is microaerophilic, oxidative stress poses an important burden on its ability to survive both in the external environment and within the host. Therefore, we tested the susceptibility of *cj1319::CAT* and protein glycosylation mutants to oxidative stress compared to WT. We performed this as a long term assay whereby diffusible discs with different concentrations of hydrogen peroxide were placed on the surface of freshly inoculated agar and zones of inhibition were measured after 24 h (Figure 31A). Short term survival was assessed by incubating cells with different concentrations of hydrogen peroxide for 30 min and then serially diluting and plating for CFU enumeration (Figure 31B). We found no difference in the long term sensitivity of the strains to oxidative stress and similarly no difference in the short term sensitivity except for *cj1121c::CAT* which was more susceptible to stress at higher concentrations of H_2O_2, however, this was an observed trend that was not determined to be statistically significant by two-way ANOVA.

Figure 31. Susceptibility of *C. jejuni* strains to oxidative stress.

(A) Long term assay measuring zone of inhibition of the hydrogen peroxide discs. Data represent the mean of six independent experiments using three discs per strain. No significant difference was found among strains by two-way ANOVA. **(B)** Short term assay measuring the survival of strains in the presence o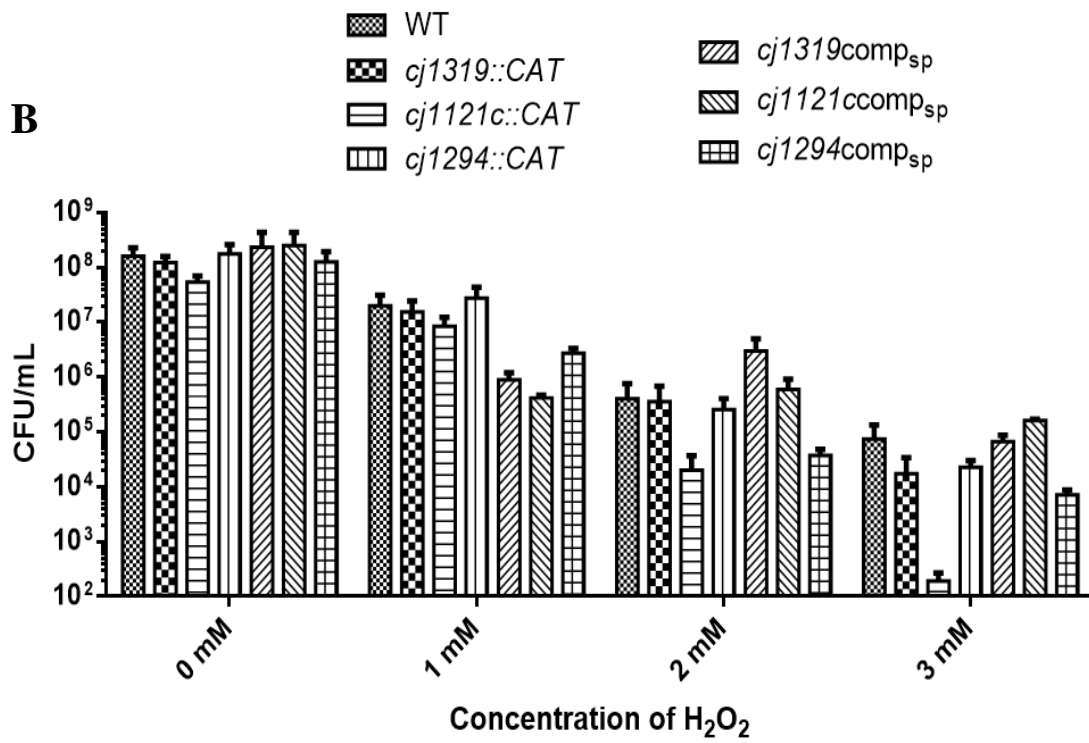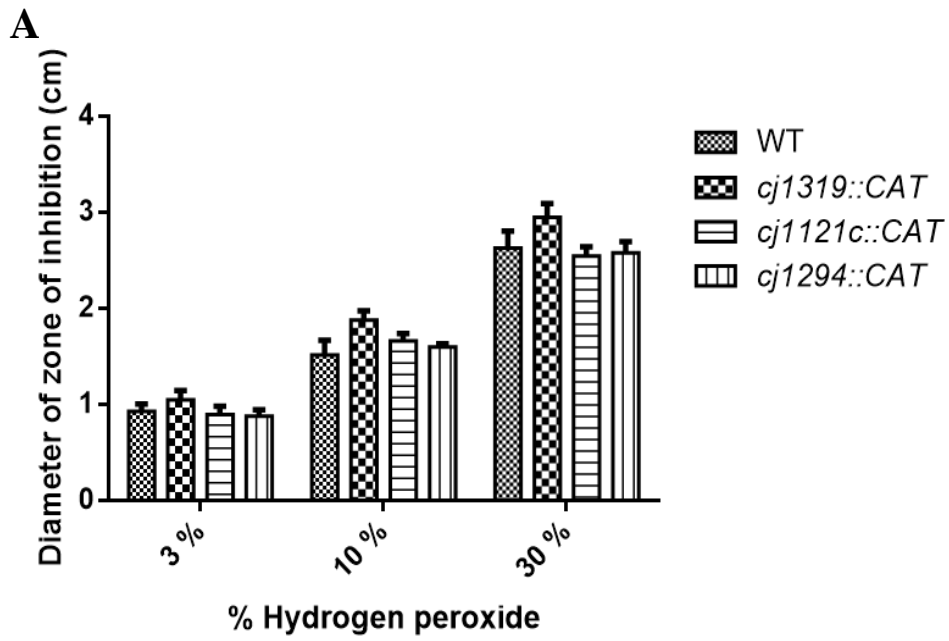f different concentrations of hydrogen peroxide. Data represent the means of six independent experiments for the WT and knockout mutants and two independent experiments for the complement strains, all performed in duplicate wells and spot plated in triplicate. Two-way ANOVA showed no significant difference among strains.

A

B

3.3.9 Effect of *cj1319* inactivation on biofilm production

Biofilm production makes use of an extracellular polymeric matrix to protect the cells within the biofilm (Joshua *et al.*, 2006). It remains unclear what this matrix is composed of, but there has been support for DNA and an α-dextran (Brown *et al.*, 2015; Jowiya *et al.*, 2015; Svensson *et al.*, 2014) It is possible that protein glycosylation pathways contribute to producing this matrix as it has been reported that *C. jejuni* produces the heptasaccharide for protein *N*-glycosylation as a free soluble form, unattached to protein, in response to osmotic stress (Nothaft *et al.*, 2009). In some bacteria, protein glycosylation mutants have been shown to have defects in biofilm formation. In *C. jejuni,* it has been shown that a mutant of the legionaminic acid pathway, *cj1324,* is defective in biofilm formation (Howard *et al.*, 2009). Therefore, we decided to determine if our mutants played a role in biofilm formation. We tried a plethora of different plastic multiwell dishes in order to increase throughput of the assay, however, no biofilms were observed on any plastic tested and thus we resorted to using borosilicate glass tubes which are typically used for *C. jejuni* biofilm studies. Additionally, since it is known that *C. jejuni* shows enhanced biofilm formation in aerobic conditions (Reuter *et al.*, 2010), we compared both aerobic and microaerobic conditions for biofilm formation. As some of the strains are nonmotile, we further tested the effect of shaking in both aerobic and microaerobic conditions. The cells were allowed to incubate for 60 h in either of these conditions and tubes were then washed in water and biofilms were stained with crystal violet. We determined that the *cj1319::CAT* mutant showed enhanced biofilm formation compared to WT under static aerobic conditions (Appendix D, Figure 53). Therefore, we pursued these conditions for further experimentation.

We performed a time course over six days, whereby we evaluated biofilm formation on days three to six for WT, *cj1319::CAT* and the two protein glycosylation pathway mutants. We determined that only *cj1319::CAT* was significantly different from the WT as it showed enhanced biofilm formation (Figure 32A).

In order to determine if this phenotype was due to the disruption of *cj1319* specifically, we tested the complement strains in the same manner (Figure 32B). Interestingly, whereas *cj1319*comp_RSP did not restore the phenotype to that of the WT, *cj1319*comp_RNP and *cj1319*comp_ONP did restore this phenotype. WT*cj1319*comp_RSP, WT*cj1319*comp_RNP and WT*cj1319*comp_ONP all produced biofilms comparable to the WT.

Figure 32. Biofilm formation is enhanced in the *cj1319::CAT* mutant.

(A) Biofilm formation comparison of *cj1319::CAT* with WT and protein glycosylation mutants. Data represent the means of three independent experiments performed in triplicate. **(B)** Comparison of biofilm formation of *cj1319::CAT* with its three respective complement strains and controls. Biofilm formation was measured for each strain every day for three to six days. These data represent the average of 9 independent experiments performed in triplicate for WT and *cj1319::CAT*, 3 for *cj1319*comp_RSP and WTcj1319comp_RSP, 6 for *cj1319*comp_RNP and WT*cj1319*comp_RNP, and 4 for *cj1319*comp_ONP and WT*cj1319*comp_ONP. Statistical analysis was performed by two-way ANOVA. Same letters indicate no significant difference with $P>0.05$. Different letters indicate significant difference with $P<0.05$. Stars indicate significance compared to WT. * $P<0.05$, ** $P<0.01$, ***$P<0.001$ and ****$P<0.0001$.
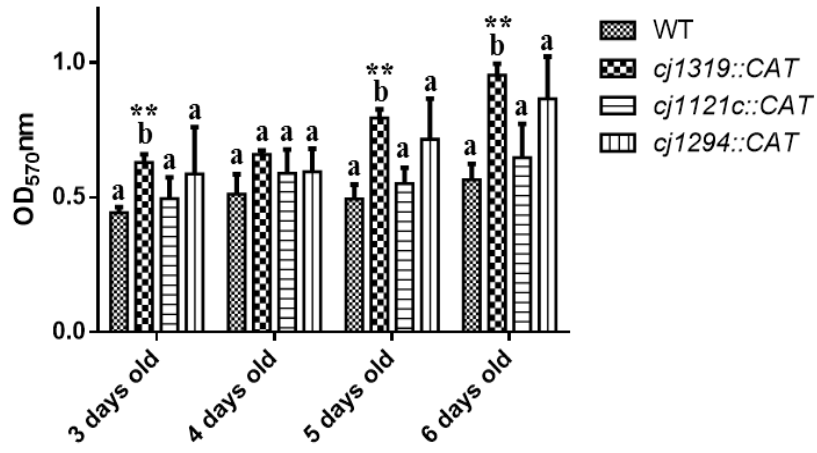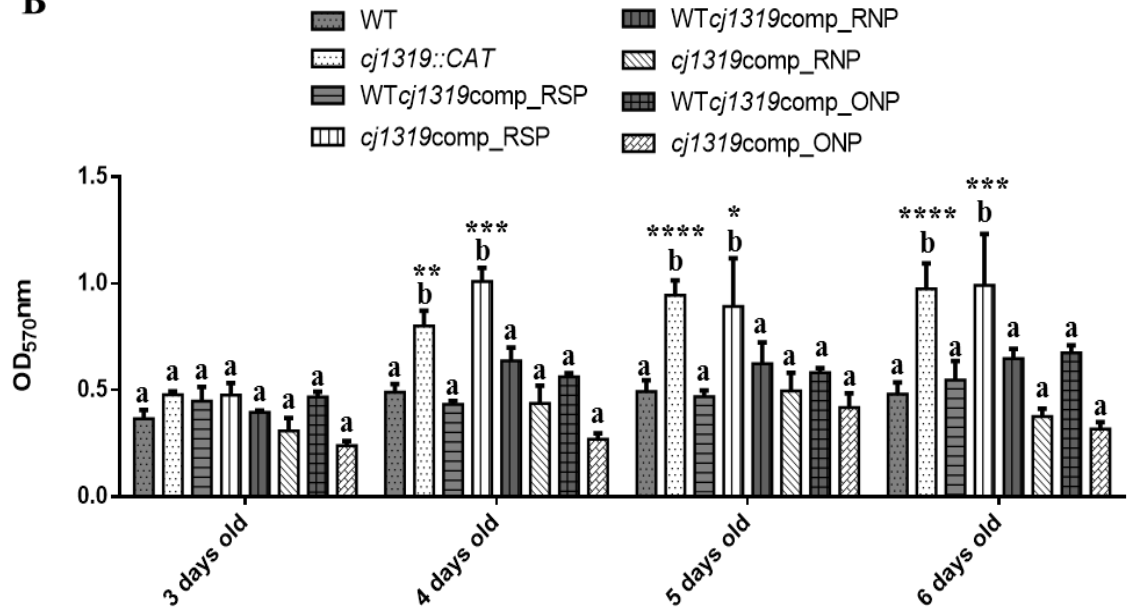
3.4 Interaction of *cj1319::CAT* mutant with eukaryotic cells and eukaryotes

Rationale: Glycosylated structures have been shown to be important for interaction of bacteria with eukaryotic cells, colonization and infection in animal models (Ishijima *et al*., 2011; Vijayakumar *et al*., 2006). Thus, we sought to explore the role of protein glycosylation in these three events. We examined the *cj1319::CAT* mutant as we hypothesize Cj1319 plays a role in protein glycosylation, in addition to each of the *N*- and *O*-protein glycosylation pathway knockout mutants.

3.4.1 Interaction of *C. jejuni* strains with *Acanthamoeba castellanii*

C. jejuni is a microaerophilic organism and thus atmospheric conditions stress these bacteria and ultimately lead to their death. Therefore, mechanisms of survival in environments external to their natural bird and cattle reservoir or human gut environemt are important for their transmissibility among hosts. It has been found that *C. jejuni* can survive within amoeba as well as externally in their presence as the amoeba provide a tolerable microenvironment by utilizing the majority of the local oxygen (Bui *et al*., 2012a, 2012b). To determine if Cj1319 and protein glycosylation plays a role in internal survival in amoeba, we conducted an internalization and short term survival assay with our mutants. We initially monitored the survival at 2.5, 5 and 24 hours post infection, however, very few bacterial counts if any were recovered after 5 hours and none at 24 hours post infection. Therefore, we performed experimental replica for 0 and 2.5 hours post infection only. Since Triton X-100 is used to lyse the amoeba prior to serial dilutions for bacterial enumeration, and the assay is performed in a defined buffer void of nutrition and performed at room temperature under normal atmospheric conditions, all of which are stressful for *C. jejuni*, we additionally tested the effect of this detergent under these conditions on our bacterial strains to determine if there were any differences in susceptibility that would influence the

CFU counts recovered between strains (Appendix B, Figure 54). Although Triton X-100 did result in killing a small portion of the bacteria, the effect was consistent among strains.

We determined that *cj1319::CAT* did not differ significantly compared to the WT in either internalization or short term survival ability (Figure 33). Similarly, all three of the *cj1319* complement strains behaved the same as WT. On the contrary, the two protein glycosylation mutants were not able to internalize and survive to the same extent as seen at 0 h post infection. This impairment could be partially restored in their respective complement strains. These two strains were often below the limit of detection at 2.5 hours post infection, or trace bacterial counts could be recovered, and thus the extent of their survival could not be determined accurately, although it was clear that their survival ability was impaired compared to WT.

Figure 33. Short term survival of *C. jejuni* **strains in** *Acanthamoeba castellanii.*

The internal survival of *C, jejuni* strains in *A. castellanii* was assessed over a period of 2.5 hours. **(A)** Amoeba were incubated in 24-well tissue culture plates for 2 hours prior to incubation with *C. jejuni* strains for 2 hours. Gentamycin was used to kill bacterial cells external to the amoeba and then bacteria were lysed immediately (0 h post infection) or 2.5 hours after antibiotic treatment (2.5 h). Bacteria were enumerated by serial dilutions and CFU counting calculated to CFU/mL. (B) Internal bacterial survival at 0 and 2.5 h post infection. **(C)** The inoculum was measured prior to incubation of the bacteria with the amoeba (Inoculum) and at the end of the experiment (Viability control). Experiments were conducted using triplicate wells/strain/time point and bacteria were enumerated by serial dilutions performed in duplicate and spot plating performed in triplicate. The data represent the average of six independent experiments for WT and *cj1319::CAT*, five for *cj1319*comp_RSP and WT*cj1319*comp_RSP, three for *cj1121c::CAT, cj1294::CAT, cj1319*comp_RNP*,* WT*cj1319*comp_RNP, *cj1319*comp_ONP, and WT*cj1319*comp_ONP, and two for *cj1121c*comp_RSP, *cj1294*comp_RSP, WT*cj1121c*comp_RSP and WT*cj1294*comp_RSP. No significant differences were determined by two-way ANOVA or Student's t-test.

A
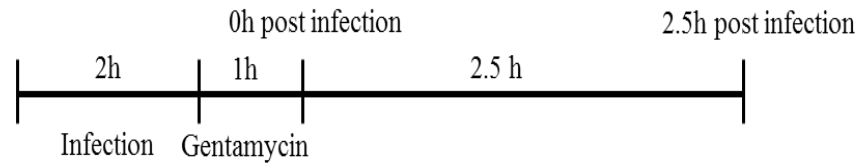
B
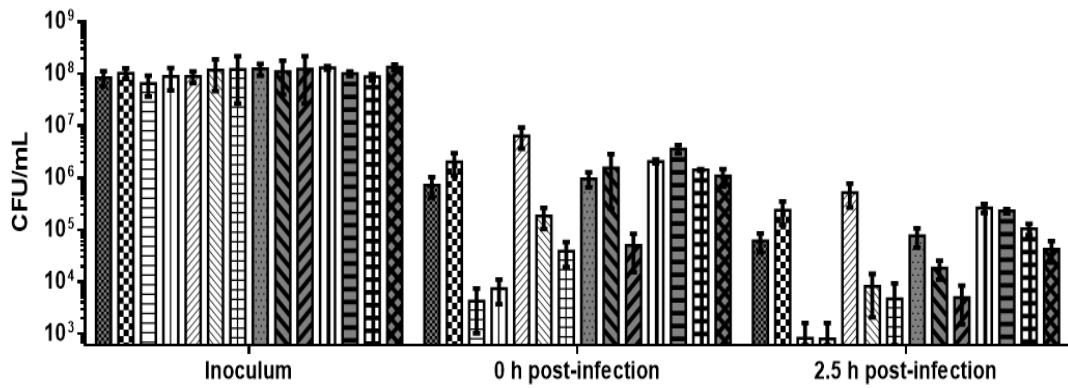
C
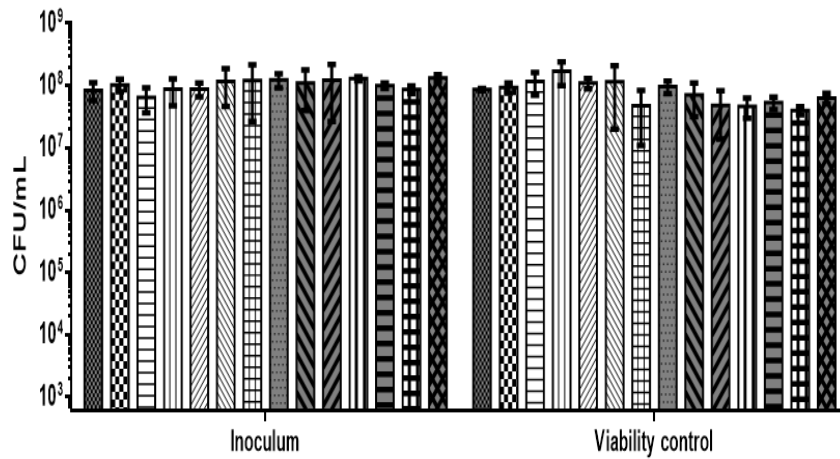
3.4.2 Interaction of *C. jejuni* strains with intestinal cells and macrophages

The mechanism of *C. jejuni* invasion of intestinal or macrophage cells is still under investigation, whereby evidence supporting aspects of both the 'zipper' and 'trigger' mechanisms have been found, thus indicating the mechanism by which *C. jejuni* invades is novel and requires further study or depends on the strain like so many other phenotypes (Ó Cróinín and Backert, 2012). It is possible that surface glycosylation including that of glycoproteins may be part of this novel mechanism. Therefore, we examined the interaction of our mutants with Caco-2 intestinal cells, an immortalized human cell line, and RAW 264.7 macrophages (mouse origin).

Once *C. jejuni* reaches the intestine of humans, it interacts with the mucins and eventually invades intestinal cells (Young *et al*., 2007). To determine if Cj1319 plays a role in this process, we performed an adhesion and invasion assay of Caco-2 intestinal cells. As in the amoeba assay, Triton X-100 is used to lyse the intestinal cells prior to serial dilutions for bacterial enumeration, but in this case the bacteria were incubated in cell culture media rich with nutrients and at 37°C under close to favourable atmospheric conditions (5% CO_2), so we assessed the effect of this detergent on our strains within this assay as well (Appendix B, Figure 55). Similarly, Triton X-100 did result in killing of a small portion of bacteria and the effect was consistent among strains. However, in this case we found that the strains replicated during the assay as a result of nearly optimal growth conditions such that the effect of the Triton X-100 killing was negligible when compared to that of the inoculum.

We did not observe a significant difference in the ability of *cj1319::CAT* to adhere and invade Caco-2 intestinal cells compared to the WT (Figure 34). We found that the *cj1121c::CAT* mutant was slightly impaired in adhesion and invasion compared to the WT. Although it was not statistically significant, the trend is in agreement with previously published work (Vijayakumar *et al*., 2006). The *cj1294::CAT* mutant had not been previously tested and we did not find a significant difference or any trend between this mutant and WT.

Figure 34. Comparison of *C. jejuni* strains ability to adhere to and invade into Caco-2 intestinal cells.

The adhesion and invasion of *C, jejuni* strains of Caco-2 intestinal cells was assessed after 5 hours of incubation. Total adhesion and invasion was assessed by CFU enumeration of bacterial counts prior to treating the wells with gentamycin and invasion only was determined through enumeration of bacteria post treatment with gentamycin. The inoculum was measured prior to incubation of the bacteria with the amoeba (Inoculum) and at the end of the experiment (Viability control). Experiments were conducted in using triplicate wells/strain and bacteria were enumerated by serial dilutions performed in duplicate and spot plating performed in triplicate. The data represent the average of 4 independent experiments.
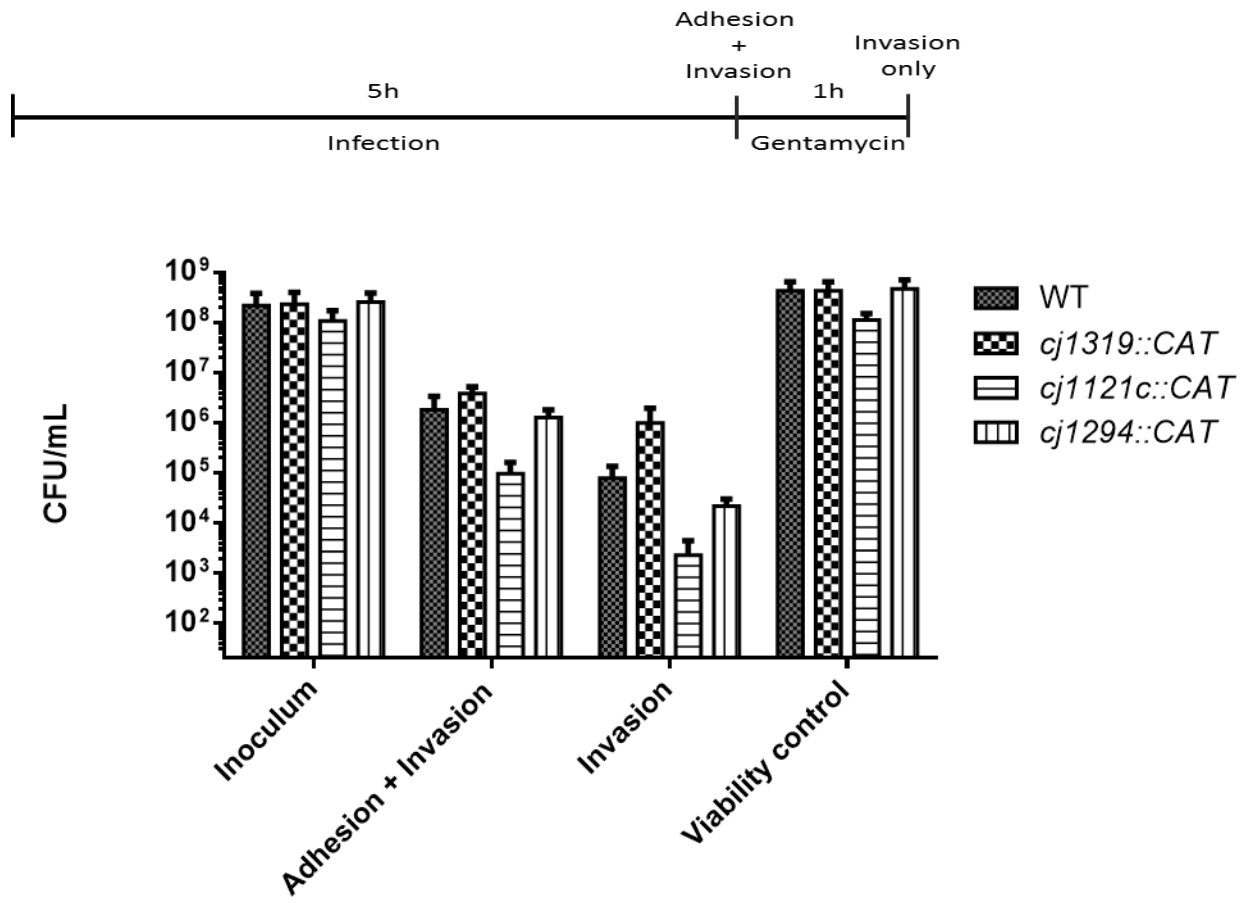
Similar to our Caco-2 cell study, we sought to determine if Cj1319 and protein glycosylation plays a role in adhesion and invasion of macrophage. *C. jejuni* are able to survive within macrophages although the mechanism is unknown (Kiehlbauch *et al.*, 1985), however, this appears to be strain specific and host specific (Wong *et al.*, 2015). The glycosylation may also have a role in internal survival.

We performed an adhesion assay at a low temperature to prevent macrophages from engulfing the bacteria which would interfere with our results. We did not find any significant difference or trend among strains in their ability to adhere to the macrophage (Figure 35A). To determine if there are any differences in the ability of the mutants to invade the macrophage, we examined internalization of the strains after incubation with the macrophage for 2 or 4 hours (Figure 35B). The duration of the incubation had no effect on recovery of internalized bacteria, signifying that that intracellular killing is counterbalanced by the entry rate. We also did not find a difference among strains in the recovery of internalized bacteria. Finally, we measured internal survival over a period of 5 hours at 2.5 hour intervals (Figure 35C). No significant difference was observed between the *cj1319::CAT* mutant and the WT or among strains at any time point. The only exception was the *cj1121::CAT* mutant which was impaired in its ability to survive short term within macrophages as detection was typically below the limit of detection at 5 hours post infection. This phenotype was recovered in *cj1121ccomp_*RSP.

Figure 35. Interaction of *C. jejuni* strains with RAW 264.7 macrophage.

(A) Adhesion of *C. jejuni* strain to macrophage. Results represent the means of three independent experiments performed in triplicate wells, duplicate serial dilutions and triplicate spot plating for all strains. **(B)** Infection time course of 2 and 4 hours. **(C)** Internal survival time course up to 5 hours post infection. Bacteria were enumerated by serial dilutions and CFU counting calculated to CFU/mL. The inoculum was measured prior to incubation of the bacteria with the amoeba (Inoculum) and at the end of the experiment (Viability control). Experiments for B and C were conducted using triplicate wells/strain/time point and bacteria were enumerated by serial dilutions performed in duplicate and spot plating performed in triplicate. The data represent the average of 4 independent experiments for WT and knockout mutants and 3 for the complement strains, and one for the complement controls in WT. The experimental scheme of each assay is represented above the bar graphs. No statistical significance was determined by two-way ANOVA, one-way ANOVA, or Student's t-test.

A

B

C
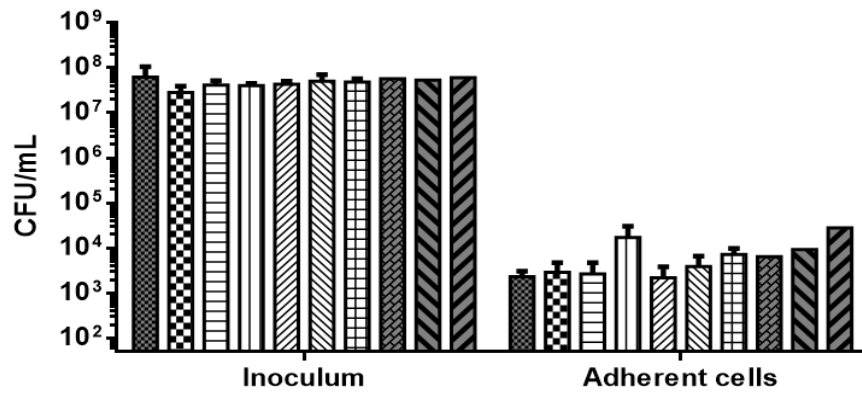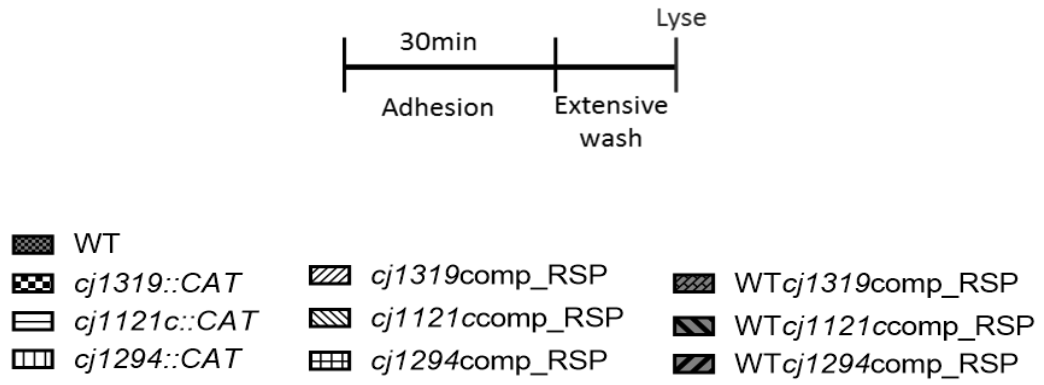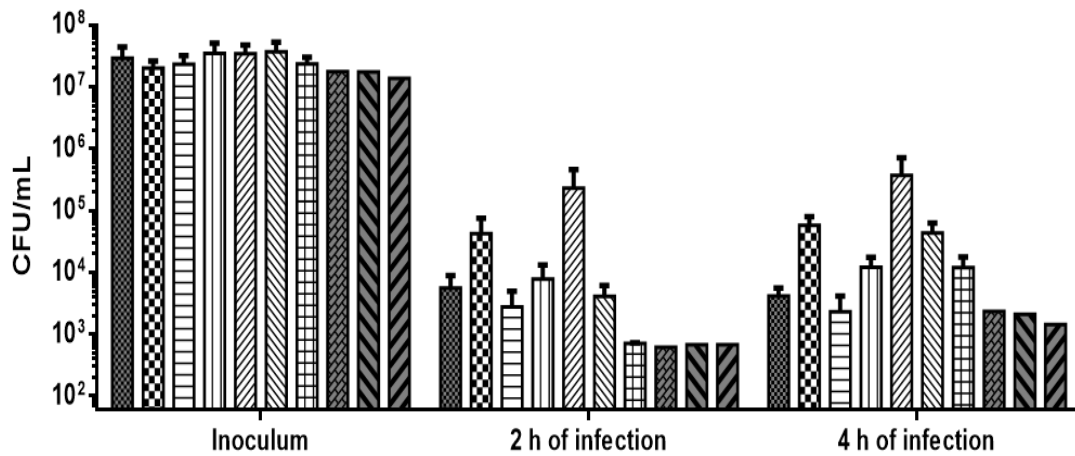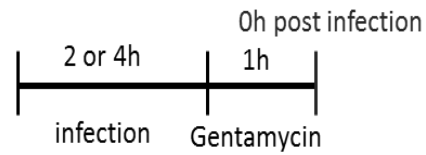
3.4.3 Infection of *Galleria mellonella* with *C. jejuni* strains

In order to assess the role of protein glycosylation in an *in vivo* infection model where innate immunity is involved, we employed *Galleria mellonella* larvae as an insect infection model that has been validated for the study of *C. jejuni* (Champion *et al*., 2010; Senior *et al*., 2011). It was necessary to optimize the dose of the WT inoculum in order to match the larvae killing rate of 100% reported in these studies. Since the WT strain that has been reported in these assays so far is a hyper virulent variant of our NCTC 11168 strain (NCTC 11168-H), the dose needed to be increased. We determined that preincubation of cells in broth for 4 hours at 37°C followed by suspending these cells in saline and using a dose of 10 ul of ~10^9 cells/mL for injecting larvae is optimal.

We determined that the *cj1319::CAT* mutant was ~30% significantly less effective at killing the larvae compared to the WT (Figure 36). This phenotype could be restored upon complementation in *cj1319*comp_RSP. Even more strikingly, the *cj1121c::CAT* mutant was found to be ~60% less efficient at killing the larvae and this phenotype could also be complemented with *cj1121c*comp_RSP. On the contrary, the *cj1294* mutant did not differ significantly from WT in its ability to kill the larvae. These results signify the importance of Cj1319 and Cj1121c in virulence in this infection model.

Figure 36. *Galleria mellonella* **show a 30% increase in survival after infection with the** *cj1319::CAT* **mutant and a 45% increase in survival after infection with the** *cj1121c::CAT* **mutant compared to those infection with WT or the** *cj1294::CAT* **mutant.**

G. mellonella were challenged with 10 µl of ~10^9 cells/mL of bacteria. Data represent percentage of larvae that survived after 24h of infection with each of the indicated strains (n=3, 10 larvae/strain/n). * $P<0.05$, ***$P<0.001$ by one-way ANOVA.
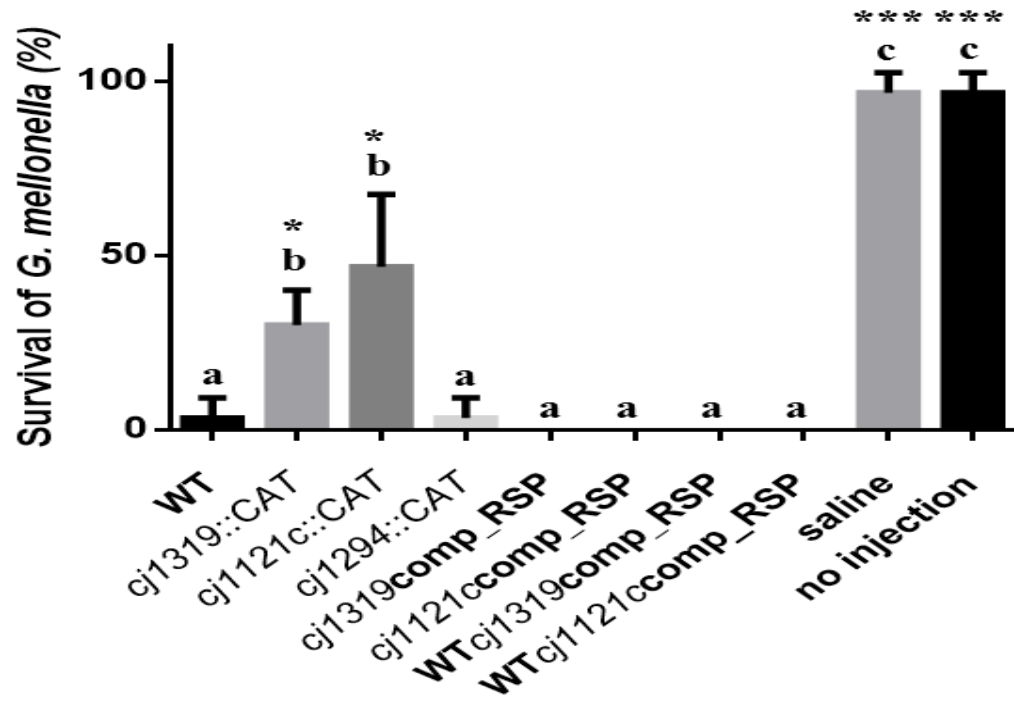
3.4.4 The *cj1319::CAT* mutant shows enhanced chicken colonization

Based on our finding that the *cj1319* knockout mutant modifies its flagellins with more Leg5AcNMe7Ac compared to WT, we sought to determine if this excess legionaminic acid incorporation on the flagella would enhance colonization of chickens, since a previous study showed that a *cj1324* knockout mutant that lacked legionaminic acid production as per metabolomic analysis showed reduced colonization in this model (Howard *et al.* 2009). Two-day old chicks were challenged orally with either WT or *cj1319* mutant and the bacterial load in the ceacum was measured after five days. There was a significant ($P<0.05$) increase in the ability of the knockout mutant to colonize the chicks compared to WT (Figure 37). We have previously published that the *cj1121c* mutant is unable to colonize chickens (Vijayakumar *et al.*, 2006). We did not test the *cj1294* mutant in this system because we infer it will also be attenuated since it is nonmotile. Furthermore, a *cj1293* mutant (Cj1293 preceeds Cj1294 in the O-glycosylation pathway) was completely attenuated in this model (Creuzenet, 2004).

Figure 37. The cj1319 knockout mutant has significantly enhanced chicken colonization compared to WT.

Two day old chicks were orally gavaged with 10^7 CFU, and their caecal content in *C. jejuni* was determined after 5 days by CFU counting of plated caecal homogenate. Significant difference compared to WT is indicated by *($P<0.05$) as determined by the Mann-Whitney test. Courtesy of Dr. Dozois (Zebian *et al.*, 2015).
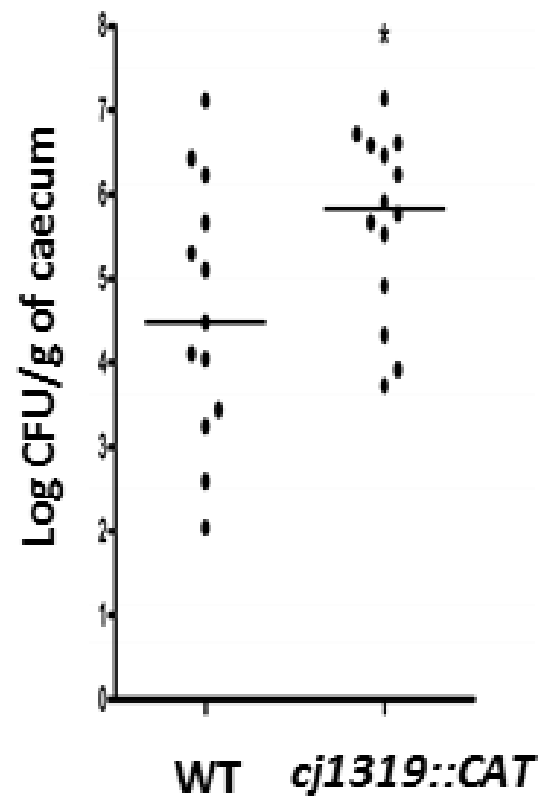
3.5 Discovery of a novel *Helicobacter pylori* outer membrane glycoprotein

3.5.1 Evidence of Le^y modified proteins

The O-antigen of LPS in pathogenic gram negatives typically plays an important role in virulence. The O-antigen of *H. pylori* is made of Lewis blood group mimics and plays a role in immune evasion in the early stages of infection (Appelmelk *et al*., 1996, 1997; Moran *et al*., 2002; Negrini *et al*., 1996). Later in infection, the host may form antibodies against the O-antigen, however, these antibodies cross react with the highly similar host blood group antigens. It has been shown in other bacteria, such as *P. aeruginosa,* that pilins can be glycosylated with the O-antigen produced by the LPS synthesis pathway (Castric *et al*., 2001; DiGiandomenico *et al*., 2002). We and others have previously demonstrated the presence of multiple glycoprotein candidates in *H. pylori* NCTC 11637 (Champasa *et al*., 2013; Hopf *et al*., 2011). Therefore, we hypothesized that it is possible for *H. pylori* to glycosylate outer membrane proteins with Lewis groups which could be exposed to the outside and potentially contribute to the host-pathogen interaction.

H. pylori NCTC 11637 expresses Le^y in its LPS

We chose to test this hypothesis by examining strain NCTC 11637 for the production of Le^y- and Le^x-modified glycoproteins since this strain was shown to produce these two Lewis O-antigens (Appelmelk *et al*., 1998; Merkx-Jacques *et al*., 2004). The expression of Lewis O-antigens is phase variable whereby the expression of fucosyltransferases may be switched on or off by slipped strand mutagenesis (Nilsson *et al*., 2006; Skoglund *et al*., 2009; Wang *et al*., 2000), leading to the generation of variable O-antigen serotypes with varying degrees of completion (Appelmelk *et al*., 1999; Wang *et al*., 1999, 2000). Le^y is a four sugar glycan, (Fuc α (1,2)-Gal β (1,4)-[Fuc α (1,3)]GlcNAc β-) and Le^x resembles Le^y but lacks the terminal fucose (Figure 38). To assemble Le^y O-antigen chains, two fucosyltransferases are required to add fucose to the Gal β (1,4)-GlcNAc β- main chain, whereas Le^x only requires one fucosyltransferase. Strain NCTC encodes for three fucosyltransferases where FutA and FutB are α (1, 3/4) fucosyltransferases and FutC is an

α (1, 2) fucosyltransferase (Appelmelk *et al*., 1999). FutA preferentially transfers fucose to internal Gal β (1,4)-GlcNAc β- units and FutB preferentially transfers fucose to this unit at the terminus of the O-antigen chain. Through sequencing, we determined that our NCTC 11637 strain contained shorter poly C tracts in *futA* (10 bases versus 13) and in *futB* (9 bases versus 13 bases) than reported for strain 26695. *futC* had the same 14-base poly C tract as strain 26695. These results indicated that both FutA and FutC were in frame, and therefore could fulfill their function to concurrently support Le^y and Le^x production, whereas FutB was out of frame. To determine if these Lewis groups incorporated into the LPS in strain NCTC 11637 under our laboratory growth conditions, we analyzed the amount, pattern and nature of LPS by SDS-PAGE and silver staining and Western blot analysis using anti- Le^y and Le^x antibodies (Figure 39). Strain 26695 expresses both Le^y and Le^x antigens and was used as a positive control. We determined that strain NCTC 11637 expresses Le^y, but not Le^x in its LPS.

Figure 38. Schematic representation of the structures of Le^y and Le^x.

Le^y

Le^x
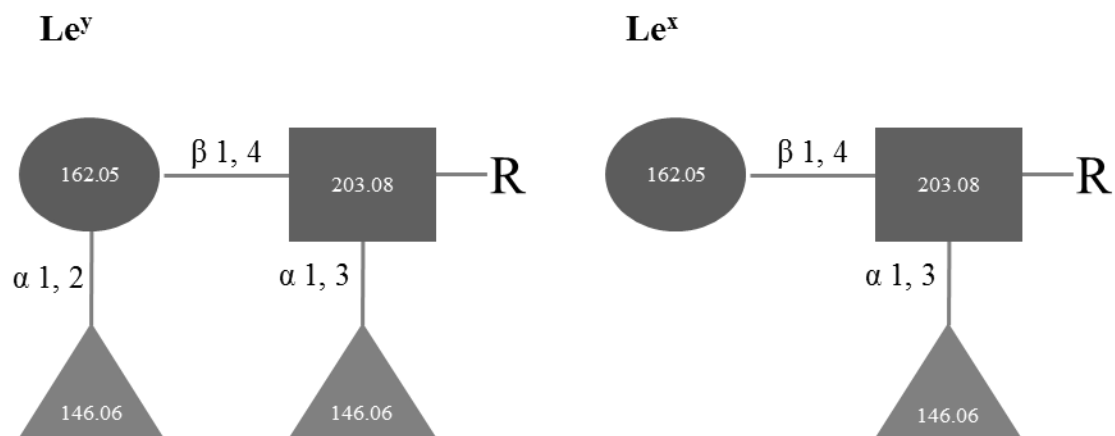
Key

GlcNAc   Gal   Fuc

Numbers correspond to the monoisotopic masses of the sugar residues.

Figure 39. Analysis of the lipopolysaccharide of *H. pylori* strains NCTC 11637 and 26695 by SDS-PAGE and detection by silver staining or anti-Lewis Western blotting.

The LPS was extracted by SDS solubilization and proteins eliminated by proteinase K treatment before SDS-PAGE. The LPS was detected by silver staining (**A**), and anti-Le^y (**B**) or anti-Le^x (**C**) Western blotting. / indicates no sample loaded. (Credit to R. Ford, MSc).

A
11637 / 26695

B
11637 / 26695

C
11637 / 26695

Silver stain   Anti-Le^y Anti-Le^x
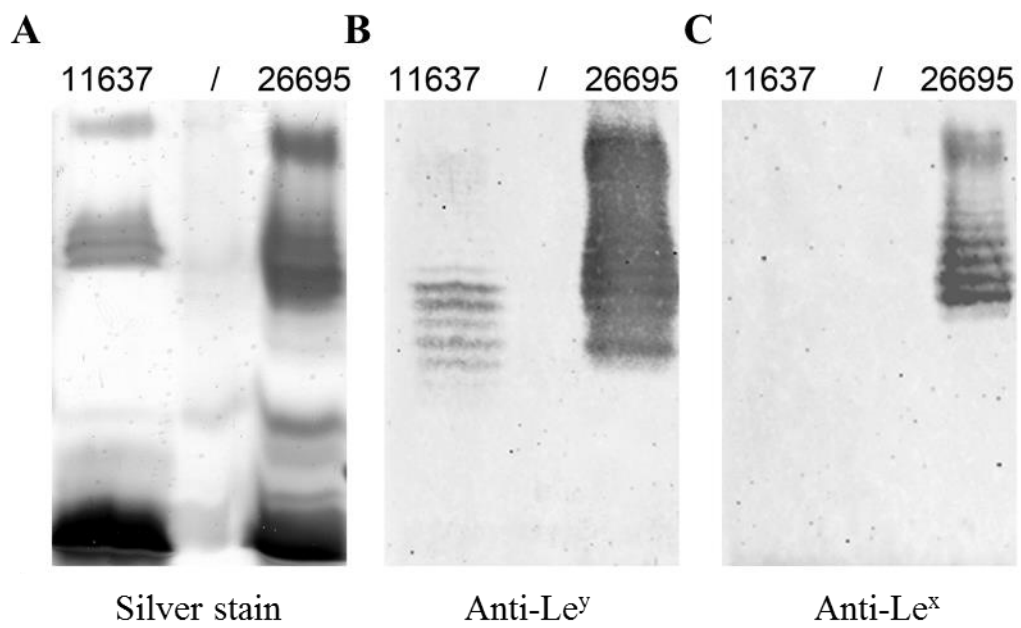
Discovery of outer membrane Le^y glycoprotein candidate

H. pylori cells were lysed and the soluble cytoplasmic and periplasmic proteins were separated from the membranes by ultracentrifugation. These membranes were screened for Le^y glycoproteins by SDS-PAGE and anti- Le^y Western blot using LPS of strain 26695 as a positive control (Figure 40). In order to distinguish signal arising from Le^y of the LPS present in the membranes from that arising from Le^y modifying proteins, we additionally treated half of the samples with proteinase K. Thus, signals disappearing after proteinase K treatment compared to signals present in untreated samples indicate the presence of Le^y modified protein candidates. One anti-Le^y reactive band that was sensitive to proteinase K treatment was observed at ~30-33 kDa. The total membranes were further treated with the detergent N-laurylsarcosine in order to solubilize the inner membrane proteins and these proteins were separated from the outer membrane proteins by ultracentrifugation (Filip *et al*., 1973; Hopf *et al*., 2011). By similar analysis, the candidate glycoprotein of 30-33 kDa was found to localize to the outer membrane. Of note, the soluble protein fraction was also screened in a similar manner, however, no Le^y positive proteins were observed.

Figure 40. Identification of glycoproteins reactive with anti- Le^y antibodies in the membrane fraction of *H. pylori* strain NCTC 11637.

Total membranes were prepared by ultracentrifugation of mechanically disrupted cells and the proteins were analysed by SDS-PAGE with detection by Ponceau S Red staining **(A)**, anti- Le^y **(B)**, and anti-Le^x Western blotting **(C)**. Outer membranes (OM) were analyzed similarly **(D)**. To facilitate distinguishing between proteins and LPS, the samples were treated with proteinase K (+ PK) or not (- PK) prior to loading on SDS-PAGE gels. The LPS of strain 26695 served as a positive control for anti- Le^y Western blots. The bracket highlights the 30-33 kDa area that reacts with anti- Le^y Western blotting and is sensitive to proteinase K treatment.

A Ponceau S Red

B Anti-Le^y

C Anti-Le^x

D
Silver stain

Ponceau S red

Anti-Le^y

kDa
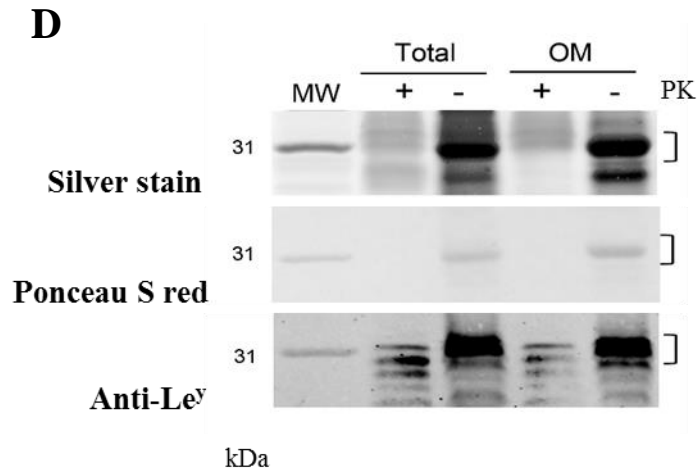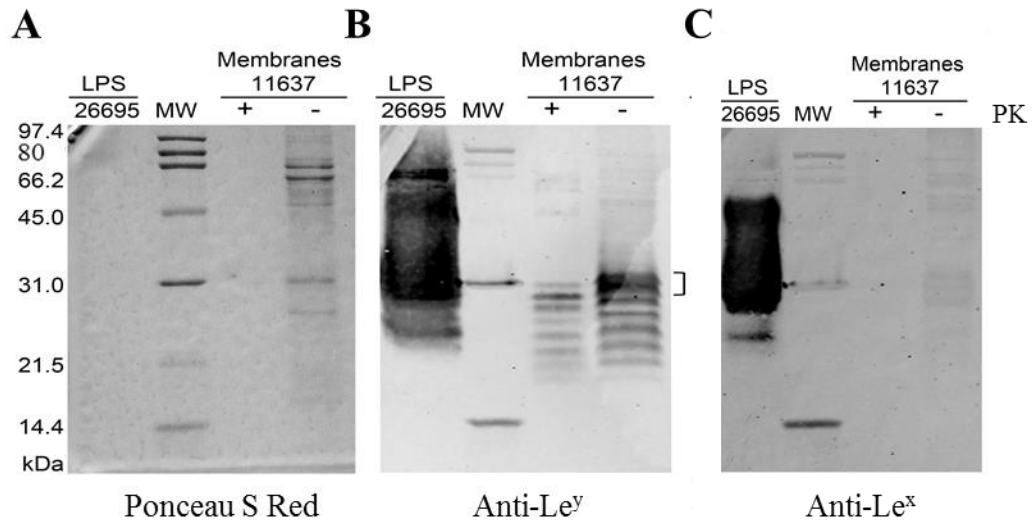
In order to identify this Le^y glycoprotein candidate and show that it is indeed glycosylated with Le^y, we needed to enrich and purify this candidate to facilitate detection and allow thorough MS analysis of its glycosylation. However, there were a number of difficulties in this case. Firstly, the outer membrane proteins cannot be solubilized without a detergent or chaotropic agent that is incompatible with downstream mass spectrometry applications. Secondly, the LPS co-purifies with the outer membrane and it is not possible to separate the LPS from the outer membrane proteins without solubilizing the proteins.

We reasoned that it was not necessary to analyze the whole glycoprotein candidate to prove its glyosylation. Based on the hydrophilic and bulky nature of the Le^y motif, glycopeptides were expected to be surface exposed which in turn would make them extractable directly from the outer membranes by protease digestion. This approach overcomes the issues of protein solubility and the presense of LPS. Therefore, outer membranes were treated with trypsin in order to release exposed tryptic peptides into the supernatant. These soluble peptides were separated from the membrane by ultracentrifugation. The supernatant containing the solubilized tryptic peptides, including those potentially carrying sugars, was analyzed by SDS-PAGE and anti- Le^y Western blot (Figure 41). The procedure was efficient at releasing four Le^y reactive peptide bands (Lane 1, Figure 41A and B), whereby the largest two were further sensitive to proteinase K digestion in the presense of detergent (Lane 2, Figure 41B), indicating that they were derived from a protein. The two smaller Le^y reactive peptides remained resistant to trypsin digestion even in the presence of the detergent signifying that they may not contain the cleavage sites for trypsin, or that the attached sugar motif prevents accessibility of the protease, or that they may have originated from released LPS (although it is unlikely).

As these Le^y reactive peptides were not pure and too large (>10 kDa) for MS analysis, the tryptic peptides were separated by SDS-PAGE, stained with Coomassie blue, and the four peptide bands of interest before Tween-20 and protease digestion were exised and digested with trypsin. The peptides were extracted from the gel and analyzed by MS.

Figure 41. Analysis of outer membrane tryptic peptides by anti- Le^y Western blot.
SDS-PAGE analysis of total outer membrane tryptic peptides (Lane 1) and outer membrane tryptic peptides further treated with trypsin in the presence of Tween-20 (Lane 2) stained with Ponceau S Red **(A)**, and anti- Le^y blot **(B)** shows four Le^y positive bands around 12 kDa, indicated by the arrows, two that are sensitive to further tryptic digestion in the presence of Tween-20.

A

MW   1   2

21.5

14.4

11.9

kDa

Ponceau S Red

B

MW   1   2
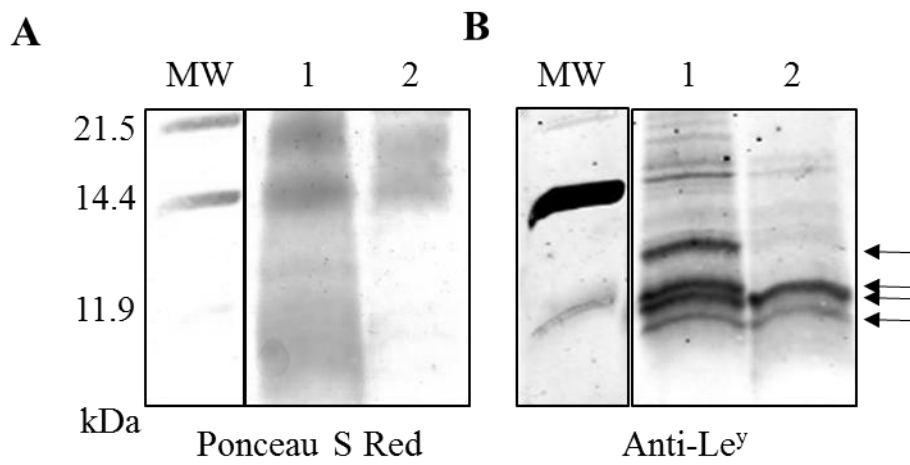
Anti-Le^y

3.5.2 Enrichment of glycopeptides by affinity chromatography

In order to further enrich Le^y carrying glycopeptides, we used affinity chromatography. An anti-Le^y antibody column would be ideal, however, due to the high cost of this antibody, we opted for a relatively inexpensive, though less specific, lectin column. We used BambL, a lectin from *B. cenocepacia* which is able to bind terminal α (1, 3) fucose of Le^y. This lectin was expressed and purified from *E. coli*. To confirm that this lectin could bind Le^y, we coupled the lectin to biotinyl-N-hydroxy-succinimide ester. Purified LPS from *H. pylori* strain SS1 was analyzed by Western blot using biotin-labelled BambL and fluorescently-labelled streptavidin and compared to an anti- Le^y Western blot of the same sample (Appendix B, Figure 56). It was concluded that BambL does bind Le^y and thus we proceeded in coupling this lectin to a sepharose column to extract the Le^y carrying peptides from the total soluble outer membrane tryptic peptide sample. Bound glycopeptides were eluted with mannose which competes with immobilized glycopeptides for BambL binding. The eluate was assumed to be enriched with glycopeptides and was analyzed by LC-MS and HCD-MS^2 as done previously (Zebian *et al*., 2015).

3.5.3 Identification of the glycoprotein candidate as HopE (HP0706) by MS

Our glycoprotein candidate is hypothesized to carry a Le^y motif which consists of four sugars as depicted in Figure 38, thus increasing the complexity of the MS analysis. An ionization energy sufficient to fragment the glycopeptide bond (the bond between the peptide and glycan), peptidic bonds (along the peptide chain) and glycosidic bonds (along the glycan) is necessary in order to obtain information on both the glycan and peptide composition. As glycan bonds (and the glycopeptide bond) are more labile compared to peptidic bonds, a lower energy is needed to fragment the glycan, however, lower energies will not suffice to fragment the peptide in the case of glycopeptides, as the energy is consumed by glycosidic fragmentation. Therefore, higher energy is required to fragment both the peptide and glycan, however, higher energies may also lead to over fragmentation

of the glycan which prevents the visualization of sugar oxonium ions that serve as signature ions for glycosylation in MS spectra. Therefore, we used HCD-MS^2 at low, medium, and high energies to obtained data for both glycan and peptide.

The extracted tryptic peptides (enriched through BambL lectin column or not) representing both unmodified peptides and Le^y carrying peptides were processed through LC-MS and HCD-MS^2. The data were analyzed with PEAKS software by *de novo* sequencing and database searching. The analysis incorporated the search for select variable PTMs including Le^y and its fragments, which were calculated based on the structure shown in Figure 38 (Table 4, Materials and Methods). Spectra were also manually inspected for sugar oxonium ions, internal peptide fragment ions, and signature sugar losses between fragment ions.

We identified a triply charged ion of 904.1143 m/z with a total mass of 2709.32 Da whose *de novo* generated sequence partially matched a sequence from *Helicobacter* outer membrane protein HopE (Figure 42B). Upon *in silico* digestion of this protein with trypsin, the sequence of the full tryptic peptide was determined to be FLSAGPNATNLYYHLK. Furthermore, we were able to manually match the ions present in our spectra to the b and y ions calculated from this sequence (Appendix B, Table 11). This peptide was also found as a triply charged ion of 603.64 m/z, with a total mass of 1807.93 Da, matching the theoretical mass of the peptide, indicating that this ion represents a peptide which is not post-translationally modified (Figure 42A). Thus, the 2709.32 Da version of this peptide carries an additional mass of 901.39 Da, which is large enough to encompass the Le^y structure, 657.25 Da, in addition to an unknown component of 244.14 Da. We obtained optimal peptide fragmentation at high energy HCD, but no obvious sugar related ions were detected (Figure 42B). At low energy HCD, we obtained poor peptide fragmentation, however, we observed an ion of 902.48 m/z, indicating a potential oxonium ion of the full 901.39 Da glycan (Figure 42C). This indicates that this additional mass occurs as one glycan chain at one amino acid site as opposed to Le^y at one site and the unknown 244.14 Da at another site. Furthermore, we also found this glycopeptide in the sample that could bind to the BambL lectin, thus supporting that this glycopeptide is fucosylated. As we could not assign the most abundant ion at 1120.58 m/z to this peptide, we investigated the

possibility that a second ion co-isolated with our peptide of interest. Examination of the LC chromatogram showed that two other peptides of similar m/z (904.11+/- 2 Da) co-eluted with our glycopeptide: 904.9728 m/z (+2 charge) corresponding to the unglycosylated FLSAGPNATNLYYHLK peptide and 904.1152 m/z (+3 charge) corresponding to the peptide GGFIALSQMGDANASIPTPQPVYYR carboxymethylated at D or M (+57 Da) from the urease subunit A. Upon close inspection of the spectra and compiling information from all scans of the 904.11 +/- 2 Da m/z ion, we determined that the ions 1120.58 and 922.48 m/z can be assigned to y ions of the urease peptide, and the 1808.94 m/z ion may represent contributions from both the FLSAGPNATNLYYHLK glycopeptide and its nonglycosylated form (stemming from the 904.9728 +2 charge ion).

Figure 42. HCD-MS^2 analysis of a peptide from HopE shown in both unglycosylated and glycosylated forms with Le^y and unknown linker.

(A) Unmodified peptide 603.64 m/z. **(B)** High energy HCD of glycosylated peptide, 904.11 m/z (+3 charge), where no sugar related ions were detected and the sequence of the full deglycosylated peptide was observed. **(C)** Low energy HCD of glycosylated peptide highlighting the entire deglycosylated peptide and ions corresponding to peptide fragments carrying sugars as well as the full glycan oxonium ion at 902.48 m/z indicated by (+). Key ions are highlighted on the spectra. Ions corresponding to the urease peptide are indicated in **bold** font.
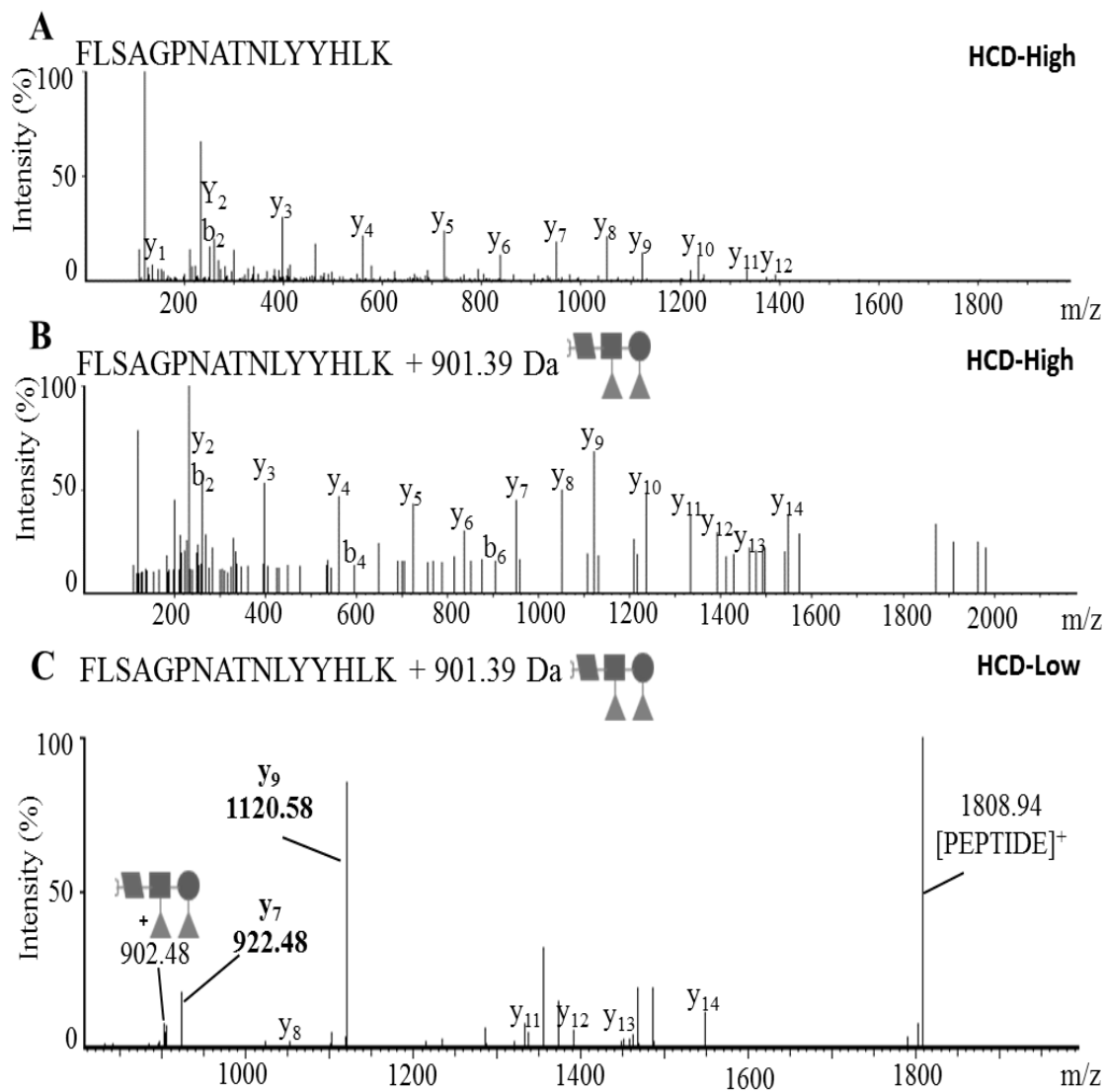
Table 8. Glycopeptide fragment ion assignment in MS^2 spectra.

Ion (m/z)	Peptide and its mass (Da)	Attached sugar and its mass (Da)	Ion type
1328.64	SAGPN 427.19	Le^y + Unknown 657.25 + 244.14	c_7 - c_2
1803.90	AGPNATNLY 902.44	Le^y + Unknown 657.25 + 244.14	c_{12} - c_3
2433.21	SAGPNATNLYYHLK 1531.77	Le^y + Unknown 657.25 + 244.14	z_{14}
2580.28	FLSAGPNATNLYYHL 1678.84	Le^y + Unknown 657.25 + 244.14	c_{15} - H

As the fragmentation observed in the HCD-MS^2 spectra of Figure 42 did not offer enough information to assign the glycosylation site(s), we used LC-MS and alternating CID- and ETD-MS^2 in order to identify the glycosylation site(s). Whereas ETD is used for glycosylation site determination since it does not cleave the glycopeptide bond, the ions generated are typically c and z ions as opposed to b and y ions which are obtained from CID and HCD, thus the alternation of ETD with CID was chosen to facilitate the analysis. Thus we first analyzed the CID spectra by a simple comparison to the low energy HCD spectra in Figure 42 to facilitate peptide sequence assignment and subsequently facilitate the analysis of the ETD spectra. Furthermore, we noted the fragmentation of the unmodified peptide, triply charged ion 603.64 m/z by ETD to facilitate the analysis of its glycosylated counterpart (Figure 43A). The glycopeptide, triply charged 904.11 m/z ion fragmented less efficiently by ETD (Figure 43B) in comparison to its unmodified counterpart (Figure 43A), whereby the fragmentation mainly occurred at the extremities of the peptide. We thus observed mostly internal ions, all carrying the extra full glycan mass of 901.39 Da as noted on the spectrum, with details to ion assignments in Table 8. As the fragmentation was not optimal, we did not obtain enough ions of the c and z series of our peptide of interest in order to be confident in our internal ion assignments. However, the observed ions precisely matched our calculated internal peptide fragments to two decimal places. This was beneficial as it allowed us to putatively map the glycosylation to N$_{247}$, suggesting potentially novel *N*-glycosylation in *H. pylori.* This was inferred from the internal peptide fragments SAGPN and AGPNATNLY (both with the full glycan attached) at 1328.64 and 1803.90 m/z respectively, whereby the first eliminates the T as being the glycosylation site and the latter similarly eliminates the S, provided that glycosylation was not heterogenous, occurring either on S or T.

Figure 43. ETD spectra of the HopE peptide in both unglycosylated and glycosylated forms.

(A) ETD of the unglycosylated peptide, 603.64 m/z. **(B)** ETD of the glycosylated peptide, 904.11 m/z. The full glycan is denoted by (⬛⬛●△△).

A FLSAGPNATNLYYHLK

B FLSAGPNATNLYYHLK + 901.39 Da

SAGP**N** +
$c_7 - c_2 + 901.39$
1328.64

AGP**N**ATNLY +
$c_{12} - c_3 + 901.39$
1803.90

$c_{15} - H + 901.39$
2580.28

$z_{14} + 901.39$
2433.21
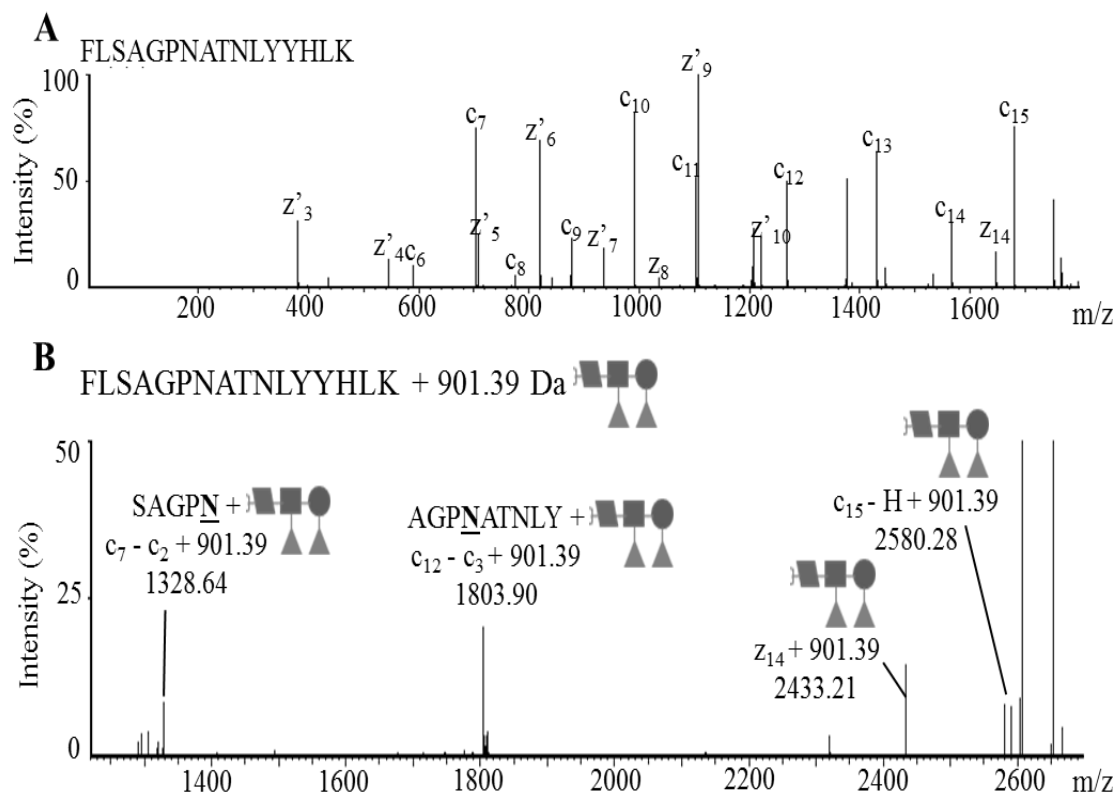
3.5.4 Confirmation that HopE is modified with Le^y

The *Helicobacter* outer membrane protein, HopE (~29 kDa), consistenly would migrate in the same MW range as that of Le^y glycoprotein candidate protein observed in Figure 40. Upon structural modelling of this protein, we determined that the glycopeptide found by MS is predicted to be part of a surface exposed loop (Figure 44), which is consistent with its release upon trypsinolysis of intact non solubilized outer membranes. Furthermore, this supports the hypothesized ability of this Le^y glycosylated protein to participate in evasion of the host immune surveillance. In order to further confirm that the identified peptide belongs to HopE and is indeed modified with Le^y, we constructed a *hopE* knockout mutant and analyzed the LPS and outer membranes by anti- Le^y Western blot compared to the WT. We confirmed that this mutant still produces Le^y LPS by both Western blot and sequencing of the phase variable fucosyltransferase genes (data not shown). We examined the outer membranes for Le^y reactivity as previously done and found that the ~30-33 kDa protein band reactive with anti- Le^y antibody in the WT sample that was absent in the *hopE* knockout mutant (Figure 45). Thus by MS analysis of WT and Western blot analysis of this knockout mutant, we conclusively showed that *H. pylori* glycosylates the outer membrane protein HopE with Le^y, supporting our hypothesis that *H. pylori* can glycosylate proteins with the O-antigen for LPS.

Figure 44. Structural model of HopE highlighting in purple the extracellular loop found to carry a Le^y motif based on MS analysis.

Outside

Glycopeptide

Outer
membrane

Periplasm
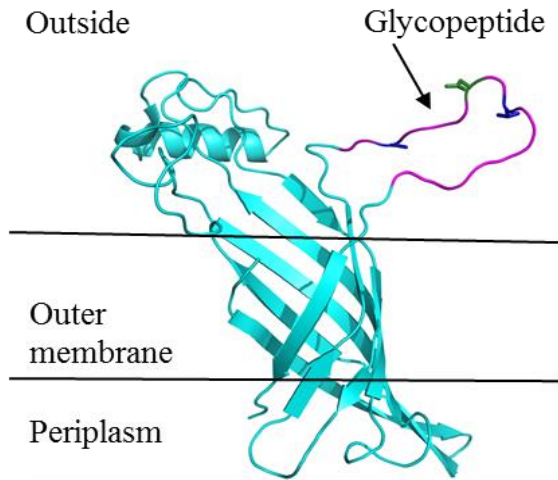
Figure 45. Analysis of *hopE*::*CAT* mutant outer membrane proteins for Le^y reactivity shows a Le^y reactive band missing in the mutant.

Panel A shows total proteins stained with Ponceau S Red. Panel B shows the anti- Le^y Western blot. The + and − signs indicate that the samples were treated with proteinase K or not respectively. The star (*) indicates the Le^y reactive band in the WT which is absent in the mutant.

A. Ponceau S Red

B. Anti-Le^y
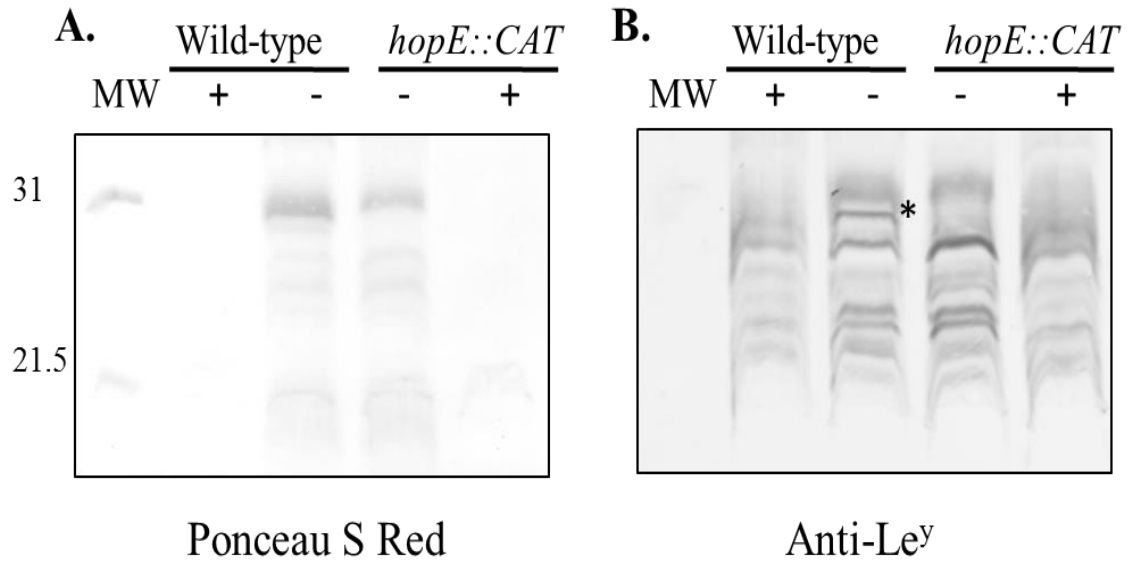
Chapter 4

4 Discussion

4.1 The role of Cj1319 in *C. jejuni*

In this work, we completed a comprehensive analysis of Cj1319 of *C. jejuni* NCTC 11168. We used an enzymology approach in parallel with phenotypic analyses of a *cj1319* knockout mutant. We were unable to determine its precise function as per enzymology, however, we did find an important role for this enzyme in virulence. Moreover, we conclusively excluded this enzyme from having a role in making capsular modified heptose or legionaminic acid for flagellin glycosylation which were proposed functions of this enzyme at the onset of our work.

4.1.1 Biochemical function of Cj1319

Cj1319 is a predicted sugar nucleotide dehydratase and enzymes with this function have been shown to initiate glycosylation pathways important for bacterial virulence in *C. jejuni, H. pylori,* and *P. aeruginosa* among others (Creuzenet, 2004; Creuzenet and Lam, 2001; Creuzenet *et al*., 2000; Schoenhofen *et al*., 2006). Thus there is potential for this enzyme to initiate a glycosylation pathway that would also impact the virulence of *C. jejuni.* Since this enzyme is homologous to GDP-mannose and GDP-*manno*-heptose dehydratases, we examined its activity on these two substrates. GDP-*manno*-heptose is the precursor in the pathway for heptose modification for capsule synthesis in *C. jejuni* NCTC 11168 which is only partially deciphered (Figure 3) (McCallum *et al*., 2013). The oxidase of the pathway has yet to be determined and, although we reasoned Cj1319 may function as the oxidase, since C-4 oxidation is also a function of C4, C6 dehydratases, we did not find that Cj1319 fulfills this function. Aside from being part of the main pathway for modifying the heptose for capsule, it is possible that Cj1319 would instead use the same precursor, but the dehydrated product would then be aminated and N-acetylated by the actions of Cj1320 and

Cj1321 respectively, which are encoded by the *cj1319* locus. Similarly, we did not find that this was the case.

As Cj1319 was not found to be the oxidase of the heptose modification pathway for capsule, other oxidase candidates need to be explored. However, there is no evident oxidase candidate for sugar nucleotide modification in the genome of *C. jejuni* based on bioinformatics. A screening approach to identify the oxidase could be performed. This may be achieved by fractionation of *C. jejuni* cell extracts and screening for activity of these fractions on GDP-*manno*-heptose whereby activity can be monitored by CE. The active protein fraction can then be further fractionated by ion exchange chromatography and the active fraction analyzed by mass spectrometry in order to determine the identities of the proteins in that fraction. Of these proteins, the most probable enzyme candidates can then be cloned and tested for oxidase activity on the said substrate. This is not an ideal approach due to the preciousness of GDP-*manno*-heptose. This sugar nucleotide is not available commercially and can only be synthesized enzymatically using four different enzymes to modify the D-sedoheptulose-7-phosphate as a precursor which is available commercially, but very costly (Kneidinger *et al*., 2001).

We determined that the 3-*O*-methyltransferase of the capsular heptose modification pathway is Cj1419 which does not methylate GDP-*manno*-heptose, but can methylate the surrogate dehydrated product produced through the activity of DdahA. Cj1319 did not use the resulting sugar, thus we could conclude that Cj1319 does not use a 3-*O*-methylated derivative of GDP-*manno*-heptose. Further studies can be pursued to determine if Cj1419 can act on other intermediates of the pathway and to analyze the kinetics of the reactions. It seems likely that this enzyme is less efficient than enzymes of the main pathway as we only observed ~50% conversion to the methylated intermediate after a 3 hour reaction compared to full conversion of GDP-*manno*-heptose to its dehydrated intermediate in 15 minutes. In addition to the fact that none of the enyzmes in this pathway require a methylated substrate, this would explain the heterogeneity in methylation of the final modified heptose product incorporated into the capsule.

Since the surrogate intermediate of the heptose modification pathway generated as a result of using DdahA, rather than the true C4 oxidase, is dehydrated, thus lacking its OH at C6, no activity for Cj1426 could be found in the surrogate pathway. Thus, when the C4 oxidase of this pathway is determined, the native 4-keto intermediate of this pathway can be generated which has a hydroxyl at C6. This will allow us to determine if Cj1426 is the true 6-*O*-methyltransferase for this pathway. In the case we do find it has a role in this pathway, we will be able to assess its substrate specificity. We could test Cj1319 on its product to determine if Cj1319 can use the 6-*O*-methylated product as its substrate. However, as the expression of Cj1426 is phase variable owing to the presence of a poly-G tract within *cj1426c*, and the expression of Cj1319 is not phase variable, it is not likely that Cj1319 would primarily use the product of Cj1426.

To determine the substrate of Cj1319, it is possible to extract the sugar nucleotide pool from cell free extracts of WT *C. jejuni* and screen for Cj1319 activity on these extracts. The sugar nucleotide extracts from WT and *cj1319* knockout mutant may also be compared by MS or CE to determine if a sugar nucleotide is accumulated in the *cj1319* mutant. If so, the metabolite of interest can be purified by anion exchange chromatography and identified by MS. We have attempted this and did not find any metabolite accumulated in the *cj1319* mutant, however, we also did not find any metabolite accumulated in the *cj1430* mutant that was used as a positive control. Cj1430 is the second enzyme in the pathway for capsular heptose modification, so one could expect an accumulation of GDP-*manno*-heptose in this mutant. However, a probable negative regulator of the pathway, WcaG, has been studied extensively and because this enzyme reduces the first oxidized intermediate of the pathway, it is likely that this prevents the accumulation of the pathway precursor (Figure 3) (McCallum *et al*., 2011). A similar mechanism may exist for the Cj1319 pathway as well. The substrate of Cj1319 may be unstable and thus is only present at a small concentration and so this substrate was undetected in our CE analysis. In addition, it may have also degraded completely as a result of the extraction conditions. Finally, the extraction methods tested may not be optimal for the extraction of the sugar nucleotide of interest, as different metabolites show different extraction efficiencies under different methods (Faijes *et al*., 2007).

GDP-mannose can be converted to up to four different sugars depending on the enzyme function following dehydration (Albermann and Piepersberg, 2001; Mäki *et al*., 2002; Wu *et al*., 2001). These four sugars have been shown to be important for virulence and include GDP-fucose. Although we did not find activity of Cj1319 on GDP-mannose, we did detect a number of glycoproteins using the fucose binding lectins BambL and PAII-L by Western blot. This suggests that *C. jejuni* NCTC 11168 may fucosylate some proteins, either as a single sugar or as a part of an oligosaccharide. However, for this to occur, there must be a GDP-mannose dehydratase encoded by the genome of this strain, but the only protein homologous to the *E. coli* GMD in our strain is Cj1319. Alternative to synthesizing GDP-fucose from GDP-mannose, it is possible that *C. jejuni* may uptake fucose and would then transfer it to proteins. Although *C. jejuni* can uptake L-fucose, this bacterium uses it as an energy source and thus not likely for protein glycosylation (Stahl *et al*., 2011). In addition, a fucosyltransferase would be needed to transfer the fucose onto proteins, which has not been noted to date. Additionally, as we only found glycoproteins binding these two lectins in the soluble protein fraction, these proteins would not be exposed to the host so it is not clear what role fucosylated proteins would play in *C. jejuni* virulence unless these proteins are secreted either as Cia proteins that can be secreted through the flagellar apparatus or by means of outer membrane vesicles (Elmi *et al*., 2012; Konkel *et al*., 2004). It is possible that these lectins may not have bound to fucose, but to another related sugar since these lectins have relaxed specificity in their binding (Audfray *et al*., 2012; Mitchell *et al*., 2005). Although these findings hint that there are yet novel glycoproteins to be discovered in *C. jejuni*, these particular ones are not related to Cj1319 as the two lectins were able to bind to the same proteins in the *cj1319* knockout mutant as in the WT.

We did not find any changes in glycoprotein profiles between the *cj1319* knockout mutant compared to WT via Western blotting with lectins or biotin hydrazide labelling of glycoproteins. However, we did find that the *cj1121c::CAT* mutant (Cj1121c is part of the N-glycosylation pathway responsible for glycosylation of over 60 proteins (Scott *et al*., 2011)) still expresses a large number of glycosylated proteins based on both biotin hydrazide labelling and the SBA lectin which was originally used to detect *N*-protein glycosylation in *C. jejuni*. Therefore, there must be another glycosylation pathway modifying these proteins in the absence of Cj1121. Thus, the *cj1121c::CAT* mutant can be

used as a tool to analyze its glycoproteins by mass spectrometry as performed previously on WT *C. jejuni* (Scott *et al*., 2011). This will reveal the glycan or sugar(s) modifying these proteins which in turn will shed light on what type of enzymes would be required for synthesis of this/these sugar(s). By doing so, this glycosylation may be traced back to Cj1319. Furthermore, as we know that the *cj1121c::CAT* mutant is nonmotile although it produces full length glycosylated flagella (Vijayakumar *et al*., 2006), the flagellin glycopeptides of this mutant can be analyzed by mass spectrometry as we have demonstrated (Zebian *et al*., 2015), in order to determine if the lack of motility is caused by a change in the glycosylation pattern of the flagellins of this mutant. Furthermore, a double mutant of *cj1121c* and *cj1319* can be generated to determine if glycosylation is abrogated.

4.1.2 Mass spectrometry analysis of flagellin glycopeptides in *C. jejuni* reveals the incorporation of legionaminic acid

As a major contribution in our study, we performed a comprehensive glycopeptide analysis of the *C. jejuni* NCTC 11168 flagellins using HCD-MS^2. We found evidence of the first glycopeptide carrying Leg5AcNMe7Ac in the WT, observing both the loss of its 329.159 Da signature mass and the presence of its oxonium ion at 330.166 m/z. We found seven glycopeptides (in their shortest digested form), five of which could be glycosylated by only one sugar at a time and one which could be glycosylated by two sugars at a time, each occupying a different site. In total, we found 22 different glycoforms of flagellin peptides in the WT. Two of the glycopeptides found could carry up to five different sugars (separately). Further showing the extensive heterogeneity of glycosylation are two glycopeptides from the *cj1319::CAT* mutant which could be glycosylated by six different glycans. This heterogeneity offers a wide combinatorial power of glycosylation patterns that produce flagellins with potentially different antigenic properties. Such properties may contribute to immune evasion and pathogenesis beyond the already established role of glycosylation in flagellin production and flagella function such as motility (Goon *et al*. 2003; Hitchen *et al.* 2010).

The extensive micro-heterogeneity found in the glycosylation of these peptides was a novel finding compared to prior reports available at onset of our studies and which indicated up

to two sugars per glycopeptide in other *C. jejuni* strains or in other bacteria in general (Logan *et al*., 2002; Thibault *et al.,* 2001; Zampronio *et al.,* 2011). Our wild-type data were corroborated by a study published during the final stages of preparation of this manuscript which also reported extensive heterogeneity of flagellin glycosylation in strain NCTC 11168 (Ulasi *et al.* 2015), including in the amino acid region 387 to 463 of flagellin A that is highly glycosylated and has been missed from all prior analyses. This extended coverage was obtained by coupling FAIMS ETD with proteinase K digestion in the Ulasi study and by coupling HCD with a double trypsin and chymotrypsin digest in our work. Overall, the same glycopeptides were identified and mapped but the Ulasi study revealed an additional glycopeptide spanning residues 427-456 as well as additional sugars on peptides 421-426 and 457-463 while our study showed the presence of a new sugar of 372.145 Da on three peptides, and most importantly our study is the only one providing unambiguous proof of the existence of legionaminic acid on flagellins.

Overall, both studies consistently highlight the high level of heterogeneity of flagellin glycosylation in *C. jejuni* strain NCTC 11168 and highlight the complexity of glycopeptide analysis whereby a combination of complex methods is necessary to capture the complete repertoire of glycopeptides. While ETD is usually considered ideal to map post-translational modifications, HCD had been used successfully to map glycosylation sites modified by GalNAc using y-ions (Segu and Mechref, 2010). Our work shows that HCD is very efficient at detecting peptides glycosylated by complex bacterial sugars and shows that mapping glycosylation sites is also possible using b-ions. It is very likely that HCD coupled with proteinase K would also have revealed an extensive number of flagellin glycopeptides in a single experiment. This also suggests the possibility of uncovering novel glycans/glycopeptides using this method in strains that were analyzed using prior methods.

To identify the potential new sugar observed at 372.145 Da, MS^3 analyses were performed. While these analyses identified several diagnostic fragments for a sugar backbone and for side chains commonly found on sugars, its identity as a new sugar can not be ascertained because of the concomitant presence of a 391.172 m/z ion in MS^2 spectra that releases common fragments upon MS^3 analysis (Logan *et al*., 2009). Thus 372.145 Da may have arisen from fragmentation of the 390.164 Da sugar during the MS^2 step. If different, this

sugar may contribute to this strain's pathogenicity and further increase the level of heterogeneity found in this strain. This finding additionally stresses the need for elucidating the functions of genes comprising *C. jejuni*'s flagellin glycosylation island in order to identify the enzymes responsible for generating this sugar.

4.1.3 Cj1319 is not required for legionaminic acid synthesis

In addition, we addressed the controversial role of Cj1319 in legionaminic acid synthesis by determining that Cj1319 is not required for legionaminic acid synthesis through the glycopeptide analysis of flagellins from the *cj1319* mutant. We showed that the enhanced detection of legionaminic acid on this mutant's peptides is specifically due to Cj1319, as determined by partial restoration of the WT phenotype in the complemented strain. Partial complementation is not unusual for glycosylation-related genes as cross-talk between glycosylation pathways and regulatory effects may occur (Demendi and Creuzenet, 2009; Howard *et al*., 2009; Wong *et al*., 2015).

Furthermore, the phenotypes we observed for the *cj1319* mutant were in contrast with the phenotypes reported for a *cj1324* knockout mutant of the legionaminic acid synthesis pathway (Howard *et al.* 2009). The *C. coli* homologue of Cj1324 is responsible for the conversion of CMP-Leg5Ac7Ac to CMP-Leg5Am7Ac (Figure 8) (McNally *et al.,* 2007). Consistently, inactivating *cj1324* in *C. coli* or in *C. jejuni* does not affect synthesis of CMP-legionaminic acid, but prevents further production of acetamidino derivatives (Howard *et al*., 2009; McNally *et al*., 2007). On the contrary, a *C. coli* mutant of the Cj1319 homologue makes more CMP-Leg5Ac7Ac as per metabolomic analysis (McNally *et al.* 2007). This is likely also the case in our *cj1319* mutant in the *C. jejuni* NCTC 11168 background since we observed enhanced incorporation of Leg5AcNMe7Ac on the flagellins by MS analysis. Finally, whereas the *C. jejuni cj1324* mutant had reduced chicken colonization compared to WT (Howard *et al.* 2009), our *cj1319* mutant showed enhanced chicken colonization. This phenotypic comparison supports that Cj1319 is not required for legionaminic acid

synthesis, but may rather negatively regulate legionaminic acid production via scavenging of the GDP-GlcNAc precursor and potentially rerouting it to the synthesis of another sugar. This implies that another dehydratase yet to be identified fulfills the role currently assigned to Cj1319 in the GDP-based legionaminic acid synthesis pathway, or that UDP-based legionaminic acid synthesis occurs when Cj1319 is absent. This latter explanation is unlikely as very little legionaminic acid could be obtained *in vitro* using the GDP-diacetamidobacillosamine modifying enzymes (Cj1328, Cj1327 and Cj1331) on UDP-diacetamidobacillosamine (Schoenhofen *et al.*, 2009). There remains the possibility that their Cj1141-Cj1143 homologues that are normally dedicated to sialic acid production for LOS synthesis would fulfill this function, however, our qRT-PCR analysis of these genes in the *cj1319::CAT* mutant suggests that this likely does not occur. Analysis of the many genes of the flagellin glycosylation island that remain uncharacterized to date may assist in understanding the mechanism of this potential negative regulation.

In vitro biochemical pathways can be misleading as, despite their specificity, sugar-nucleotide modifying enzymes can be used artificially *in vitro* in pathways that they do not belong to biologically. For example, the N-acetyltransferase Cj1123c from the general protein N-glycosylation pathway can also acetylate an intermediate of the pseudaminic acid synthesis pathway for flagellin O-glycosylation (Demendi and Creuzenet, 2009) although both pathways have been shown to be independent by mutagenesis studies (Goon *et al.*, 2003; Vijayakumar *et al.*, 2006). Further evidence of cross-talk between both pathways was also demonstrated for the initiating enzymes Cj1120c and Cj1293c (Creuzenet, 2004; Guerry *et al.*, 2007).

4.1.4 The role of Cj1319 in *C. jejuni*

Knockout mutants in *C. jejuni* are routinely created by insertional gene inactivation with an antibiotic resistance cassette. This leads to some polarity effects on surrounding genes in an operon when the promoter of the antibiotic cassette is stronger than that of the native

promoter of downstream genes. This can be avoided by addition of a transcriptional terminator downstream of the antibiotic resistance cassette, however, this would stop transcription of the downstream genes in operon. We did not introduce a terminator sequence into the mutant constructs for this reason. As such, we observed that the downstream genes were upregulated in our *cj1319::CAT* mutant, although this was not deemed significant by Student's t test. To our knowledge, there has been no system developed for in-frame deletion mutants with no insertional antibiotic cassette for *C. jejuni* and thus we were unable to avoid this effect. However, in order to assess that the phenotypes we detected in our *cj1319::CAT* mutant were indeed due to the loss of Cj1319 and not due to polarity and pleiotropic effects, we designed three different complements in our study. Because complementation *in trans* by use of a shuttle vector results in unstable strains in which the vector is rapidly lost through repeated culturing, all three complement constructs were prepared on a suicide vector which was transformed into *C. jejuni* and inserted into the genome by homologous recombination to create stable strains. Specifically, integration was engineered into a redundant tRNA site. As detailed in section 3.2, the two additional complement strains were developed due to inability to complement the biofilm, capsule, and LOS phenotypes with *cj1319*comp_RSP. This was thought to be due to either the overexpression of Cj1319, other mutations or a combination of both which may vary depending on the phenotype studied. The capsule and LOS were found to be altered due to phase variation of genes within the LOS or capsule biosynthesis clusters.

The enhanced biofilm phenotype in the *cj1319* knockout mutant was concluded to be due to the *cj1319* mutation. This was interpreted based on the ability to complement this phenotype with *cj1319*comp_RNP and *cj1319*comp_ONP. As we could not complement this phenotype with *cj1319*comp_RSP, this indicates that overexpression of *cj1319* inferred from qRT-PCR caused complications. The bulk of the overexpressed protein may precipitate and thus result in limited amounts of soluble and active Cj1319 available which may have been sufficient to complement some phenotypes but not others. We ruled out growth rate, motility and flagella as being the causes for the increased biofilm production since *cj1319*comp_RNP and *cj1319*comp_ONP grow at the same rate as *cj1319::CAT*, *cj1319*comp_RSP is nonmotile yet still makes enhanced biofilms, and *cj1294::CAT* which lacks flagella formed biofilms comparable to WT. The enhancement in biofilm formation

in the *cj1319::CAT* mutant only occurred under aerobic static conditions and did not occur under shaking conditions or microaerobic conditions. This suggests that oxidative stress may affect the mutant more than the WT, however, we did not find that the two strains differ significantly in their sensitivity to oxidative stress. There must be another stressor that this mutant is susceptible to which causes it to form biofilms more readily. As shaking abolished this effect, this suggests that the biofilm created by the *cj1319* mutant may be more fragile in its early stages compared to the WT and so the shaking slows down the rate of biofilm formation in the mutant.

The loss of motility of the *cj1319*comp_RSP strain and partial loss of motility in the *cj1319*comp_RNP and *cj1319*comp_ONP strains remain an enigma that may be investigated. We know the *cj1319*comp_RSP produces and assembles flagella which are glycosylated similarly to WT based on our ability to shear this structure from the cells, EM analysis and our mass spectrometry analysis. We could clearly see that this complement still makes normal (bi)polar flagella. There was no striking difference in the amount of flagella sheared among the strains, no evidence of truncated flagella formation, or lateral flagella formation which has been shown to occur in some *C. jejuni* mutants and impair motility (Balaban *et al*., 2009). Therefore, it is most likely that there is some change that occurred in this strain that affected the flagellar motor proteins or proteins involved in flagellar regulation.

From our analyses, we can conclude that Cj1319 is not required for synthesis of capsular or LOS sugars, nor is it required for legionaminic acid synthesis. We did find however, that it may have a negative regulatory role on legionaminic acid expression as a legionaminic acid derivative was detected more readily in the *cj1319* knockout mutant. Although we could not detect any glycoproteins dependent on Cj1319 for glycosylation based on our analysis of glycoprotein profiles via Western blot, it is possible that Cj1319 is responsible for glycosylation of proteins involved in legionaminic acid synthesis and/or export. These Cj1319 dependent glycoproteins would be repressors of legionaminic acid synthesis and/or export, whose activity is dependent on their glycosylation. Thus, in the absence of Cj1319, they would no longer be glycosylated and thus would no longer be able to perform their repressor role. This would then explain the effect of the complement strains on motility

since there is an upregulation of *cj1320* and *cj1321* which would mean an upregulation of the whole predicted Cj1319 pathway. Since there is an over expression of *cj1319* in *cj1319*comp_RSP, there is an increase in the glycosylation of repressor proteins by this pathway which could shut down motility. In the *cj1319*comp_RNP, there is only an increase in *cj1320* and *cj1321* which limits the increase in glycosylation and thus less repressor proteins would be glycosylated compared to the prior complement strain, and thus motility is only partially lost. It is presumed the same would apply to the *cj1319*comp_ONP strain, since this strain has a kanamycin resistance cassette just upstream of *cj1320* which may also result in an upregulation of its transcription and also that of *cj1321*.

4.1.5 Importance of Cj1319 in the interactions with eukaryotic cells and eukaryotes

We determined that Cj1319 was not important for interactions of *C. jejuni* NCTC 11168 with *A. castellanii.* On the other hand, both protein glycosylation pathway mutants were impaired in their survival within these protists, suggesting that both general protein glycosylation with the *N*-linked heptasaccharide and flagellar glycosylation were essential for survival. Whereas the enhanced killing of *cj1121::CAT* may be due to its increased susceptibility to oxidative stress, the *cj1294::CAT* mutant did not differ in its sensitivity to this stressor compared to WT. The lack of motility was ruled out as the causative factor due to the *cj1319*comp_RSP mutant which was nonmotile but did not differ from WT in its survival within the amoeba. Thus it appears that the glycosylation of the flagella may play a role in prolonging survival of *C. jejuni* within amoeba. However, at this stage we do not know by what mechanism this may occur.

An important difference between the interaction of *C. jejuni* with chickens compared to humans is that *C. jejuni* invades human intestinal cells more than chickens' (Young *et al.*, 2007), signifying that this phenomenon is key to understanding what triggers this chicken commensal to become pathogenic in humans. It is possible that human intestinal cells have

receptors that interact with surface glycoproteins expressed by *C. jejuni* which allow for its internalization. Although Cj1319 did not appear to have any effect on adherence or invasion of the cell lines tested, the *N*-protein glycosylation pathway was evidently important in invasion of Caco-2 cells (Vijayakumar *et al*., 2006) and macrophages. Since a large number of proteins are glycosylated by this pathway, this was not surprising. As the number of bacteria from each strain recovered from macrophage was not affected by infection time, this suggests that the strains were being killed by macrophage at a constant rate compared to the internalization rate. Similarly, the strains were not internalized at different rates, which suggests that the initial internalization was mostly influenced by the macrophage phagocytosing the bacteria. As we demonstrated that *cj1319::CAT* was not significantly different compared to WT in its sensitivity to both nitrosative and oxidative damage which are encountered in the phagosome or secreted into the media by the macrophage, it was not surprising that the mutant survived the internalization to the same extent as the WT. Consistently, the *cj1121::CAT* mutant was more susceptible to oxidative stress which explains its impaired survival in this system.

In the insect model of infection, Cj1319 and Cj1121c were clearly important for killing *G. mellonella.* Motility and flagellar glycosylation were ruled out as factors influencing virulence in this model as the nonmotile *cj1294::CAT* mutant did not differ from WT in its ability to kill the larvae. In *G. mellonella,* the innate immune response is very similar to that of mammals and acts as a first line of defense (Browne *et al*., 2013). This includes eight types of hemocytes, including a phagocytic cell type called a plasmatocyte, circulating in the hemolymph throughout the insect's body. Furthermore, these insects also have a humoral response whereby they secrete anti-microbial peptides, melanin, complement-like proteins, and products of proteolytic pathways to combat pathogens. Since our *cj1319::CAT* mutant was more sensitive to killing by serum containing these effectors, this indicates that the larvae could clear this mutant faster and in turn they were able to survive better upon challenge with *cj1319::CAT*. This was interesting since the excess capsule produced by this mutant which should protect it from serum killing failed to do so (Keo *et al*., 2011). This suggests that Cj1319 has an important role in serum resistance which even excess capsule cannot compensate for. Athough we did not test *cj1121c*::*CAT* for serum susceptibility, this may also be the reason for enhanced survival

of the larvae challenged with this mutant. As such, the glycosylation resulting from both Cj1319 and Cj1121 pathways is important for evading killing by complement or anti-microbial peptides.

As legionaminic acid has been largely associated with livestock isolates from chicken, bovine, and ovine origin (Champion *et al.* 2005), this modification may be used by *Campylobacter* to enhance colonization in livestock. Since more legionaminic acid decorates the *cj1319* mutant's flagellins compared to WT, this provided an opportunity to assess whether enhanced legionaminic acid presented on flagellins offered an advantage with regards to chicken colonization. We showed that our mutant did indeed colonize chicken caecum significantly better than the WT with ~1.1 log difference between both strains. The complemented strain was not tested in this system in light of the partial complementation highlighted by the flagellin analysis which, combined with the variability of the *in vivo* assay and the relatively small difference between wild-type and mutant, would likely prevent reaching statistical significance even upon using a very large number of chicks. The enhanced colonization seen in the mutant may not be solely attributed to the increased legionaminic acid incorporation on flagellins, but may also be due to the currently unknown specific function of Cj1319 that is lacking in this mutant. Further research needs to be done to understand this complex glycosylation machinery and how this complexity contributes to the virulence of *C. jejuni*, its ability to colonize poultry and its ability to survive in seemingly unsuitable growth environments during transmission.

4.1.6 Concluding remarks

In conclusion, although *cj1319* did not appear to have a significant role in interactions with the tested cells lines, we showed that it does have an important role *in vivo*, whereby it affects both colonization and infection potential. Protein glycosylation, particularly the *N*-glycosylation pathway, appears to have an important role in colonization and virulence and survival in macrophage. Studies extended to human macrophages and to chicken epithelial cells and macrophages may be performed in order to address the potential role of Cj1319 in host specificity. This can be done using the new *cj1319::CAT* mutant clone void of point mutations in the LOS genes. The level of different cytokines produced by these cell lines can also be examined as it is possible that Cj1319 indirectly alters the immune response

which may explain why we observe less larvae killing upon challenge with this mutant compared to WT. Larvae immune cells may be extracted and cultured to examine the interactions of *C. jejuni* strains on these primary immune cells to shed light on the mechanism behind the decreased virulence in both *cj1319::CAT* and *cj1121c::CAT* mutants.

We have generated three complement strains with respective control strains which allow us to distinguish effects resulting from our desired mutation from those generated by randomly occurring phase variations. To facilitate future analyses, we have produced a new *cj1319::CAT* mutant that we have confirmed is not a LOS phase variant. This mutant can be utilized for future experimentation as misleading phenotypes arising due to the LOS truncation and excess capsule will be absent.

4.2   Protein glycosylation in *H. pylori*

The major findings presented in this work are the discovery of a Le^y-modified outer membrane glycoprotein HopE and potential *N*-linked glycosylation. This was achieved through a series of anti-Le^y Western blotting for initial detection, extraction of glycopeptides by trypsinolysis treatment of outer membranes coupled with SDS-PAGE and/or lectin chromatography, and the combination of three modern MS fragmentation methods. The significance of these findings is discussed below.

We are the first group who performed MS analysis of an intact glycopeptide from an *H. pylori* glycoprotein and were able to map the glycosylation site with the glycan remaining attached to the peptide using ETD-MS^2. This analysis of an intact glycopeptide is in contrast with the analysis of the *H. pylori* flagellin subunits, FlaA and FlaB (Schirm *et al.*, 2003). FlaA was shown to carry seven Pse5Ac7Ac residues and FlaB could carry up to 10 of these sugars, each at a unique S/T residue, however, the mapping of the glycosylation sites was determined through a comparison of glycosylated and chemically deglycosylated

flagellin peptides following extensive peptide digestion. Similarly, the other glycoproteins in *H. pylori* were identified on the basis of MS analysis of the sugars released from protein samples (Hopf *et al*., 2011) or MS analysis of glycoproteins after chemical deglycosylation (Champasa *et al*., 2013). Noteworthy, neither of these studies had identified HopE as a glycoprotein candidate. This can be explained simply by the prior study only analyzing the soluble protein fraction by MS and not including Le^y or the newly identified 244.14 Da linker in the MS analysis inclusion list during data analysis of released sugars. The latter study did look at outer membrane proteins but used azide-labelled free GlcNAc which acts as a metabolic intermediate for making UDP-GlcNAz, which becomes incorporate into glycoproteins (Vocadlo *et al*., 2003). This labelled GlcNAz variant is used as a basis for tagging these unknown proteins with a FLAG-His-tag via the reaction between the azide and a phosphine that had been incorporated into the FLAG-His-tag. β-elimination was used to release *O*-linked sugars and these proteins were analyzed by mass spectrometry. Since the GlcNAc of Le^y is linked to both fucose and galactose, ligation with the FLAG-His-tag is likely inhibited or much less efficient due to steric hindrance. This is provided that GlcNAz would be incorporated into Le^y. Thus the Le^y modified HopE remained undetected in these studies.

Although the *N*-glycosylation consensus sequence was thought to consist of (D/E)-X-N-X-(S/T) (where X≠P) in bacteria (Kowarik *et al*., 2006), this no longer appears to be the case as the sequence of N-X-(S/T) (where X≠P) was found to be sufficient in some bacteria (Schwarz and Aebi, 2011; Schwarz *et al*., 2011b). The glycopeptide mapped to HopE contains <u>N</u>AT, belonging to the minimal consensus sequence, which suggests potential for this peptide to be modified by Lewis Y via *N*-glycosylation. However, there remains the possibility that the peptide is *O*-glycosylated at either S or T. It was not possible to determine the precise site of glycosylation due to the co-elution of a peptide from the urease subunit A protein which was abundantly found in our samples. Urease is constitutively highly expressed in *H. pylori* and has been shown to associate with outer membranes (Phadnis et al., 1996). The urease peptide was found to be carboxymethylated as a result of the alkylation performed prior to tryptic digestion and thus in order to prevent this peptide from co-eluting and co-isolating with the HopE peptide of interest in the future, no alkylation will be performed *in vitro*. Furthermore, to map the glycosylation site, the

potential glycosylated residues may be mutated by site-directed mutagenesis. The recombinant protein can be analyzed for glycosylation in order to definitively assign the modified residues conclusively.

The enzymes for LPS synthesis in *H. pylori* have been shown to be evolutionarily related to those required for protein *N*-glycosylation in other bacteria such as the Pgl enzymes encoded by *C. jejuni* (Hug *et al*., 2010). In both protein glycosylation and LPS synthesis, oligosaccharides or polysaccharides are assembled onto the lipid carrier undecaprenol pyrophosphate (UndPP) (Hug and Feldman, 2011). To date, most bacteria producing glycans linked to UndPP have been shown to use these glycans either for protein glycosylation or as the O-antigens for LPS, but not for both. *P. aeruginosa* and *A. actinomycetemcomitans* are exceptions that use UndPP-linked glycans for both protein glycosylation and LPS synthesis (Faridmoayer *et al*., 2007; Tang and Mintz, 2010). In these cases, whereas the O-antigen ligase for incorporation of the UndPP-linked glycan onto the core oligosaccharide of LPS is known, the protein responsible for transfer of the glycan onto proteins remains unknown. We also have yet to determine the oligosaccharyl transferase responsible for transfer of the Le^y motif onto HopE. In light of the discovery of the yet to be characterized 244.14 Da linker, it is possible that this linker is the key determinant in which O-antigen chains are transferred onto the LPS core versus those that are transferred by the unknown Oligosaccharyl transferase for protein glycosylation.

The identification of an outer membrane protein glycosylated with Le^y signifies the importance of molecular mimicry in *H. pylori* colonization and infection since we have shown that it is extended beyond the O-antigen of the LPS. The localization of this glycoprotein to the outer membrane further suggests a role for this protein in interactions with the host and the potential for modulation of the immune response. Indeed, several studies have shown the importance of HopE in immune activation and its antigenic properties. HopE purified from *H. pylori* was shown to stimulate cytokine production, including tumour necrosis factor alpha, interleukin 6 (IL-6), IL-8, interferon gamma and granulocyte macrophage colony stimulating factor, from monocytes and lymphocytes *in vitro*, whereby the release of cytokines was dependent on the concentration of HopE and the duration of incubation with this porin (Tufano *et al*., 1994). This porin was also found

in all clinical isolates from asymptomatic carriers and duodenal ulcer and gastric cancer patients, along with BabA and Omp11 (Carlsohn *et al*., 2006). This is not surprising due to its conserved nature among *H. pylori* strains. HopE was ranked as the fourth best candidate antigen as a vaccine target in an analysis of the ANTIGENome of *H. pylori* (Meinke *et al*., 2009). Further studies to understand the role of glycosylation on the function of HopE as an immune modulator can be conducted comparing recombinant HopE expressed and purified from *E. coli*, which would be unglycosylated due to the lack of Le^y synthesis machinery, and HopE purified from *H. pylori*, which would be found in both glycosylated and potentially unglycosylated forms, in their ability to stimulate cytokine production from immune cells. Alternatively, upon determination of the glycosylation site of HopE, this residue can be changed by site-directed mutagenesis to prevent glycosylation while keeping the protein structure (Miller *et al*., 2004).

HopE, originally called Omp15 (Outer membrane protein 15), is the name denoted for HP0706, a member of the *Helicobacter* outer membrane porins (Hops) (Doig *et al*., 1995; Tufano *et al*., 1994), which are conserved among *H. pylori* strains, but not in other *Helicobacter spp.* (Doig and Trust, 1994). This protein is one of the more abundant outer membrane proteins and is a non-specific, large, water-filled channel, with a conductance of 1.5 nS in 1.0M KCl that is present as a homotrimer in the outer membrane (Doig *et al*., 1995), signifying the potential for a wide variety of molecules to be transported through this porin. Porins from gram negatives are comprised of β-barrels unique to bacteria, save those found in mitochondria and chloroplasts (Walther et al., 2009) and have been shown to be immunogenic, such as those expressed by *Salmonella typhimurium* and *E. coli* (Galdiero *et al*., 2012; Liu *et al*., 2012a). Glycosylation may mask the immunogenic epitopes. There is no identified porin-specific signaling receptor on host cells, however, porins are considered as pathogen associated molecular patterns that may be recognized by a number of host cell receptors. There has been evidence of interactions of porins with toll-like receptor 1 (TLR-1), TLR-2, and TLR-6 (Banerjee *et al*., 2008; Galdiero *et al*., 2004; Massari *et al*., 2002, 2006), however, since there are a broad range of porins, these interactions do not appear to be specific. The porins of a number of gram negatives have been shown to have a ring of positively charged residues on their extracellular surface-exposed side, which has been shown to interact with the negatively charged LPS to

maintain stability in the membrane (Ferguson *et al*., 2000; Zeth *et al*., 2000). In addition, the TLR-1/2 heterodimer has been shown to have two predominantly negatively charged ectodomains, which mediate recognition of bound ligands (Jin *et al*., 2007), and thus it has been proposed that the nonspecific electrostatic interactions between the positively charged ring of porins and the negatively charged ectodomains of the TLR receptors may be the basis for recognition and signal transduction in host cells (Galdiero *et al*., 2012). Based on this, it is possible that the glycosylation of HopE by Le^y not only modulates the immune response through molecular mimicry, but may also serve to block the interaction between HopE and TLRs, thus preventing immune activation by these glycoproteins. Since we detected nonglycosylated versions of the HopE glycopeptide, it is possible that not all molecules are glycosylated. These unglycosylated versions of HopE may still activate the immune response, but perhaps the glycosylation of some HopE molecules functions to dampen the response.

HopE is the first *H. pylori* porin to be shown to be glycosylated. In general, only two other bacterial porins have been shown to be glycosylated to date. The *C. jejuni* MOMP porin is *O*-glycosylated with a glycan chain of three GalNAc and one galactose residue and this glycosylation was shown to influence the conformation of the protein such that it improves binding to histo-human blood group antigens (Mahdavi *et al*., 2014). Importantly, the glycosylation was observed to occur at T_{268}, which is in a surface exposed loop as we found in HopE. In *P. aeruginosa,* the porin OrpD was shown to be sialylated and this modification caused increased resistance to β-lactam uptake, thus hinting to a novel mechanism for antibiotic resistance (Khatua *et al*., 2014). Thus it is possible that the glycosylation of HopE also contributes to antibiotic resistance.

In summary, we showed that HopE is glycosylated with the O-antigen Le^y, a highly novel finding as this indicates that *H. pylori* can glycosylate proteins with Lewis O-antigens which were presumed to be exclusively associated with LPS. This also shows that glycosylation in this bacterium is linked to the LPS synthesis pathway. Further studies are needed to determine the precise relationship between the two processes in which the key lies in the identification of the oligosaccharyl transferase responsible for transfer of the O-antigen chain to proteins. Another important finding was that this novel glycosylation was

found to occur through an unknown linker of 244.14 Da. It is presumed that this is a sugar, however, further analysis is required to determine its structure and subsequently the origin of this molecule. We have found a potentially important role for HopE in enhancing host mimicry during *H. pylori* infection based on the role assigned to Le^y motifs in previous literature and thus it is well worth investigating the role that glycosylation with Le^y has on the immunogenicity of HopE and its importance in colonization and infection of the stomach.

4.3   General discussion

This work examined aspects of protein glycosylation in both *C. jejuni* and *H. pylori* in relation to the synthesis of different glycolipids. In *C. jejuni*, we focused on studying Cj1319 to uncover a novel protein glycosylation pathway which may share a precursor with the heptose modification pathway for capsule synthesis. On the other hand, in *H. pylori*, we had preliminary data suggesting that proteins may be glycosylated with the LPS O-antigen. Thus, although our analysis was performed on two different microorganisms, we had a similar focus in both. Protein glycosylation is a complex process that is studied at three levels: the glycosylation pathways, the glycoproteins, and the function of glycosylation. Our work in *C. jejuni* focused on the first and third areas of study, whereas in *H. pylori* the work focused on the second. If we had been successful in determining the pathway of Cj1319 through the identification of its substrate, we would have proceeded to identify the glycoproteins in a similar manner as done in *H. pylori*. Thus, combining the work performed in both bacteria provided a continuum of the methodology undertaken for studying protein glycosylation.

In *C. jejuni*, we dispelled the assumptions that Cj1319 plays a role in modification of the heptose found in the capsule. Although we rejected our original hypothesis that Cj1319 provides a link between capsule synthesis and protein glycosylation, we did not exclude or examine if the capsular K-units may be incorporated onto proteins as has been shown to occur in *A. baumannii* (Lees-Miller *et al.*, 2013). We showed that even in the absence of the general *N*-protein glycosylation pathway, *C. jejuni* still glycosylates a significant

number of proteins and that the glycosylation of these proteins was not dependent on Cj1319. Therefore, nothing excludes the possibility that at least some of these glycoproteins may be glycosylated by capsule K-units. However, being independent of Cj1319, this was not a focus of this work. Importantly, we showed that although Cj1319 can be used in a pathway for making legionaminic acid *in vitro*, this was not the case *in vivo*. Instead, we found that Cj1319 likely plays a role in negative regulation of legionaminic acid synthesis since more legionaminic acid was detected on the flagellins of the *cj1319* knockout mutant. This increase in legionaminic acid expression was correlated with an increase in chicken colonization, thus showing the importance of this modification for interaction of *C. jejuni* with its host. The role of Cj1319 in *C. jejuni* virulence was shown to be significant in the insect model of infection, highlighting that it is worth investigating the basis of attenuation of the *cj1319* knockout mutant in this system.

We found a link between LPS synthesis and protein glycosylation in *H. pylori* by showing that the outer membrane protein HopE is glycosylated by the Le^y O-antigen of the LPS. We showed this through a comprehensive MS analysis of a HopE glycopeptide that was found to be modified with Le^y. The importance of this glycosylation may also be investigated in the future to determine the role that this glycosylation has on both the protein function and its interaction with the host.

We report novel findings related to protein glycosylation in these bacteria. Our study highlights that many glycoproteins in *C. jejuni* have yet to be identified. This further indicates that there are protein glycosylation pathways beyond the general *N*-protein glycosylation pathway and the flagellar *O*-glycosylation pathway. The discovery of Le^y-modified HopE in *H. pylori* provides new insight into mechanisms that this pathogen uses to evade the host immune response and persist in long term colonization.

References

Albermann, C., and Piepersberg, W. (2001). Expression and identification of the RfbE protein from *Vibrio cholerae* O1 and its use for the enzymatic synthesis of GDP-D-perosamine. Glycobiology *11*, 655–661.

Allen, K.J., and Griffiths, M.W. (2001). Effect of environmental and chemotactic stimuli on the activity of the *Campylobacter jejuni* flaA sigma(28) promoter. FEMS Microbiol. Lett. *205*, 43–48.

Alphen, L.B. van, Wenzel, C.Q., Richards, M.R., Fodor, C., Ashmus, R.A., Stahl, M., Karlyshev, A.V., Wren, B.W., Stintzi, A., Miller, W.G., et al. (2014). Biological roles of the O -methyl phosphoramidate capsule modification in *Campylobacter jejuni*. PLOS ONE *9*, e87051.

Appelmelk, B.J., Simoons-Smit, I., Negrini, R., Moran, A.P., Aspinall, G.O., Forte, J.G., Vries, T.D., Quan, H., Verboom, T., Maaskant, J.J., et al. (1996). Potential role of molecular mimicry between *Helicobacter pylori* lipopolysaccharide and host Lewis blood group antigens in autoimmunity. Infect. Immun. *64*, 2031–2040.

Appelmelk, B.J., Negrini, R., Moran, A.P., and Kuipers, E.J. (1997). Molecular mimicry between *Helicobacter pylori* and the host. Trends Microbiol. *5*, 70–73.

Appelmelk, B.J., Shiberu, B., Trinks, C., Tapsi, N., Zheng, P.Y., Verboom, T., Maaskant, J., Hokke, C.H., Schiphorst, W.E.C.M., Blanchard, D., et al. (1998). Phase Variation in *Helicobacter pylori* Lipopolysaccharide. Infect. Immun. *66*, 70–76.

Appelmelk, B.J., Martin, S.L., Monteiro, M.A., Clayton, C.A., McColm, A.A., Zheng, P., Verboom, T., Maaskant, J.J., van den Eijnden, D.H., Hokke, C.H., et al. (1999). Phase variation in *Helicobacter pylori* lipopolysaccharide due to changes in the lengths of poly(C) tracts in alpha3-fucosyltransferase genes. Infect. Immun. *67*, 5361–5366.

Arnold, K., Bordoli, L., Kopp, J., and Schwede, T. (2006). The SWISS-MODEL workspace: a web-based environment for protein structure homology modelling. Bioinforma. Oxf. Engl. *22*, 195–201.

Arsenault, J., Berke, O., Michel, P., Ravel, A., and Gosselin, P. (2012). Environmental and demographic risk factors for campylobacteriosis: do various geographical scales tell the same story? BMC Infect. Dis. *12*, 318.

Aspinall, G.O., McDonald, A.G., and Pang, H. (1992). Structures of the O chains from lipopolysaccharides of *Campylobacter jejuni* serotypes O:23 and O:36. Carbohydr. Res. *231*, 13–30.

Aspinall, G.O., McDonald, A.G., Pang, H., Kurjanczyk, L.A., and Penner, J.L. (1993). An antigenic polysaccharide from *Campylobacter coli* serotype O:30. Structure of a

teichoic acid-like antigenic polysaccharide associated with the lipopolysaccharide. J. Biol. Chem. *268*, 18321–18329.

Aspinall, G.O., Monteiro, M.A., Pang, H., Kurjanczyk, L.A., and Penner, J.L. (1995a). Lipo-oligosaccharide of *Campylobacter lari* strain PC 637. Structure of the liberated oligosaccharide and an associated extracellular polysaccharide. Carbohydr. Res. *279*, 227–244.

Aspinall, G.O., Lynch, C.M., Pang, H., Shaver, R.T., and Moran, A.P. (1995b). Chemical structures of the core region of *Campylobacter jejuni* O:3 lipopolysaccharide and an associated polysaccharide. Eur. J. Biochem. FEBS *231*, 570–578.

Aspinall, G.O., Lynch, C.M., Pang, H., Shaver, R.T., and Moran, A.P. (1995c). Chemical structures of the core region of *Campylobacter jejuni* O:3 lipopolysaccharide and an associated polysaccharide. Eur. J. Biochem. FEBS *231*, 570–578.

Audfray, A., Claudinon, J., Abounit, S., Ruvoën-Clouet, N., Larson, G., Smith, D.F., Wimmerová, M., Pendu, J.L., Römer, W., Varrot, A., et al. (2012). Fucose-binding Lectin from Opportunistic Pathogen *Burkholderia ambifaria* Binds to Both Plant and Human Oligosaccharidic Epitopes. J. Biol. Chem. *287*, 4335–4347.

Balaban, M., Joslin, S.N., and Hendrixson, D.R. (2009). FlhF and its GTPase activity are required for distinct processes in flagellar gene regulation and biosynthesis in *Campylobacter jejuni.* J. Bacteriol. *191*, 6602–6611.

Banerjee, P., Biswas, A., and Biswas, T. (2008). Porin-incorporated liposome induces Toll-like receptors 2- and 6-dependent maturation and type 1 response of dendritic cell. Int. Immunol. *20*, 1551–1563.

Batz, M.B., Hoffmann, S., and Morris, J., J. Glenn (2012). Ranking the Disease Burden of 14 Pathogens in food sources in the United States using attribution data from outbreak investigations and expert elicitation. J. Food Prot. *75*, 1278–1291.

Bause, E. (1983). Structural requirements of N-glycosylation of proteins. Studies with proline peptides as conformational probes. Biochem. J. *209*, 331–336.

Bergman, M.P., Engering, A., Smits, H.H., van Vliet, S.J., van Bodegraven, A.A., Wirth, H.-P., Kapsenberg, M.L., Vandenbroucke-Grauls, C.M.J.E., van Kooyk, Y., and Appelmelk, B.J. (2004). *Helicobacter pylori* modulates the T helper cell 1/T helper cell 2 balance through phase-variable interaction between lipopolysaccharide and DC-SIGN. J. Exp. Med. *200*, 979–990.

Borén, T., Falk, P., Roth, K.A., Larson, G., and Normark, S. (1993). Attachment of *Helicobacter pylori* to human gastric epithelium mediated by blood group antigens. Science *262*, 1892–1895.

Brandt, S., Kwok, T., Hartig, R., König, W., and Backert, S. (2005). NF-kappaB activation and potentiation of proinflammatory responses by the *Helicobacter pylori* CagA protein. Proc. Natl. Acad. Sci. U. S. A. *102*, 9300–9305.

Bronowski, C., James, C.E., and Winstanley, C. (2014). Role of environmental survival in transmission of *Campylobacter jejuni*. FEMS Microbiol. Lett. *356*, 8–19.

Brown, H.L., Hanman, K., Reuter, M., Betts, R.P., and van Vliet, A.H.M. (2015). *Campylobacter jejuni* biofilms contain extracellular DNA and are sensitive to DNase I treatment. Front. Microbiol. *6*.

Browne, N., Heelan, M., and Kavanagh, K. (2013). An analysis of the structural and functional similarities of insect hemocytes and mammalian phagocytes. Virulence *4*, 597–603.

Bui, T.X., Winding, A., Qvortrup, K., Wolff, A., Bang, D.D., and Creuzenet, C. (2012a). Survival of *Campylobacter jejuni* in co-culture with *Acanthamoeba castellanii:* role of amoeba-mediated depletion of dissolved oxygen. Environ. Microbiol. *14*, 2034–2047.

Bui, X.T., Qvortrup, K., Wolff, A., Bang, D.D., and Creuzenet, C. (2012b). Effect of environmental stress factors on the uptake and survival of *Campylobacter jejuni* in *Acanthamoeba castellanii.* BMC Microbiol. *12*, 232.

Butty, F.D., Aucoin, M., Morrison, L., Ho, N., Shaw, G., and Creuzenet, C. (2009). Elucidating the formation of 6-deoxyheptose: biochemical characterization of the GDP-D-*glycero*-d-*manno*-heptose C6 dehydratase, DmhA, and its associated C4 reductase, DmhB. Biochemistry (Mosc.) *48*, 7764–7775.

Butzler, J.P., Dekeyser, P., Detrain, M., and Dehaen, F. (1973). Related vibrio in stools. J. Pediatr. *82*, 493–495.

Byrne, C.M., Clyne, M., and Bourke, B. (2007). *Campylobacter jejuni* adhere to and invade chicken intestinal epithelial cells in vitro. Microbiol. Read. Engl. *153*, 561–569.

Calvano, C.D., Zambonin, C.G., and Jensen, O.N. (2008). Assessment of lectin and HILIC based enrichment protocols for characterization of serum glycoproteins by mass spectrometry. J. Proteomics *71*, 304–317.

Carlsohn, E., Nyström, J., Karlsson, H., Svennerholm, A.-M., and Nilsson, C.L. (2006). Characterization of the outer membrane protein profile from disease-related *Helicobacter pylori* isolates by subcellular fractionation and nano-LC FT-ICR MS analysis. J. Proteome Res. *5*, 3197–3204.

Castric, P., Cassels, F.J., and Carlson, R.W. (2001). Structural characterization of the *Pseudomonas aeruginosa* 1244 pilin glycan. J. Biol. Chem. *276*, 26479–26485.

Chait, B.T. (2006). Mass spectrometry: Bottom-up or top-down? Science *314*, 65–66.

Champasa, K., Longwell, S.A., Eldridge, A.M., Stemmler, E.A., and Dube, D.H. (2013). Targeted identification of glycosylated proteins in the gastric pathogen *Helicobacter pylori* (Hp). Mol. Cell. Proteomics MCP *12*, 2568–2586.

Champion, O.L., Karlyshev, A.V., Senior, N.J., Woodward, M., La Ragione, R., Howard, S.L., Wren, B.W., and Titball, R.W. (2010). Insect infection model for *Campylobacter jejuni* reveals that O-methyl phosphoramidate has insecticidal activity. J. Infect. Dis. *201*, 776–782.

Chen, Y.-H., Poly, F., Pakulski, Z., Guerry, P., and Monteiro, M.A. (2008). The chemical structure and genetic locus of *Campylobacter jejuni* CG8486 (serotype HS:4) capsular polysaccharide: the identification of 6-deoxy-D-ido-heptopyranose. Carbohydr. Res. *343*, 1034–1040.

Chou, W.K., Dick, S., Wakarchuk, W.W., and Tanner, M.E. (2005). Identification and Characterization of NeuB3 from *Campylobacter jejuni* as a Pseudaminic Acid Synthase. J. Biol. Chem. *280*, 35922–35928.

Corcoran, A.T., Annuk, H., and Moran, A.P. (2006). The structure of the lipid anchor of *Campylobacter jejuni* polysaccharide. FEMS Microbiol. Lett. *257*, 228–235.

Creuzenet, C. (2004). Characterization of CJ1293, a new UDP-GlcNAc C6 dehydratase from *Campylobacter jejuni*. FEBS Lett. *559*, 136–140.

Creuzenet, C., and Lam, J.S. (2001). Topological and functional characterization of WbpM, an inner membrane UDP-GlcNAc C6 dehydratase essential for lipopolysaccharide biosynthesis in *Pseudomonas aeruginosa*. Mol. Microbiol. *41*, 1295–1310.

Creuzenet, C., Schur, M.J., Li, J., Wakarchuk, W.W., and Lam, J.S. (2000). FlaA1, a new bifunctional UDP-GlcNAc C6 Dehydratase/ C4 reductase from *Helicobacter pylori*. J. Biol. Chem. *275*, 34873–34880.

Dasti, J.I. (2010). *Campylobacter jejuni*: A brief overview on pathogenicity-associated factors and disease-mediating mechanisms. Int. J. Med. Microbiol. *300*, 205–211.

Day, C.J., Tiralongo, J., Hartnell, R.D., Logue, C.-A., Wilson, J.C., von Itzstein, M., and Korolik, V. (2009). Differential carbohydrate recognition by *Campylobacter jejuni* strain 11168: influences of temperature and growth conditions. PloS One *4*, e4927.

Day, C.J., Semchenko, E.A., and Korolik, V. (2012). Glycoconjugates play a key role in *Campylobacter jejuni* infection: Interactions between host and pathogen. Front. Cell. Infect. Microbiol. *2*.

Day, W.A., Sajecki, J.L., Pitts, T.M., and Joens, L.A. (2000). Role of catalase in *Campylobacter jejuni* intracellular survival. Infect. Immun. *68*, 6337–6345.

Delchier, J.C., Malfertheiner, P., and Thieroff-Ekerdt, R. (2014). Use of a combination formulation of bismuth, metronidazole and tetracycline with omeprazole as a rescue therapy for eradication of *Helicobacter pylori*. Aliment. Pharmacol. Ther. *40*, 171–177.

Dell, A., Galadari, A., Sastre, F., Hitchen, P., Dell, A., Galadari, A., Sastre, F., and Hitchen, P. (2011). Similarities and differences in the glycosylation mechanisms in prokaryotes and eukaryotes. Int. J. Microbiol. Int. J. Microbiol. *2010, 2010*, e148178.

Del Rocio Leon-Kempis, M., Guccione, E., Mulholland, F., Williamson, M.P., and Kelly, D.J. (2006). The *Campylobacter jejuni* PEB1a adhesin is an aspartate/glutamate-binding protein of an ABC transporter essential for microaerobic growth on dicarboxylic amino acids. Mol. Microbiol. *60*, 1262–1275.

Deltenre, M.A.L. (2012). Economics of *Helicobacter pylori* eradication therapy. J. Gastroenterol.

Demendi, M., and Creuzenet, C. (2009). Cj1123c (PglD), a multifaceted acetyltransferase from *Campylobacter jejuni*. Biochem. Cell Biol. Biochim. Biol. Cell. *87*, 469–483.

DiGiandomenico, A., Matewish, M.J., Bisaillon, A., Stehle, J.R., Lam, J.S., and Castric, P. (2002). Glycosylation of *Pseudomonas aeruginosa* 1244 pilin: glycan substrate specificity. Mol. Microbiol. *46*, 519–530.

Dirks, B.P., and Quinlan, J.J. (2014). Development of a modified gentamicin protection assay to investigate the interaction between *Campylobacter jejuni* and *Acanthamoeba castellanii* ATCC 30010. Exp. Parasitol. *140*, 39–43.

Doig, P., and Trust, T.J. (1994). Identification of surface-exposed outer membrane antigens of *Helicobacter pylori*. Infect. Immun. *62*, 4526–4533.

Doig, P., Exner, M.M., Hancock, R.E., and Trust, T.J. (1995). Isolation and characterization of a conserved porin protein from *Helicobacter pylori*. J. Bacteriol. *177*, 5447–5452.

Dorrell, N., and Wren, B.W. (2007). The second century of *Campylobacter* research: recent advances, new opportunities and old problems. Curr. Opin. Infect. Dis. *20*, 514–518.

Dugar, G., Herbig, A., Förstner, K.U., Heidrich, N., Reinhardt, R., Nieselt, K., and Sharma, C.M. (2013). High-resolution transcriptome maps reveal strain-specific regulatory features of multiple *Campylobacter jejuni* isolates. PLoS Genet *9*, e1003495.

Eaton, K.A., Brooks, C.L., Morgan, D.R., and Krakowka, S. (1991). Essential role of urease in pathogenesis of gastritis induced by *Helicobacter pylori* in gnotobiotic piglets. Infect. Immun. *59*, 2470–2475.

Edge, A.S.B. (2003). Deglycosylation of glycoproteins with trifluoromethanesulphonic acid: elucidation of molecular structure and function. Biochem. J. *376*, 339–350.

Elmi, A., Watson, E., Sandu, P., Gundogdu, O., Mills, D.C., Inglis, N.F., Manson, E., Imrie, L., Bajaj-Elliott, M., Wren, B.W., et al. (2012). *Campylobacter jejuni* outer membrane vesicles play an important role in bacterial interactions with human intestinal epithelial cells. Infect. Immun. *80*, 4089–4098.

Escherich, T. (1886). Articles adding to the knowledge of intestinal bacteria, III. on the existence of *vibrios* in the intestines and feces of babies. Muench Med Wochenschr *33*, 815–817.

Faijes, M., Mars, A.E., and Smid, E.J. (2007). Comparison of quenching and extraction methodologies for metabolome analysis of *Lactobacillus plantarum*. Microb. Cell Factories *6*, 27.

Faridmoayer, A., Fentabil, M.A., Mills, D.C., Klassen, J.S., and Feldman, M.F. (2007). Functional characterization of bacterial oligosaccharyltransferases involved in O-linked protein glycosylation. J. Bacteriol. *189*, 8088–8098.

Feldman, M.F., Wacker, M., Hernandez, M., Hitchen, P.G., Marolda, C.L., Kowarik, M., Morris, H.R., Dell, A., Valvano, M.A., and Aebi, M. (2005). Engineering N-linked protein glycosylation with diverse O antigen lipopolysaccharide structures in Escherichia coli. Proc. Natl. Acad. Sci. U. S. A. *102*, 3016–3021.

Ferguson, A.D., Welte, W., Hofmann, E., Lindner, B., Holst, O., Coulton, J.W., and Diederichs, K. (2000). A conserved structural motif for lipopolysaccharide recognition by procaryotic and eucaryotic proteins. Structure *8*, 585–592.

Ferrero, R.L., and Lee, A. (1988). Motility of *Campylobacter jejuni* in a viscous environment: comparison with conventional rod-shaped bacteria. J. Gen. Microbiol. *134*, 53–59.

Filip, C., Fletcher, G., Wulff, J.L., and Earhart, C.F. (1973). Solubilization of the cytoplasmic membrane of *Escherichia coli* by the ionic detergent sodium-Lauryl sarcosinate. J. Bacteriol. *115*, 717–722.

Flanagan, R.C., Neal-McKinney, J.M., Dhillon, A.S., Miller, W.G., and Konkel, M.E. (2009). Examination of *Campylobacter jejuni* putative adhesins leads to the identification of a new protein, designated FlpA, required for chicken colonization. Infect. Immun. *77*, 2399–2407.

Fomsgaard, A., Freudenberg, M.A., and Galanos, C. (1990). Modification of the silver staining technique to detect lipopolysaccharide in polyacrylamide gels. J. Clin. Microbiol. *28*, 2627–2631.

Ford, A.C., Forman, D., Hunt, R.H., Yuan, Y., and Moayyedi, P. (2014). *Helicobacter pylori* eradication therapy to prevent gastric cancer in healthy asymptomatic infected individuals: systematic review and meta-analysis of randomised controlled trials. BMJ *348*, g3174.

Frank, A., and Pevzner, P. (2005). PepNovo: *De novo* peptide sequencing via probabilistic network modeling. Anal. Chem. *77*, 964–973.

Frirdich, E., Biboy, J., Adams, C., Lee, J., Ellermeier, J., Gielda, L.D., DiRita, V.J., Girardin, S.E., Vollmer, W., and Gaynor, E.C. (2012). Peptidoglycan-modifying enzyme Pgp1 Is required for helical cell shape and pathogenicity traits in *Campylobacter jejuni*. PLoS Pathog *8*, e1002602.

Galdiero, M., Galdiero, M., Finamore, E., Rossano, F., Gambuzza, M., Catania, M.R., Teti, G., Midiri, A., and Mancuso, G. (2004). *Haemophilus influenzae* porin induces Toll-like receptor 2-mediated cytokine production in human monocytes and mouse macrophages. Infect. Immun. *72*, 1204–1209.

Galdiero, S., Falanga, A., Cantisani, M., Tarallo, R., Elena Della Pepa, M., D'Oriano, V., and Galdiero, M. (2012). Microbe-host interactions: Structure and role of Gram-negative bacterial porins. Curr. Protein Pept. Sci. *13*, 843–854.

Gatta, L., Vakil, N., Vaira, D., and Scarpignato, C. (2013). Global eradication rates for *Helicobacter pylori* infection: systematic review and meta-analysis of sequential therapy. BMJ *347*, f4587.

Geis, G., Suerbaum, S., Forsthoff, B., Leying, H., and Opferkuch, W. (1993). Ultrastructure and biochemical studies of the flagellar sheath of *Helicobacter pylori*. J. Med. Microbiol. *38*, 371–377.

Gisbert, J.P., Romano, M., Gravina, A.G., Solís-Muñoz, P., Bermejo, F., Molina-Infante, J., Castro-Fernández, M., Ortuño, J., Lucendo, A.J., Herranz, M., et al. (2015). *Helicobacter pylori* second-line rescue therapy with levofloxacin- and bismuth-containing quadruple therapy, after failure of standard triple or non-bismuth quadruple treatments. Aliment. Pharmacol. Ther. *41*, 768–775.

Glaze, P.A., Watson, D.C., Young, N.M., and Tanner, M.E. (2008). Biosynthesis of CMP-N,N′-Diacetyllegionaminic acid from UDP-N,N′-diacetylbacillosamine in *Legionella pneumophila*†. Biochemistry (Mosc.) *47*, 3272–3282.

Godschalk, P.C.R., Kuijf, M.L., Li, J., Michael, F.S., Ang, C.W., Jacobs, B.C., Karwaski, M.-F., Brochu, D., Moterassed, A., Endtz, H.P., et al. (2007). Structural characterization of *Campylobacter jejuni* lipooligosaccharide outer cores associated with Guillain-Barré and Miller Fisher Syndromes. Infect. Immun. *75*, 1245–1254.

Goon, S., Kelly, J.F., Logan, S.M., Ewing, C.P., and Guerry, P. (2003). Pseudaminic acid, the major modification on *Campylobacter* flagellin, is synthesized via the Cj1293 gene. Mol. Microbiol. *50*, 659–671.

Gradel, K.O., Nielsen, H.L., Schønheyder, H.C., Ejlertsen, T., Kristensen, B., and Nielsen, H. (2009). Increased short- and long-term risk of inflammatory bowel disease after *Salmonella* or *Campylobacter* gastroenteritis. Gastroenterology *137*, 495–501.

Grant, C.C., Konkel, M.E., Cieplak, W., and Tompkins, L.S. (1993). Role of flagella in adherence, internalization, and translocation of *Campylobacter jejuni* in nonpolarized and polarized epithelial cell cultures. Infect. Immun. *61*, 1764–1771.

Guerry, P., Alm, R.A., Power, M.E., Logan, S.M., and Trust, T.J. (1991). Role of two flagellin genes in *Campylobacter* motility. J. Bacteriol. *173*, 4757–4764.

Guerry, P., Ewing, C.P., Schirm, M., Lorenzo, M., Kelly, J., Pattarini, D., Majam, G., Thibault, P., and Logan, S. (2006). Changes in flagellin glycosylation affect *Campylobacter* autoagglutination and virulence. Mol. Microbiol. *60*, 299–311.

Guerry, P., Poly, F., Riddle, M., Maue, A.C., Chen, Y.-H., and Monteiro, M.A. (2012). *Campylobacter* polysaccharide capsules: Virulence and vaccines. Front. Cell. Infect. Microbiol. *2*.

Gundogdu, O., Bentley, S.D., Holden, M.T., Parkhill, J., Dorrell, N., and Wren, B.W. (2007). Re-annotation and re-analysis of the *Campylobacter jejuni* NCTC11168 genome sequence. BMC Genomics *8*, 162.

Gundogdu, O., Mills, D.C., Elmi, A., Martin, M.J., Wren, B.W., and Dorrell, N. (2011). The *Campylobacter jejuni* transcriptional regulator Cj1556 plays a role in the oxidative and aerobic stress response and is important for bacterial survival *in vivo*. J. Bacteriol. *193*, 4238–4249.

Hakomori, S. (1992). Le(X) and related structures as adhesion molecules. Histochem. J. *24*, 771–776.

Han, L., and Costello, C.E. (2013). Mass spectrometry of glycans. Biochem. Biokhimiia *78*, 710–720.

Hanisch, F.-G. (2011). Top-down sequencing of O-glycoproteins by in-source decay matrix-assisted laser desorption ionization mass spectrometry for glycosylation site analysis. Anal. Chem. *83*, 4829–4837.

Hanniffy, O.M., Shashkov, A.S., Moran, A.P., Prendergast, M.M., Senchenkova, S.N., Knirel, Y.A., and Savage, A.V. (1999). Chemical structure of a polysaccharide from *Campylobacter jejuni* 176.83 (serotype O:41) containing only furanose sugars. Carbohydr. Res. *319*, 124–132.

Hanning, I., Jarquin, R., and Slavik, M. (2008). *Campylobacter jejuni* as a secondary colonizer of poultry biofilms. J. Appl. Microbiol. *105*, 1199–1208.

Hara-Kudo, Y., and Takatori, K. (2011). Contamination level and ingestion dose of foodborne pathogens associated with infections. Epidemiol. Infect. *139*, 1505–1510.

Heckman, K.L., and Pease, L.R. (2007). Gene splicing and mutagenesis by PCR-driven overlap extension. Nat. Protoc. *2*, 924–932.

Heikema, A.P., Islam, Z., Horst-Kreft, D., Huizinga, R., Jacobs, B.C., Wagenaar, J.A., Poly, F., Guerry, P., van Belkum, A., Parker, C.T., et al. (2015). *Campylobacter jejuni* capsular genotypes are related to Guillain–Barré syndrome. Clin. Microbiol. Infect. *21*, 852.e1–e852.e9.

Heneghan, M.A., McCarthy, C.F., and Moran, A.P. (2000). Relationship of blood group determinants on *Helicobacter pylori* lipopolysaccharide with host Lewis phenotype and inflammatory response. Infect. Immun. *68*, 937–941.

Hickey, T.E., Majam, G., and Guerry, P. (2005). Intracellular survival of *Campylobacter jejuni* in human monocytic cells and induction of apoptotic death by cytholethal distending toxin. Infect. Immun. *73*, 5194–5197.

Hitchcock, P.J., and Brown, T.M. (1983). Morphological heterogeneity among *Salmonella* lipopolysaccharide chemotypes in silver-stained polyacrylamide gels. J. Bacteriol. *154*, 269–277.

Hitchen, P., Brzostek, J., Panico, M., Butler, J.A., Morris, H.R., Dell, A., and Linton, D. (2010). Modification of the *Campylobacter jejuni* flagellin glycan by the product of the Cj1295 homopolymeric-tract-containing gene. Microbiology *156*, 1953–1962.

Ho, N., Kondakova, A.N., Knirel, Y.A., and Creuzenet, C. (2008). The biosynthesis and biological role of 6-deoxyheptose in the lipopolysaccharide O-antigen of *Yersinia pseudotuberculosis*. Mol. Microbiol. *68*, 424–447.

Hopf, P.S., Ford, R.S., Zebian, N., Merkx-Jacques, A., Vijayakumar, S., Ratnayake, D., Hayworth, J., and Creuzenet, C. (2011). Protein glycosylation in *Helicobacter pylori:* beyond the flagellins? PloS One *6*, e25722.

Houliston, R.S., Vinogradov, E., Dzieciatkowska, M., Li, J., Michael, F.S., Karwaski, M.-F., Brochu, D., Jarrell, H.C., Parker, C.T., Yuki, N., et al. (2011). Lipooligosaccharide of *Campylobacter jejuni* similarity with multiple types of mammalian glycans beyond gangliosides. J. Biol. Chem. *286*, 12361–12370.

Howard, S.L., Jagannathan, A., Soo, E.C., Hui, J.P.M., Aubry, A.J., Ahmed, I., Karlyshev, A., Kelly, J.F., Jones, M.A., Stevens, M.P., et al. (2009). *Campylobacter jejuni* glycosylation island important in cell charge, legionaminic acid biosynthesis, and colonization of chickens. Infect. Immun. *77*, 2544–2556.

Huang, B., Zhao, D., Fang, N.-X., Hall, A., Eglezos, S., and Blair, B. (2013). An optimized binary typing panel improves the typing capability for *Campylobacter jejuni.* Diagn. Microbiol. Infect. Dis. *77*, 312–315.

Hug, I., and Feldman, M.F. (2011). Analogies and homologies in lipopolysaccharide and glycoprotein biosynthesis in bacteria. Glycobiology *21*, 138–151.

Hug, I., Couturier, M.R., Rooker, M.M., Taylor, D.E., Stein, M., and Feldman, M.F. (2010). *Helicobacter pylori* lipopolysaccharide is synthesized via a novel pathway with an evolutionary connection to protein N-glycosylation. PLoS Pathog *6*, e1000819.

Humphrey, T. Campylobacters as zoonotic pathogens: A food production perspective. Int. J. Food Microbiol. *117*, 237–257.

Humphrey, S., Chaloner, G., Kemmett, K., Davidson, N., Williams, N., Kipar, A., Humphrey, T., and Wigley, P. (2014). *Campylobacter jejuni* is not merely a commensal in commercial broiler chickens and affects bird welfare. mBio *5*, e01364–14.

Ica, T., Caner, V., Istanbullu, O., Nguyen, H.D., Ahmed, B., Call, D.R., and Beyenal, H. (2012). Characterization of mono- and mixed-culture *Campylobacter jejuni* biofilms. Appl. Environ. Microbiol. *78*, 1033–1038.

Ielmini, M.V. (2011). *Desulfovibrio desulfuricans* PglB homolog possesses oligosaccharyltransferase activity with relaxed glycan specificity and distinct protein acceptor sequence requirements†. Glycobiology *21*, 734–742.

Ierardi, E., Giorgio, F., Losurdo, G., Di Leo, A., and Principi, M. (2013). How antibiotic resistances could change *Helicobacter pylori* treatment: A matter of geography? World J. Gastroenterol. WJG *19*, 8168–8180.

Ilver, D., Arnqvist, A., Ogren, J., Frick, I.M., Kersulyte, D., Incecik, E.T., Berg, D.E., Covacci, A., Engstrand, L., and Borén, T. (1998). *Helicobacter pylori* adhesin binding fucosylated histo-blood group antigens revealed by retagging. Science *279*, 373–377.

Iovine, N.M., Pursnani, S., Voldman, A., Wasserman, G., Blaser, M.J., and Weinrauch, Y. (2008). Reactive nitrogen species contribute to innate host defense against *Campylobacter jejuni*. Infect. Immun. *76*, 986–993.

Ishijima, N., Suzuki, M., Ashida, H., Ichikawa, Y., Kanegae, Y., Saito, I., Borén, T., Haas, R., Sasakawa, C., and Mimuro, H. (2011). BabA-mediated adherence is a potentiator of the *Helicobacter pylori* type IV secretion system activity. J. Biol. Chem. *286*, 25256–25264.

Islam, Z., Gilbert, M., Mohammad, Q.D., Klaij, K., Li, J., van Rijs, W., Tio-Gillen, A.P., Talukder, K.A., Willison, H.J., van Belkum, A., et al. (2012). Guillain-Barré syndrome-related *Campylobacter jejuni* in Bangladesh: ganglioside mimicry and cross-reactive antibodies. PloS One *7*, e43976.

Israeli, E., Agmon-Levin, N., Blank, M., Chapman, J., and Shoenfeld, Y. (2010). Guillain–Barré Syndrome—A classical autoimmune disease triggered by infection or vaccination. Clin. Rev. Allergy Immunol. *42*, 121–130.

Jheng, G.-H., Wu, I.-C., Shih, H.-Y., Wu, M.-C., Kuo, F.-C., Hu, H.-M., Liu, C.-J., Hsu, W.-H., Hu, C.-T., Bair, M.-J., et al. (2015). Comparison of second-line quadruple therapies with or without bismuth for *Helicobacter pylori* Infection, Comparison of

Second-Line Quadruple Therapies with or without Bismuth for *Helicobacter pylori* Infection. BioMed Res. Int. BioMed Res. Int. *2015, 2015*, e163960.

Jin, M.S., Kim, S.E., Heo, J.Y., Lee, M.E., Kim, H.M., Paik, S.-G., Lee, H., and Lee, J.-O. (2007). Crystal structure of the TLR1-TLR2 heterodimer induced by binding of a tri-acylated lipopeptide. Cell *130*, 1071–1082.

Jin, S., Joe, A., Lynett, J., Hani, E.K., Sherman, P., and Chan, V.L. (2001). JlpA, a novel surface-exposed lipoprotein specific to *Campylobacter jejuni,* mediates adherence to host epithelial cells. Mol. Microbiol. *39*, 1225–1236.

Josenhans, C., Labigne, A., and Suerbaum, S. (1995). Comparative ultrastructural and functional studies of *Helicobacter pylori* and *Helicobacter mustelae* flagellin mutants: both flagellin subunits, FlaA and FlaB, are necessary for full motility in *Helicobacter* species. J. Bacteriol. *177*, 3010–3020.

Josenhans, C., Vossebein, L., Friedrich, S., and Suerbaum, S. (2002). The neuA/flmD gene cluster of *Helicobacter pylori* is involved in flagellar biosynthesis and flagellin glycosylation. FEMS Microbiol. Lett. *210*, 165–172.

Joshua, G.W.P., Guthrie-Irons, C., Karlyshev, A.V., and Wren, B.W. (2006). Biofilm formation in *Campylobacter jejuni*. Microbiology *152*, 387–396.

Jowiya, W., Brunner, K., Abouelhadid, S., Hussain, H.A., Nair, S.P., Sadiq, S., Williams, L.K., Trantham, E.K., Stephenson, H., Wren, B.W., et al. (2015). Pancreatic amylase is an environmental signal for regulation of biofilm formation and host interaction in *Campylobacter jejuni.* Infect. Immun. *83*, 4884–4895.

Juge, N. (2012). Microbial adhesins to gastrointestinal mucus. Trends Microbiol. *20*, 30–39.

Kaakoush, N.O., Castaño-Rodríguez, N., Mitchell, H.M., and Man, S.M. (2015). Global epidemiology of *Campylobacter* infection. Clin. Microbiol. Rev. *28*, 687–720.

Kale, A., Phansopa, C., Suwannachart, C., Craven, C.J., Rafferty, J.B., and Kelly, D.J. (2011). The Virulence factor PEB4 (Cj0596) and the periplasmic protein Cj1289 are two structurally related SurA-like chaperones in the human pathogen *Campylobacter jejuni.* J. Biol. Chem. *286*, 21254–21265.

Karlyshev, A.V., and Wren, B.W. (2005). Development and application of an insertional system for gene delivery and expression in *Campylobacter jejuni*. Appl. Environ. Microbiol. *71*, 4004–4013.

Karlyshev, A.V., Linton, D., Gregson, N.A., Lastovica, A.J., and Wren, B.W. (2000). Genetic and biochemical evidence of a *Campylobacter jejuni* capsular polysaccharide that accounts for Penner serotype specificity. Mol. Microbiol. *35*, 529–541.

Karlyshev, A.V., Champion, O.L., Churcher, C., Brisson, J.-R., Jarrell, H.C., Gilbert, M., Brochu, D., St Michael, F., Li, J., Wakarchuk, W.W., et al. (2005a). Analysis of *Campylobacter jejuni* capsular loci reveals multiple mechanisms for the generation of structural diversity and the ability to form complex heptoses. Mol. Microbiol. *55*, 90–103.

Karlyshev, A.V., Ketley, J.M., and Wren, B.W. (2005b). The *Campylobacter jejuni* glycome. FEMS Microbiol. Rev. *29*, 377–390.

Keegan, V.A., Majowicz, S.E., Pearl, D.L., Marshall, B.J., Sittler, N., Knowles, L., and Wilson, J.B. (2009). Epidemiology of enteric disease in C-EnterNet's pilot site - Waterloo region, Ontario, 1990 to 2004. Can. J. Infect. Dis. Med. Microbiol. J. Can. Mal. Infect. Microbiol. Médicale AMMI Can. *20*, 79–87.

Keenan, J.I., Davis, K.A., Beaugie, C.R., McGovern, J.J., and Moran, A.P. (2008). Alterations in *Helicobacter pylori* outer membrane and outer membrane vesicle-associated lipopolysaccharides under iron-limiting growth conditions. Innate Immun. *14*, 279–290.

Kelly, D. j. (2001). The physiology and metabolism of *Campylobacter jejuni a*nd Helicobacter pylori. J. Appl. Microbiol. *90*, 16S – 24S.

Kelly, D.J. (2008). Complexity and versatility in the physiology and metabolism of *Campylobacter jejuni*. In Campylobacter, Third Edition, M.J. Blaser, I. Nachamkin, and C.M. Szymanski, eds. (American Society of Microbiology), pp. 41–61.

Kelly, J., Jarrell, H., Millar, L., Tessier, L., Fiori, L.M., Lau, P.C., Allan, B., and Szymanski, C.M. (2006). Biosynthesis of the N-Linked glycan in *Campylobacter jejuni* and addition onto protein through block transfer. J. Bacteriol. *188*, 2427–2434.

Keo, T., Collins, J., Kunwar, P., Blaser, M.J., and Iovine, N.M. (2011). *Campylobacter* capsule and lipooligosaccharide confer resistance to serum and cationic antimicrobials. Virulence *2*, 30–40.

Khan, I.U.H., Gannon, V., Jokinen, C.C., Kent, R., Koning, W., Lapen, D.R., Medeiros, D., Miller, J., Neumann, N.F., Phillips, R., et al. (2014). A national investigation of the prevalence and diversity of thermophilic *Campylobacter* species in agricultural watersheds in Canada. Water Res. *61*, 243–252.

Khatua, B., Vleet, J.V., Choudhury, B.P., Chaudhry, R., and Mandal, C. (2014). Sialylation of outer membrane porin protein D: A mechanistic basis of antibiotic uptake in *Pseudomonas aeruginosa.* Mol. Cell. Proteomics MCP *13*, 1412–1428.

Kiehlbauch, J., Albach, R., Baum, L., and Chang, K. (1985). Phagocytosis of *Campylobacter jejuni* and its intracellular survival in mononuclear phagocytes. Infect. Immun. *48*, 446–451.

Kim, M.-S., and Pandey, A. (2012). Electron transfer dissociation mass spectrometry in proteomics. Proteomics *12*, 530–542.

Klena, J.D., Gray, S.A., and Konkel, M.E. (1998). Cloning, sequencing, and characterization of the lipopolysaccharide biosynthetic enzyme heptosyltransferase I gene (waaC) from *Campylobacter jejuni* and *Campylobacter coli*. Gene *222*, 177–185.

Kneidinger, B., Graninger, M., Puchberger, M., Kosma, P., and Messner, P. (2001). Biosynthesis of nucleotide-activated-glycero-d-manno-heptose. J. Biol. Chem. *276*, 20935–20944.

Kneidinger, B., Marolda, C., Graninger, M., Zamyatina, A., McArthur, F., Kosma, P., Valvano, M.A., and Messner, P. (2002). Biosynthesis pathway of ADP-l-glycero-β-d-manno-heptose in *Escherichia coli*. J. Bacteriol. *184*, 363–369.

Kondakova, A.N., Ho, N., Bystrova, O.V., Shashkov, A.S., Lindner, B., Creuzenet, C., and Knirel, Y.A. (2008). Structural studies of the O-antigens of *Yersinia pseudotuberculosis* O:2a and mutants thereof with impaired 6-deoxy-d-manno-heptose biosynthesis pathway. Carbohydr. Res. *343*, 1383–1389.

Konkel, M.E., Garvis, S.G., Tipton, S.L., Anderson, J., Donald E., and Cieplak, J., Witold (1997). Identification and molecular cloning of a gene encoding a fibronectin-binding protein (CadF) from *Campylobacter jejuni*. Mol. Microbiol. *24*, 953–963.

Konkel, M.E., Klena, J.D., Rivera-Amill, V., Monteville, M.R., Biswas, D., Raphael, B., and Mickelson, J. (2004). Secretion of virulence proteins from *Campylobacter jejuni* is dependent on a functional flagellar export apparatus. J. Bacteriol. *186*, 3296–3303.

Koolman, L., Whyte, P., Burgess, C., and Bolton, D. (2016). Virulence gene expression, adhesion and invasion of *Campylobacter jejuni* exposed to oxidative stress (H2O2). Int. J. Food Microbiol. *220*, 33–38.

Kowarik, M., Young, N.M., Numao, S., Schulz, B.L., Hug, I., Callewaert, N., Mills, D.C., Watson, D.C., Hernandez, M., Kelly, J.F., et al. (2006). Definition of the bacterial N-glycosylation site consensus sequence. EMBO J. *25*, 1957–1966.

Laemmli, U.K. (1970). Cleavage of Structural Proteins during the Assembly of the Head of Bacteriophage T4. Nature *227*, 680–685.

Lairson, L.L., Henrissat, B., Davies, G.J., and Withers, S.G. (2008). Glycosyltransferases: structures, functions, and mechanisms. Annu. Rev. Biochem. *77*, 521–555.

Lameignere, E., Malinovská, L., Sláviková, M., Duchaud, E., Mitchell, E.P., Varrot, A., Šedo, O., Imberty, A., and Wimmerová, M. (2008). Structural basis for mannose recognition by a lectin from opportunistic bacteria *Burkholderia cenocepacia*. Biochem. J. *411*, 307–318.

Larson, C.L., Shah, D.H., Dhillon, A.S., Call, D.R., Ahn, S., Haldorson, G.J., Davitt, C., and Konkel, M.E. (2008). *Campylobacter jejuni* invade chicken LMH cells inefficiently and stimulate differential expression of the chicken CXCLi1 and CXCLi2 cytokines. Microbiol. Read. Engl. *154*, 3835–3847.

Lees-Miller, R.G., Iwashkiw, J.A., Scott, N.E., Seper, A., Vinogradov, E., Schild, S., and Feldman, M.F. (2013). A common pathway for O-linked protein-glycosylation and synthesis of capsule in *Acinetobacter baumannii*. Mol. Microbiol. *89*, 816–830.

Lehtola, M.J., Pitkänen, T., Miebach, L., and Miettinen, I.T. (2006). Survival of *Campylobacter jejuni* in potable water biofilms: a comparative study with different detection methods. Water Sci. Technol. J. Int. Assoc. Water Pollut. Res. *54*, 57–61.

Lerouge, I., and Vanderleyden, J. (2002). O-antigen structural variation: mechanisms and possible roles in animal/plant–microbe interactions. FEMS Microbiol. Rev. *26*, 17–47.

Linden, S.K., Sutton, P., Karlsson, N.G., Korolik, V., and McGuckin, M.A. (2008). Mucins in the mucosal barrier to infection. Mucosal Immunol. *1*, 183–197.

Linton, D., Gilbert, M., Hitchen, P.G., Dell, A., Morris, H.R., Wakarchuk, W.W., Gregson, N.A., and Wren, B.W. (2000). Phase variation of a β-1,3 galactosyltransferase involved in generation of the ganglioside GM1-like lipo-oligosaccharide of *Campylobacter jejuni*. Mol. Microbiol. *37*, 501–514.

Linton, D., Dorrell, N., Hitchen, P.G., Amber, S., Karlyshev, A.V., Morris, H.R., Dell, A., Valvano, M.A., Aebi, M., and Wren, B.W. (2005). Functional analysis of the *Campylobacter jejuni* N-linked protein glycosylation pathway. Mol. Microbiol. *55*, 1695–1703.

Lisowska, E., and Jaskiewicz, E. (2001). Protein glycosylation, an overview. In eLS, (John Wiley & Sons, Ltd),.

Liu, C., Chen, Z., Tan, C., Liu, W., Xu, Z., Zhou, R., and Chen, H. (2012a). Immunogenic characterization of outer membrane porins OmpC and OmpF of porcine extraintestinal pathogenic *Escherichia coli*. FEMS Microbiol. Lett. *337*, 104–111.

Liu, H., Zhang, N., Wan, D., Cui, M., Liu, Z., and Liu, S. (2014). Mass spectrometry-based analysis of glycoproteins and its clinical applications in cancer biomarker discovery. Clin. Proteomics *11*, 14.

Liu, X., Han, Y., Yuen, D., and Ma, B. (2009). Automated protein (re)sequencing with MS/MS and a homologous database yields almost full coverage and accuracy. Bioinforma. Oxf. Engl. *25*, 2174–2180.

Liu, X., Gao, B., Novik, V., and Galán, J.E. (2012b). Quantitative proteomics of intracellular *Campylobacter jejuni* reveals metabolic reprogramming. PLoS Pathog *8*, e1002562.

Liu, Y.-W., Denkmann, K., Kosciow, K., Dahl, C., and Kelly, D.J. (2013). Tetrathionate stimulated growth of *Campylobacter jejuni* identifies a new type of bi-functional tetrathionate reductase (TsdA) that is widely distributed in bacteria. Mol. Microbiol. *88*, 173–188.

Logan, S.M., and Trust, T.J. (1984). Structural and antigenic heterogeneity of lipopolysaccharides of *Campylobacter jejuni* and *Campylobacter coli.* Infect. Immun. *45*, 210–216.

Logan, S.M., Kelly, J.F., Thibault, P., Ewing, C.P., and Guerry, P. (2002). Structural heterogeneity of carbohydrate modifications affects serospecificity of *Campylobacter* flagellins. Mol. Microbiol. *46*, 587–597.

Logan, S.M., Hui, J.P.M., Vinogradov, E., Aubry, A.J., Melanson, J.E., Kelly, J.F., Nothaft, H., and Soo, E.C. (2009). Identification of novel carbohydrate modifications on *Campylobacter jejuni* 11168 flagellin using metabolomics-based approaches. FEBS J. *276*, 1014–1023.

Lundborg, M. (2010). Glycosyltransferase functions of E. coli O-antigens. Glycobiology *20*, 366–368.

Ma, B. (2003). PEAKS: powerful software for peptide de novo sequencing by tandem mass spectrometry. Rapid Commun. Mass Spectrom. *17*, 2337–2342.

Ma, B., Simala-Grant, J.L., and Taylor, D.E. (2006). Fucosylation in prokaryotes and eukaryotes. Glycobiology *16*, 158R – 184R.

Maal-Bared, R., Bartlett, K.H., Bowie, W.R., and Hall, E.R. (2012). *Campylobacter s*pp. distribution in biofilms on different surfaces in an agricultural watershed (Elk Creek, British Columbia): using biofilms to monitor for *Campylobacter.* Int. J. Hyg. Environ. Health *215*, 270–278.

Magalhães, A., Gomes, J., Ismail, M.N., Haslam, S.M., Mendes, N., Osório, H., David, L., Le Pendu, J., Haas, R., Dell, A., et al. (2009). Fut2-null mice display an altered glycosylation profile and impaired BabA-mediated *Helicobacter pylori* adhesion to gastric mucosa. Glycobiology *19*, 1525–1536.

Magalhães, A., Ismail, M.N., and Reis, C.A. (2010). Sweet receptors mediate the adhesion of the gastric pathogen *Helicobacter pylori*: glycoproteomic strategies. Expert Rev. Proteomics *7*, 307–310.

Mahdavi, J., Sondén, B., Hurtig, M., Olfat, F.O., Forsberg, L., Roche, N., Angstrom, J., Larsson, T., Teneberg, S., Karlsson, K.-A., et al. (2002). *Helicobacter pylori* SabA adhesin in persistent infection and chronic inflammation. Science *297*, 573–578.

Mahdavi, J., Pirinccioglu, N., Oldfield, N.J., Carlsohn, E., Stoof, J., Aslam, A., Self, T., Cawthraw, S.A., Petrovska, L., Colborne, N., et al. (2014). A novel O-linked glycan

modulates *Campylobacter jejuni* major outer membrane protein-mediated adhesion to human histo-blood group antigens and chicken colonization. Open Biol. *4*, 130202.

Mäki, M., Järvinen, N., Räbinä, J., Roos, C., Maaheimo, H., Renkonen, R., Pirkko, and Mattila (2002). Functional expression of *Pseudomonas aeruginosa* GDP-4-keto-6-deoxy-D-mannose reductase which synthesizes GDP-rhamnose. Eur. J. Biochem. FEBS *269*, 593–601.

Maleknia, S.D., and Johnson, R. (2011). Mass Spectrometry of amino acids and proteins. in amino acids, peptides and proteins in organic chemistry, A.B. Hughes, ed. (Wiley-VCH Verlag GmbH & Co. KGaA), pp. 1–50.

Malfertheiner, P., Megraud, F., O'Morain, C.A., Atherton, J., Axon, A.T.R., Bazzoli, F., Gensini, G.F., Gisbert, J.P., Graham, D.Y., Rokkas, T., et al. (2012). Management of *Helicobacter pylori* infection—the Maastricht IV/ Florence Consensus Report. Gut *61*, 646–664.

Malfertheiner, P., Link, A., and Selgrad, M. (2014). Helicobacter pylori: perspectives and time trends. Nat. Rev. Gastroenterol. Hepatol. *advance online publication*.

Man, S.M. (2011). The clinical importance of emerging *Campylobacter* species. Nat. Rev. Gastroenterol. Hepatol. *8*, 669–685.

Marchetti, R., Malinovska, L., Lameignère, E., Adamova, L., Castro, C. de, Cioci, G., Stanetty, C., Kosma, P., Molinaro, A., Wimmerova, M., et al. (2012). *Burkholderia cenocepacia* lectin A binding to heptoses from the bacterial lipopolysaccharide. Glycobiology *22*, 1387–1398.

Marshall, B.J., and Warren, J.R. (1984). Unidentified curved bacilli in the stomach of patients with gastritis and peptic ulceration. Lancet Lond. Engl. *1*, 1311–1315.

Marshall, B.J., Armstrong, J.A., McGechie, D.B., and Glancy, R.J. (1985). Attempt to fulfil Koch's postulates for pyloric *Campylobacter*. Med. J. Aust. *142*, 436–439.

Marshall, D.G., Hynes, S.O., Coleman, D.C., O'Morain, C.A., Smyth, C.J., and Moran, A.P. (1999). Lack of a relationship between Lewis antigen expression and cagA, CagA, vacA and VacA status of Irish *Helicobacter pylori* isolates. FEMS Immunol. Med. Microbiol. *24*, 79–90.

Masoodi, M., Talebi-Taher, M., Tabatabaie, K., Khaleghi, S., Faghihi, A., Agah, S., and Asadi, R. (2015). Clarithromycin vs. gemifloxacin in quadruple therapy regimens for empiric primary treatment of *Helicobacter pylori* Infection: A Randomized Clinical Trial. Middle East J. Dig. Dis. MEJDD *7*, 88–93.

Massari, P., Henneke, P., Ho, Y., Latz, E., Golenbock, D.T., and Wetzler, L.M. (2002). Cutting edge: Immune stimulation by neisserial porins is toll-like receptor 2 and MyD88 dependent. J. Immunol. Baltim. Md 1950 *168*, 1533–1537.

Massari, P., Visintin, A., Gunawardana, J., Halmen, K.A., King, C.A., Golenbock, D.T., and Wetzler, L.M. (2006). Meningococcal porin PorB binds to TLR2 and requires TLR1 for signaling. J. Immunol. Baltim. Md 1950 *176*, 2373–2380.

McAuley, J.L., Linden, S.K., Png, C.W., King, R.M., Pennington, H.L., Gendler, S.J., Florin, T.H., Hill, G.R., Korolik, V., and McGuckin, M.A. (2007). MUC1 cell surface mucin is a critical element of the mucosal barrier to infection. J. Clin. Invest. *117*, 2313–2324.

McCallum, M., Shaw, G.S., and Creuzenet, C. (2011). Characterization of the dehydratase WcbK and the reductase WcaG involved in GDP-6-deoxy-manno-heptose biosynthesis in *Campylobacter jejuni*. Biochem. J. *439*, 235–248.

McCallum, M., Shaw, S.D., Shaw, G.S., and Creuzenet, C. (2012). Complete 6-deoxy-D-altro-heptose biosynthesis pathway from *Campylobacter jejuni:* more complex than anticipated. J. Biol. Chem. *287*, 29776–29788.

McCallum, M., Shaw, G.S., and Creuzenet, C. (2013). Comparison of predicted epimerases and reductases of the *Campylobacter jejuni* D-*altro-* and L-*gluco*-heptose synthesis pathways. J. Biol. Chem. *288*, 19569–19580.

McFadyean, J., and Stockman, S. (1913). Report of the departmental committee appointed by the Board of Agriculture and Fisheries to inquire into Epizootic Abortion. Part III. Abortion in sheep. London: HMSO.

McFarland, L.V., Huang, Y., Wang, L., and Malfertheiner, P. (2015). Systematic review and meta-analysis: Multi-strain probiotics as adjunct therapy for *Helicobacter pylori* eradication and prevention of adverse events. United Eur. Gastroenterol. J. 2050640615617358.

McNally, D.J., Jarrell, H.C., Li, J., Khieu, N.H., Vinogradov, E., Szymanski, C.M., and Brisson, J.-R. (2005). The HS:1 serostrain of *Campylobacter jejuni* has a complex teichoic acid-like capsular polysaccharide with nonstoichiometric fructofuranose branches and O-methyl phosphoramidate groups. FEBS J. *272*, 4407–4422.

McNally, D.J., Aubry, A.J., Hui, J.P.M., Khieu, N.H., Whitfield, D., Ewing, C.P., Guerry, P., Brisson, J.-R., Logan, S.M., and Soo, E.C. (2007a). Targeted metabolomics analysis of *Campylobacter coli* VC167 reveals legionaminic acid derivatives as novel flagellar glycans. J. Biol. Chem. *282*, 14463–14475.

McNally, D.J., Lamoureux, M.P., Karlyshev, A.V., Fiori, L.M., Li, J., Thacker, G., Coleman, R.A., Khieu, N.H., Wren, B.W., Brisson, J.-R., et al. (2007b). Commonality and biosynthesis of the O-methyl phosphoramidate capsule modification in *Campylobacter jejuni.* J. Biol. Chem. *282*, 28566–28576.

Meinke, A., Storm, M., Henics, T., Gelbmann, D., Prustomersky, S., Kovács, Z., Minh, D.B., Noiges, B., Stierschneider, U., Berger, M., et al. (2009). Composition of the

ANTIGENome of *Helicobacter pylori* defined by human serum antibodies. Vaccine *27*, 3251–3259.

Merkle, R.K., and Poppe, I. (1994). Carbohydrate composition analysis of glycoconjugates by gas-liquid chromatography/mass spectrometry. Methods Enzymol. *230*, 1–15.

Merkx-Jacques, A., Obhi, R.K., Bethune, G., and Creuzenet, C. (2004). The *Helicobacter pylori* flaA1 and wbpB genes control lipopolysaccharide and flagellum synthesis and function. J. Bacteriol. *186*, 2253–2265.

Mescher, M.F., and Strominger, J.L. (1976). Purification and characterization of a prokaryotic glucoprotein from the cell envelope of *Halobacterium salinarium*. J. Biol. Chem. *251*, 2005–2014.

Michael, F.S., Szymanski, C.M., Li, J., Chan, K.H., Khieu, N.H., Larocque, S., Wakarchuk, W.W., Brisson, J.-R., and Monteiro, M.A. (2002). The structures of the lipooligosaccharide and capsule polysaccharide of *Campylobacter jejuni* genome sequenced strain NCTC 11168. Eur. J. Biochem. *269*, 5119–5136.

Mihaljevic, R.R., Sikic, M., Klancnik, A., Brumini, G., Mozina, S.S., and Abram, M. (2007). Environmental stress factors affecting survival and virulence of *Campylobacter jejuni.* Microb. Pathog. *43*, 120–125.

Mikesh, L.M., Ueberheide, B., Chi, A., Coon, J.J., Syka, J.E.P., Shabanowitz, J., and Hunt, D.F. (2006). The utility of ETD mass spectrometry in proteomic analysis. Biochem. Biophys. Acta *1764*, 1811–1822.

Miller, G.C., Long, C.J., Bojilova, E.D., Marchadier, D., Badellino, K.O., Blanchard, N., Fuki, I.V., Glick, J.M., and Rader, D.J. (2004). Role of N-linked glycosylation in the secretion and activity of endothelial lipase. J. Lipid Res. *45*, 2080–2087.

Misawa, N., and Blaser, M.J. (2000). Detection and characterization of autoagglutination activity by *Campylobacter jejuni*. Infect. Immun. *68*, 6168–6175.

Mitchell, E.P., Sabin, C., Šnajdrová, L., Pokorná, M., Perret, S., Gautier, C., Hofr, C., Gilboa-Garber, N., Koča, J., Wimmerová, M., et al. (2005). High affinity fucose binding of *Pseudomonas aeruginosa* lectin PA-IIL: 1.0 Å resolution crystal structure of the complex combined with thermodynamics and computational chemistry approaches. Proteins Struct. Funct. Bioinforma. *58*, 735–746.

Mitchell Wells, J., and McLuckey, S.A. (2005). Collision-Induced Dissociation (CID) of Peptides and Proteins. B.-M. in Enzymology, ed. (Academic Press), pp. 148–185.

Monteiro, M.A., Chan, K.H., Rasko, D.A., Taylor, D.E., Zheng, P.Y., Appelmelk, B.J., Wirth, H.P., Yang, M., Blaser, M.J., Hynes, S.O., et al. (1998). Simultaneous expression of type 1 and type 2 Lewis blood group antigens by *Helicobacter pylori*

lipopolysaccharides. Molecular mimicry between *H. pylori* lipopolysaccharides and human gastric epithelial cell surface glycoforms. J. Biol. Chem. *273*, 11533–11543.

Monteiro, M.A., Zheng, P., Ho, B., Yokota, S., Amano, K., Pan, Z., Berg, D.E., Chan, K.H., MacLean, L.L., and Perry, M.B. (2000). Expression of histo-blood group antigens by lipopolysaccharides of *Helicobacter pylori* strains from Asian hosts: the propensity to express type 1 blood-group antigens. Glycobiology *10*, 701–713.

Monteville, M.R., Yoon, J.E., and Konkel, M.E. (2003). Maximal adherence and invasion of INT 407 cells by *Campylobacter jejuni* requires the CadF outer-membrane protein and microfilament reorganization. Microbiol. Read. Engl. *149*, 153–165.

Moran, A.P. (2008). Relevance of fucosylation and Lewis antigen expression in the bacterial gastroduodenal pathogen *Helicobacter pylori.* Carbohydr. Res. *343*, 1952–1965.

Moran, A.P., Prendergast, M.M., and Appelmelk, B.J. (1996). Molecular mimicry of host structures by bacterial lipopolysaccharides and its contribution to disease. FEMS Immunol. Med. Microbiol. *16*, 105–115.

Moran, A.P., Knirel, Y.A., Senchenkova, S.N., Widmalm, G., Hynes, S.O., and Jansson, P.-E. (2002). Phenotypic variation in molecular mimicry between *Helicobacter pylori* lipopolysaccharides and human gastric epithelial cell surface glycoforms. Acid-induced phase variation in Lewis(x) and Lewis(y) expression by *H. pylori* lipopolysaccharides. J. Biol. Chem. *277*, 5785–5795.

Morelle, W., and Michalski, J.-C. (2007). Analysis of protein glycosylation by mass spectrometry. Nat. Protoc. *2*, 1585–1602.

Muldoon, J., Shashkov, A.S., Moran, A.P., Ferris, J.A., Senchenkova, S.N., and Savage, A.V. (2002). Structures of two polysaccharides of *Campylobacter jejuni* 81116. Carbohydr. Res. *337*, 2223–2229.

Murphy, C., Carroll, C., and Jordan, K.N. (2006). Environmental survival mechanisms of the foodborne pathogen *Campylobacter jejuni.* J. Appl. Microbiol. *100*, 623–632.

Murray, C.J.L., Vos, T., Lozano, R., Naghavi, M., Flaxman, A.D., Michaud, C., Ezzati, M., Shibuya, K., Salomon, J.A., Abdalla, S., et al. (2012). Disability-adjusted life years (DALYs) for 291 diseases and injuries in 21 regions, 1990-2010: a systematic analysis for the Global Burden of Disease Study 2010. Lancet Lond. Engl. *380*, 2197–2223.

Nachamkin, I., Yang, X.H., and Stern, N.J. (1993). Role of *Campylobacter jejuni* flagella as colonization factors for three-day-old chicks: analysis with flagellar mutants. Appl. Environ. Microbiol. *59*, 1269–1273.

Nachamkin, I., Allos, B.M., and Ho, T. (1998). *Campylobacter* species and Guillain-Barré Syndrome. Clin. Microbiol. Rev. *11*, 555–567.

Naito, M., Frirdich, E., Fields, J.A., Pryjma, M., Li, J., Cameron, A., Gilbert, M., Thompson, S.A., and Gaynor, E.C. (2010). Effects of sequential *Campylobacter jejuni* 81-176 lipooligosaccharide core truncations on biofilm formation, stress survival, and pathogenesis. J. Bacteriol. *192*, 2182–2192.

Naja, F., Kreiger, N., and Sullivan, T. (2007). *Helicobacter pylori* infection in Ontario: prevalence and risk factors. Can. J. Gastroenterol. J. Can. Gastroenterol. *21*, 501–506.

Negrini, R., Savio, A., Poiesi, C., Appelmelk, B., Buffoli, F., Paterlini, A., Cesari, P., Graffeo, M., Vaira, D., and Franzin, G. (1996). Antigenic mimicry between *Helicobacter pylori* and gastric mucosa in the pathogenesis of body atrophic gastritis. Gastroenterology *111*, 655–665.

Newton, D.T., and Mangroo, D. (1999). Mapping the active site of the *Haemophilus influenzae* methionyl-tRNA formyltransferase: residues important for catalysis and tRNA binding. Biochem. J. *339*, 63–69.

Nielsen, L.N. (2010). MLST clustering of Campylobacter jejuni isolates from patients with gastroenteritis, reactive arthritis and Guillain–Barré syndrome. J. Appl. Microbiol. *108*, 591–599.

Nilsson, C., Skoglund, A., Moran, A.P., Annuk, H., Engstrand, L., and Normark, S. (2006). An enzymatic ruler modulates Lewis antigen glycosylation of *Helicobacter pylori* LPS during persistent infection. Proc. Natl. Acad. Sci. U. S. A. *103*, 2863–2868.

Nilsson, C., Skoglund, A., Moran, A.P., Annuk, H., Engstrand, L., and Normark, S. (2008). Lipopolysaccharide diversity evolving in *Helicobacter pylori* communities through genetic modifications in fucosyltransferases. PLoS ONE *3*, e3811.

Nita-Lazar, M., Wacker, M., Schegg, B., Amber, S., and Aebi, M. (2005). The N-X-S/T consensus sequence is required but not sufficient for bacterial N-linked protein glycosylation. Glycobiology *15*, 361–367.

Nothaft, H., and Szymanski, C.M. (2010). Protein glycosylation in bacteria: sweeter than ever. Nat. Rev. Microbiol. *8*, 765–778.

Nothaft, H., Liu, X., McNally, D.J., Li, J., and Szymanski, C.M. (2009). Study of free oligosaccharides derived from the bacterial N-glycosylation pathway. Proc. Natl. Acad. Sci. U. S. A. *106*, 15019–15024.

Novik, V., Hofreuter, D., and Galán, J.E. (2010). Identification of *Campylobacter jejuni* genes involved in its interaction with epithelial cells. Infect. Immun. *78*, 3540–3553.

Obhi, R.K., and Creuzenet, C. (2005). Biochemical characterization of the *Campylobacter jejuni* Cj1294, a novel UDP-4-keto-6-deoxy-GlcNAc aminotransferase that generates UDP-4-amino-4,6-dideoxy-GalNAc. J. Biol. Chem. *280*, 20902–20908.

Ó Cróinín, T., and Backert, S. (2012). Host Epithelial Cell Invasion by *Campylobacter jejuni*: Trigger or Zipper Mechanism? Front. Cell. Infect. Microbiol. *2*.

Oldfield, N.J., Moran, A.P., Millar, L.A., Prendergast, M.M., and Ketley, J.M. (2002). Characterization of the *Campylobacter jejuni* heptosyltransferase II gene, waaF, provides genetic evidence that extracellular polysaccharide is lipid A core independent. J. Bacteriol. *184*, 2100–2107.

Oliver, J.D. (2005). The viable but nonculturable state in bacteria. J. Microbiol. Seoul Korea *43 Spec No*, 93–100.

Olofsson, J., Axelsson-Olsson, D., Brudin, L., Olsen, B., and Ellström, P. (2013). *Campylobacter jejuni* actively invades the amoeba *Acanthamoeba polyphaga* and survives within non digestive vacuoles. PLoS ONE *8*, e78873.

Olofsson, J., Berglund, P.G., Olsen, B., Ellström, P., and Axelsson-Olsson, D. (2015). The abundant free-living amoeba, *Acanthamoeba polyphaga*, increases the survival of *Campylobacter jejuni* in milk and orange juice. Infect. Ecol. Epidemiol. *5*.

Olsen, J.V., Macek, B., Lange, O., Makarov, A., Horning, S., and Mann, M. (2007). Higher-energy C-trap dissociation for peptide modification analysis. Nat. Methods *4*, 709–712.

On, S. l. w. (2001). Taxonomy of *Campylobacter, Arcobacter, Helicobacter* and related bacteria: current status, future prospects and immediate concerns. J. Appl. Microbiol. *90*, 1S − 15S.

Ongay, S., Boichenko, A., Govorukhina, N., and Bischoff, R. (2012). Glycopeptide enrichment and separation for protein glycosylation analysis. J. Sep. Sci. *35*, 2341–2372.

Osborn, M.J., Gander, J.E., and Parisi, E. (1972). Mechanism of assembly of the outer membrane of *Salmonella typhimurium* site of synthesis of lipopolysaccharide. J. Biol. Chem. *247*, 3973–3986.

O. Westphal, J.K.J. (1964). Bacterial lipopolysaccharide. Extraction with phenol-water and further applications of the procedure. Methods Carbohydr Chem *43*, 83–91.

Papamichael, K., and Mantzaris, G.J. (2012). Pathogenesis of *Helicobacter pylori* infection: colonization, virulence factors of the bacterium and immune and non-immune host response. Hosp. Chron. *7*, 32–38.

Park, S.F. (2002). The physiology of *Campylobacter* species and its relevance to their role as foodborne pathogens. Int. J. Food Microbiol. *74*, 177–188.

Parkhill, J., Wren, B.W., Mungall, K., Ketley, J.M., Churcher, C., Basham, D., Chillingworth, T., Davies, R.M., Feltwell, T., Holroyd, S., et al. (2000). The genome sequence of the food-borne pathogen *Campylobacter jejuni* reveals hypervariable sequences. Nature *403*, 665–668.

Patrie, S.M., Roth, M.J., and Kohler, J.J. (2013). Introduction to glycosylation and mass spectrometry. Methods Mol. Biol. Clifton NJ *951*, 1–17.

Pavlovskis, O.R., Rollins, D.M., Haberberger, R.L., Green, A.E., Habash, L., Strocko, S., and Walker, R.I. (1991). Significance of flagella in colonization resistance of rabbits immunized with *Campylobacter* spp. Infect. Immun. *59*, 2259–2264.

Pei, Z.H., Ellison, R.T., and Blaser, M.J. (1991). Identification, purification, and characterization of major antigenic proteins of *Campylobacter jejuni*. J. Biol. Chem. *266*, 16363–16369.

Peleteiro, B., Bastos, A., Ferro, A., and Lunet, N. (2014). Prevalence of *Helicobacter pylori* infection worldwide: A systematic review of studies with national coverage. Dig. Dis. Sci. *59*, 1698–1709.

Penner, J. (1983). Serotyping of *Campylobacter jejuni* and *Campylobacter coli* on the basis of thermostable antigens. Eur. J. Clin. Microbiol. *2*, 378–383.

Penner, J.L., and Hennessy, J.N. (1980). Passive hemagglutination technique for serotyping *Campylobacter fetus* subsp. *jejuni* on the basis of soluble heat-stable antigens. J. Clin. Microbiol. *12*, 732–737.

Persson, B., Bray, J.E., Bruford, E., Dellaporta, S.L., Favia, A.D., Gonzalez Duarte, R., Jörnvall, H., Kallberg, Y., Kavanagh, K.L., Kedishvili, N., et al. (2009). The SDR (short-chain dehydrogenase/reductase and related enzymes) nomenclature initiative. Chem. Biol. Interact. *178*, 94–98.

Phadnis, S.H., Parlow, M.H., Levy, M., Ilver, D., Caulkins, C.M., Connors, J.B., and Dunn, B.E. (1996). Surface localization of *Helicobacter pylori* urease and a heat shock protein homolog requires bacterial autolysis. Infect. Immun. *64*, 905–912.

Pike, B.L., Guerry, P., and Poly, F. (2013). Global distribution of *Campylobacter jejuni* Penner Serotypes: A Systematic Review. PLoS ONE *8*, e67375.

Pittman, M.S., Elvers, K.T., Lee, L., Jones, M.A., Poole, R.K., Park, S.F., and Kelly, D.J. (2007). Growth of *Campylobacter jejuni* on nitrate and nitrite: electron transport to NapA and NrfA via NrfH and distinct roles for NrfA and the globin Cgb in protection against nitrosative stress. Mol. Microbiol. *63*, 575–590.

Plummer, M., Franceschi, S., Vignat, J., Forman, D., and de Martel, C. (2015). Global burden of gastric cancer attributable to *Helicobacter pylori*. Int. J. Cancer *136*, 487–490.

Poly, F., Serichatalergs, O., Schulman, M., Ju, J., Cates, C.N., Kanipes, M., Mason, C., and Guerry, P. (2011). Discrimination of major capsular types of *Campylobacter jejuni* by multiplex PCR ▽ . J. Clin. Microbiol. *49*, 1750–1757.

Poropatich, K.O., Walker, C.L.F., and Black, R.E. (2010). Quantifying the association between *Campylobacter* infection and Guillain-Barré syndrome: A systematic review. J. Health Popul. Nutr. *28*, 545–552.

Portner, D.C., Leuschner, R.G.K., and Murray, B.S. (2007). Optimising the viability during storage of freeze-dried cell preparations of *Campylobacter jejuni*. Cryobiology *54*, 265–270.

Power, P.M., Seib, K.L., and Jennings, M.P. (2006). Pilin glycosylation in *Neisseria meningitidis* occurs by a similar pathway to wzy-dependent O-antigen biosynthesis in *Escherichia coli.* Biochem. Biophys. Res. Commun. *347*, 904–908.

Qutyan, M., Paliotti, M., and Castric, P. (2007). PilO of *Pseudomonas aeruginosa* 1244: subcellular location and domain assignment. Mol. Microbiol. *66*, 1444–1458.

Raman, R., Raguram, S., Venkataraman, G., Paulson, J.C., and Sasisekharan, R. (2005). Glycomics: an integrated systems approach to structure-function relationships of glycans. Nat. Methods *2*, 817+.

Reuter, M., Mallett, A., Pearson, B.M., and Vliet, A.H.M. van (2010). Biofilm formation by *Campylobacter jejuni* is increased under aerobic conditions. Appl. Environ. Microbiol. *76*, 2122–2128.

Roepstorff, P., and Fohlman, J. (1984). Letter to the editors. Biol. Mass Spectrom. *11*, 601–601.

Rossez, Y., Gosset, P., Boneca, I.G., Magalhães, A., Ecobichon, C., Reis, C.A., Cieniewski-Bernard, C., Joncquel Chevalier Curt, M., Léonard, R., Maes, E., et al. (2014). The lacdiNAc-specific adhesin LabA mediates adhesion of *Helicobacter pylori* to human gastric mucosa. J. Infect. Dis. *210*, 1286–1295.

Rubin, E.J., and Trent, M.S. (2013). Colonize, evade, flourish. Gut Microbes *4*, 439–453.

Ruhaak, L.R., Zauner, G., Huhn, C., Bruggink, C., Deelder, A.M., and Wuhrer, M. (2010). Glycan labeling strategies and their use in identification and quantification. Anal. Bioanal. Chem. *397*, 3457–3481.

Schägger, H. (2006). Tricine-SDS-PAGE. Nat. Protoc. *1*, 16–22.

Schirm, M., Soo, E.C., Aubry, A.J., Austin, J., Thibault, P., and Logan, S.M. (2003). Structural, genetic and functional characterization of the flagellin glycosylation process in *Helicobacter pylori*. Mol. Microbiol. *48*, 1579–1592.

Schirm, M., Schoenhofen, I.C., Logan, S.M., Waldron, K.C., and Thibault, P. (2005). Identification of unusual bacterial glycosylation by tandem mass spectrometry analyses of intact proteins. Anal. Chem. *77*, 7774–7782.

Schoenhofen, I.C., McNally, D.J., Vinogradov, E., Whitfield, D., Young, N.M., Dick, S., Wakarchuk, W.W., Brisson, J.-R., and Logan, S.M. (2006). Functional characterization of dehydratase/aminotransferase pairs from *Helicobacter* and *Campylobacter* enzymes distinguishing the pseudaminic acid and bacillosamine biosynthetic pathways. J. Biol. Chem. *281*, 723–732.

Schoenhofen, I.C., Vinogradov, E., Whitfield, D.M., Brisson, J.-R., and Logan, S.M. (2009). The CMP-legionaminic acid pathway in *Campylobacter*: Biosynthesis involving novel GDP-linked precursors. Glycobiology *19*, 715–725.

Schwarz, F., and Aebi, M. (2011). Mechanisms and principles of N-linked protein glycosylation. Curr. Opin. Struct. Biol. *21*, 576–582.

Schwarz, F., Fan, Y.-Y., Schubert, M., and Aebi, M. (2011a). Cytoplasmic N-glycosyltransferase of *Actinobacillus pleuropneumoniae* Is an inverting enzyme and recognizes the NX(S/T) consensus sequence. J. Biol. Chem. *286*, 35267–35274.

Schwarz, F., Lizak, C., Fan, Y.-Y., Fleurkens, S., Kowarik, M., and Aebi, M. (2011b). Relaxed acceptor site specificity of bacterial oligosaccharyltransferase in vivo. Glycobiology *21*, 45–54.

Scott, D.R., Weeks, D., Hong, C., Postius, S., Melchers, K., and Sachs, G. (1998). The role of internal urease in acid resistance of *Helicobacter pylori*. Gastroenterology *114*, 58–70.

Scott, N.E., Marzook, N.B., Deutscher, A., Falconer, L., Crossett, B., Djordjevic, S.P., and Cordwell, S.J. (2010). Mass spectrometric characterization of the *Campylobacter jejuni* adherence factor CadF reveals post-translational processing that removes immunogenicity while retaining fibronectin binding. PROTEOMICS *10*, 277–288.

Scott, N.E., Parker, B.L., Connolly, A.M., Paulech, J., Edwards, A.V.G., Crossett, B., Falconer, L., Kolarich, D., Djordjevic, S.P., Højrup, P., et al. (2011). Simultaneous glycan-peptide characterization using hydrophilic interaction chromatography and parallel fragmentation by CID, higher energy collisional dissociation, and electron transfer dissociation MS applied to the N-linked glycoproteome of *Campylobacter jejuni*. Mol. Cell. Proteomics MCP *10*, M000031–MCP201.

Sebald, M., and Veron, M. (1963). Base DNA content and classification of *vibrios*. Ann. Inst. Pasteur *105*, 897–910.

Segu, Z.M., and Mechref, Y. (2010). Characterizing protein glycosylation sites through higher-energy C-trap dissociation. Rapid Commun. Mass Spectrom. *24*, 1217–1225.

Sellars, M.J., Hall, S.J., and Kelly, D.J. (2002). Growth of *Campylobacter jejuni* supported by respiration of fumarate, nitrate, nitrite, trimethylamine-N-oxide, or dimethyl sulfoxide requires oxygen. J. Bacteriol. *184*, 4187–4196.

Semchenko, E.A., Day, C.J., Moutin, M., Wilson, J.C., Tiralongo, J., and Korolik, V. (2012). Structural heterogeneity of terminal glycans in *Campylobacter jejuni* lipooligosaccharides. PLoS ONE *7*.

Senior, N.J., Bagnall, M.C., Champion, O.L., Reynolds, S.E., La Ragione, R.M., Woodward, M.J., Salguero, F.J., and Titball, R.W. (2011). *Galleria mellonella* as an infection model for *Campylobacter jejuni* virulence. J. Med. Microbiol. *60*, 661–669.

Šikić Pogačar, M. (2009). Survival of stress exposed *Campylobacter jejuni* in the murine macrophage J774 cell line. Int. J. Food Microbiol. *129*, 68–73.

Simoons-Smit, I.M., Appelmelk, B.J., Verboom, T., Negrini, R., Penner, J.L., Aspinall, G.O., Moran, A.P., Fei, S.F., Shi, B.S., Rudnica, W., et al. (1996). Typing of *Helicobacter pylori* with monoclonal antibodies against Lewis antigens in lipopolysaccharide. J. Clin. Microbiol. *34*, 2196–2200.

Skirrow, M.B. (1977). *Campylobacter* enteritis: a "new" disease. Br. Med. J. *2*, 9–11.

Skoglund, A., Bäckhed, H.K., Nilsson, C., Björkholm, B., Normark, S., and Engstrand, L. (2009). A changing gastric environment leads to adaptation of lipopolysaccharide variants in *Helicobacter pylori* populations during colonization. PloS One *4*, e5885.

Sleytr, U.B., and Thorne, K.J. (1976). Chemical characterization of the regularly arranged surface layers of *Clostridium thermosaccharolyticum* and *Clostridium thermohydrosulfuricum*. J. Bacteriol. *126*, 377–383.

Slynko, V., Schubert, M., Numao, S., Kowarik, M., Aebi, M., and Allain, F.H.-T. (2009). NMR structure determination of a segmentally labeled glycoprotein using in vitro glycosylation. J. Am. Chem. Soc. *131*, 1274–1281.

Stahl, M., Friis, L.M., Nothaft, H., Liu, X., Li, J., Szymanski, C.M., and Stintzi, A. (2011). L-fucose utilization provides *Campylobacter jejuni* with a competitive advantage. Proc. Natl. Acad. Sci. U. S. A. *108*, 7194–7199.

Stanley, P., Schachter, H., and Taniguchi, N. (2009). N-Glycans. In Essentials of Glycobiology, A. Varki, R.D. Cummings, J.D. Esko, H.H. Freeze, P. Stanley, C.R. Bertozzi, G.W. Hart, and M.E. Etzler, eds. (Cold Spring Harbor (NY): Cold Spring Harbor Laboratory Press),.

Sternberg, M.J.E., Tamaddoni-Nezhad, A., Lesk, V.I., Kay, E., Hitchen, P.G., Cootes, A., van Alphen, L.B., Lamoureux, M.P., Jarrell, H.C., Rawlings, C.J., et al. (2013). Gene function hypotheses for the *Campylobacter jejuni* glycome generated by a logic-based Approach. J. Mol. Biol. *425*, 186–197.

Svensson, S.L., Davis, L.M., MacKichan, J.K., Allan, B.J., Pajaniappan, M., Thompson, S.A., and Gaynor, E.C. (2009). The CprS sensor kinase of the zoonotic pathogen *Campylobacter jejuni* influences biofilm formation and is required for optimal chick colonization. Mol. Microbiol. *71*, 253–272.

Svensson, S.L., Pryjma, M., and Gaynor, E.C. (2014). Flagella-mediated adhesion and extracellular DNA release contribute to biofilm formation and stress tolerance of *Campylobacter jejuni*. PLoS ONE *9*.

Syka, J.E.P., Coon, J.J., Schroeder, M.J., Shabanowitz, J., and Hunt, D.F. (2004). Peptide and protein sequence analysis by electron transfer dissociation mass spectrometry. Proc. Natl. Acad. Sci. U. S. A. *101*, 9528–9533.

Szymanski, C.M. (1999). Evidence for a system of general protein glycosylation in *Campylobacter jejuni*. Mol. Microbiol. *32*, 1022–1030.

Szymanski, C.M., Burr, D.H., and Guerry, P. (2002). *Campylobacter* protein glycosylation affects host cell interactions. Infect. Immun. *70*, 2242–2244.

Szymanski, C.M., Michael, F.S., Jarrell, H.C., Li, J., Gilbert, M., Larocque, S., Vinogradov, E., and Brisson, J.-R. (2003). Detection of conserved N-Linked glycans and phase-variable lipooligosaccharides and capsules from *Campylobacter* cells by mass spectrometry and high resolution magic angle spinning NMR Spectroscopy. J. Biol. Chem. *278*, 24509–24520.

Tang, G., and Mintz, K.P. (2010). Glycosylation of the collagen adhesin EmaA of *Aggregatibacter actinomycetemcomitans* is dependent upon the lipopolysaccharide biosynthetic pathway. J. Bacteriol. *192*, 1395–1404.

Thibault, P., Logan, S.M., Kelly, J.F., Brisson, J.R., Ewing, C.P., Trust, T.J., and Guerry, P. (2001). Identification of the carbohydrate moieties and glycosylation motifs in *Campylobacter jejuni* flagellin. J. Biol. Chem. *276*, 34862–34870.

Trachoo, N., Frank, J.F., and Stern, N.J. (2002). Survival of *Campylobacter jejuni* in biofilms isolated from chicken houses. J. Food Prot. *65*, 1110–1116.

Tufano, M.A., Rossano, F., Catalanotti, P., Liguori, G., Capasso, C., Ceccarelli, M.T., and Marinelli, P. (1994). Immunobiological activities of *Helicobacter pylori* porins. Infect. Immun. *62*, 1392–1399.

Ulasi, G.N., Creese, A.J., Hui, S.X., Penn, C.W., and Cooper, H.J. (2015). Comprehensive mapping of O-glycosylation in flagellin from *Campylobacter jejuni* 11168: A multi-enzyme differential ion mobility mass spectrometry approach. PROTEOMICS n/a – n/a.

Vandamme, P. (2000). Taxonomy of the family *Campylobacteraceae*. In Campylobacter, Eds, (Washington, DC: ASM), pp. 3–27.

Verdu, E.F., Mauro, M., Bourgeois, J., and Armstrong, D. (2007). Clinical onset of celiac disease after an episode of *Campylobacter jejuni* enteritis. Can. J. Gastroenterol. J. Can. Gastroenterol. *21*, 453–455.

Veron, M., and Chatelain, R. (1973). Taxonomic study of the genus *Campylobacter* Sebald and Véron and Designation of the Neotype Strain for the Type Species, Campylobacter fetus (Smith and Taylor) Sebald and Véron. Int. J. Sys. Bacteriol *23*.

Viala, J., Chaput, C., Boneca, I.G., Cardona, A., Girardin, S.E., Moran, A.P., Athman, R., Mémet, S., Huerre, M.R., Coyle, A.J., et al. (2004). Nod1 responds to peptidoglycan delivered by the *Helicobacter pylori* cag pathogenicity island. Nat. Immunol. *5*, 1166–1174.

Vijayakumar, S., Merkx-Jacques, A., Ratnayake, D.B., Gryski, I., Obhi, R.K., Houle, S., Dozois, C.M., and Creuzenet, C. (2006). Cj1121c, a Novel UDP-4-keto-6-deoxy-GlcNAc C-4 Aminotransferase Essential for Protein Glycosylation and Virulence in *Campylobacter jejuni.* J. Biol. Chem. *281*, 27733–27743.

Vocadlo, D.J., Hang, H.C., Kim, E.-J., Hanover, J.A., and Bertozzi, C.R. (2003). A chemical approach for identifying O-GlcNAc-modified proteins in cells. Proc. Natl. Acad. Sci. *100*, 9116–9121.

Wacker, M., Linton, D., Hitchen, P.G., Nita-Lazar, M., Haslam, S.M., North, S.J., Panico, M., Morris, H.R., Dell, A., Wren, B.W., et al. (2002). N-linked glycosylation in *Campylobacter jejuni* and its functional transfer into E. coli. Science *298*, 1790–1793.

Wang, G., Rasko, D.A., Sherburne, R., and Taylor, D.E. (1999). Molecular genetic basis for the variable expression of Lewis Y antigen in *Helicobacter pylori*: analysis of the alpha (1,2) fucosyltransferase gene. Mol. Microbiol. *31*, 1265–1274.

Wang, G., Ge, Z., Rasko, D.A., and Taylor, D.E. (2000). Lewis antigens in *Helicobacter pylori:* biosynthesis and phase variation. Mol. Microbiol. *36*, 1187–1196.

Wassenaar, T.M., Bleumink-Pluym, N.M., and van der Zeijst, B.A. (1991). Inactivation of *Campylobacter jejuni* flagellin genes by homologous recombination demonstrates that flaA but not flaB is required for invasion. EMBO J. *10*, 2055–2061.

Wassenaar, T.M., van der Zeijst, B.A., Ayling, R., and Newell, D.G. (1993). Colonization of chicks by motility mutants of *Campylobacter jejuni* demonstrates the importance of flagellin A expression. J. Gen. Microbiol. *139 Pt 6*, 1171–1175.

Wassenaar, T.M., Engelskirchen, M., Park, S., and Lastovica, A. (1997). Differential uptake and killing potential of *Campylobacter jejuni* by human peripheral monocytes/macrophages. Med. Microbiol. Immunol. (Berl.) *186*, 139–144.

Watson, R.O., and Galán, J.E. (2008). *Campylobacter jejuni* survives within epithelial cells by avoiding delivery to lysosomes. PLoS Pathog. *4*, e14.

Weingarten, R.A., Taveirne, M.E., and Olson, J.W. (2009). The dual-functioning fumarate reductase is the sole succinate:quinone reductase in *Campylobacter jejuni* and is required for full host colonization. J. Bacteriol. *191*, 5293–5300.

Weisent, J. (2010). Comparison of three time-series models for predicting campylobacteriosis risk. Epidemiol. Infect. *138*, 898–906.

Whitfield, C. (2006). Biosynthesis and assembly of capsular polysaccharides in *Escherichia coli.* Annu. Rev. Biochem. *75*, 39–68.

Willis, L.M., Stupak, J., Richards, M.R., Lowary, T.L., Li, J., and Whitfield, C. (2013). Conserved glycolipid termini in capsular polysaccharides synthesized by ATP-binding cassette transporter-dependent pathways in Gram-negative pathogens. Proc. Natl. Acad. Sci. *110*, 7868–7873.

Wilson, N.L., Schulz, B.L., Karlsson, N.G., and Packer, N.H. (2002). Sequential analysis of N- and O-Linked glycosylation of 2D-PAGE separated glycoproteins. J. Proteome Res. *1*, 521–529.

Wirth, H.P., Yang, M., Karita, M., and Blaser, M.J. (1996). Expression of the human cell surface glycoconjugates Lewis x and Lewis y by *Helicobacter pylori* isolates is related to cagA status. Infect. Immun. *64*, 4598–4605.

Wong, A., Lange, D., Houle, S., Arbatsky, N.P., Valvano, M.A., Knirel, Y.A., Dozois, C.M., and Creuzenet, C. (2015). Role of capsular modified heptose in the virulence of *C ampylobacter jejuni*: Role of modified heptose in virulence of *C. jejuni*. Mol. Microbiol. 1136–1158.

Wu, B., Zhang, Y., and Wang, P.G. (2001). Identification and characterization of GDP-d-mannose 4,6-dehydratase and GDP-l-fucose synthetase in a GDP-l-fucose biosynthetic gene cluster from *Helicobacter pylori*. Biochem. Biophys. Res. Commun. *285*, 364–371.

Yan, Q., and Lennarz, W.J. (2002). Studies on the function of oligosaccharyl transferase subunits. Stt3p is directly involved in the glycosylation process. J. Biol. Chem. *277*, 47692–47700.

Yang, J.-C., Lu, C.-W., and Lin, C.-J. (2014). Treatment of *Helicobacter pylori* infection: Current status and future concepts. World J. Gastroenterol. WJG *20*, 5283–5293.

Yao, R., Alm, R.A., Trust, T.J., and Guerry, P. (1993). Construction of new *Campylobacter* cloning vectors and a new mutational cat cassette. Gene *130*, 127–130.

Ye, H., Boyne, M.T., Buhse, L.F., and Hill, J. (2013). Direct approach for qualitative and quantitative characterization of glycoproteins using tandem mass tags and an LTQ Orbitrap XL electron transfer dissociation hybrid mass spectrometer. Anal. Chem. *85*, 1531–1539.

York, W.S., Darvill, A.G., McNeil, M., Stevenson, T.T., and Albersheim, P. (1986). Isolation and characterization of plant cell walls and cell wall components. B.-M. in Enzymology, ed. (Academic Press), pp. 3–40.

Young, K.T., Davis, L.M., and DiRita, V.J. (2007). *Campylobacter jejuni*: molecular biology and pathogenesis. Nat. Rev. Microbiol. *5*, 665–679.

Young, N.M., Brisson, J.-R., Kelly, J., Watson, D.C., Tessier, L., Lanthier, P.H., Jarrell, H.C., Cadotte, N., Michael, F.S., Aberg, E., et al. (2002). Structure of the N-Linked glycan present on multiple glycoproteins in the gram-negative bacterium, *Campylobacter jejuni*. J. Biol. Chem. *277*, 42530–42539.

Yu, L., Li, X., Guo, Z., Zhang, X., and Liang, X. (2009). Hydrophilic interaction chromatography based enrichment of glycopeptides by using click maltose: a matrix with high selectivity and glycosylation heterogeneity coverage. Chem. Weinh. Bergstr. Ger. *15*, 12618–12626.

Yuki, N., Susuki, K., Koga, M., Nishimoto, Y., Odaka, M., Hirata, K., Taguchi, K., Miyatake, T., Furukawa, K., Kobata, T., et al. (2004). Carbohydrate mimicry between human ganglioside GM1 and *Campylobacter jejuni* lipooligosaccharide causes Guillain–Barré syndrome. Proc. Natl. Acad. Sci. U. S. A. *101*, 11404–11409.

Zampronio, C.G., Blackwell, G., Penn, C.W., and Cooper, H.J. (2011). Novel glycosylation sites localized in *Campylobacter jejuni* flagellin FlaA by liquid chromatography electron capture dissociation tandem mass spectrometry. J. Proteome Res. *10*, 1238–1245.

Zebian, N., Merkx-Jacques, A., Pittock, P.P., Houle, S., Dozois, C.M., Lajoie, G.A., and Creuzenet, C. (2015). Comprehensive analysis of flagellin glycosylation in *Campylobacter jejuni* NCTC 11168 reveals incorporation of legionaminic acid and its importance for host colonization. Glycobiology cwv104.

Zeth, K., Diederichs, K., Welte, W., and Engelhardt, H. (2000). Crystal structure of Omp32, the anion-selective porin from *Comamonas acidovorans*, in complex with a periplasmic peptide at 2.1 A resolution. Struct. Lond. Engl. 1993 *8*, 981–992.

Zhang, J., Xin, L., Shan, B., Chen, W., Xie, M., Yuen, D., Zhang, W., Zhang, Z., Lajoie, G.A., and Ma, B. (2012). PEAKS DB: De novo sequencing assisted database search for sensitive and accurate peptide identification. Mol. Cell. Proteomics *11*, M111.010587.

Zhang, Y., Fonslow, B.R., Shan, B., Baek, M.-C., and Yates, J.R. (2013). Protein analysis by shotgun/bottom-up proteomics. Chem. Rev. *113*, 2343–2394.

Zhou, W., and Håkansson, K. (2011). Structural characterization of carbohydrates by fourier transform tandem mass spectrometry. Curr. Proteomics *8*, 297–308.

Zielinska, D.F., Gnad, F., Wiśniewski, J.R., and Mann, M. (2010). Precision mapping of an in vivo N-glycoproteome reveals rigid topological and sequence constraints. Cell *141*, 897–907.

Ziprin, R.L., Young, C.R., Stanker, L.H., Hume, M.E., and Konkel, M.E. (1999). The absence of cecal colonization of chicks by a mutant of *Campylobacter jejuni* not expressing bacterial fibronectin-binding protein. Avian Dis. *43*, 586–589.

(1994). Schistosomes, liver flukes and *Helicobacter pylori.* IARC Working Group on the Evaluation of Carcinogenic Risks to Humans. Lyon, 7-14 June 1994. IARC Monogr. Eval. Carcinog. Risks Hum. World Health Organ. Int. Agency Res. Cancer *61*, 1–241.

Appendices

Appendix A: Copyright statements.

Appendix B: Supplementary figures and tables.

Table 9. Primers used in this study.

Primer name	Primer sequence
Cloning	
CJ1319P1	AGGGTCCATGGATGGAAAGGGTGAG
CJ1319P2	GCGTCGGATCCTTAAACATTATAAAGCTCGC

CJ1319P3	GTGGGTACCGTGCTAGATACTTGCGAG
CJ1319P4	ATGCTAGGGCCCCGCTTGTTGAGGTGTGGA
CJ1319P9	GGAAGACCATATGGATGGAAAGGGTGA
CJ1319P10	ATAGTTTCGCGGCAACATTATAAAGCTCGCTT
CJ1319P13	GCCTCGAATTCTTAAACATTATAAAGCTCGC
CJ1319P14	AAGACGGATCCATGGATGGAAAGGGTGAG
CJ1319P16	TAATTTTTGACAAGGAGAATTCTCATGAGAAATATTTTAGTTACAGGTG
CJ1319P17	CACCTGTAACTAAAATATTTCTATGAGAATTCTCCTTGTCAAAAATTA
CJ1319P18	ATAAAAGCGAGCTTTATAATGTTTAAGAAACCCAGCGAACCATTTGAG
CJ1319P19	CTCAAATGGTTCGCTGGGTTTCTTAAACATTATAAAGCTCGCTTTTAT
Aph3-p3-NcoI	AGGTACCATGGTGACATCTAAATCTAGGTACT
Cj1319p25-NdeI	TGGGAATTCCATATGAACATTATAAAGCTCGCTTTTATAATTTTC
16s-Rev-Bglll	GAAGATCTGGAGGTGATCCAACCGC
1318Pr-Bglll	GAAGATCTAAAGTTGAAACTCATAGTATATGGCTTT
Aph3-For-His-NdeI	TGGGAATTCCATATGCACCACCACCACCACCACTGGATAAACCCAGCG AACCATTTG
CJ1320P1	AGGGTCCATGGGCATGTTTAAAAAAGAAATTTCTTTTATAAAAGTCT
CJ1320P2	GCGTCGGATCCTCATTCCTTTTTATTTGCTATTCTAACG
16S rRNA Top Primer – KpnI	GGGGTACCCTGGAACTCAACTGACGCTAA
23S rRNA Bottom NotI	ATAAGAATGCGGCCGCTCTTGCACATTGCAGTCCTA
CJ1419P1	AGGTACCATGGGCATGCAAAAACTAGTAGAACAA
CJ1419P2	GCGTCGGATCCTTATATTTTTTTAGCACTCCAAC
CJ1426P1	AGGTACCATGGGCATGAAAAAAGAACAATTGGAAGTATTA
CJ1426P2	GCGTCGGATCCTCATATCCAATCAAGTAAAATATTTG
Sequencing	
HP0379P1	GAATCTTGGGGGCGTTATTGG
HP0379P2	CCGGTGTAAAACACTCGTTTAG

HP0651P1	GGTGGTTTGCTTCAGCGGAG
HP0094P1	CAACACCTCCCCAAGCTAGT
HP0094P2	CAAGATTGCATGAGCAGCATG
qPCR	
CJ1142P1	TGCATGGTGATAGAGTGGAGC
CJ1142P2	GATTTCTCATCTTCACCCATTTGT
CJ1141P1	TAGATGCGGCCAAAAGAGCA
CJ1141P2	ACCAAACCTTGCTTCTCTACAT
CJ1142P1	CCTGCCATACAAAGAGGTGT
CJ1142P2	ATAAGCCACTCATCTTGCGGT
CJ1121RT-F	AAACCTCCATTTGCGCTACG
CJ1121RT-R	TCACCACTTCAGGTGGAGGTA
CJ1294RT-F	ATTTTGCGGGCAATAGCGTT
CJ1294RT-R	CCACAGCCCCACCTTCAAAA
CJ1319RT-F	TTTATCCACACCTCAACAAGCG
CJ1319RT-R	GGTGTTAAAAGGGCGTGCAA
CJ1318RT-F	ACCGAGGCTTATGGAGGAAATG
CJ1318RT-R	TGGTTCCTTCTATCCTTGCTCC
CJ1320RT-F	GCCCTACATGAGCCTTGCTT
CJ1320RT-R	ATATGAAGGGCTGCTGTGCC
CJ1321RT-F	AGGACAAGGGGTTATAGTGTGTC
CJ1321RT-R	GCAAGGCAACAGGCTAACTC
CJ1419RT-F	AGCCTGTTGCTCTAACCCAG
CJ1419RT-R	GTCGCTGATATCGGTGCAGG
CJ1426RT-F	TTATCGACATAAAGCATCTTGTAAAAAA
CJ1426RT-R	ATTGATAATCATCAGCAAGCTAGGAA

|	
CJ1120RT-F	AGTTCTCCCCCTTTTGCGAT
CJ1120RT-R	TGCTTGTGTGCGTTTTGGTA
CJ1293RT-F	TTAATCACGGGCGGAACAGG
CJ1293RT-R	CACATCACGCATAGCAGCAC
CJ1427RT-F	CCGCATGCACTTTATCGATCCCA
CJ1427RT-R	CTGATATTATTATTCCTCTAGCTGCT
CJ1428RT-F	CAAGCGGTTGCTAAATTTTTTAAAGAA
CJ1428RT-R	AAATCACCTTGAAATAAATATTCCTCTT
CJ1429RT-F	GCTTGTACCAAAGTAATTGTATTCTC
CJ1429RT-R	GAATAGGTGGTAATGGAGATGGTG
CJ1430RT-F	CAGATGGAATTAAATTTAAGCATGACA
CJ1430RT-R	TGGTGGTAATAAAATAAGTTGCTGATT
AcetylRT-F	TAGCCCCAATCCTTGCACAAGCT
AcetylRT-R	AATGTCTTGATCGTCATATGAAAACAA
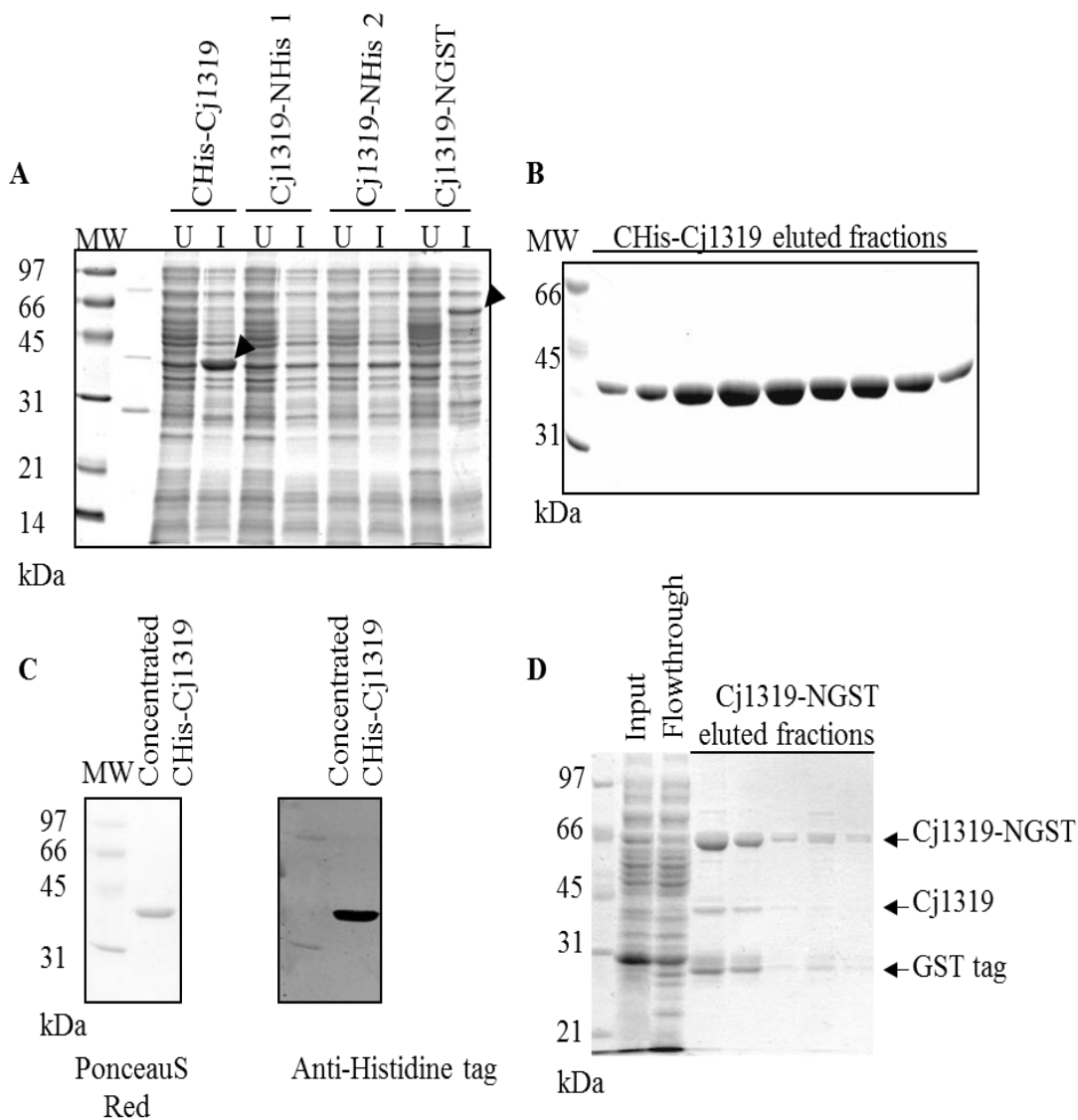
Figure 46. Expression and purification of Cj1319 tagged clones.

SDS-PAGE stained with Coomassie blue showing the induced expression of Cj1319 from four expression clones and highlighting that expression was successful with Cj1319-CHis and Cj1319-NGST (A). The pure Cj1319-CHis elution fractions stained with Coomassie blue (B) and detected by anti-His Western blot (C). Analysis of Cj1319-NGST purification and thrombin cleavage by SDS-SDS-PAGE and Coomassie blue staining.

Table 10. Compositonal analysis of the LOS and capsule by GC-MS of *C. jejuni* WT and *cj1319::CAT*.

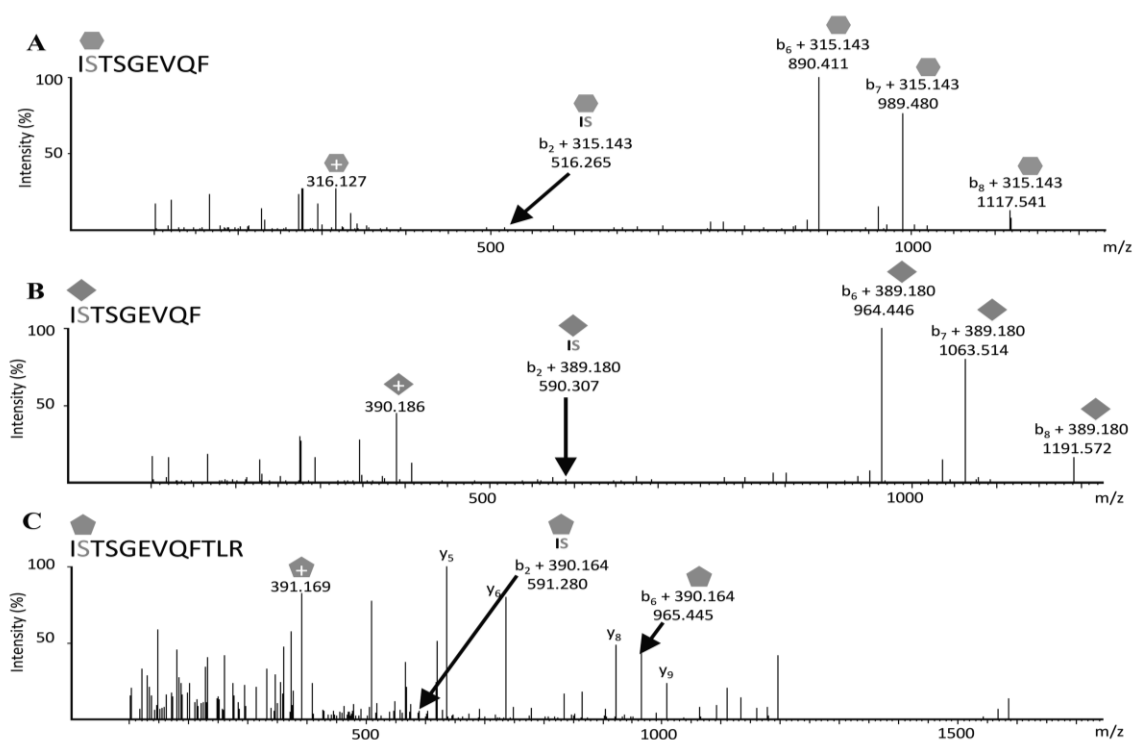| Sugar	WT (mol %)	*cj1319::CAT* (mol %)	WT Ratio of sugars to GalNAc	*cj1319::CAT* Ratio of sugars to GalNAc
LOS				
Galactose (Gal)	29.4	25.2	4.39	3.32
Glucose (Glc)	13.4	14.0	2	1.84
N-Acetyl Galactosamine (GalNAc)	6.7	7.6	1	1
Neuraminic acid (NANA)	6.7	6.3	1	0.83
Heptose	18.3	19.7	2.73	2.59
KDO	22.1	22.8	3.30	3
Capsule				
GlcA	22.7	22.8	1.6	1.52
Modified heptose	11.7	7.8	0.82	0.52
GalNAc	14.2	15.0	1	1
Ribose	51.4	54.4	3.6	3.6

Figure 47. HCD-MS^2 analysis of WT glycopeptide showing multiple glycoforms.

(A) Peptide modified with Pse5Ac7Am/Leg5Am7Ac (● 315.143 Da). **(B)** Peptide modified with Pse5AcGriMe7Am (◆ 389.180 m/z). **(C)** Peptide modified with Pse5AcGriMe7Ac (⬠ 390.164 m/z).
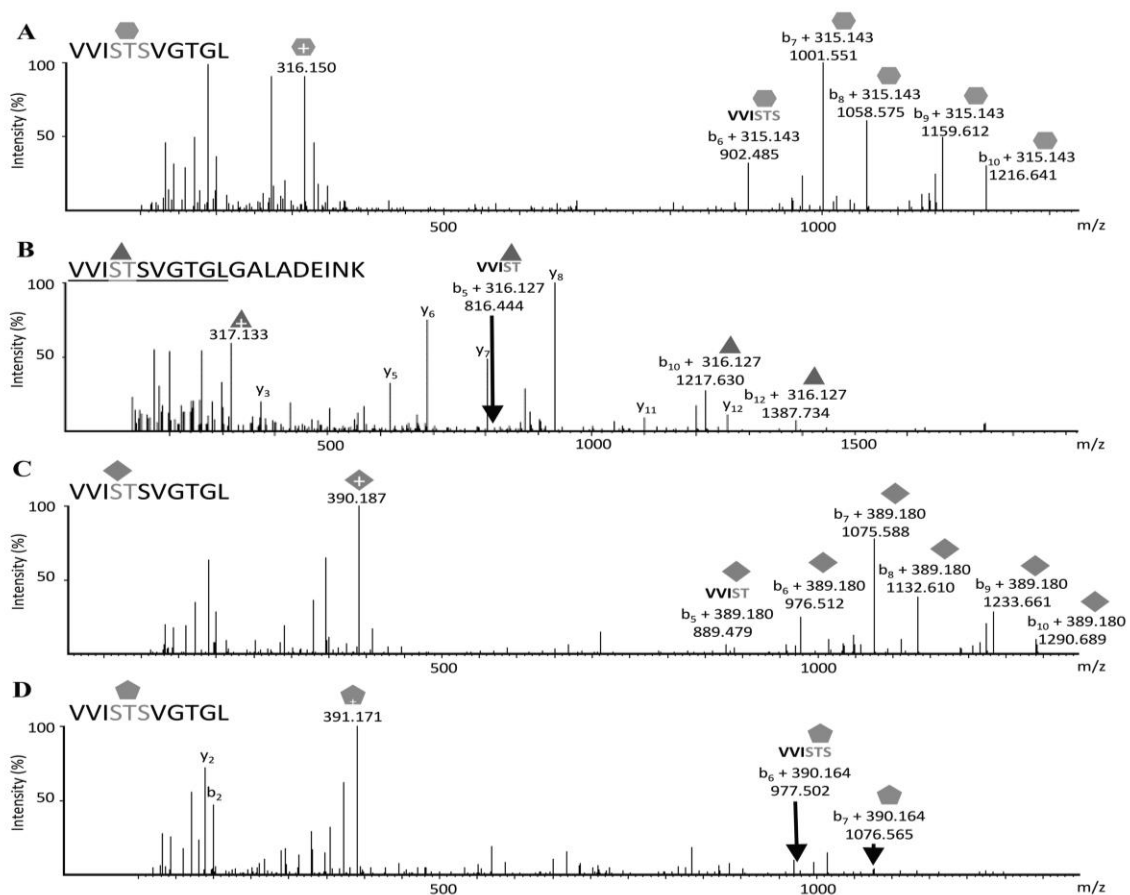
Figure 48. HCD-MS² analysis of WT glycopeptide showing multiple glycoforms.

(**A**) Peptide modified with Pse5Ac7Am/Leg5Am7Ac (⬡ 315.143 Da). (**B**) Peptide modified with Pse5Ac7Ac/Leg5Ac7Ac (▲ 316.127 Da). (**C**) Peptide modified with Pse5AcGriMe7Am (◆ 389.180 m/z). (**D**) Peptide modified with Pse5AcGriMe7Ac (⬠ 390.164 m/z).
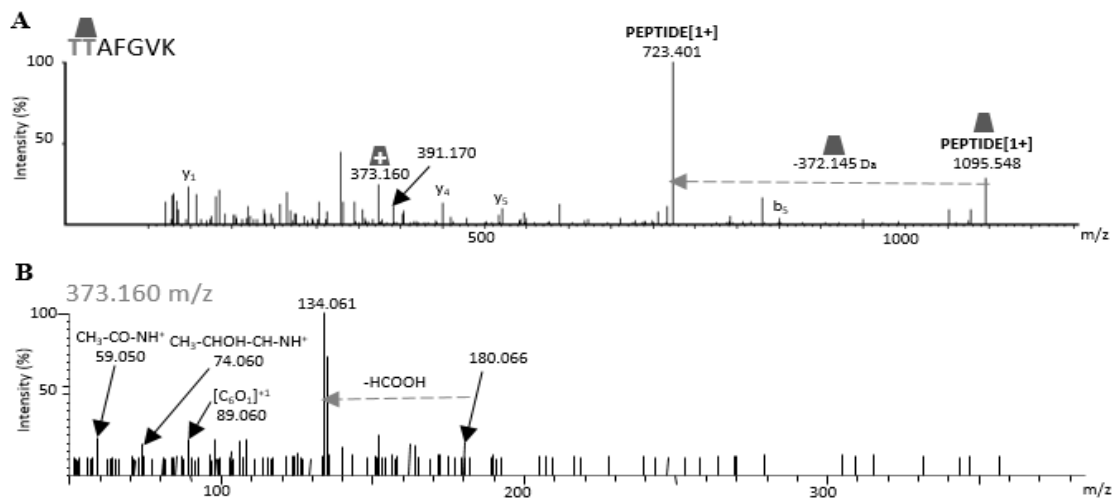
Figure 49. Targeted MS analysis of the 372.145 Da (▲) modification.

(**A**) HCD-MS^2 of peptide TTAFGVK carrying the 372.145 Da modification seen as ion at 373.160 (▲). (**B**) HCD-MS^3 of the 373.160 m/z ion acquired from HCD-MS^2 data. Key ions are noted and potential chemical formulas are indicated where applicable.
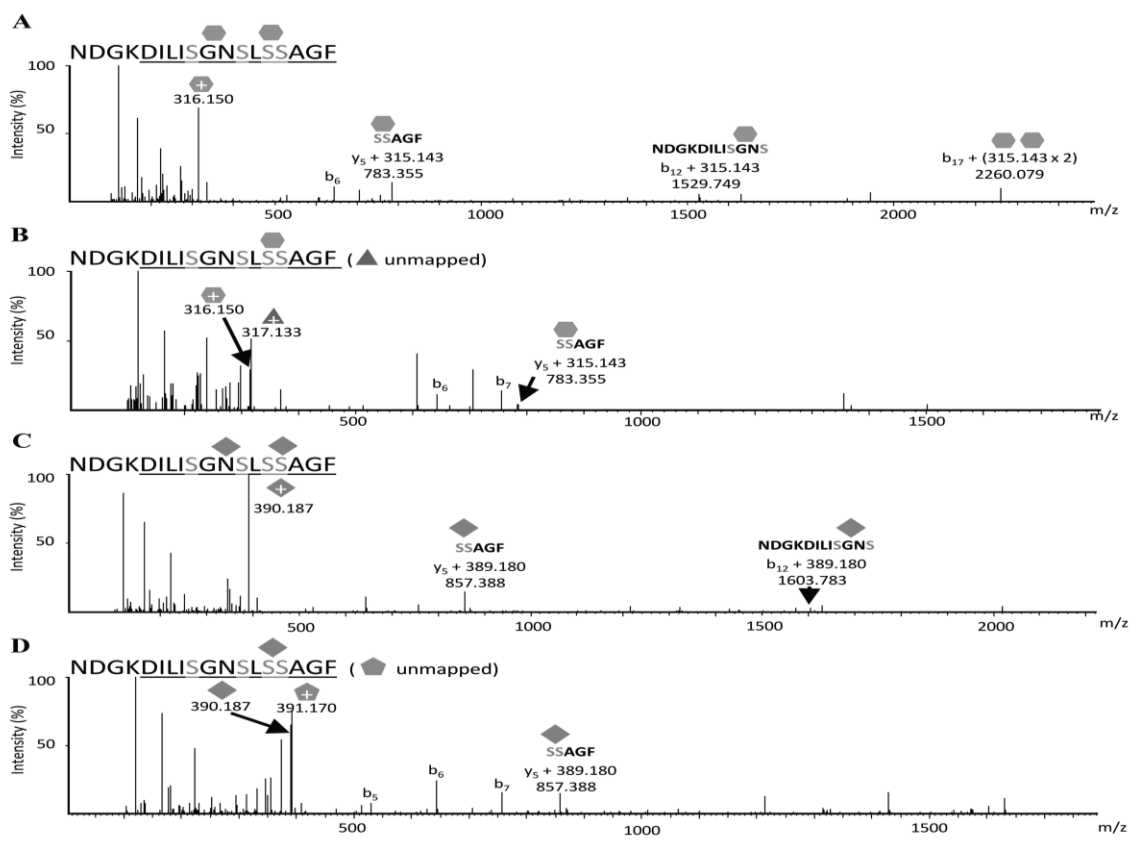
Figure 50. HCD-MS² analysis of WT glycopeptide glycosylated with two sugars showing multiple glycoforms.

(A) Peptide modified with two residues of Pse5Ac7Am/Leg5Am7Ac (● 315.143 Da). **(B)** Peptide modified with Pse5Ac7Ac/Leg5Ac7Ac (▲ 316.127 Da) and Pse5Ac7Am/Leg5Am7Ac. **(C)** Peptide modified with two residues of Pse5AcGriMe7Am (◆ 389.180 Da). **(D)** Peptide modified with Pse5AcGriMe7Ac (⬠ 390.164 Da) and Pse5AcGriMe7Am.

Figure 51. HCD-MS^2 analysis of two WT glycopeptides only found after a sequential digest with trypsin followed by chymotrypsin.

 (A) Peptide modified with Pse5Ac7Am/Leg5Am7Ac (⬤ 315.143 Da). **(B)** Peptide modified with Pse5AcGriMe7Am (◆ 389.180 Da).
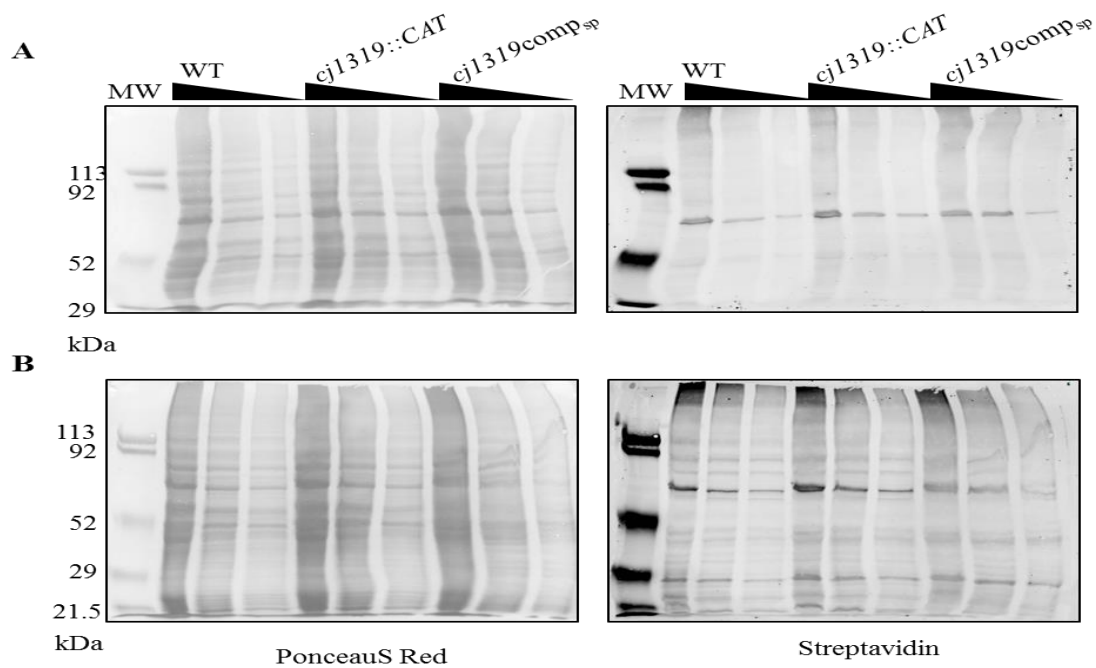
Figure 52. BambL and PAII-L lectin blots of soluble proteins.

Analysis of soluble protein with **(A)** PAII-L and **(B)** BambL by Western blot using strepatividin.

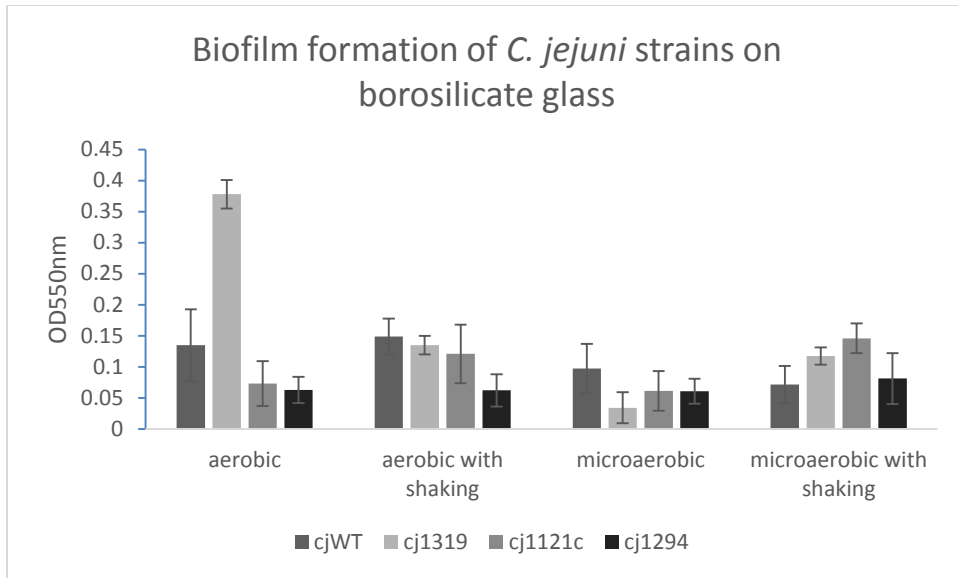Biofilm formation of *C. jejuni* strains on borosilicate glass

Figure 53. Biofilm formation of *C. jejuni* strains 60 hours under aerobic or microaerobic conditions with or without shaking.
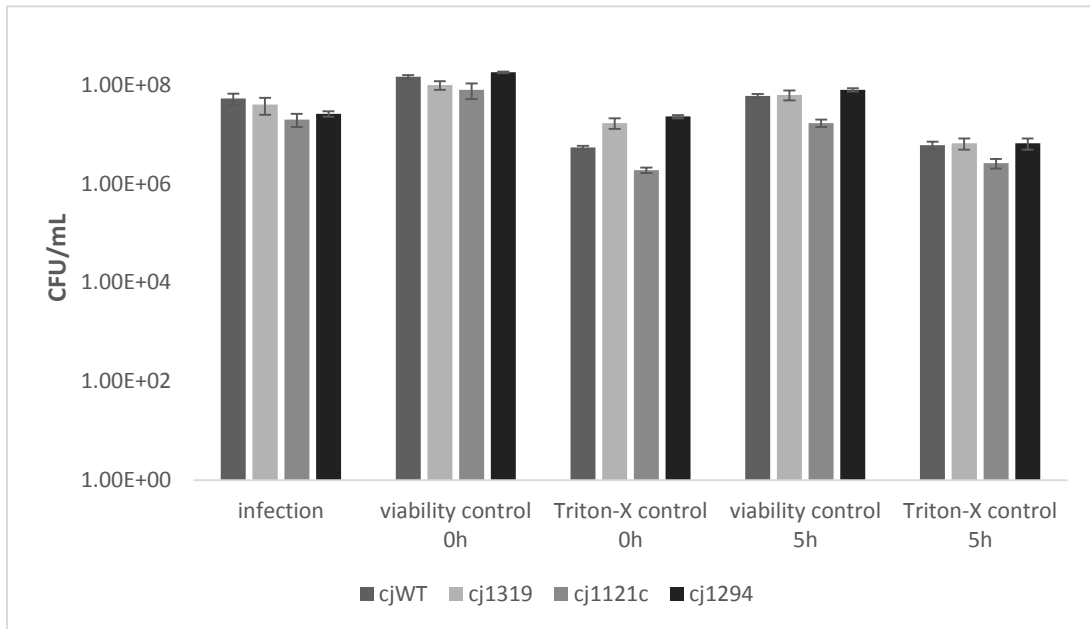

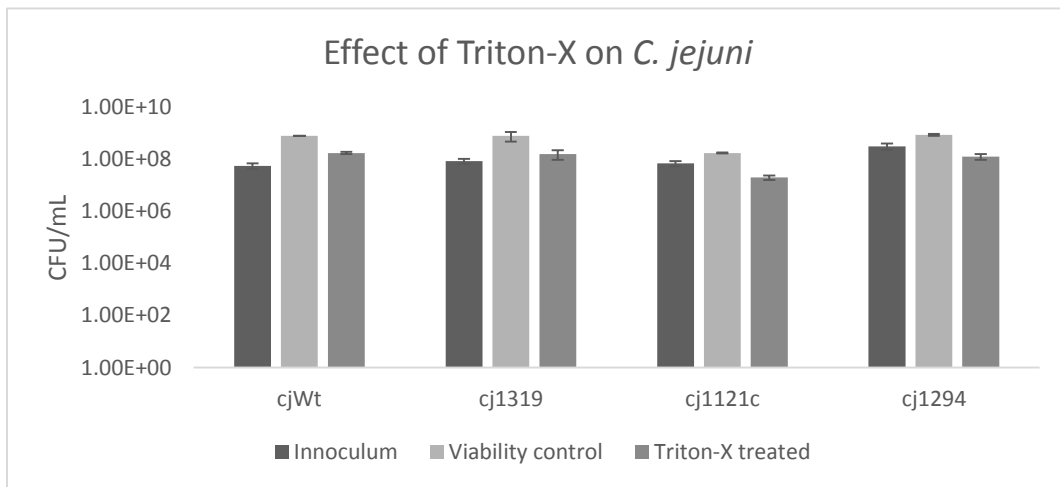**Figure 54. Effect of Triton X-100 on *C. jejuni* strains in amoeba assay.**

Figure 55. Effect of Triton X-100 on *C. jejuni* strains in Caco-2 cell assay.

Table 11. Monoisotopic fragment ions of the peptide FLSAGPNATNLYYHLK.

Seq	#	A	B	C	X	Y	Z	# (+1)
F	1	120.08137	148.07628	165.10283	-	1808.93358	1791.90704	16
L	2	233.16543	261.16035	278.18690	1687.84444	1661.86517	1644.83862	15
S	3	320.19746	348.19238	365.21892	1574.76037	1548.78111	1531.75456	14
A	4	391.23457	419.22949	436.25604	1487.72834	1461.74908	1444.72253	13
G	5	448.25604	476.25095	493.27750	1416.69123	1390.71197	1373.68542	12
P	6	545.30880	573.30372	590.33027	1359.66977	1333.69050	1316.66395	11
N	7	659.35173	687.34664	704.37319	1262.61700	1236.63774	1219.61119	10
A	8	730.38884	758.38376	775.41031	1148.57408	1122.59481	1105.56826	9
T	9	831.43652	859.43144	876.45798	1077.53696	1051.55770	1034.53115	8
N	10	945.47945	973.47436	990.50091	976.48928	950.51002	933.48347	7
L	11	1058.56351	1086.55843	1103.58498	862.44636	836.46709	819.44054	6
Y	12	1221.62684	1249.62175	1266.64830	749.36229	723.38303	706.35648	5
Y	13	1384.69017	1412.68508	1429.71163	586.29897	560.31970	543.29315	4
H	14	1521.74908	1549.74399	1566.77054	423.23564	397.25637	380.22982	3
L	15	1634.83314	1662.82806	1679.85461	286.17673	260.19746	243.17091	2
K	16	1762.92811	1790.92302	-	173.09266	147.11340	130.08685	1

Table produced through the Fragment Ion Calculator tool on

http://db.systemsbiology.net/.
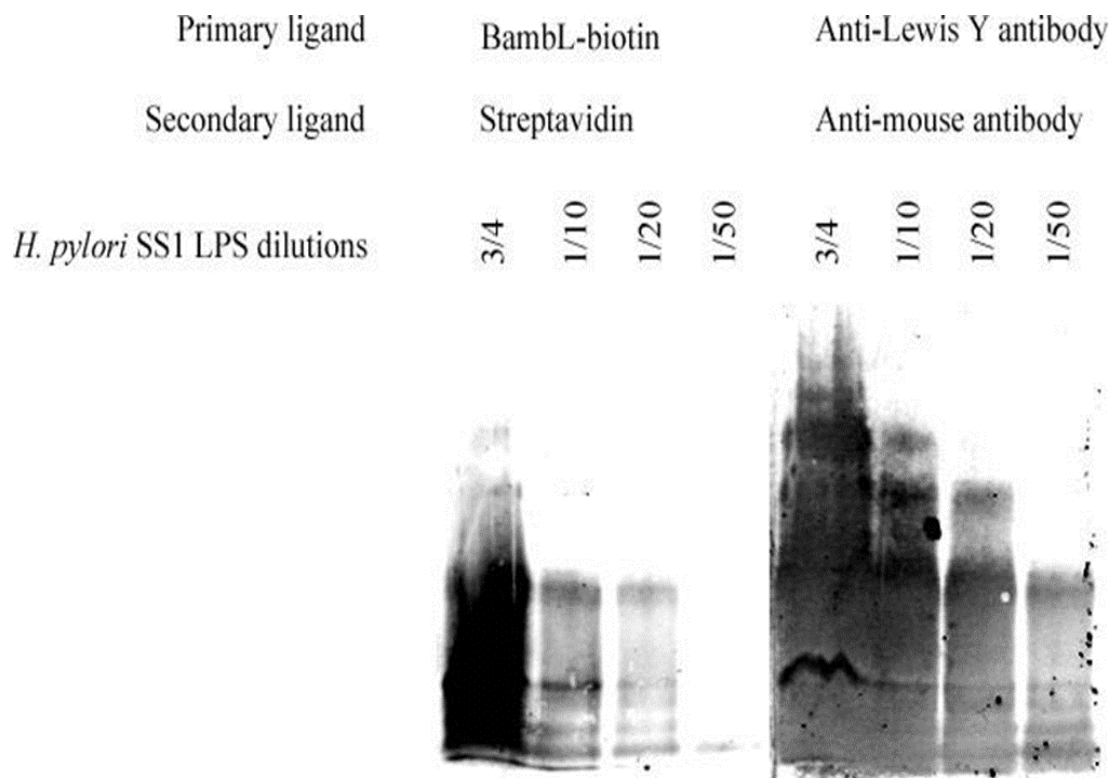
Figure 56. BambL binds to Le^y of *H. pylori* SS1. (Credit to A. Oberc).

Curriculum Vitae

Name:	Najwa Zebian

Post-secondary Education and Degrees:	Western University
	London, Ontario, Canada
	May 2011-April 2016
	Ph.D candidate
	Western University
	London, Ontario, Canada
	Sept. 2007-April 2011
	BMSc Honours Specialization in Microbiology and Immunology

Honours and Awards:	Terry Beveridge Poster Award -2015
	(Canadian Society of Microbiology)
	$500.00
	Dr. Frederick W. Luney Graduate Travel Award -2013, 2014, 2015
	Department of MNI, Western University
	$1000.00
	Ontario Graduate Scholarship – 2012-2013 & 2014-2015
	$15,000.00
	Graduate Thesis Research Award -2012, 2013
	Western University
	$850
	Western Graduate Research Scholarship - 2011 – 2016

Western University

$7,500.00/year

Western Scholarship of Excellence – 2007

$1500.00

Related Work   Teaching Assistant

Experience   Western University

M&I 3610F: Microbiology Laboratory

Sept 2014- Dec 2016

Teaching Assistant

The University of Western Ontario

M&I 2100A: Biology of Prokaryotes

Sept 2012- Dec 2013

Publications:

Zebian, N., Merkx-Jacques, A., Pittock, P.P., Houle, S., Dozois, C.M., Lajoie, G.A., and Creuzenet, C. (2015). Comprehensive analysis of flagellin glycosylation in *Campylobacter jejuni* NCTC 11168 reveals incorporation of legionaminic acid and its importance for host colonization. *Glycobiology* cwv104.

Hopf, P.S., Ford, R.S., **Zebian, N**., Merkx-Jacques, A., Vijayakumar, S., Ratnayake, D., Hayworth, J., and Creuzenet, C. (2011). Protein Glycosylation in *Helicobacter pylori*: Beyond the Flagellins? *PLoS One* 6, e25722.

Oral and Poster Presentations:

1- **Nov 6, 2015:** <u>*Poster*</u> presentation for Infection and Immunity Research Forum

Title: A comprehensive study of Sbe1 reveals incorporation of legionaminic acid in the flagellins, a regulatory role on capsule synthesis and a role in virulence of *Campylobacter jejuni*

Authors: Najwa Zebian, Paula P. Pittock, Gilles A. Lajoie, and Carole Creuzenet

2- **June 15-18, 2015:** *Poster* presentation for student competition at the Canadian Society of Microbiology - **WINNER**
Title: The role of Sbe1 in protein glycosylation and capsule synthesis
Authors: Najwa Zebian, Paula P. Pittock, Gilles A. Lajoie, and Carole Creuzenet

3- **April 1, 2015:** *Poster* presentation for London Health Research Day
Title: The role of Sbe1 in flagellin glycosylation and capsule synthesis
Authors: Najwa Zebian, Paula P. Pittock, Gilles A. Lajoie, and Carole Creuzenet

4- **Nov 6, 2014:** *Poster* presentation for Infection and Immunity Research Forum
Title: Investigation of the role of a sugar biosynthetic enzyme in flagellar glycosylation and capsule synthesis
Authors: Najwa Zebian, Paula P. Pittock, Gilles A. Lajoie, and Carole Creuzenet

5- **March 18, 2014:** *Poster* presentation for London Health Research Day

Title: SBE1 and its role in the virulence of *Campylobacter jejuni*
Authors: Najwa Zebian and Carole Creuzenet

6- **Feb 10, 2014:** *Poster* presentation for CDDW – Main conference

Title: Investigating the function of SBE1 and its potential link to the virulence of *Campylobacter jejuni*
Authors: Najwa Zebian and Carole Creuzenet

7- **Nov 1, 2013:** *Poster* presentation for Infection and Immunity Research forum

Title: Investigating the function of SBE1 and its potential link to the virulence of *Campylobacter jejuni*
Authors: Najwa Zebian and Carole Creuzenet

8- **March 19, 2013:** *Poster* presentation for London Health Research Day

Title: sbe1: A novel sugar biosynthetic enzyme involved in protein glycosylation in *Campylobacter jejuni*
Authors: Najwa Zebian and Carole Creuzenet

9- **March 1-4, 2013**: *Poster* presentation for CDDW – main conference

Title: Determining the function of a novel sugar biosynthetic enzyme and its role in the pathogenesis of *Campylobacter jejuni*
Authors: Najwa Zebian and Carole Creuzenet

10- **Feb 27-28, 2013**: _Oral_ Presentation for CDDW –Research Topics
Title: Determining the function of a novel sugar biosynthetic enzyme and its role in the pathogenesis of *Campylobacter jejuni*
Authors: Najwa Zebian and Carole Creuzenet

11- **Nov 30, 2012:** _Poster_ presentation for Infection and Immunity Research Forum
Title: Determining the function of a novel sugar biosynthetic enzyme and its role in the pathogenesis of *Campylobacter jejuni*
Authors: Najwa Zebian and Carole Creuzenet

12- **March 20, 2012:** _Poster_ presentation for London Health Research Day
Title: Characterization of two putative glycoproteins in *Helicobacter pylori*
Authors: Najwa Zebian and Carole Creuzenet

13- **Nov 4, 2011:** _Poster_ presentation for Infection and Immunity Research Forum
Title: Protein glycosylation in *Helicobacter pylori*
Authors: Najwa Zebian and Carole Creuzenet